Production of methanol/DME from biomass

EFP06

Ahrenfeldt, Jesper; Henriksen, Ulrik Birk; Münster-Swendsen, Janus; Fink, Anders; Clausen, Lasse Røngaard; Christensen, Jakob Munkholt; Qin, Ke; Lin, Weigang; Jensen, Peter Arendt; Jensen, Anker Degn

Publication date:
2011

EFP06

Production of methanol/DME from biomass

Jesper Ahrenfeldt
Ulrik Birk Henriksen
Janus Münster-Swendsen
Anders Fink
Lasse Røngaard Clausen
Jakob Munkholt Christensen
Ke Qin
Weigang Lin
Peter Arendt Jensen
Anker Degn Jensen

National Laboratory for Sustainable Energy (Risø DTU)
Department of Mechanical Engineering (DTU Mekanik - MEK)
Department of Chemical and Biochemical Engineering (DTU Kemiteknik - KT)
TECHNICAL UNIVERSITY OF DENMARK

2011

Table of Contents

Abstract

In this project the production of DME/methanol from biomass has been investigated. Production of DME/methanol from biomass requires the use of a gasifier to transform the solid fuel to a synthesis gas (syngas) - this syngas can then be catalytically converted to DME/methanol. Two different gasifier types have been investigated in this project:

- The Two-Stage Gasifier (Viking Gasifier), designed to produce a very clean gas to be used in a gas engine, has been connected to a lab-scale methanol plant, to prove that the gas from the gasifier could be used for methanol production with a minimum of gas cleaning. This was proved by experiments.
  Thermodynamic computer models of DME and methanol plants based on using the Two-Stage Gasification concept were created to show the potential of such plants. The models showed that the potential biomass to DME/methanol + net electricity energy efficiency was 51-58% (LHV). By using waste heat from the plants for district heating, the total energy efficiencies could reach 87-88% (LHV).
- A lab-scale electrically heated entrained flow gasifier has been used to gasify wood and straw. Entrained flow gasifiers are today the preferred gasifier type for commercial coal gasification, but little information exists on using these types of gasifiers for biomass gasification. The experiments performed provided quantitative data on product and gas composition as a function of operation conditions. Biomass can be gasified with less oxygen consumption compared to coal. The organic fraction of the biomass that is not converted to gas appears as soot.
  Thermodynamic computer models of DME and methanol plants based on using entrained flow gasification were created to show the potential of such plants. These models showed that the potential torrefied biomass to DME/methanol + net electricity energy efficiency was 65-71% (LHV).

Different routes to produce liquid transport fuels from biomass are possible. They include production of RME (rapeseed oil methyl ester), ethanol from fermentation or gasification based synthesis of DME, methanol, Fisher Tropsch fuels etc.
A comparison of these different methods to provide biomass based transport fuels has shown that the gasification based route is an attractive and efficient technology.

Resumé

I dette projekt undersøges produktion af DME/metanol ud fra biomasse. Produktion af DME/metanol ud fra biomasse indbefatter brugen af en forgasser for at transformere det faste biomassebrændsel til en syntesegas (syngas) - denne syngas kan herefter katalytisk konvertes til DME/metanol. To forskellige forgassertyper er blevet undersøgt i dette projekt:

- To-trins-forgasseren (Viking Forgasseren), som blev designet til at producere en meget ren gas til brug i en gas motor, er blevet forbundet til et lab-scale metanolanlæg for at vise, at den rene forgasningsgas kan bruges til metanolproduktion med et minimum af gasrensning. Dette blev eftervist ved eksperimenter.
  Termodynamiske computermodeller af DME- og metanol-anlæg baseret på at bruge to-trins forgasningsprocessen blev lavet for at undersøge potentialet for sådanne anlæg. Modellerne viste at anlæggene kunne konvertere 51-58% (LHV) af energien i biomassen til DME/metanol + elektricitet (netto). Ved at bruge spildvarmen fra anlæggene til fjernvarmeproduktion, blev der opnået totalvirkningsgrader på 87-88% (LHV).
- En lab-scale elektrisk opvarmet entrained flow forgasser er blevet brugt til forgasning af træ og halm. Entrained flow forgassere er i dag den foretrukne forgassertype til kommerciel kulforgasning, men man har kun begrænset erfaring med brug af denne forgassertype til forgasning af biomasse. De udførte eksperimenter gav kvantitative data om produkt- og gas-sammensætning som funktion af driftbetingelserne. Biomasse kan forgasses med et mindre ilt-forbrug sammenlignet med kul. Den organiske del af biomassen som ikke omdannes til gas omdannes til sod.
  Termodynamiske computermodeller af DME- og metanol-anlæg baseret på at bruge entrained flow forgasning af biomasse blev lavet for at undersøge potentialet for sådanne anlæg. Modellerne viste at anlæggene kunne konvertere 65-71% (LHV) af energien i torreficeret biomasse til DME/metanol + elektricitet (netto).

Der findes flere forskellige måder hvorpå flydende brændstoffer til transportsektoren kan produceres ud fra biomasse. De omfatter produktion af RME (rapeseed oil methyl ester), etanol produceret ved fermentering, og forgasningsbaserede brændstoffer som DME, metanol og Fisher Tropsch brændsler osv.
En sammenligning af disse forskellige metoder har vist, at de forgasningsbasere ruter er attrative og energieffektive.

Personnel

National Laboratory for Sustainable Energy (Risø DTU)
Senior Scientist Jesper Ahrenfeldt
Associate professor Ulrik Birk Henriksen

Department of Mechanical Engineering (DTU Mekanik - MEK)
Student Janus Münster-Swendsen
Student Anders Fink
PostDoc Lasse Røngaard Clausen

Department of Chemical and Biochemical Engineering (DTU Kemiteknik - KT)
Student Jakob Munkholt Christensen
Ph.D student Ke Qin
Associate professor Weigang Lin
Associate professor Peter Arendt Jensen
Professor Anker Degn Jensen

Publication list

(all publications are appended this report)

A. Münster-Swendsen J, Fink A. "Methanol production from gasified biomass". Bachelor report, Department of Mechanical Engineering, Technical University of Denmark, 2007.
B. Clausen LR, Elmegaard B, Ahrenfeldt J, Henriksen U. "Thermodynamic analysis of small-scale DME and methanol plants based on the efficient Two-stage gasifier". Submitted to Energy (manuscript number: EGY-D-11-00180), 2011.
C. Clausen LR, Elmegaard B, Houbak N. "Technoeconomic analysis of a low CO2 emission dimethyl ether (DME) plant based on gasification of torrefied biomass". Energy 2010;35(12):4831-4842.
D. Weigang Lin. Report: Modification of the Entrained Flow Reactor for Gasification Experiments.
E. Ke Qin, Weigang Lin, Peter Arendt Jensen, Anker Degn Jensen. Report: Atmospheric pressure entrained flow gasification of biomass.
F. Ke Qin, Weigang Lin, Peter Arendt Jensen, Anker Degn Jensen, Helge Egsgaard. Conference paper: Influence of operating conditions on gas composition, soot and tar in entrained flow gasification of biomass. International Conference on Polygeneration strategies, Vienna, September 2009.
G. Jakob Munkholt Christensen, Anker Degn Jensen, Peter Arendt Jensen. Report: synthesis of liquid fuels from biomass in a Danish context (Syntese af væskeformige brændsler fra biomasse i en dansk kontekst). (in danish)

1. Project background

Research in the production of DME/methanol from biomass is promoted by the Danish Energy Agency in they bio-fuel strategy (”Strategi for forskning og udvikling vedr. fremstilling af flydende biobrændsler”).
A main research area is the use of the two-stage biomass gasification concept (e.g. the “Viking Gasifier”) for production of syngas that can be used for DME/methanol production. The reason why the Two-Stage Gasifier is suited for DME/methanol production is that the gas is very clean, and that the energy efficiency of the gasifier is very high.
The two-stage biomass gasification concept is demonstrated at 70 kWth (the “Viking Gasifier”) and at 700 kWth. Both gasifiers are air-blown and operate at atmospheric pressure. The Viking Gasifier is situated at Risø DTU and has been in operation for over 4000 hours.
The two-stage biomass gasification concept could especially be suited for once-through synthesis because of the high content of inerts due to air-blown gasification.
In a once-through plnat, the unconverted syngas could be used in a gas engine to produce electricity, and the plant waste heat could be used for district heating. Such a plant could achieve a high total energy efficiency. The ratio between liquid fuel and electricity production can also be changed according to the demand for electricity.

A main supplier of technology for DME/methanol synthesis, and of syngas cleaning technology, is Haldor Topsøe. Equipment from Haldor Topsøe is used in a lab-scale methanol synthesis plant situated near the “Viking Gasifier”. This lab-scale methanol plant has been operated on a bottle gas mixture simulating the gas composition from the “Viking Gasifier”.

Pressurized entrained flow gasification of biomass can be an important process in a future renewable energy supply system. The technology can be utilized in different concepts, or combination of concepts, to obtain an optimal use of biomass and thereby minimize fossil fuel CO_2 emissions. Some possible energy conversion plants that could use the pressurized entrained flow gasification are:

- Plants to produce transport fuels from Biomass. A synthesis gas rich in H_2 and CO are produced in the gasifier and the gas is used to make a catalytic based production of methanol, DME or gasoline.
- The technology can be used for electricity production with a high efficiency in an integrated gasification combined cycle plant (IGCC)
- The entrained flow gasifier can be used as a ‘pre-combustion’ technology for CO_2 sequestration. The produced gas is led to a shift reactor whereby CO is removed and CO_2 and H_2 are produced. The CO_2 is sequestered and the H_2 is used for electricity production using a combustion process that only produces water.

The entrained flow gasification technology is normally used in large pressurized oxygen blown units that apply coal as fuel. No commercial large scale biomass entrained flow gasifiers are operated presently.

Entrained flow gasifiers have lower energy efficiency than what is achieved with the two-stage biomass gasification concept, but the use of entrained flow gasifiers enable a higher conversion of the syngas to DME/methanol.

2. Objectives

The objectives were:

- To prove that the gas from the “Viking Gasifier” can be used for DME/methanol production with a minimum of gas cleaning. Eventual problems related to the use of the gas from the “Viking Gasifier” with the synthesis and gas cleaning equipment supplied by Haldor Topsøe were identified.
- To model DME/methanol plants based on: 1. the two-stage biomass gasification concept, and 2. large-scale entrained flow gasification of torrefied biomass. The models were used for prediction of achievable energy efficiencies. The results from the models were compared.
- To investigate the possibilities to make efficient entrained flow gasification of biomass by performing experiments with an atmospheric pressure electrically heated laboratory entrained flow reactor, and investigate how reactor operation conditions influence the composition of the product gas.
- To compare different technologies used for production of transport fuels from biomass by doing a literature review.

3. Tasks

Task 1: Synthesis of DME/methanol with gas from the "Viking Gasifier" (experimental – Risø/MEK)
The exsisting lab-scale methanol synthesis plant located at Risø was used to produce methanol from a syngas generated from bottled gas. Different syngas compositions were tested.
The "Viking Gasifier" was then connected to the lab-scale methanol synthesis plant and methanol was produced.
The results from the tests were compared, mainly regarding the methanol yield.

The effect of adding a CO_2 removal step (potassium hydroxide pills) before the methanol synthesis was investigated.

Note: The original plan included operation of the methanol plant ("Viking Gasifier" + methanol synthesis) for more than a 1000 hours, to investigate the long-term effects on the gas cleaning and synthesis equipment (e.g. catalyst deactivation). This was, in agreement with EFP, reduced to short proof-of-concept tests.

Task 2: Modeling of DME/methanol plants (MEK/Risø)
Numerical models of DME/methanol plants, based on using a two-stage biomass gasifier, were created. The models were used for prediction of the achievable energy efficiencies. The following plant concepts were investigated:

- Once-through methanol synthesis
- Once-through DME synthesis
- Recycle methanol synthesis
- Recycle DME synthesis

The different plant concepts were compared on the methanol/DME yield and on the co-production of electricity and district heating.

The results from the modeling of DME/methanol plants based on the two-stage biomass gasification concept were compared with results from numerical models of DME/methanol plants based on entrained flow gasification of biomass.

Task 3: Modification of entrained flow reactor (KT)
The CHEC high temperature entrained flow reactor was constructed to perform experiments with combustion, ash transformation and pyrolysis of solid fuels in a suspension flow reactor mode. In the present project, the reactor is used to perform experiments on biomass gasification at entrained flow gasifier conditions. Major modifications of the reactor included steam injection, adequate solid and gas sampling of the product gas and modification of the safety system.

Task 4: Entrained flow gasification of biomass (experimental - KT)
The optimal gasification process on an entrained flow gasifier should provide a gas for liquid fuel synthesis with a high content of CO and H_2 and with a minimal content of larger hydrocarbons, tar and soot. Entrained flow gasification of biomass was investigated by performing laboratory experiments and equilibrium calculations. Experiments with gasification of two types of biomass, wood and straw, were performed in the CHEC atmospheric pressure electrically heated entrained flow reactor. Additionally a few experiments with coal gasification were performed.

Task 5: Comparison of different methods to produce transport fuels from biomass (KT)
Different routes to produce liquid transport fuels from biomass are possible. They include production of RME (rapeseed oil methyl ester), ethanol from fermentation or gasification based synthesis of DME, methanol, Fisher Tropsch fuels etc. The energy efficiency and the CO_2 reduction potential of the different technologies have been calculated. This was done by calculation of the possible obtainable transport distance by applying the biomass from one hectare using a specific conversion technology.

4. Summary of results

Task 1: Synthesis of DME/methanol with gas from the "Viking Gasifier" (experimental – Risø/MEK)
The exsisting lab-scale methanol synthesis plant was used to produce methanol from a syngas generated from bottled gas. When using a syngas composition similar to the syngas composition expected from the "Viking Gasifier" - with CO_2 removal – 14.6 g of methanol was produced over a period of 30 minutes.
When coupling the "Viking Gasifier" to the lab-scale methanol plant, without CO_2 removal, 2.9 g of methanol was produced over a period of 30 minutes.

The CO_2 removal system based on using potassium hydroxide pills did not work probaply. This meant that only 0.3 g of methanol was produced over a period of a few minutes when the CO_2 removal system was coupled to the "Viking Gasifier".

These results therefor show that it is possible to produce methanol based on a gas generated by a two-stage gasifier such as the "Viking Gasifier". The results also show that the methanol yield depends greatly on the CO_2 content of the syngas - as expected. The long-term effects of using a gas generated by a two-stage gasifier, on e.g. the methanol catalyst, are however still not known.

See Appendix A for further information.

Task 2: Modeling of DME/methanol plants (MEK/Risø)
Numerical models of small-scale DME/methanol plants, based on the two-stage biomass gasification concept, were created. The plant models showed energy efficiencies from biomass (wood chips) to DME/methanol of 45-58% (LHV). The highest yields were achieved when using recycle synthesis, and the lowest yields when using once-through synthesis.
The unconverted syngas was used in a gas engine to produce electricity to cover the on-site electricity consumption and, in the case of the once-through plants, for export to the grid. The biomass to DME/methanol + net electricity efficiencies achieved were 51-58% (LHV). By using waste heat from the plants for district heating, the total energy efficiencies became 87-88%.
The difference in energy efficiencies between the methanol plants and the DME plants showed to be very small, but because the DME plants are somewhat more complex due to the use of a refrigeration plant, the methanol plants may be the preffered option.

Numerical models of DME plants based on entrained flow gasification of biomass were also created. A commercial large-scale entrained flow gasifier operating on torrefied biomass pellets was modeled. The gasifier was pressurized and oxygen-blown.
The plant models showed energy efficiencies from torrefied biomass to DME of 49-66% (LHV). If it is assumed that 10% of the heating value in the biomass is lost in the

torrefaction process, the untreated biomass to DME energy efficiencies becomes 44-59%.
The plants co-produced electricity by utilizing plant waste heat in a steam cycle, and unconverted syngas in a gas turbine. The torrefied biomass to DME + net electricity efficiencies achieved were 65-71% (LHV).

When comparing the results from the small-scale DME/methanol plants to the large-scale DME plants, it can be seen that the large-scale DME plants achieve the highest fuel + net electricity energy efficiencies. However, if the maximum fuel + net electricity energy efficiencies are compared on an "untreated biomass" basis, the difference is relatively small (58% vs. 64%).
Litterature on biomass-to-liquids (BTL) plants concludes that large-scale fuel production is more feasible than small-scale, due to economy of scale. The economy of scale more than outweighs the increased biomass transportation costs. The advantage with small-scale biomass-to-liquids (BTL) plants could however be a better utilization of a district heating co-production.

See Appendix B and Appendix C for further information.

Task 3: Modification of entrained flow reactor (KT)

The PI diagram of the modified entrained flow gasifier facility is shown in Figure 1. The modification of the reactor setup included the following tasks:

1. Mounting of a steam injection system
2. Mounting of a new hot probe gas and particle sample extraction system making it possible to measure the content of tar, soot and char as well as the composition of the gas product flow from the gasifier.
3. Modification of the exhaust gas system to make a controlled combustion of the product gas
4. Modification of the facility PLC safety system to stop fuel feeding at high room CO level and if the exhaust flame was extinct.
5. Mounting of a gas shell around the reactor for the removal of gas leaking out of the reactor
6. Including a GC in the system to make measurements of light hydrocarbons possible.

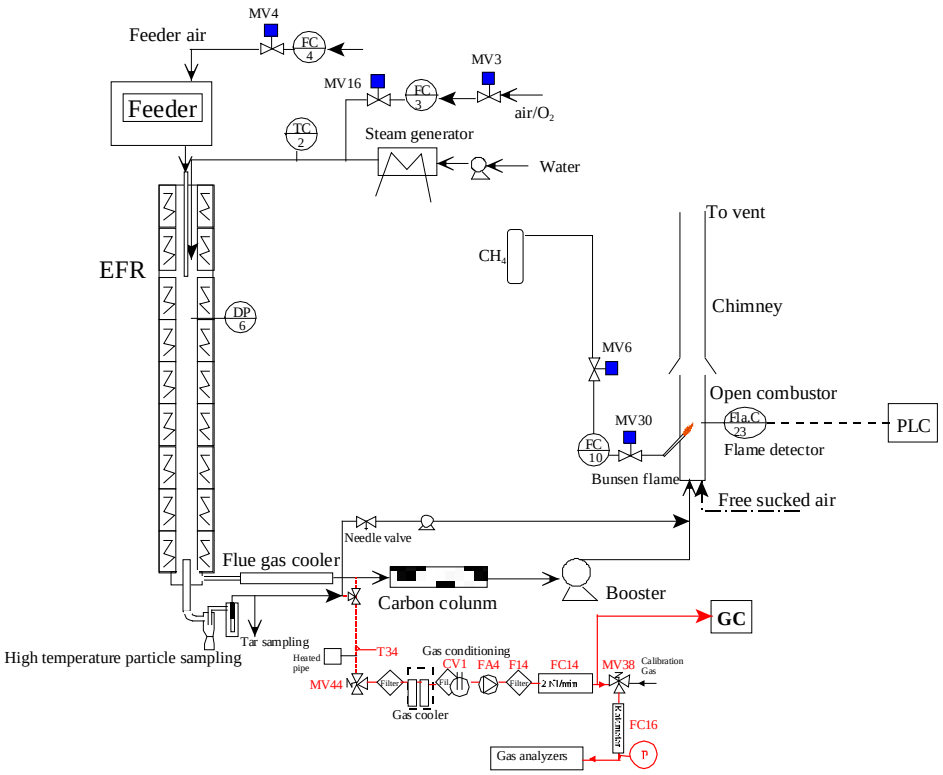

Figure 1. PI diagram of the entrained flow gasifier after modification

See Appendix D for further information.

Task 4: Entrained flow gasification of biomass (experimental - KT)

Experiments with gasification of two types of biomass, wood and straw, were performed in the CHEC atmospheric pressure electrically heated entrained flow reactor.

The feeding rate of fuel into the reactor was 550 – 1000 g/h, and the gasification process took place in a two meter long ceramic tube with an inner diameter of 8 cm. It was the objective to quantify the influence of reactor operation conditions on the products composition of gas, tar, char and soot.

The applied operation range included reactor temperatures of 1000 to 1350°C, oxygen inlet concentrations of 2 to 34 vol % O_2, steam carbon molar ratios of 0 – 1,25 H_2O/C (steam inlet to fuel carbon molar ratio), and excess air ratios of λ = 0.2-0.9. The obtained reactor residence time was from 2.1 to 4.7 seconds. In all biomass experiments, the fuel was completely converted and no char was found in the reactor outlet products. At reactor temperatures of 1200°C and 1350°C, all carbon mass balance closures were reasonable, typically within ±9%. At 1000°C the carbon mass balance has a large deviation (22 wt %) probably due to a high content of unmeasured tar and larger hydrocarbons in the product gas. The product gas were besides N_2 dominated by H_2 (0.15-0.7 Nm^3/kg fuel), CO (0.35-0.75 Nm^3/kg fuel), CO_2 (0.15-0.3 Nm^3/kg fuel), and a small amount of light hydrocarbons, less than 0.08 Nm^3/kg fuel (CH_4+C_2H_4+C_3H_8). Increasing the reactor temperature from 1000 to 1350°C at otherwise maintained operation conditions led to increased yields of product gas (defined as the sum of H_2,

CO, CO_2 and C_xH_y (hydrocarbons up to C_3 species)), H_2 and CO; and a decreased yield of CO_2 and C_xH_y. As seen on Figure 3 at 1350°C, a significant yield of soot was produced (~40g/kg fuel at λ=0.25, H_2O/C=0), while there was nearly no tar formation. Conversely, at 1000°C, the soot yield was lowest, whereas the amount of tar was highest. Thus, there is a tradeoff between soot and tar formation.

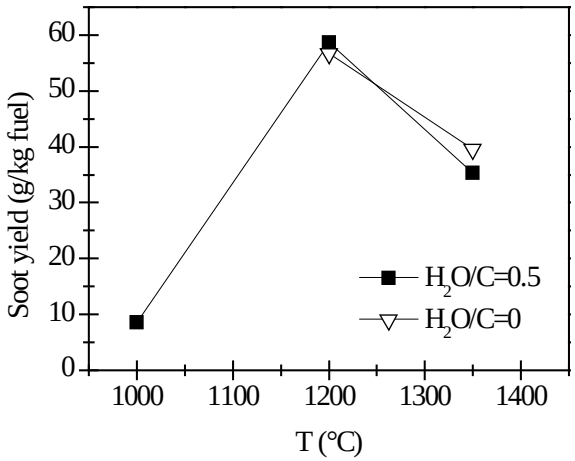

Figure 3. Effect of reactor temperature on the soot yield of wood gasification at λ=0.25.

The influence of changes in oxygen to fuel ratio was investigated. An increased oxygen to fuel ratio (λ = 0.2-0.9) was obtained by increasing the gas inlet oxygen content from 3 to 17 vol%. The increased oxygen to fuel ratio lead to decreased outlet contents of H_2, CO, C_xH_y and soot, while the CO_2 content increased and the gas heating value decreased. The increased amount of oxygen simply caused an oxidation of the H_2, CO, C_xH_y and soot.

The influence of increased oxygen inlet concentration with otherwise maintained operation conditions at an excess air ratio of λ=0.25, a reactor temperature of 1350°C and no steam injection were investigated. The increased oxygen concentration was obtained by decreasing the N_2 flow to the reactor and this leads to an increased reactor residence time, and probably an increased temperature in the top of the reactor. The soot formation increased from 3 mol/kg fuel at an inlet oxygen concentration of 5 vol% up to 11 mol soot/kg fuel at an inlet oxygen concentration of 34 vol%. The reason for the large soot formation at high oxygen inlet concentrations is presently not known. Increased steam injection and thereby increased reactor H_2O/C ratio pushed the water shift reaction towards an increased formation of H_2 and CO_2. However, even a high amount of water injection (H_2O/C ratio changed from 0 to 1) typically caused a H_2 dry gas content increase of only 20%. A moderate reduction of the soot formation in the range of 20-50% can be obtained by increasing the steam injection from 0 to H2O/C=1. A comparison of product gas composition when using wood and straw fuel showed similar results. This indicates that the high straw fuel alkali content do not significantly influences the gasification process. Using coal as gasifier fuel showed that at conditions

(1350°C, λ=0.25, H_2O/C=1.25) where biomass was completely converted to gas (except a small amount of soot) a large amount of unconverted coal char was collected. This indicates that a smaller amount of oxygen is needed to gasifie biomass compared to gasification of coal with similar energy content.
Generally some soot was produced in all experiments conducted at 1200 and 1350°C using low λ values. A minimum amount of soot of 2 mol/kg fuel at λ = 0.25 were observed at the operation conditions 1350°C, inlet O_2= 5 vol% and a steam injection level of H_2O/C = 1.0. STA (simultaneous Thermal Analysis) tests showed that the combustion reactivity of soot from straw gasification is higher than that of soot from wood gasification.
Thermodynamic equilibrium calculations were performed by using the Factsage software. The equilibrium calculations were performed using conditions that correspond to entrained flow gasification of wood. Effects of temperature (800-1600°C), steam/carbon molar ratio (0 – 2.0 mol steam added relative to fuel C mol input), excess air ratio (λ = 0.0-1.0), and pressure (1 – 100 Bar) were investigated. As a standard condition were used a temperature of 1350°C, a steam/carbon molar ratio of 0, an excess air ratio λ = 0.25 and a pressure of 1 Bar. Using a λ value of 0.2 to 0.25 lead to a maximum CO yield, while using a value of λ below 0.2 formation of carbon was predicted. Changes of temperature above 800°C only induced small changes in the gas composition. By increased water injection an increased level of H_2 and CO_2 and a decreased level of CO were observed. Increasing the pressure from 1 to 100 Bar only changed the gas composition slightly; a small amount of methane was predicted to be formed at high pressures. The gasification product distributions obtained by the experiments and equilibrium calculations were compared. It was observed that at 1350 and 1200°C with no steam addition the experiments gave rise to some soot and hydrocarbon formation that was not predicted by the equilibrium calculations. At 1350°C with steam addition smaller amounts of hydrocarbon and soot was formed, and generally the equilibrium calculations provided reasonable predictions of the gas H_2, CO and CO_2 contents.

See Appendix E and Appendix F for further information.

Task 5: Comparison of different methods to produce transport fuels from biomass (KT)

The results shown in Figure 2 are the obtainable driving distance in a standard size family car using the harvest from one hectare of Danish land, and then use a particular technology to produce a transport fuel. The results are calculated by combining the crop yield from the field, the conversion efficiency to a transport fuel and the obtained transport distance by a car. The highest distance is obtained by an electric car followed by hydrogen driven fuel cell car. For fuels used in diesel or gasoline engines the DME option is the most efficient followed by methanol. Synthetic gasoline, FT diesel, higher alcohols and bio-ethanol provides nearly similar transport distances, while RME is the least efficient method. The electrical car based concept is very efficient, but large

changes in infrastructure and the car park inventory are needed to implement the technology.
If the technologies based on gasification followed by fuel synthesis are combined with electricity production they generally provides a larger CO_2 displacement than the routes using bio-ethanol and RME. This work illuminates the potential of the production of gasification based transport fuels.

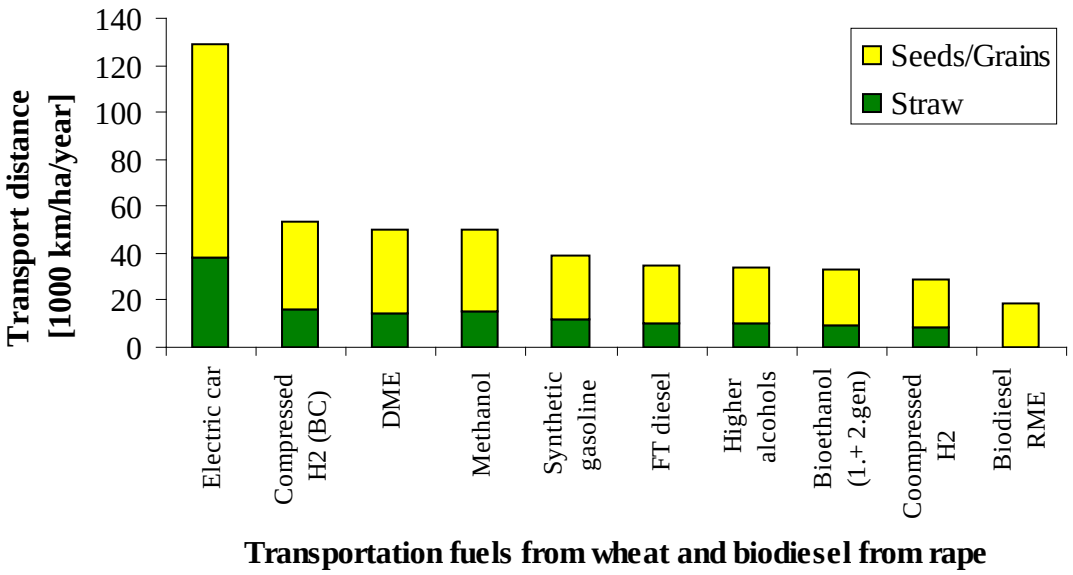

Figure2. The distance an average car can travel using the yearly harvest of the whole wheat crop (straw + grain) from one hectare of land. Bio-diesel (RME) is derived from rape. Compressed hydrogen (BC) is based on using hydrogen driven fuel cell. The hydrogen is produced by biomass gasification.

See Appendix G for further information.

5. Conclusions

The conclusions are:

- It was shown that the gas from the "Viking Gasifier" can be used for DME/methanol production with a minimum of gas cleaning. The long-term effects on gas cleaning and synthesis equipment were however not investigated.
- Numerical models of DME/methanol plants based on: 1. the two-stage biomass gasification concept, and 2. large-scale entrained flow gasification of torrefied biomass, showed that biomass could be converted to DME/methanol + electricity with an energy efficiencies of 51-71%. The highest efficiencies were achieved by the large scale plants based on entrained flow gasification of torrefied biomass.
- Entrained flow gasification experiments have provided quantitative data on product and gas composition as a function of operation conditions. Biomass can be gasified with less oxygen consumption compared to coal. The organic fraction of the biomass that is not converted to gas appears as soot.
- A comparison of different methods to provide biomass based transport fuels has shown that the gasification based route is an attractive and efficient technology.

Further work regarding entrained flow biomass gasifiers (KT)

This study have only dealt with some of the knowledge needed to design reliable and optimized biomass entrained flow gasifiers used to a liquid fuel synthesis processes. Some of the areas needing further studies are:

- Development of computer models describing the gasification process
- Investigations on how to minimize soot formation
- Study of biomass ash behavior in an entrained flow reactor process
- Study of the auto thermal gasification process (without electrical reactor heating) at high inlet oxygen contents (above 35 vol %) and at pressurized conditions
- Further optimization with respect to use of a minimum of oxygen to conduct the gasification process
- Optimization of gas cleaning processes

Appendix A. Methanol production from gasified biomass

Bachelor report
Münster-Swendsen J, Fink A. “Methanol production from gasified biomass”. Bachelor report, Department of Mechanical Engineering, Technical University of Denmark, 2007.

METHANOL PRODUCTION FROM GASIFIED BIOMASS

Janus Münster-Swendsen s042269
Anders Fink s041996

Technical University of Denmark
Department of Mechanical Engineering
Supervisors: Anker Degn Jensen, Jesper Ahrenfeldt and Ulrik Birk Henriksen
19. juni 2007

DTU

0.1 Summary

0.1.1 Introduction

This report presents a study in methanol and DME (DiMethylEther) production from gasified biomass. The study is done at the section for energy engineering at MEK (Department of Mechanical Engineering) at the Technical University of Denmark (DTU). This bachelor project has been carried out by Anders Fink and Janus Münster-Swendsen, supervised by Anker Degn Jensen (Professor), Jesper Ahrenfeldt (Assistant Professor) and Ulrik Birk Henriksen (Associate Professor).

The study is based on the work and facility made by Henrik Iversen in his Master Thesis from 2006.

This bachelor project is part of a larger research project called EFP (Energy Research Programme). The purpose with the EFP project is to create productions of methanol and DME from biomass. The participants are MEK (DTU), KT (Department of Chemical Engineering - DTU), Haldor Topsøe and Elsam Engineering.

This report describes production of methanol directly from synthesis gas (syngas) from the Viking gasifier. The important parameters for this production will be identified and the possibilities to modify the methanol facility to produce DME is evaluated.

0.1.2 Objectives

The purpose of this project is to demonstrate methanol production from gasified biomass and consider possibilities for DME production from gasified biomass.

The main objectives of the report:

1. A literature study of DME and other alternative bio fuels to evaluate the prospects of DME.
2. Methanol production by synthesis of syngas from the Viking gasifier. Including implementation of several cleaning devices to remove unwanted components in the syngas.
3. Creating a theoretical correct model of methanol and DME synthesis in order to evaluate the different parameters in the methanol and DME production.

0.1.3 Conclusions

Conclusions on the established objectives:

1. DME is versatile, it can be used for many different things and can be produced in various ways.

   Bio DME (DME produced from biomass) has many interesting properties as diesel engine fuel. It has a minimum of emissions, is CO_2 neutral and have the best well to wheel efficiency compared with the other alternative bio fuels.

There are some problems with implementing DME as a diesel engine fuel. Especially the distribution net and engine lubrication are problems that needs to be solved.

2. The experiments showed that it is possible to produce methanol from syngas from the Viking gasifier.

   The CO_2 scrubber with pills of potassium hydroxide did not work as intended.

   Experiments showed that chemical equilibrium in the methanol reactor is not reach with flows higher than 0,75 Nm^3/h.

   The gas composition has large influence on the methanol outcome.

3. The created model has large deviations from the experimental results.

   An investigation indicates that it is the measured temperature of the methanol synthesis and not the model, that is the main source of error.

   The model uses the ideal gas equation of state which is verified with the theoretic better Soave-Redlich-Kwong (SRK) equation of state. The ideal gas equation is a good assumption for the used gas composition, different operating temperatures and pressures.

   Calculations shows that with gas from the Viking gasifier condensation temperatures must be below -50 °C for more than 80% DME to be condensed. If the amount of DME in the gas increases so does the condensation temperature.

0.2 Danish summery – resume

0.2.1 Introduktion

Denne rapport studerer metanol og DME produktion fra forgasset biomasse. Studiet er foretaget ved sektionen for energiteknik på institut for Mekanik, Energi og Konstruktion (MEK) på DTU. Bachelorprojektet er udarbejdet af Anders Fink og Janus Münster-Swendsen og vejledt af Lektor Anker Degn Jensen, Adjunkt Jesper Ahrenfeldt og Lektor Ulrik Birk Henriksen.

Dette studie er baseret på Henrik Iversens eksamensprojekt fra 2006 og det anlæg, der blev konstrueret i forbindelse med dette projekt.

Dette bachelorprojekt er del af et større forskningsprojekt ved navn EFP (Energiforskningsprogrammet). EFP projektet omhandler produktion af methanol og DME fra biomasse. Deltagerne i dette projekt er MEK, KT (Kemiteknik - DTU), Haldor Topsøe og Elsam Engineering.

Denne rapport beskriver metanolproduktion direkte fra syntesegas fra Viking forgasseren. De vigtige parametre for denne produktion vil blive identificeret og mulighederne for at modificere anlægget til DME produktion vil blive vurderet.

0.2.2 Formål

Formålet med dette projekt er at demonstrere methanol produktion fra forgasset biomasse og overveje mulighederne for DME produktion.

De primære formål i rapporten er:

1. Et litteraturstudie af DME og de andre alternative biobrændsler for at vurdere muligheder for DME.
2. Metanolproduktion ud fra syntesegas fra Viking forgasseren. Herunder implementering af de nødvendige renseenheder til at fjerne uønskede komponenter i syntesegassen.
3. Konstruere en teoretisk korrekt model for metanol og DME for at kunne vurdere de forskellige parametre ved metanol og DME produktion.

0.2.3 Konklusion

Konklusioner på de opstillede formål:

1. DME er alsidigt. Det kan benyttes til mange forskellige formål og kan produceres ud fra forskellige råmaterialer.

   BioDME (DME produceret fra biomasse) har mange interessante egenskaber som brændstof i en dieselmotor. Det har et minimum af emissioner, er CO_2 neutral og har den bedste "well to wheel" effektivitet sammenlignet med de andre alternative biobrændstoffer.

   Der er dog nogle problemer med implementering af DME som diesel brændstof. Specielt distributionsnettet og smøring i motoren er problemer, der skal løses.

2. Forsøgene viste, at det var muligt at producere metanol direkte fra syntesegas fra Viking forgasseren.

   CO_2 vaskeren med kaliumhydroxid piller fungerede ikke som forventet.

   Forsøg viste, at kemisk ligevægt i methanolreaktoren ikke opnås ved flow over 0,75 Nm^3/h.

   Gassammensætningen har stor effekt på methanol udbyttet.

3. Den konstruerede model har store afvigelser fra de eksperimentelle resultater.

   En undersøgelse tyder dog på, at denne afvigelse ikke skyldes modellen, men den målte temperatur ved methanolsyntesen.

   Modellen benytter sig af idealgas tilstandsligningen og denne er sammenlignet med den teoretisk bedre SRK tilstandsligning. Det kan konkluderes, at idealgasligningen er tilstrækkelig med den givne gassammensætning og de forskellige tryk og temperaturer, der opereres med til metanol og DME produktion.

Beregninger viser at med gas fra Viking forgasseren, skal DME kondenseringstemperaturerne være lavere end -50 °C, hvis mere end 80% skal kondenseres. Hvis DME indholdet af gassen forøges, så er der mulighed for højere kondenseringstemperaturer.

Contents

0.3 Preface

This report is the result of the bachelor project made at the section for energy engineering at MEK, DTU. The project constitutes 15 ECTS points pr student and was made in the period of 19 February 2007 to 19 June 2007.

A large group of experts within the different aspects of the subject have assisted in providing valuable information for the project and for practical implementing of the facility. In this regard, we would particularly like to thank Georgios Kontogeorgis (IVC-SEP), Kaj Thomsen (IVC-SEP), Steen Nielsen (Assistant Engineer), Freddy Christensen (Assistant Engineer), Erik Hansen (Technician), Joachim Paul (Professor), Spencer C Sorensen (Docent) and Haldor Topsøe.

Special thanks are given to our project supervisors Anker Degn Jensen (Professor), Jesper Ahrenfeldt (Assistant Professor) and Ulrik Birk Henriksen (Associate Professor).

June - 2007

Anders Fink (s041996)

Janus Münster-Swendsen (s042269)

0.4 Introduction

The idea behind this project is to try to produce DME from biomass so CO_2 neutral fuels could be an option in the future.

This study is interesting because of the rising demand for renewable and CO_2 neutral fuels and because DME can be used in many different ways. DME could be advantageous to both the local and global environment.

Wednesday the 6. of June a debate program about global warming was aired on DR2 (Danish Television). Here different experts, representatives from the press and members from all the parties of the Danish Parliament discussed domestic energy issues and the role of Denmark in international energy politic.

The former environment minister Svend Auken and the present environment minister Connie Hedegaard both agreed that global warming is a serious human-induced problem and action needs to be taken to stop this tendency.
They agree that the solution is more research and development in new technologies and mechanisms to transfer these new technologies to underdeveloped parts of the world.

In the program the transport sector was named the Achilles heel of global warming. CO_2 is the main gas responsible for climate change[1]. So far CO_2 emissions from the transport sector has been rising in Denmark and this tendency will most likely continue because the demand for cargo and use of cars is rising. As a response, the Danish government express that they are interested in more research and development in new bio fuels to help reduce the CO_2 emissions.

On a global scale, a third of all global greenhouse gasses comes from the transport sector, and the number of cars will properly increase drastic in the future if the current tendency is continuing. This means that the need for fuel is rising, while the amount of fossil fuel is declining. The increase will especially come from Asia. It has been estimated that from 2000 to 2020 there will be a 24-factor increase of cars in China while a three to four factor increase of cars in India.[1]

So there is a growing interest in finding efficient and economically feasible ways to produce CO_2-neutral automotive fuels, by using biomass as the raw material.[1]

0.5 Problem statement

The scope of this project is to produce methanol from biomass and investigate if there is possibilities for the facility to produce DME from syngas.

The syngas is provided by DTU´s Viking gasifier. This syngas contains certain components that needs to be removed before the syngas is reformed to methanol via catalytic processes.

An existing facility is able to produce methanol from bottled gas. This facility must be developed further to run on syngas from biomass.

The second scope of the project is to create a model based on the valid theory describing the process of methanol and DME production and verify this with literature and practical experiments.

Furthermore the existing literature will be studied to evaluate the prospects of bio DME contra other bio-fuels.

0.6 Project delimitations

The literature study is focused on DME and only briefly on other bio fuels. This is because DME has interesting perspectives especially when it is produced from biomass. DTU have a great interest in the development of bio DME. Already DTU has success with the Ecocar and the success will be even greater, if the Ecocar could run on bio DME. A economic study was not possible because this facility is only a demonstration facility and therefore calculations of economic perspectives would not have a solid foundation.

After the literature study it was concluded that there have not been reported production of bio DME. Therefore this was the main focus. But before producing bio DME several other tests was necessary to ensure that the different steps of the facility worked as planned. This part of the project is easily affected by external factors, which could alter the practical success criteria. First methanol was to be produced directly from syngas with all the cleaning devices in use and then change the facility to produce DME. Efficiencies of the facility are not evaluated because it is a demonstration facility designed to proof the concept of bio DME production without considering energy-efficient solutions.

It was prioritized to study the chemistry behind such a production and make a model from the applicable theoretical background.
So far the available models developed on DTU assume ideal gas which seemed incorrect with operational pressure at 40-50 baro and the condense process with low temperature and high pressure.
Therefore a thorough study was made, but it was desired to obtain an equal degree of theory and practical work. Since this is a bachelor project reaction kinetics has been excluded from the theoretical model.

Chapter 1

Biofuels

In the following section the different alternative bio fuels are briefly described to evaluate bio DME.
In order to estimate an acceptable price level for bio DME, an overview of production prices of the other alternatives are summarized.
Then follows a thorough analysis of DME, in which the usages, problems and possibilities are reviewed.

1.1 Alternatives

Focus is on fuels that can be produced from biomass. It is important to distinguish between 1. generation bio fuels and 2. generation.

1. generation bio fuels is primary produced from raw material containing starch or sugar such as corn, sugar beets and sugar canes, which are normally used in the food manufacturing business.
2. generation bio fuels is primary produced from by-products from the industry, the silviculture and the agriculture such as trees, straw, animal fat and plant scrap.

A large advantage with 2. generation bio fuels is that it in general does not grow on cultivated land. Therefore the food manufacturing business remain unaffected by the production of 2. generation bio fuel.
The cultivation of the raw material for 2. generation bio fuels (if there is any) can be less intensive than for ordinary agricultural crops. The lower intensity of the cultivation will therefore generate fewer green house gasses.[2]

None of these new bio fuels can compete in effectiveness with Danish powerplants. But as said in the introduction, research and development in new alternative fuels is very important, especially on a global scale.

One of the advantages with biomass is the opportunity to make decentralized facilities which can help local communities and use raw materials that so far have not been used efficiently in many places of the world.

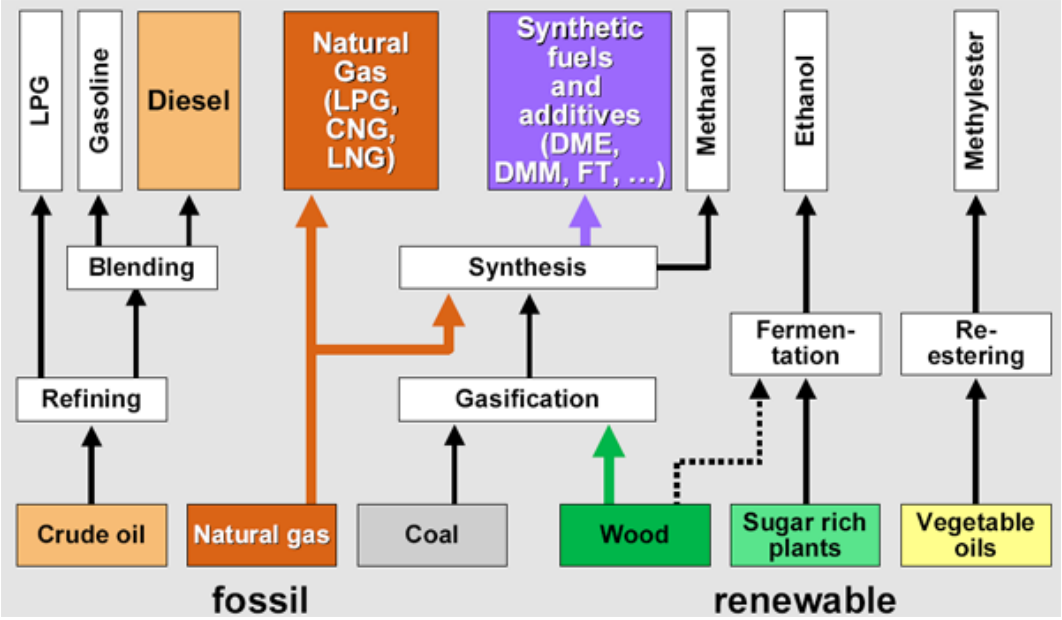

Figure 1.1: Overview of different conversion technologies [3]

1.1.1 Bio diesel

Bio diesel can be obtained from several different products, including rape (RME - Rape Methyl Ester) and soy (SME - Soy Methyl Ester). Fat from deep-friers and animal leftovers can also be used - this is referred to as 2. generation bio diesel.
Bio diesel is a so called flexible fuel, because it is miscible with fossil diesel and can be used in existing vehicles. Problems might occur in fuel systems because of bio diesels dissolving effect on certain plastics and rubbers. EU-standards states that all diesel cars must be able to drive on B5 (95% fossil diesel and 5% bio diesel). Many bigger engines (heavy duty vehicles) are already able to handle pure bio diesel, B100. Bio diesel has lower particle emissions, but higher NO_x emissions than fossil diesel.[4]

Production efficiency (estimated from [5], see App. A.0.1) = 40,2 %

1.1.2 Bio ethanol

Bio ethanol can be produced from crops containing sugar or starch e.g. sugar beets, fruits, wheat and maize. This is referred to as 1. generation bio ethanol and the process requires relatively much energy for pre-treatment, distillation etc.
2. generation bio ethanol is produced from fibre rich biomass (lignocellulose). Enzymes decomposes these fibers and microorganisms can then transform this into ethanol (fermentation).
Up to 5% fossil gasoline can be replaced by ethanol and used in the car population of today. Engines needs to be changed if the mixing rate is higher. Ethanol has a lower calorific value, hence more fuel is needed. On the other hand the compression ratio can be increased which gives better utilization. It should be noted that FFV (Flexible Fuel Vehicles) can use mixtures of 85% ethanol and 15% gasoline (E85).[4][6]

Bio ethanol production generates some by-products. This can vary from animal fodder to biogas or solid bio fuel than can be used for combined heat/power production. Proper use of these by-products are important to increase cost effectiveness of the production.

As mentioned earlier energy is used in the production process. For 1. generation between 30-55% of the energy content is used in production. For 2. generation bio ethanol produced on residual products (straw) this is about 10% of the energy content.[4]
Furthermore one must consider that energy has been used to cultivate the land and natural gas has been converted to fertilizer.[6]

Efficiency of production of bio ethanol can be up to 40%[7]. Ad to this the usage of the by-products.

1.1.3 Biogas

Biogas primarily consists of CH_4 and CO_2. It can be produced from liquid manure, biomass and organic waste. Degasification of liquid manure does not yield a lot of gas, but it has other advantages. Degasified manure is easier absorbed in plants, which means there will be less nutrient leaching. Furthermore there will be less odour nuisance and fewer GHG emissions (methane and laughing gas) from the manure. Methane and laughing gas are very powerful green house gasses, which means that substituting gasoline with biogas can lead to 167% reductions in GHG emissions.[4]

Biogas can be used for combined heat/power generation, or if the CO_2 is removed it can be pressurized and used in SI (Spark Ignition) engines.

Biogas produced from biomass yields 70% of the energy content of the biomass (dry basis). But energy for heat, pumps etc. must be subtracted. This gives a total efficiency of 52%. If CO_2 must be removed and the biogas compressed to 200 bar the total efficiency becomes 35%.[7]

1.1.4 Methanol

Methanol can be used in the engines of today with some modifications. Just like ethanol much more fuel (about double amount) is needed, but the compression ratio can be increased.
Methanol is toxic and should be handled with care. It is aggressive towards some materials, which means some components might have to be changed.
Emissions are of the same magnitude as from gasoline engines, though NO_x emission may be slightly lower. On the other hand formaldehyde emissions could cause problems and unburned fuel will be toxic because of the methanol.[6]
Methanol can also be used in fuel cells (DMFC - Direct Methanol Fuel cell). But currently it is a problem to get high efficiencies, because of minor leakages through the electrolyte. The power output is not as high as from hydrogen fuel cells, because the process is slower.[8]
Studies on bio methanol produced from biomass reports production efficiencies about 54%.[7]

1.1.5 Fischer Trophs

Fischer Trophs (FT) diesel is a synthetic fuel of high quality that can be used in diesel engines without any alterations. The process to produce the fuel was invented in Germany in the 1920s.

The FT process is a catalyzed chemical reaction. The FT diesel can be produced from either coal, natural gas or biomass. These three processes are called Coal-To-Liquids (CTL), Gas-To-Liquids (GTL) or Biomass-To-Liquids (BTL).

The fuel is ready for the present distribution net, which is a great advantage.

Furthermore FT diesel could be used as hydrogen source for fuel cell vehicles via on-board reforming. This is because it is free of sulphur.

FT also partly reduce local air pollution compared to diesel.

The FT production costs on a short term basis is about 2-4 times the production costs for fossil diesel and FT diesel also seems 40-50 percent more expensive than biomass derived methanol or hydrogen.[9]

FT from biomass can only become economically competitive when the oil prices rise significant or if political decisions prioritize the environmental benefits of green FT diesel.

To make the process competitive with diesel fuel the production needs to be at least 100-200 MWh input.[9]

Production efficiency is about 45%.[7]

1.1.6 Overview of production cost

Fuel	Production costs
Bio diesel	$4 - 4,42\ dkr/l$
1. generation Bio ethanol	3,5 dkr/l
2. generation Bio ethanol	$2,5 - 4,5\ dkr/l$
Biogas	$4dkr/l$
Methanol	$3 - 3,5\ dkr/l$
Fischer-Tropsch	$4,65 - 6,5\ dkr/l$

Table 1.1: Overview of cost effectiveness of alternative bio fuels.[4]

This overview of cost effectiveness of bio fuels is made to estimate at what price level bio DME is competitive with other bio fuels. Table 1.1 shows a price range of 2,5-4,5 dkr/l.

The costs in the overview is collected from a report done by the Danish Board of Technology which should be an objective evaluating.

For DME to be cost competitive in the general fuel market, plant capacities of 1-2 million t/y is needed[10]

1.2 Perspectives of DME

Even though DME is relatively new on global energy markets, it is already widely used. The first publications about DME was made in 1995 [11] and now 12 years later production facilities of DME is growing. China has large DME productions from coal and Japan has extensive production facilities based on natural gas (plants > 100.000 t/year [12]).
DME can be used as aerosol propellant, in gas turbines and for cooking and heating. But DME also has excellent combustion characteristics and is worldwide being tested as fuel. The many different ways that DME can be used and the fact that it can be produced in various ways makes studies of DME important.
First the different uses of DME is reviewed.

1.2.1 Aerosol propellant

Today DME is mostly used as an aerosol propellant in spray cans, inhalers etc. - about 150.000 t/y. DME can be used because it is neither toxic, carcinogenic or mutagenic. It is very volatile, which means that it has very little effect on surrounding environment. Furthermore is has a very low reactivity, short half-life period in the troposphere (easily degraded to water and carbon dioxide) and does not deplete ozone (unlike the previously used CFC gasses).[11][13]

1.2.2 Gas turbines

DME can be used in existing gas turbines with emissions and operating parameters similar to those of natural gas. Power generation efficiency is a little higher (1.6 - 2.8 %).[14]
Storage- and degassing costs are lower for DME than for LNG (Liquefied Natural Gas).[10]
DME has potential as gas turbine fuel at markets that cannot be reached directly by cheap natural gas suppliers (e.g. Japan, Korea and Taiwan). Bio DME production facilities are relatively simple and small, which gives even greater potential for niche markets not reachable with cheap natural gas.[14]

1.2.3 Cooking and heating

Open fires used for cooking and heating are not very efficient and pollutes a great deal more than burning gas, hence leading to a very unhealthy indoor climate. This is a big problem in the rural areas of the developing world. Indoor air pollution is the second largest environmental risk in causing premature mortality, WHO (World Health Organization) estimates that it annually results in 1.62 million premature deaths. The World Bank estimates health damage costs in China of 4 - 6 billion $ per year which is 35 - 100 $ per capita/year. Shifting to clean cooking fuels (e.g. DME or LPG - Liquefied Petroleum Gas) costs about 20 $ per capita/year. [15]
LPG is commonly used for both cooking and heating around the world. The properties of DME and LPG are somewhat similar. Hence 25-30% of the LPG can be substituted with DME and used in LPG appliances, such as a cooking heater, without any modifications. This is a very large potential marked for DME, especially in countries as China, India and Korea which all have rapidly increasing energy demands. The Japanese company JFE estimates the total DME demand of Asia to 38.6 million t/year in 2010. [10][11]
LPG prices follows oil prices closely, which means that higher oil prices leads to higher LPG prices. DME (from coal, natural gas or biomass) has potential to be cheaper and more available. Fossil resources are located at specific places, contrary to biomass that can be grown in several places. Because DME can also be produced from coal or natural gas, it can be produced more places in the world.[15]
Technologies developed to LPG can be used for DME transportation and storage with slight modifications to gaskets, seals and pumps. This already existing infrastructure would make an introduction of DME much cheaper and easier. Estimations of the capital investment (production plants and infrastructure) for DME introduction in USA is 4 billion $. In comparison capital investments for hydrogen is estimated to 18 billion $ and ethanol is 5 billion $.[16]
Cooking and heating devices can of course also be made to run solely on DME. This would however mean that new devices and bigger fuel tanks are needed, because of lower heating value.

1.2.4 Engine fuel

Diesel engines (CI engines - Combustion Ignition) operated on DME does not exhaust any smoke and particle emissions are therefore very low. The only particles emitted originates from the lubricating oil of the engine and not the DME. This is of course a great advantage since particles emitted from diesel engines are a great health concern. The absence of particles enables adjustments to minimize NO_x emissions, which is another health threat caused by engines. Emissions from diesel operated engines can be reduced with particle filters and NO_x absorbers. But with DME these can be spared making the CI engine operated on DME cheaper than a diesel engine with filters and catalysts, even though the DME fuel system is more expensive.[13]

Compared to emissions from standard diesel engines without filters and catalysts, DME performs much better. No smoke and NO_x reductions as large as 84%. But when the NO_x emissions are lowest, the CO emissions are very high. Therefore an oxidation catalyst is necessary to get acceptable CO emissions.[13]

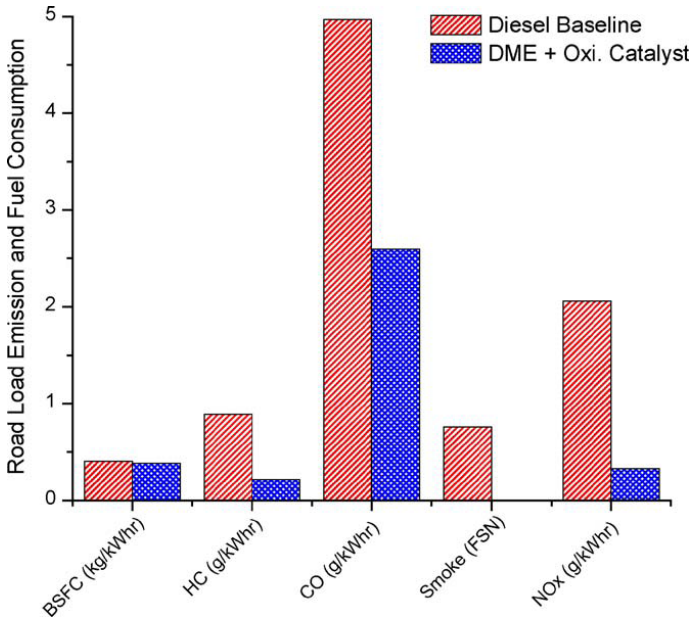

Figure 1.2: Engine emission[16] (Diesel baseline is a high quality diesel)

Figure 1.2 shows that emission are significantly lower for the DME operated engine, though the CO emissions are lowered by a catalyst.

Emissions can be reduced significantly if the diesel engine is equipped with a particle filter to remove particles, CO and HC (HydroCarbons) and a SCR (Selective Catalytic Reduction) catalyst to remove NO_x. But exhaust treatment can also be used to reduce emissions from DME engines even further (figure 1.3).

EGR (Exhaust Gas Recirculation) is an effective way to reduce NO_x emissions. DME operates better than conventional diesel with high levels of EGR, because of the oxygen contained within the DME molecule (table 1.2). This means that it is easier to fulfil emission standards at lower loads using DME as fuel.[11]

Furthermore DME contains no sulphur, which means SO_x reductions are 100%. Sulphur is damaging to catalysts in exhaust treatment systems. Therefore after treatment will be easier

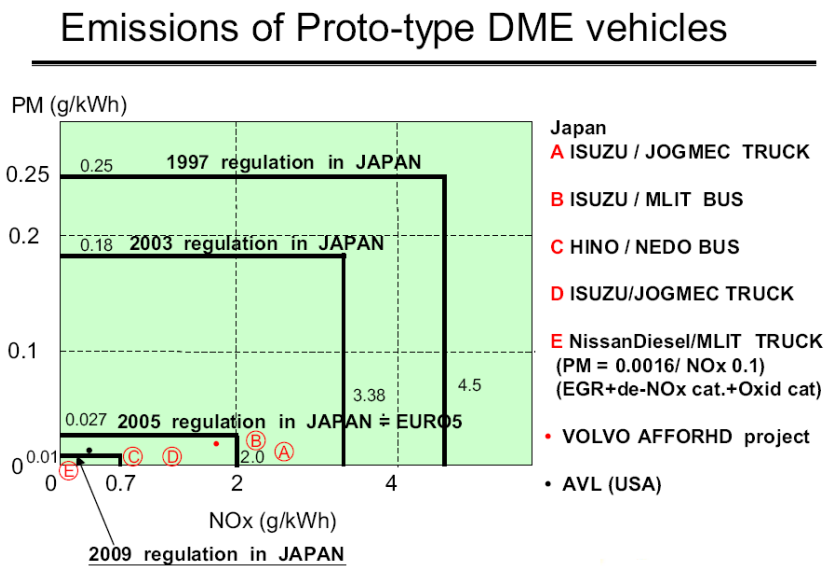

Figure 1.3: Emission standards and DME performance[11]

and more efficient.[7]

DME fuelled engines has greater output torque than diesel fuelled engines, especially at low speeds (figure 1.4). Since there is no smoke limitation with DME the power output can be increased by adding more fuel. This gives advantages to frequently starting and stopping and heavy-duty vehicles, for instance a city bus.[17]

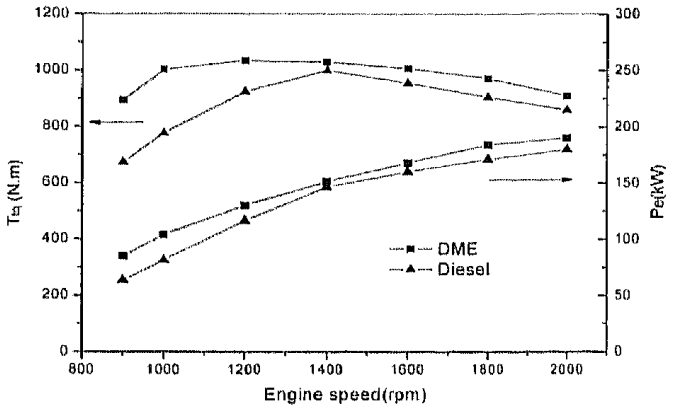

Figure 1.4: Torque and power at full load[17]

DME has a high cetane number, which means that it easily ignites when injected into the cylinder. This makes DME well suited for CI engines. This is fortunate since the CI engines has the highest efficiencies - about 30% better fuel economy than SI engines.[13]
Due to the high cetane number of DME it has lower pressure rise rate upon combustion than conventional diesel. This results in less noise than conventional diesel.

NO.	Item	Diesel	DME
1	The noise of accelerating outside engine dB(A)	82.9	80.8
2	Noise in bus dB(A)	80.8	76.4

Figure 1.5: Engine noise[17]

	unit	Diesel	DME
Chemical Formula	-	$C_nH_{1,8n}$	CH_3OCH_3
Molecular weight	g/mol	>120	46
Oxygen content	mass %	0	34,8
Stoichiometric air fuel ratio	kg/kg	14,8	9,1
Lower heating value	kJ/kg	42.500	28.800
Liquid density	g/ml at 15 °C	0,8 - 0,85	0,668
Boiling point	°C	>150	-24,9
Viscosity	$kg/(m \cdot s)$	2 - 4	0.122
Vapor pressure	bar	<0,01	5,1
Ignition temperature	°C	450 - 500	235
Cetane number	-	40 - 55	>>55

Table 1.2: Properties af typical diesel fuel og DME [6]

As examples on DME used in diesel engines several cases is worth mentioning. Students at DTU has in the last couple of years developed vehicles which operates on DME. These vehicles has won several first prizes in Shells eco-marathon, including driving the longest distance on what equates to 1 liter of gasoline.[18]

Volvo is developing heavy duty vehicles that operates on DME. From the technology roadmap from that project, it is seen that Volvo is focusing on doing large field tests of about 30 heavy duty vehicles until 2010 and having the vehicles ready for commercial sale after these tests.[19][11]

In China a fleet of DME city busses has been driving around Shanghai since 2006. Such a bus can contain 75 passengers and is free of smoke emissions.[12]

1.2.5 Other markets

DME can also be used to produce olefins (plastic). The demand for olefins is vast - about the same as for natural gas.[11]
In Moscow test are currently running on using DME as refrigerant, replacing fluoro-hydrocarbons for conservation of the ozone layer. DME can also be used as a resin foaming agent, replacing toxic chemicals. Japan is using DME for polystyrene foaming.[10]

1.2.6 Advantages

Bio DME production facilities are relatively simple (compared to eg. FT) and can vary in size. Economy of scale will enable big facilities to reduce production costs. Smaller facilities can produce the DME locally, create local workplaces and reduce transportation costs. The biomass can come from surrounding environment and the DME can be used in the local society. DME synthesis is very selective which means that the DME produced is very pure and there are no by-products.
If the facility is used as a combined heat/power station with fuel production the overall efficiency will be higher.
In comparison synthesis to liquid hydrocarbons yields a variety of by-products, from gasses to waxes. These products must be treated additionally in order to make usage of them. This results in big expensive facilities which must be very large in order to be profitable.

Production of DME from biomass has the highest efficiency compared to methanol, ethanol,

methane (biogas) and FT. All these efficiencies are reported in the same source[7] (except production efficiency of bio diesel, which is estimated from [5], Appendix A.0.1).
Fuels are often compared on well-to-wheel basis, which means the efficiency for the whole system (from feedstock to end use). As mentioned earlier DME is used in CI engines which have higher efficiencies than SI engines. The well-to-wheel efficiency is therefore highest for DME.

Fuel	Production	Well-to-wheel	Heating Value	Density
DME	55,0%	9,5%	28,8 MJ/kg	0,66 kg/l
Methanol	52,2%	9,0%	19,7 MJ/kg	0,79 kg/l
Biodiesel	40,2%	7,0%	39 MJ/kg	0,88 kg/l
Ethanol	44,9%	7,8%	26,8 MJ/kg	0,79 kg/l
Fischer-Tropsch	43,4%	7,5%	43,5 MJ/kg	-
Biogas	52,7%	7,2%	19,588 MJ/kg	-

Table 1.3: Production and well-to-wheel (conventional car) efficiencies of different biofuels.[7]

Another advantage with bio DME is that EU has exempted bio fuels from taxations since 2003. This is important for DME to be able to be price competitive in the future. It is however up to each country to implement this law.

1.2.7 Problems

As written above DME has many promising properties and uses, but there are some reasons why DME still is relatively unknown to the public.

- DME is a gas at normal temperature and pressure. Containers must be pressurized to get liquid DME. (see table 1.2)
- DME has lower heating value than diesel, which means more fuel is needed. (see table 1.2)
- The lubricity of DME is very low. This increases wear in e.g. fuel systems
- DME is very aggressive towards materials (especially rubber and plastic).
- Low viscosity can give leakage problems.

None of these problems are crucial, they just make the use of DME a little less attractive. The problems should be manageable: Lubricant additives can decrease wear, materials already exists that can withstand DME and leakage can be eliminated with proper manufacturing.

Infrastructure is a problem for DME. As mentioned earlier LPG infrastructure can relatively easy be modified to DME. But infrastructure is not build unless there is a market. A market needs enormous production facilities, which will not be made unless there is a market. This seems like a big problem, but the many uses of DME and the fact that it can be made from coal gives it some advantages. China has vast coal resources, but relies greatly on oil import. In 2004 42 % of domestic oil consumption in China was imported (122.7 mill. tons). DME can solve some of China's problems and major production facilities are being planned, installed or already up and running. Within the next 5 years DME production capacity in China will be 4-5 million tons per year. Here DME will be used in busses, for power generation and blended with LPG.[12]

Chapter 2

Theoretic model

2.1 Introduction

To be able to optimize the configuration of a bio DME facility a model is constructed. Different parameters can be changed in order to evaluate outcome, yield etc. This model will be compared to results from the existing methanol demonstration facility. The model will also play an important role in the upgrade of the facility from methanol to DME synthesis. The construction of a DME facility depends on the amount of DME in the gas after synthesis (section 2.3.5).

The model will be constructed in the equation program EES (Engineering Equation Solver). It will be simplified and only consider basic parameters within the facility.
EES can solve any number of equations with the same number of unknowns. It is important to define upper and lower limits of some of the variables in the model. Otherwise EES can get solutions with negative quantities of components for instance. Therefore all molar fractions are limited to the interval $[0; 1]$. Supplying EES with reasonable guesses of certain values can be necessary to get accurate results. EES contains a number of built-in functions to determined e.g. saturated pressure of a component.

The facility is originally designed to produce methanol from bottled gas. The facility has been upgraded to be able to run on synthesis gas from the Viking gasifier. The model was therefore first created for methanol synthesis and tested against experiments made on the facility (see section 3.5.3).
The model was then further developed to describe the DME synthesis. This model will be compared with results from the literature, because we had no time to upgrade the facility to DME production.
The DME model will be described in the following chapter. Since the methanol model is contained in the DME model, the description of the DME model will describe the methanol model meanwhile.

There are two different setups to produce DME in the facility.

1. Two reactors with different catalysts pills.
2. One reactor with mixed pills.

A model is created for both, and reviewed in section 2.4

These are the two main reactions for producing DME.[20]

$$3\,CO + 3\,H_2 \rightleftharpoons CH_3OCH_3 + CO_2 \tag{1.1}$$
$$2\,CO + 4\,H_2 \rightleftharpoons CH_3OCH_3 + H_2O \tag{1.2}$$

The two different reactions to produce DME uses different amounts of CO and H_2. Reaction (1.1) performs best with a H_2/CO ratio of 1, while reaction (1.2) prefers a ratio to be 2.
DME can be produced either by direct DME synthesis or by methanol dehydration. The catalysts used in this facility are for methanol synthesis (eq. 1.3) and methanol dehydration (eq. (1.5)).
The two reactions for DME production ((1.1), (1.2)) can be formed from the methanol synthesis, the water-gas-shift (eq. 1.4) and the methanol dehydration. Since the two main reactions are linear combinations of these three, the model will be based on these reactions.

$$CO + 2\,H_2 \rightleftharpoons CH_3OH \tag{1.3}$$
$$CO_2 + H_2 \rightleftharpoons CO + H_2O \tag{1.4}$$
$$2\,CH_3OH \rightleftharpoons CH_3OCH_3 + H_2O \tag{1.5}$$

Assumptions
Following assumptions are made in the model.

- Only the three reactions (eq. (1.3)-(1.5)) will be considered.
- Components not occurring in these reactions are inert.
- Stationary conditions.
- Thermal equilibrium
- Chemical equilibrium is assumed in reactors.
- Ideal gas behavior is assumed.

The argumentation for these assumptions are presented in the following section.

2.2 Argumentation for assumptions

The selectivity of the catalysts for methanol and DME synthesis is very high [21]. It is therefore considered unlikely that other reactions should occur.

Conditions in the facility are kept constant. Therefore there is no change in time and stationary conditions can be assumed.

Thermal equilibrium is assumed because heat transfer is not calculated. Temperature of the methanol synthesis is assumed to the same temperature as the gas out of the reactor.

Chemical equilibrium in the reactors must be assumed because the model do not calculate

reactions kinetics of synthesis processes. These calculations cannot be made because the kinetics for this specific catalyst are unknown. The assumption will be evaluated in later experiments (section 3.5.2).

2.2.1 Equation of state

Ideal gas behavior can normally be assumed at high temperatures and low pressures. Assuming ideal gas behavior neglects the volume of the molecules and the intermolecular forces.[22]
The question is, is this a reasonable assumption in this model?

Many improvements have been suggested to the ideal gas equation, to make it valid for real gasses. The first was the Van der Waal equation:

$$\left(P + \frac{a \cdot n^2}{V^2}\right)(V - nb) = nRT \tag{2.6}$$

The constants a and b are specific for each substance. The constant a accounts for intermolecular forces and b for the size of the molecules.
The range of applications of Van der Waals equation is however very narrow[23]. Therefore improvements have been suggested.

In mechanical engineering equations of state are based on enthalpy and are called Helmholtz type equations. These equations use a huge amount of experimental data to obtain reproducibility with a high precision. But this means these equations becomes very complex because there can be more then a 100 constants involved in the equation. This type of equation of state for DME has therefore not yet been reported in the literature.[24]

In chemical engineering the equations of state are based on a P-V-T relationship. Here pressure is given as a function of temperature and molar volume.[25] Compared with a Helmholtz type equation these equations are less reproducible for the various physical properties of a pure substance. But the constants for these equations can be calculated from some physical properties such as critical pressure and temperature. These equations can be used for a multi component system such as this DME system, because the needed constants are available[24] [25].
Therefore the focus for this report is equations of state which are based on a P-V-T relationship. Normally the pressure or compressibility type equations of state are divided into cubic, semi-empirical perturbed hard sphere, and virial expansion equations.
In the literature, the cubic equation is the most common for the prediction of phase equilibrium, therefore these are used in this report. [25][24]

The two most used cubic equation of state in the refinery and gas processing industries for the prediction of vapor-liquid equilibria is the Peng-Robinson (PR) and the Soave-Redlich-Kwong (SRK). These are widely used because of their simplicity and accuracy. The difference between these are negligible (cf. Figure 2.1) [26]

SRK is primarily used in Europe and PR in USA. Use of the SRK equation (eq. 2.7) will be investigated.
SRK

$$P = \frac{RT}{v - b} - \frac{a}{v^2 + bv} \tag{2.7}$$

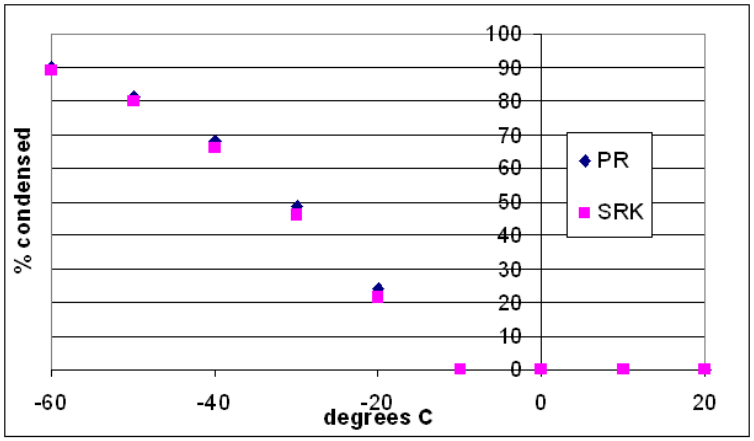

Figure 2.1: Comparison of the SRK and PR equation of state. Calculated with the SPECS program (App. B.0.2)

where

$$v = \frac{V}{n}$$

When applied to mixtures the constants a and b are found from the quadratic mixing rules. Mixing rules for vapor mixtures of C components are [23]

$$a = \sum_{i=1}^{C} \left(\sum_{j=1}^{C} y_i y_j (a_i a_j)^{0.5} (1 - k_{ij}) \right) \tag{2.8}$$

$$b = \sum_{i=1}^{C} y_i b_i \tag{2.9}$$

The k_{ij} is a binary interaction coefficient that describes the interaction between 2 specific components, and is determined from experiments. The term k_{ij} has been added as an error correction because the model does not perform accurately at all times. This correction is small with simple and alike components (like H_2 and N_2) and can then reasonably be assumed to be 0. But especially polar molecules (like H_2O and CH_3OH) gives larger values of k_{ij}. The SRK equation of state should perform better than the ideal gas equation, even when values for k_{ij} are not know.[27]

Because the syngas contains fairly many components these calculations will be quite complicated.

The k_{ij} values for DME and some of the other mixes of components in the system do not exist in the literature. It was possible to find the k_{ij} values listed in table 2.1, the values not found are assumed 0.

The deviation when the k_{ij} values are added to the SRK equation of state is evaluated. Figure 2.2 shows calculations made with the program SPECS of a gas with very high DME content. The difference is very small.

Components	CO	CO_2	N_2	H_2	H_2O	CH_4	CH_3OH	CH_3OCH_3
CO	0	0	0.0374	0.0919	0	0.0322	0	0
CO_2	0	0	-0.315	-0.3426	0.0737	0.0933	0.0141	0
N_2	0.0374	-0.0315	0	0	0	0.0278	-0.2141	0
H_2	0.0919	-0.3426	0	0	0	-0.0222	0	0
H_2O	0	0.0737	0	0	0	0	-0.0789	0
CH_4	0.0322	0.0933	0.0278	-0.0222	0	0	0	0
CH_3OH	0	0.0141	-0.2141	0	-0.0789	0	0	0
CH_3OCH_3	0	0	0	0	0	0	0	0

Table 2.1: The available k_{ij} values from the literature[28]

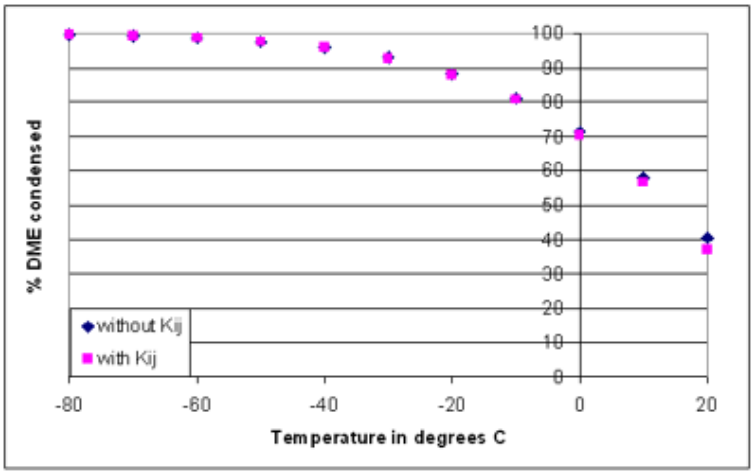

Figure 2.2: The deviation with and without k_{ij} values.

2.2.2 Fugacity

A way to control whether the ideal gas equation applies in a particular situation, is to examine the fugacity of the gas. The physical interpretation of fugacity would be the tendency of a component to escape i.e. how likely is the molecule to flee from one phase to another.
The equilibrium constant is given by

$$K = K_\phi K_y P^\nu \tag{2.10}$$

where

$$\nu = \sum \nu_i \quad ; \quad K_\phi = \prod \phi_i^{\nu_i} \quad ; \quad K_y = \prod y_i^{\nu_i} \tag{2.11}$$

ν is called the *stoichiometric coefficients* and is the numbers of molecules in the reaction. They are negative for reactants and positive for products.[25]
i.e. equilibrium constant for reaction 1.3 becomes

$$K = \frac{\phi_{CH_3OH}}{\phi_{CO}\,\phi_{H_2}^2} \frac{y_{CH_3OH}}{y_{CO}\,y_{H_2}^2} \frac{1}{P^2}$$

For ideal gasses the fugacity $K_\phi = 1$. Then the equation becomes equal to equation (3.34) which is derived later and is based on ideal gas behavior.

At the facility entry the pressure and temperature is near atmospheric, and ideal gas behavior can reasonably be assumed.

The synthesis of methanol and DME occurs in the reactors at temperatures around 250 °C and pressures from $40 - 50$ bar. Ideal gas behavior can normally be assumed at high temperatures and low pressures. The fugacities are examined to check if ideal gas behavior can be assumed.

The vapor phase fugacity (ϕ_i) of a component in a mixture is given by[29]

$$ln(\phi_i) = ln\left(\frac{V}{V-b}\right) + \frac{b_i}{V-b} - ln(Z) + \frac{ab_i}{RTb^2}\left(ln\left(\frac{V+b}{V}\right) - \frac{b}{V+b}\right) - \frac{2\sum_j y_i a_{ij}}{RTb} ln\left(\frac{V+b}{V}\right) \tag{2.12}$$

With the compressibility Z given by

$$Z = \frac{V}{V-b} - \frac{a}{RT}\left(\frac{1}{V+b}\right) \tag{2.13}$$

The fugacity of each component is calculated using the program SPECS (results are shown i App. B.2). The enthalpy of the components in the syngas is calculated for a typical mixture at 250 °C and 40 bars.

Component	Enthalpy
CO	1,0192
H_2	1,0171
CH_4	1,0090
H_2	0,9606
N_2	1,0195
CO_2	0,9984
CH_3OH	0,9714
CH_3OCH_3	0,9896

Table 2.2: Enthalpy calculated with SPECS

Values of K_ϕ (see eq. (2.10)) for reactions (1.3)-(1.5) are calculated

$$K1_\phi = 0,9380 \tag{2.14}$$
$$K2_\phi = 0,9641 \tag{2.15}$$
$$K3_\phi = 1,0073 \tag{2.16}$$

These values does not deviate much from one. Using the found fugacity coefficients as an extra term in the ideal gas equation does not make sense. Either equation (eq. 2.10) is used with fugacity calculations and the SRK equation of state or else ideal gas behavior must be assumed[27]. As the fugacity coefficients are close to one, assuming ideal gas behavior seems reasonable. Equilibrium calculations using SRK equation and fugacity will become much more complex. It is important to investigate if such extensive calculations are needed, or if other insecurities of the model makes ideal gas assumption sufficient.
The ideal gas assumption will be compared with SRK calculations in section 2.5.

2.2.3 Vapor liquid equilibrium

The ideal gas equation of state is used when all the components are in a gaseous phase. But after the synthesis reactions, the methanol and DME needs to be condensed in order to separate the fuel from the syngas. Therefore both gas and liquid volumes will be present at the same time.
The high pressure is maintained and the temperature is lowered to condense as much fuel as possible. High pressures, low temperatures and components in 2 phases are normally conditions where the ideal gas equation does not provide very accurate results.

As mentioned in section 2.2.2 the fugacity coefficient is a way to verify if the ideal gas is a good assumption. If the fugacity coefficient for the different components deviates from one, the ideal gas assumption is not very good.[27]

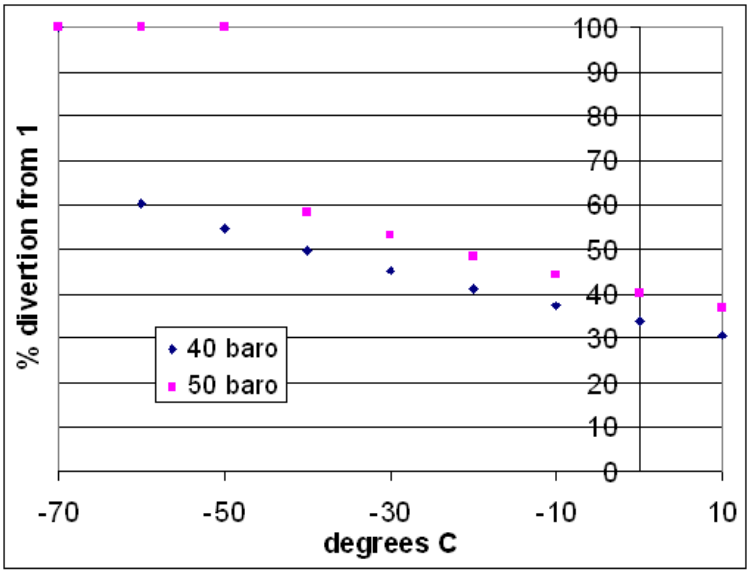

Figure 2.3: The deviation of fugacity coefficients at different temperatures and pressures

Figure 2.3 shows that lower temperatures and higher pressures increases the fugacity deviation from one, and making ideal gas assumption less accurate.
The SRK equation of state will used to calculate the vapor liquid equilibrium during the condensation process. These calculations are made with SPECS. (App. B.0.2)

2.3 The model step by step

2.3.1 Gas composition

Measurements of gas composition is given in volume%. Since ideal gas behavior is assumed the volumes of the molecules is neglected. Therefore the composition on molar basis becomes the same as the volume based composition.
Molar fractions are given by

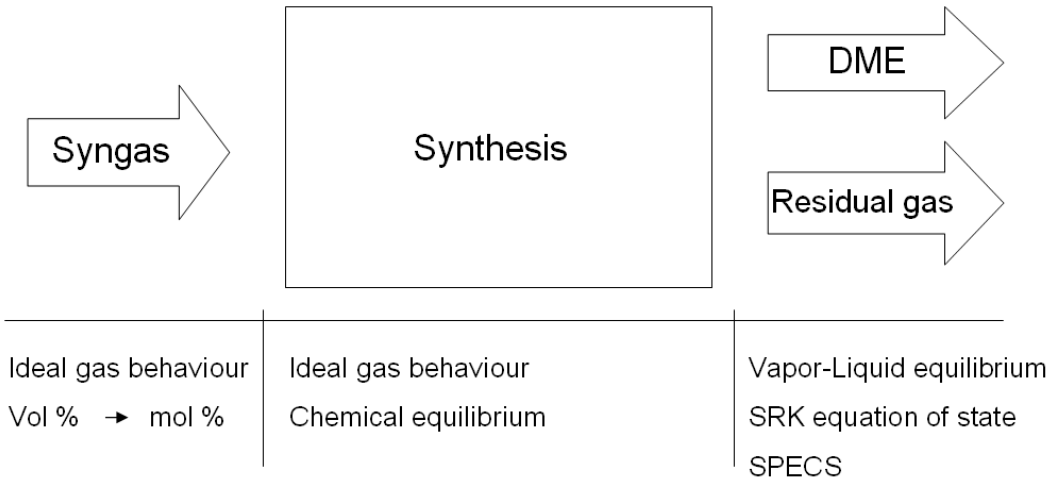

Figure 2.4: Process diagram of DME facility model

$$y_i = \frac{n_i}{n_{tot}} \tag{3.17}$$

The equilibrium calculations in the model are based on one mole of wet gas. Hence the number of moles of the specific component are calculated from.

$$n_i = y_{i,dry} \cdot n_{tot,dry}$$

with the total number of moles on dry basis is derived from

$$n_{tot,wet} = n_{tot,dry} + n_{H_2O} = 1$$

Values of $y_{i,dry}$ are found from gas composition measurements. Only CO, CO_2, H_2 and CH_4 are measured.
As water is not included in the measurements this must be added. It is assumed that the gas is saturated with water in the NH_3 scrubber (section 3.3.4). Temperature is measured in the NH_3 scrubber and saturation pressure of water at this temperature is found using the function incorporated in EES. The ideal gas equation is used to calculate the number of moles of water vapour.

$$n_{H_2O} = \frac{p_{sat,H_2O}}{p_{tot}} n_{tot,wet}$$

The rest of the gas is assumed to be N_2.
The molar fractions on wet basis equals the number of moles because the total number of moles on wet basis is defined as 1.

2.3.2 Compressor

Work done by the compressor is calculated from enthalpy of the gas before and after compression. This is found with the build in enthalpy function in EES. Given the temperature or internal energy this function returns the specific enthalpy of the given substance assuming ideal gas behavior. The enthalpy of the gas can then be calculated.

$$h_{gas} = \sum_{i=substance} h_i \cdot y_i \tag{3.18}$$

By assuming ideal gas behavior, constant specific heats, the efficiency of the compressor η_c and the specific heat ratio γ, the temperature after compression can be determined.
Isentropic compression gives[30]:

$$T_{after,s} = T_{before}\left(\frac{p_{after}}{p_{before}}\right)^{\frac{\gamma-1}{\gamma}} \tag{3.19}$$

$$T_{after} = T_{before} + \frac{T_{after,s} - T_{before}}{\eta_c} \tag{3.20}$$

The enthalpy function can now be used to find the enthalpy after compression with the use of the temperature.
The first law of thermodynamics can now be used to find the work done by the compressor. Steady state is assumed and kinetic and potential energy is neglected. An adiabatic compression gives following revised first law[30].

$$\dot{W}_c = \dot{m}(h_{after} - h_{before}) \tag{3.21}$$

But since EES returns the enthalpy's in $\frac{J}{mol}$ the equation becomes

$$\dot{W}_c = \dot{n}(h_{after} - h_{before}) \tag{3.22}$$

2.3.3 Synthesis

As mentioned in section 2.1 the model is based on equilibrium of these three reactions.

Methanol synthesis:

	CO	$+$	$2H_2$	$\rightleftharpoons$	CH_3OH
$before:$	n_{CO}		n_{H_2}		0
$after:$	$n_{CO} - x$		$n_{H_2} - 2x$		x

Gas-water shift:

	CO_2	$+$	H_2	$\rightleftharpoons$	CO	$+$	H_2O
$before:$	n_{CO_2}		n_{H_2}		n_{CO}		n_{H_2O}
$after:$	$n_{CO_2} - y$		$n_{H_2} - 2x - y$		$n_{CO} - x + y$		$n_{H_2O} + y$

DME synthesis:

	$2CH_3OH$	$\rightleftharpoons$	CH_3OCH_3	$+$	H_2O
$before:$	x		0		$n_{H_2O} + y$
$after:$	$x - 2z$		z		$n_{H_2O} + y + z$

The equilibrium equations (eq. (1.3-1.5)) leads to the following equations

$$n_{CO,after} = n_{CO} - x + y \tag{3.23}$$
$$n_{H_2,after} = n_{H_2} - 2x - y \tag{3.24}$$
$$n_{CO_2,after} = n_{CO_2} - y \tag{3.25}$$
$$n_{CH_3OH,after} = x - 2z \tag{3.26}$$
$$n_{H_2O,after} = n_{H_2O} + y + z \tag{3.27}$$
$$n_{CH_3OCH_3,after} = z \tag{3.28}$$

x,y and z are constants indicating how many moles of each substance reacts.
Every time a process takes place and DME is formed methanol must first be produced. This consumes 2 moles of gas every time one mole methanol is produced (eq. (1.3)). The number of moles are the same after the DME synthesis since 2 moles of methanol produces 1 mole of DME and one of water (eq. (1.5)). Hence conservation of matter gives the following equation:

$$n_{after} = n_{before} - 2x \tag{3.29}$$

Three equations are needed to calculate the three constants x,y and z. These equations comes from the equilibrium assumption.
The equilibrium constants can be described by the partial pressures of reactants and products. Given the equation

$$aA(g) \rightleftharpoons bB(g) \tag{3.30}$$

The equilibrium constant becomes[22]

$$K_p = \frac{P_B^b}{P_A^a} \tag{3.31}$$

Equilibrium constant for equation (1.3) then becomes

$$k_1 = \frac{p_{CH_3OH}}{p_{CO} \cdot (p_{H_2})^2} \tag{3.32}$$

Ideal gas behavior is assumed. The ideal gas equation gives

$$k_1 = \frac{\frac{n_{CH_3OH}}{V}RT}{\frac{n_{CO}}{V}RT \cdot (\frac{n_{H_2}}{V}RT)^2} = \frac{n_{CH_3OH}}{n_{CO} \cdot (n_{H_2})^2} \frac{1}{(\frac{RT}{V})^2} \tag{3.33}$$

The equation for molar fraction (eq. (3.17)) and ideal gas equation is used to simplify expression

$$k_1 = \frac{y_{CH_3OH}}{y_{CO} \cdot (y_{H_2})^2} \frac{1}{(\frac{n_{tot}}{V}RT)^2} = \frac{y_{CH_3OH}}{y_{CO} \cdot (y_{H_2})^2} \frac{1}{p^2} \tag{3.34}$$

The calculations of k_2 and k_3 are similar and gives

$$k_2 = \frac{y_{CO} \cdot y_{H_2O}}{y_{H_2} \cdot y_{CO_2}} \tag{3.35}$$

$$k_3 = \frac{y_{CH_3OCH_3} \cdot y_{H_2O}}{(y_{CH_3OH})^2} \tag{3.36}$$

The molar fractions used in eq. (3.34)-(3.36) are all after the reaction. These are called $y_{i,after}$ in the model.

The equilibrium constant for a given reaction can be found from equilibrium constants for the formation reactions [30]. The expression for linear combination of reactions is used to find expressions for the equilibrium constants.

$$log(K) = \sum_{i=1}^{C} \nu_i \, log(K_{i,f}) \tag{3.37}$$

Hence the expression for reaction (1.3) becomes

$$log(K) = log(K_{CH_3OH,f}) - log(K_{CO,f}) - 2\, log(K_{H_2,f}) \tag{3.38}$$

Values for log(K) can be found from a NASA database[31]. This database provides thermodynamical properties for a large amount of substances over a wide range of temperatures, the data used can be found in appendix B.0.3.

To find an expression for the calculated values of the equilibrium constants an exponential regression was made . These expressions are very accurate for the short data range $(500K - 540K)$ with $r^2 > 0.999$ (see figures 2.5-2.7).

$$K_1 = 1,7938 \cdot 10^7 \, e^{-0,04374\,T} \tag{3.39}$$
$$K_2 = 1,0851 \cdot 10^{-6} \, e^{0,01764\,T} \tag{3.40}$$
$$K_3 = 2878,3 \, e^{-0,00970\,T} \tag{3.41}$$

These expressions are compared to expressions found in the literature[20].

$$K_1 = e^{(21,225+(\frac{9143,6}{T})-7,492 \cdot ln(T)+4,076 \cdot 10^{(-3)} \cdot T-7,161 \cdot 10^{(-8)} \cdot T^2)} \tag{3.42}$$
$$K_2 = e^{(13,148+(\frac{5639,5}{T})-1,077 \cdot ln(T)-5,44 \cdot 10^{(-4)} \cdot T+1,125 \cdot 10^{(-7)} \cdot T^2+\frac{49170}{T^2})} \tag{3.43}$$
$$K_3 = e^{-2,205+\frac{2708,6317}{T}} \tag{3.44}$$

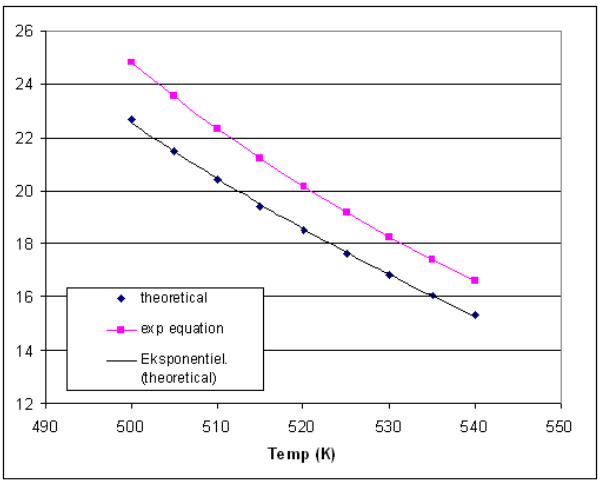

Figure 2.5: values of k1

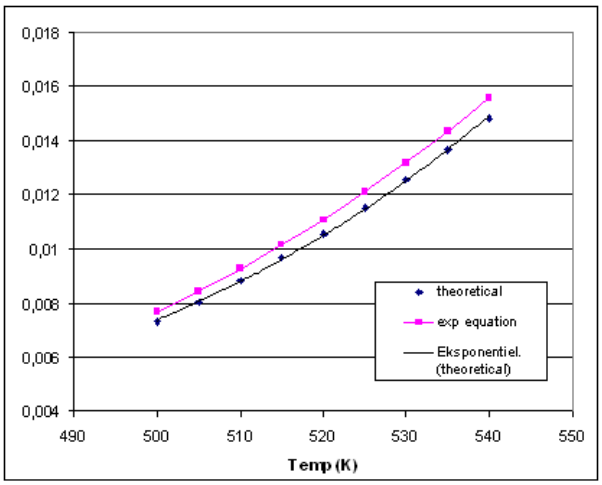

Figure 2.6: values of k2

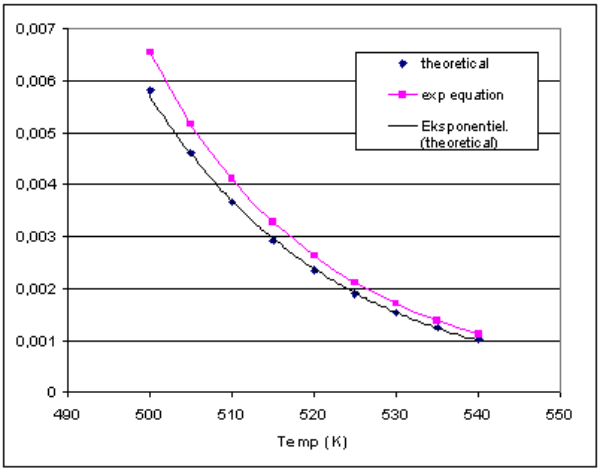

Figure 2.7: values of k3

The expressions used by Henrik Iversen in his Master Thesis (eq. (3.42)-(3.44)) are called exp. equations in the figures 2.5-2.7. The expressions calculated in this report gives lower values of the equilibrium constants. This means that the model will calculate a little bit lower yields with the same conditions (about 7,5 %). A Preliminary test (App. C.1) indicates that the model calculates much higher yields than what is actually measured from the facility. As the values from the expressions derived in this report (eq. (3.39)-(3.41)) gives lower yields, it could seem that these new expressions are a little more accurate.

Another report[32] reports a lower value of K_3 (section 2.5). The calculated value from yet another report is used for comparison. A programme called ASPEN calculated the following values for equilibrium concentrations at 523 K and 36 bar.[33]

$$\begin{aligned}[CH_3OCH_3] &= 0,068\\ [H_2O] &= 0,068\\ [CH_3OH] &= 0,017\end{aligned}$$

The equilibrium constant equation (concentrations can be used instead of partial pressures - equation (3.36) returns

$$K_3 = \frac{[CH_3OCH_3][H_2O]}{[CH_3OH]} = \frac{0,068^2}{0,017^2} = 16$$

The exponential regression (eq. 3.41) returns $K_3 = 18$. This is accepted as a verification of the exponential regressions derived in this report (eq. 3.39-3.41). These will be used in the model.

The number of moles of the products can now be determined from the equilibrium constant equations ((3.34)-(3.36)) and the equilibrium equations ((3.23)-(3.28)).
The molar fractions, after equilibrium is obtained, are determined from equation (3.17).

2.3.4 Flows

The model requires input of volume flow or the volume of the residual gas. The latter is measured by a gas meter, which is temperature compensated. The measurements are given in Nm^3 following the DIN 1343 standard, meaning that the volume of the gas is corrected to 0 °C (273,15 K). Therefore the molar flow is calculated by following ideal gas equation.

$$\dot{n}_{res.gas} = \frac{p_{atm} \cdot \dot{V}_{in}}{R \cdot 273,15\ K} \tag{3.45}$$

With p_{atm} being the pressure at the gas measurement (atmospheric), and R being the gas constant.

Molar flow after equilibrium

$$\dot{n}_{after} = \dot{n}_{in} \cdot n_{after} \tag{3.46}$$

n_{after} is found with equation (3.29)
Molar flows of components can now be calculated

$$\dot{n}_{i,in} = y_{i,in} \cdot \dot{n}_{in} \tag{3.47}$$

$$\dot{n}_{i,after} = y_{i,after} \cdot \dot{n}_{after} \tag{3.48}$$

2.3.5 Condensation

The condensation process is a bit complicated. How much gas will condense is a result of vapor-liquid equilibrium. Ideal gas equation is normally said to have errors around 10-15 % within the 2 phase area[26]. Therefore the more advanced SRK equation of state is applied. We have chosen to do so with the use of the SPECS program. Unfortunately the SPECS calculations cannot be incorporated in the EES model.
In the EES model condensation are calculated from saturation pressure of the components and the ideal gas equation. Results from the 2 different methods are compared.

SPECS
The input in SPECS is the composition, temperature and pressure of the gas and if possible values for k_{ij} (see section 2.2). SPECS then returns the molar fractions of each component in every present phase. For additional info on SPECS see appendix B.0.2.
The gas composition after synthesis is found from the EES model, this means that the only difference between the results from SPECS and the model will be the condensation process.

EES
The build in EES function P_SAT yields the saturation pressure of a given substance at a given temperature. Assuming that this pressure is due to the amount of gas that will not condense at the given temperature, the number of moles on gaseous form are found from the ideal gas equation.

$$\dot{n}_{i,res.gas} = \frac{p_{i,sat}}{p} \dot{n}_{after} \tag{3.49}$$

The amount of the component that is condensed

$$\dot{n}_{i,cond} = \dot{n}_{i,after} - \dot{n}_{i,res.gas} \tag{3.50}$$

An IF sentence is used in the programming to ensure that if the molar flow in the residual gas is higher than the molar flow produced by the reactions, then the condensed molar flow is 0 rather

than negative ($\dot{n}_{i,res.gas} > \dot{n}_{i,after}$ then $\dot{n}_{i,cond} = 0$).
EES has thermodynamical data for many substances but not for DME, hence another way of expressing the vapor pressure must be used. The Wagner equation gives the vapor pressure of a substance as a function of temperature. The error is reported to be less than 1% and temperature range is larger than for the model itself.[29]

$$ln(p_{vp,r}) = \frac{a\tau + b\tau^{1.5} + c\tau^3 + d\tau^6}{T_r} \tag{3.51}$$

where

$$\tau = 1 - T_r \quad ; \quad T_r = \frac{T}{T_c} \quad ; \quad p_r = \frac{p}{p_c} \tag{3.52}$$

This gives

$$p_{vp} = e^{\frac{a\tau + b\tau^{1.5} + c\tau^3 + d\tau^6}{T_r}} \cdot p_c \tag{3.53}$$

The critical temperature and pressure and the constants a,b,c and d for DME can all be found in the litterature[29].

Comparison
First the condensation percentage of methanol at methanol synthesis is calculated. The gas composition used is the typical values from the Viking gasifier, however with assumptions of CO_2 percentage reduced to 4 % and the gas saturated with water vapor at 10 °C (this compares to the gas composition after cleaning devices).

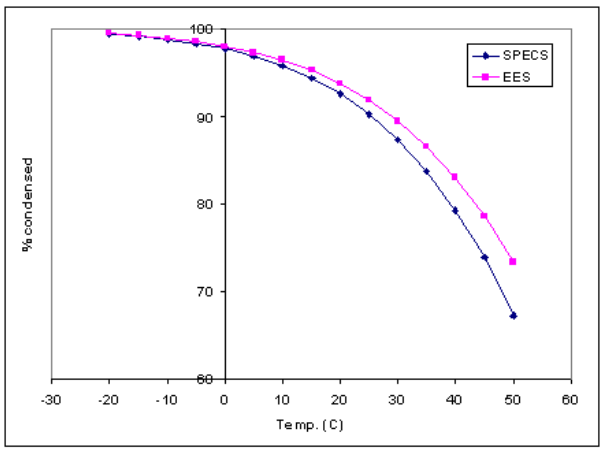

Figure 2.8: Calculations of % methanol condensed at different temperatures

Figure 2.8 shows that the values calculated with SPECS are slightly lower than the results from the model. The difference is however nowhere near the reported 10-15 %. At condensation temperatures of 20 °C the difference in the two calculations is 1,3 %. Considering the assumptions and uncertainties within other parts of the model the calculations in EES proves to be accurate enough. There is no need to use SRK when calculating methanol condensation.
Because DME is a gas at normal temperature and pressure the condensation of DME occurs at much lower temperatures. The results of SPECS and EES are compared once again (figure 2.9). The 2 different compositions comes from the 2 different DME scenarios with separate synthesis (mix1) or mixed pills (mix2). Mix 1 contain 4,67 % DME and mix 2 contain 9,14 %. (For total gas composition see Appendix B.2)
The difference between the calculations are still small, but it appears that this difference increases with higher DME percentages.

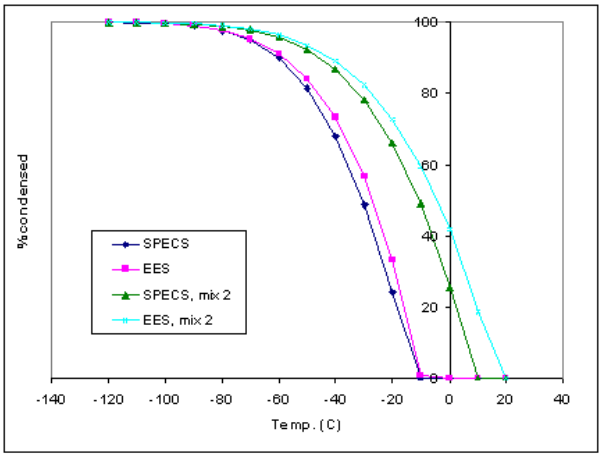

Figure 2.9: Calculations of % DME condensed at different temperatures

When concentrations of DME are higher, the temperatures needed to condense the DME are higher as well. This is because the partial pressure of the DME increases. This is an important factor to consider.

2.3.6 Yield and selectivity

The yield and selectivity are important parameters in the synthesis of methanol and DME. Yield is in this report defined as the amount of fuel compared to the initial CO content of the syngas, i.e. how much CO has reacted to fuel.

$$Y_{met} = \frac{n_{met,after}}{n_{CO,in}} \cdot 100\% \tag{3.54}$$

$$Y_{DME} = \frac{2 \cdot n_{DME,after}}{n_{CO,in}} \cdot 100\% \tag{3.55}$$

$n_{DME,after}$ is multiplied with 2 because it takes two CO molecules to form one DME molecule (see equations (1.3) and (1.5)).
Selectivity is defined as the amount of fuel per reacted CO molecule.

$$S_{DME} = \frac{n_{DME,after}}{n_{CO,in} - n_{CO,after}} \cdot 100\% \tag{3.56}$$

$$S_{DME} = \frac{2 \cdot n_{DME,after}}{n_{CO,in} - n_{CO,after}} \cdot 100\% \tag{3.57}$$

It should be noted that there are different definitions of yield and selectivity in the literature. Therefore care must be taken when comparing these with results from other reports.

2.3.7 Heating value

When evaluating efficiencies it is important to know the inputs and outputs of the facility. But because this is a demonstration facility there has been little or no focus on these efficiencies. For instance is the power consumption of the heat blowers not included anywhere. The focus of this report is proving the concepts of producing methanol and DME from biomass. The model does however calculate heating values of the syngas feed and the residual gas.

The heating value at a given temperature can be calculated from the build in enthalpy function in EES.
As an example, the reaction for complete combustion of H_2 is:

$$2\,H_2 + O_2 \rightarrow 2\,H_2O \tag{3.58}$$

The combustion is assumed to be a stationary flow process with no changes in potential and kinetic energy, hence the net calorific value can be determined from the enthalpy of the components.[30]

$$h_i^0(H_2) = \frac{1}{2}(2\,h^0(H_2) + h^0(0_2) - 2\,h^0(H_2O)) \tag{3.59}$$

This gives the net calorific value in kJ/mol. If the unit kJ/kg is needed the value can be divided with the molar mass M (g/mol).
Net calorific values for H_2, CO and CH_4 are determined this way. This way the energy within the syngas feed can be determined.
Table values are used for net calorific values for methanol and DME. Since the goal is to use DME and methanol as fuel or something alike, it makes sense to use the table values.

Calculating the input power, the different efficiencies of the facility can be estimated.

$$P_{in} = \sum_{i=1}^{C} \dot{n}_{i,in} \cdot H_{u,i} \tag{3.60}$$

$H_{u,i}$ is the net calorific value of component i.
A fuel efficiency for the production would be

$$\eta_{fuel} = \frac{P_{fuel}}{P_{in}} \tag{3.61}$$

2.4 Weaknesses of the model

As mentioned earlier does the model only take some aspects of the synthesis into account. Chemical equilibrium is assumed within the reactors because the model does not take reaction kinetics into account. This assumption is evaluated with experiments in section 3.5.2.
Furthermore the model does not view the activity of the catalysts. The methanol and DME synthesis are active at relatively low temperatures, and higher conversion efficiencies can be reached by lowering the temperature which will shift the equilibrium towards higher fuel production. However the catalysts activity suffers at lower temperatures. The catalysts has higher activity at higher temperatures[21]. This means if the temperature is too low the synthesis will not occur because the activity of the catalyst are too low. But if the temperature is too high the synthesis will not occur because the synthesis reactions will stop. Hence balancing the temperature between high selectivity and high activity gives the highest yield (figure 2.11). The model however does not take the activity of the catalysts into account. Therefore the model will get higher and higher yields when lowering the temperature.
Another temperature related effect not regarded in the model is sintering of the catalysts. If temperatures are to high sintering will deactivate the catalysts. The effects of sintering are beginning to show at temperature higher than 275 °C[34].

There are other parameters than temperature affecting the activity of the catalysts. It is reported in the literature that small amounts of CO_2 increases the speed of the methanol synthesis up to a 100 times[21].

On the other hand can addition of to much CO_2 also be a problem. The water gas shift reaction formes water by reacting CO_2 and H_2. Large amounts of CO_2 will form large amounts of water. Water lowers the activity of the catalysts by blocking the active sites of the catalysts[34].
As reaction speed and activity is not considered in the model neither of these effects are taken into account.

The two different models of a DME facility are created because there are 2 ways of constructing such a facility. Either the methanol and DME catalysts can be mixed to complete the DME synthesis all at once. Otherwise one reactor can be used for methanol synthesis and then another separate reactor for the DME synthesis.
If the catalysts are mixed the equilibrium yield will be higher. The methanol synthesis is limited by equilibrium, the DME production removes methanol at the same time methanol is produced. Because the methanol synthesis is still active more methanol will be produced which means more DME in the output.
The activity of the catalysts can however become a problem. Mixed in one reactor the temperature is the same for methanol and DME synthesis. The literature reports a temperature range for methanol synthesis of 220-300 °C[20]. The catalysts are supplied by Haldor Topsøe, who suggests a synthesis temperature of 260-350 °C for DME synthesis. Because activity is not evaluated in the model, the mixed pills model will probably give results of yield and outcome that are too high. Section 3.6 shows how sensitive the synthesis process is to changes in temperature.
In reality the temperature selected in the reactor with mixed pills will probably end up with a compromise between methanol and DME synthesis.
In two separate reactors optimum temperatures for each synthesis can be used.
Which solution is the best cannot be determined with this model, experiments are necessary.

2.5 Comparison with literature

The model is compared to two studies found in the literature.

- Theoretic analysis that is using the SRK equation of state for equilibrium calculations[32]
- A series of experiments concerning the effects of operating conditions on the DME synthesis.[34]

2.5.1 SRK equation of state

?? In the argumentation (section 2.2.1) we found that the ideal gas equation was sufficient for the equilibrium calculations. In another study the same SRK equation of state has been used to calculate the equilibrium. No experimental data is known, hence values for k_ij are all 0. Values of equilibrium constants in that study are calculated with a equilibrium program programmed by Dr. Yamazaki. These values are compared to the values calculated in section 2.3.3.

	This report	SRK report
K_1	0,00208	0,00211
K_2	0,01102	0,01161
K_3	18,027	3,959

Table 2.3: Comparison of equilibrium constants at T = 523 K

The values for K_1 and K_2 are very close, but K_3 is different. It is difficult to comment on this difference, since we have no access to the calculations used in the SRK report. The calculations in this work are described and verified in section 2.3.3. The point of this comparison is solely to evaluate the ideal gas assumption against the theoretical more accurate SRK equation.

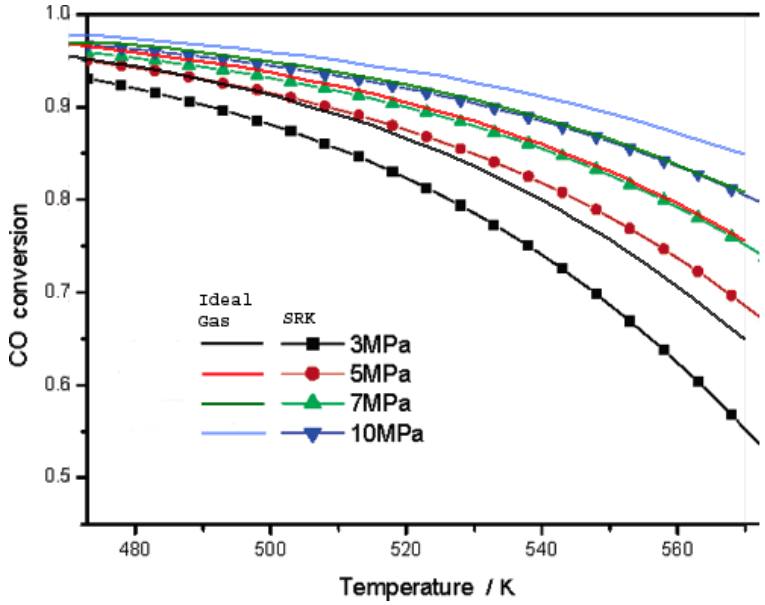

Figure 2.10: CO conversion at different temperatures with SRK or ideal gas equation

Figure 2.10 shows a graph from the SRK report[32] with a similar graph constructed from the mixed pills model from this report on top. The axis uses same scale and the two graphs has been fitted so the values coincide. The curves look the same, but the results of this work are higher than the SRK report. It must be added that if lower values of K_3 are used in the model from this report the curves will move downward.
Because the parameters used in the equations are not exactly the same, it can be hard to conclude much. But it can be seen that the results obtained by the two different methods are not far from each other. The error within the pressure and temperature intervals of this report (40-50 bar; 503,15-543,15 K) looks to be less than 10%. Compared to other sources of error and the accuracy of the model this is acceptable (see section 3.5.3)
Unfortunately the comparison cannot be used to evaluate at which conditions the ideal gas assumptions is best. In theory SRK and ideal gas should be closest at low pressures and high temperatures, but the difference in K_3 can easily disguise this.

2.5.2 Activity

As mentioned in section 2.4, activity of the catalysts are not a part of the model. Experiments of DME synthesis has been carried out at the University of Pais Vasco in Spain[34]. The gas composition and other parameters are not evident in the report which makes direct comparison impossible. But tendencies can be seen and assumptions evaluated.

The affects of catalyst activity becomes obvious when watching figure 2.11 and 2.12. When temperatures are to low the synthesis stops, which cannot be seen in the model. This is an important factor to consider. The model states that the lower temperature the better, which clearly is not the case. The comparison is only interesting from above 275 °C.

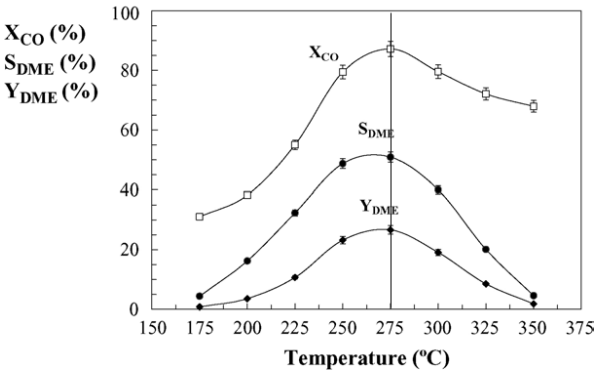

Figure 2.11: Experimental data from the litterature[34] (X_{CO} is CO conversion)

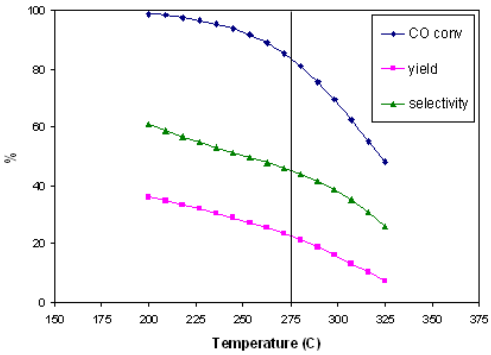

Figure 2.12: Simulation from this report

It should be noted that the experimental report uses different definitions of selectivity and yield.

$$S_{DME} = \frac{2 \cdot n_{DME,after}}{n_{CH_4,after} + 2 \cdot n_{DME,after} + n_{CH3OH,after} + (n_{CO,in} - n_{CO,after}) + (n_{CO_2,in} - n_{CO_2,after})} \cdot 100\%$$

$$Y_{DME} = \frac{2 \cdot n_{DME,after}}{n_{CO,in} + n_{CO_2,in}} \cdot 100\%$$

Figure 2.12 is constructed from the model with these definitions of yield and selectivity for the sake of comparison.
When the temperatures gets higher the synthesis stop because of thermodynamic restrictions as described in section 2.4. The decrease in yield at higher temperatures can also be contributed to sintering of the catalysts, which lowers the activity.[34] This affect is neither taken into consideration in the model.

2.5.3 Review

When considering the limitations of the model it perform well. The results are very close to the theoretical better SRK model (figure 2.10).
Apart from the lack of catalyst activity the model results resemble the experimental data (figures 2.11, 2.12).
When using the model it is very important to know its limitations. But with these considered, the model can help predict tendencies and make decisions about design and configuration.
Section 3.5.2 compares the model with experiments and in section 3.7 the model is basis for decisions about further developments of the facility.

Chapter 3

Experiments

3.1 Method of measurements

The methods for the different measurements is described in this section.
The data processing is primary done in Excel, but also in the EES model and the SPECS program.

3.1.1 Gas analysis

The gas analysis uses different metering methods to measure the different components. CO_2, CO and CH_4 with the NDIR method, H_2 with a thermal conductivity measure and O_2 with a paramagnetic measurement[35]. The gas analysis is calibrated before use with a known gas. The gas composition is monitored by a program called Labview. (cf. Figure 3.1)

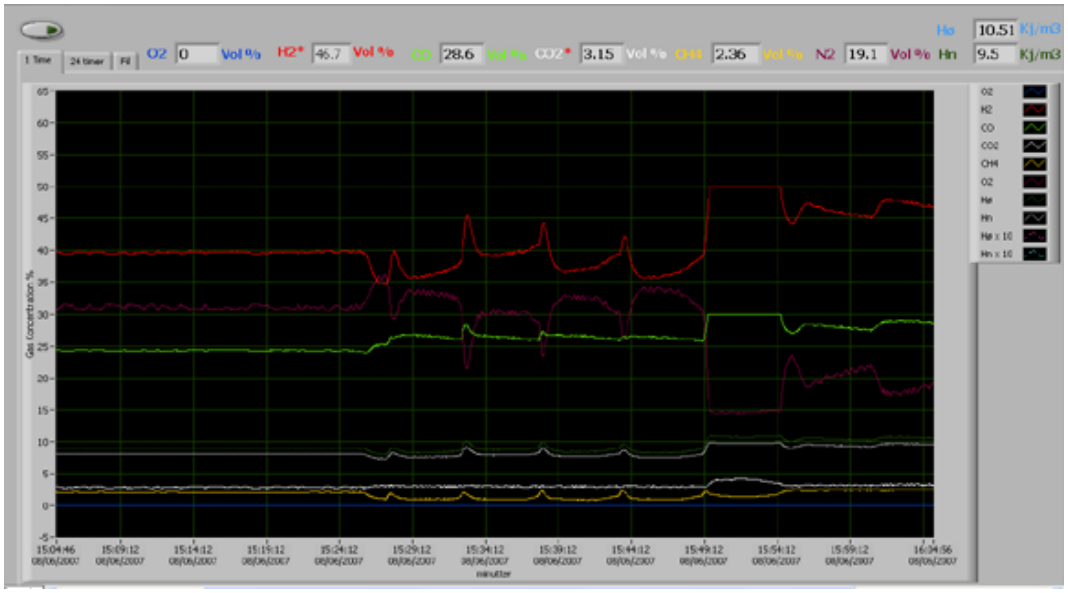

Figure 3.1: Monitoring the gas composition

Gas analysis was done three places in the experiments. The gas compositions was collected every minute with Labview.
In experiments with syngas from the Viking gasifier, gas analysis was made before the cleaning devices, after the cleaning devices and of the residual gas.
In experiments with bottle gas, gas analysis was made after the gas mixer, after the first volume meter and of the residual gas.

The gas analysis delivers the data in dry vol%. This is fine because the water vapour content in the gas is not interesting for the calculations.

For further use of these data the average value for the most stable periods is calculated in Excel.

The gas analysis do not measure the nitrogen content, but all the other components. Therefore the amount of nitrogen is calculated with molar fractions as:

$$y_{N_2} = 1 - y_{CO} - y_{CO_2} - y_{CH_4} - y_{H_2}$$

3.1.2 Pressure

The pressure in the experimental workshop was collected online from DMI (The Danish Meteorological Institute). Data from different monitoring stations around DTU was evaluated and a proper average value was used. The deviation between the different monitoring station was minimal.

A liquid manometer is installed over the CO_2 scrubber to check for choking. This is a absolute pressure measurement.

On the output of the facility a manometer measures the output pressure. This is also a absolute pressure measurement.

On the first volume meter a manometer is installed which can measure both positive and negative pressure. This proofed to be very important for leakage detection in the cleaning devices (cf. section 3.4).

3.1.3 Volume

The volume readings is done at the beginning and at the end at each experiment.

The two metering devices is a Gallus 2100 TCE. Which is a mechanical diaphragm gas meter that is temperature compensated (see figure 3.2).

The output is temperature adjusted to the DIN 1343 standard (0 °C - 1 atm)

Because the flow meter needs to by adjusted to the specific gas composition and the pressure drop, the flow meter is only used for adjusting the flow not to collect data (se figure 3.3).

3.1.4 Temperature

For temperature measurements thermo elements of the type K is used. They consist of the conductive materials nickel and chrome wrapped in a stainless steel jacket. These measurements is taken every second. When used for calculations an average value was calculated in Excel. The temperature in the experimental workshop was also collected with a thermoelement.

Figure 3.2: The volume meter

Figure 3.3: The flow meter

All of these data are handled in a the software program Labview. Labview makes it possible to create a specific program completely adjusted to this facility. With this program it is possible to monitor all the actual temperatures (see figure 3.4 and 3.5), the changes in the different temperatures and the changing gas composition.

There is a overview table in Appendix C.3 of all the thermoelements.

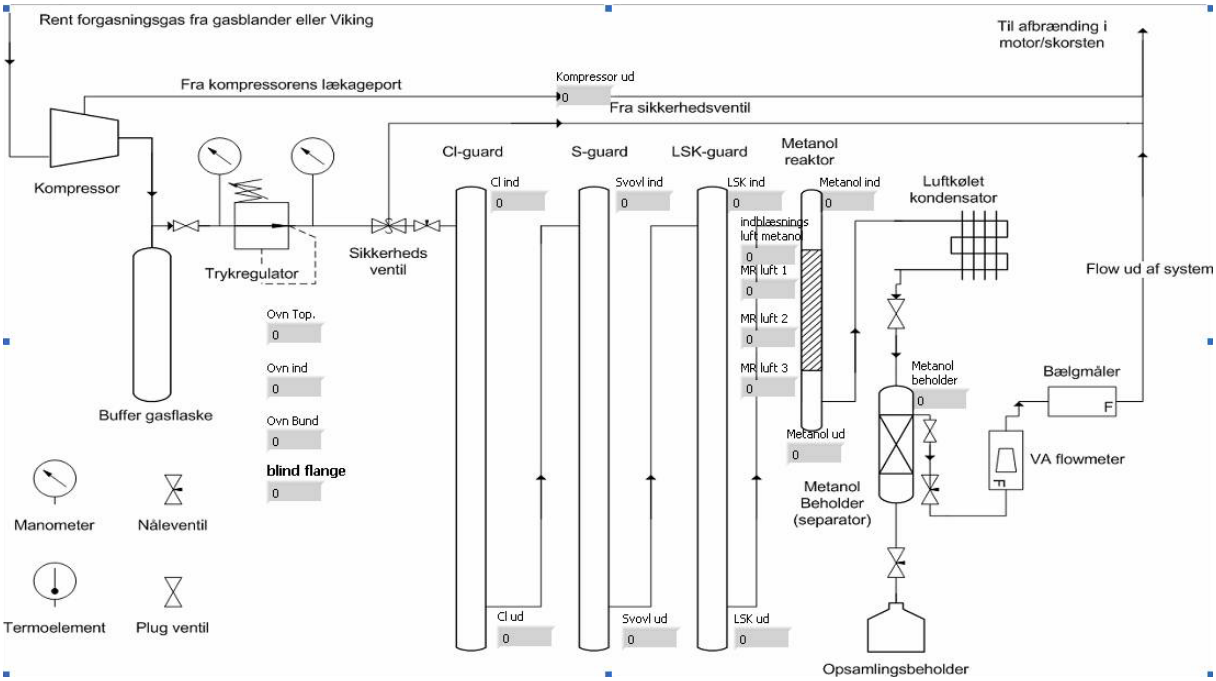

Figure 3.4: Temperature overview of the main facility

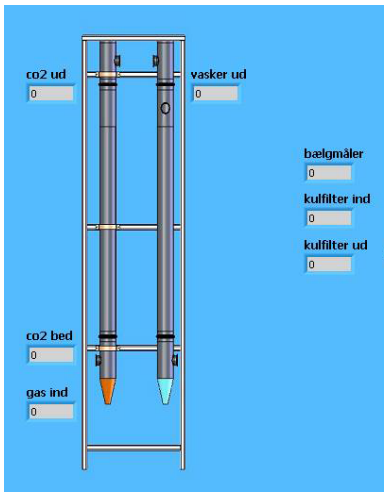

Figure 3.5: emperature overview of the CO_2 srubber and the NH_3 washing tower

3.1.5 Verification of methanol

Because Haldor Topsøe did not actively participate in the project and DTU do not have the facilities to analyze the condensable parts the only test made was a burning test. Henrik Iversen produced verified methanol from the same catalysts pills with the same conditions, it is therefore assumed that the condensed liquid has the same composition as the one Henrik Iversen obtained, which contained about 88% methanol, 4% water and 8% other components.

3.2 Facility Description

The goal is to make a facility where it is possible to reform syngas from the Viking gasifier to methanol and DME. This is a demonstration facility so the modifications are often the fastest, easiest and most practical solutions. It is important that many parameters easily can be adjusted.

A facility that can produce methanol from bottled gas has been further developed. This facility was constructed by Henrik Iversen for his exam project on DTU. Henrik Iversen successfully produced methanol from bottle gas. In his report he described some changes that needs to be done so his facility can use syngas from The Viking gasifier.
We have incorporated some of these changes and added others.

In order to upgrade the facility from bottled gas to gasified syngas, some cleaning is necessary. The challenge was to integrate some devices that can remove certain components or lower their percentage of the syngas. This is necessary to ensure high efficiency and because the catalyst used to produce methanol and DME are very sensitive.[20]

The catalysts are supplied by HTAS (Haldor Topsøe A/S) and there is no description of what these catalysts can tolerate or data concerning acticity.
From the literature it is known that it is necessary to clean the gasified biomass from NH_3, CO_2, tar, sulphur and other particles.[20]

The syngas provided from the Viking gasifier has the following composition.

The syngas is really clean compared to syngas from other gasifiers (the tar content is very low). This makes it realistic to produce bio DME directly from syngas.[20]

Gas component	CH_4	CO	CO_2	H_2	$N2$
Percentage	1,56 %	13,87 %	17,48 %	24,04 %	43,06 %

Table 3.1: The gas composition in percent from the Viking gasifier

3.2.1 Test run

Before we changed the existing facility a test run was made to ensure that the facility still was able to produce methanol from bottle gas and that the facility have not suffered any damaged since it was last used.

The facility was held under operational pressure (40 baro) for 48 hours. The facility had no leakage. The actual test run was made from bottled gas mixed with a gas mixer. (see C.1) for more data) From this test run it was concluded that the facility still was able to produce methanol (sec. 3.1.5).

3.2.2 Short facility description

The syngas from the Viking gasifier is cleaned in four separate cleaning devices for NH_3, CO_2, tar and sulphur.

After these cleaning devices the syngas is led to a compressor that compresses the syngas to about 40 to 50 baro.

The main facility is a big oven. The temperature is adjusted to the wanted temperature with 4 heat blowers. Then the syngas is let through three cleaning devices a Cl-, S- and LSK-guard before it is let into the methanol reactor. It is in the reactor the synthesis takes place.

After the reactor the condensable parts are condensed by cooling the gas.
The residual gas consists primarily of unreacted syngas and uncondensed methanol.

Figure 3.6 is an overview of the facility and figure 3.7 shows a picture of the actual facility.

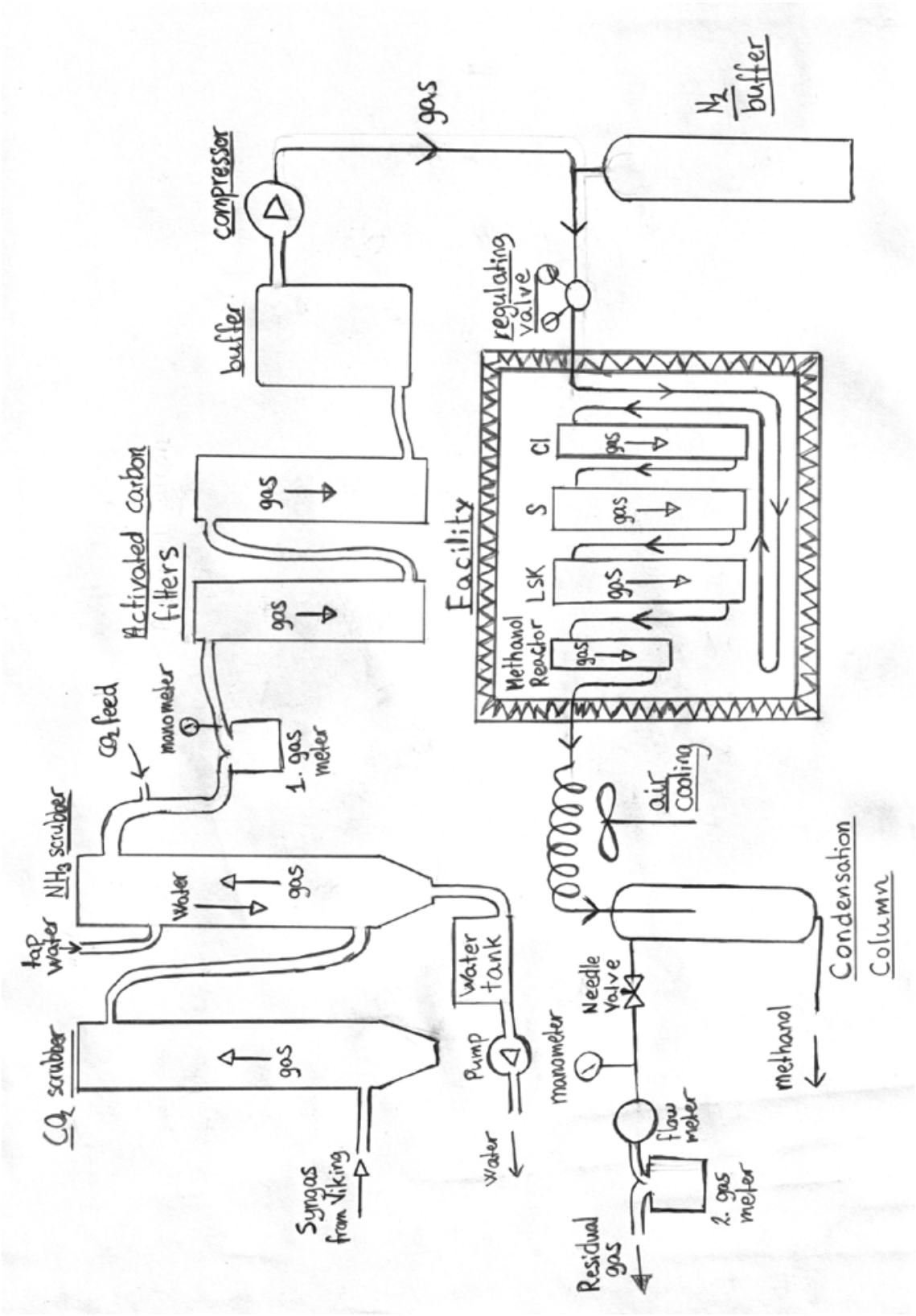

Figure 3.6: Schematic drawing of facility

Figure 3.7: The actual facility

3.3 Detailed facility description

3.3.1 The Viking gasifier

This is a fixed bed co-flow gasifier based on a two-step process, where the pyrolysis and gasifier is spilt in the separate units. (cf. figure 3.8) [20]

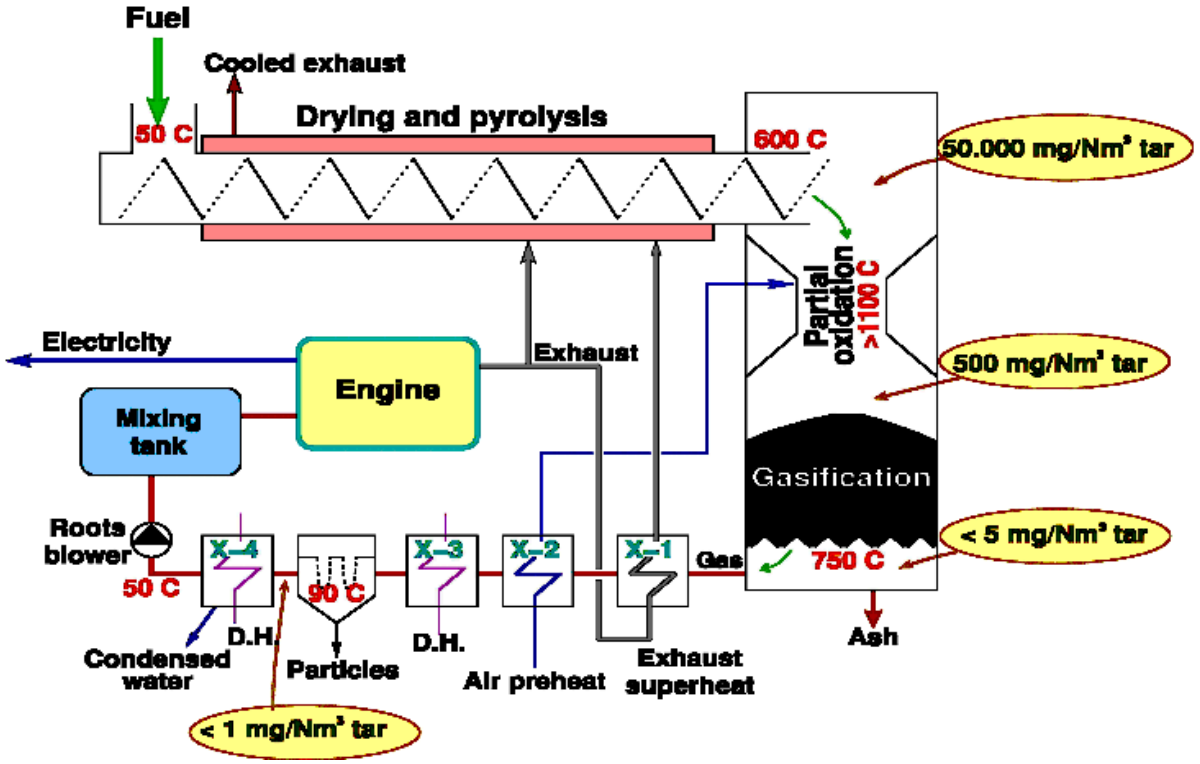

Figure 3.8: System overview of the Viking gassifier

3.3.2 Cleaning devices

The product gas from a biomass gasifier contains different components that needs to be removed before used in a synthesis facility. These components are particles, alkali connections, tar, sulphur and chlorine.

There are some basic technologies to remove the unwanted components.

Particles can be removed with cyclones, bag filters for low temperatures, ceramic filters for high temperatures, electrostatic filters and water based scrubbers.

Tar can be removed by physical- or catalytic process or by thermic destruction.

Physical removal contains water based scrubber, oil based scrubbers and electrostatic filters

Destruction of tar can be done with high temperatures (about 800 C) or by thermic cracking at temperatures over 1300 C.

Ammoniac can be removed by washing with water while sulphur connection and chlorine is removed by passing absorbers. [20]

3.3.3 The CO_2 scrubber

This cleaning device removes all the CO_2 from the syngas using pills of potassium hydroxide. The gas comes in at the bottom and rises to the top. The gas is heated with a burner to above 100 °C. The reaction with the CO_2 produces water. The gas is heated to evaporate this and prevent the potassium hydroxide from turning into a paste. A manometer is installed to monitor if the potassium hydroxide blocks the pipe.
The NH_3 scrubber installed after the CO_2 scrubber lowers the temperature after the heating.

3.3.4 The NH3 cleaner

A washing tower is used to remove ammonia from the syngas. The syngas enters at the bottom of the washing tower and rises up. In the top of the washing tower a nozzle head sprays pure tap water in a 60 degree angel. The tower is filled with plastic fillers. This set-up makes the water trickle downwards and gets mixed with the gas. The plastic fillers generates a large surface area and because ammonia is easily dissolved in water the ammonia is removed from the syngas. The water is picked up in a reservoir. This reservoir is connect to a pump that operated by a floating switch. When the reservoir is full, the pump will start. The water in the reservoir enables operating pressures different than those of the surrounding.
To ensure that the water does not travels with the gas as little drops, several layers of filtering elements (demister) and sleeve are placed in the top of the cleaning device. All of this is held back with a grate.
Figure 3.9 shows a picture of the CO_2 and the NH_3 scrubbers.

3.3.5 CO_2 adjustment

CO_2 is added to the syngas. This is because there needs to be a little CO_2 in the gas for optimal conditions for methanol synthesis. How much CO_2 is needed is uncertain but the literature suggests 4-8 %.[21]. It was easier to add some CO_2, rather than constructing a bypass on the

Figure 3.9: The CO_2 scrubber is on the left and the NH_3 scrubber on the right. The reservoir and pump are in the foreground

Figure 3.10: The activated carbon filters.

Figure 3.11: The pump to ensure high flow

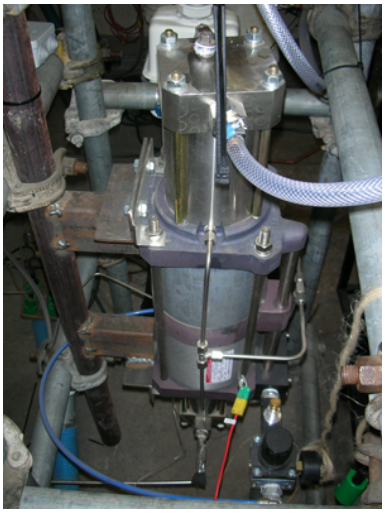

Figure 3.12: The compressor

CO_2 scrubber. The addition of CO_2 is easily controlled, which is important if experiments concerning the CO_2 content is to be carried out.

3.3.6 Pump and activated carbon filters

The gas from the NH_3 scrubber is cooled and saturated with water. A pump is installed before the activated carbon filters to raise the pressure to about 1-2 baro. This will increase the temperature and thereby preventing water from precipitating in the filters. The pump is important because it ensures that it is possible to operate with high flows (see section 3.3.8).

There are two activated carbon filters. The first one removes tar components from the gas and the other removes sulphur. The carbon particles are small and form a large surface area that makes it possible to remove larger particles as tar and sulphur. One could consider having a filter to avoid carbon dust trough the facility.

3.3.7 Buffer container

A buffer container ensures that there is always syngas to feed the compressor. Because the gas is completely mixed, gas analysis can be made from this tank. A tap is installed on the buffer container to enable emptying to the outside surroundings.

3.3.8 Compressor

The compressor (figure 3.12) is driven by pressurized air. It is possible to adjust how fast the compressor works, and at what outlet pressure it should stop. If the syngas is not pressurized before entering, then the compressor cannot deliver flow higher than 1,5 Nm^3/h at 40 bar.

3.3.9 N_2 buffer tank

The pressurized N_2 buffer tank is filled with compressed nitrogen at high pressure (40 - 50 baro) and works as a buffer to ensure a continual pressure and flow through the facility. Without it the pressure would change with the compressor rhythm of work. The buffer container is also very important concerning safety. Because the facility is running at pressurized flammable gasses, a safety plan is important. If any internal reactions should go out of control it is possible to turn off the syngas feed and scavenge the facility with nitrogen from the buffer container. The nitrogen is inert and will therefore neutralize the reactions out of control. The temperature can of course always be turned off, but the reactions inside the oven are exothermic and therefore it is not enough to turn off the heat.
The syngas will inevitably mix a little with the nitrogen. This means that the nitrogen content in the facility may be a little higher than measured before the compressor and that the emergency scavenging gas is not completely inert.

Figure 3.13: The buffer tank

Figure 3.14: Pressure controller and plug valve

3.3.10 Regulating valve

A plug valve after the container can close the flow from the compressor and container. A regulating valve after the plug valve adjusts the pressure in the facility (cf. figure 3.14). It is important that the pressure on the compressor side of the valve is high enough to deliver the proper test pressure. If the compressor cannot handle the flow through the facility this pressure will slowly drop. Because of the large volume of the N_2 buffer tank it can take a while before this pressure drop is registered.

3.3.11 Safety valve

A safety valve ensures that the facility pressure does not exceed a certain limit. The safety valve is adjusted to 54 baro. The safety valve is connected to the ventilation.

3.3.12 The main facility

Inside the oven the syngas is heated in 4 meters of pipe before entering the first reactor

Figure 3.15: The inside of the facility

The first reactor is a Cl guard which removes chlorine compounds. The reactor is filled with scrub material in pill form. The syngas goes into the Cl guard from the top and comes cleaned out trough the bottom.

Then the syngas is led trough two more reactors, a S-guard and a LSK- guard. The only

difference of the three reactors is the cleaning material. The S-guard removes sulphur compound and the LSK- guard is a thorough clean-up device that withhold different compounds that did not get removed from the first two devices.

Then the syngas is led to the methanol reactor for the methanol synthesis. This reactor is smaller than the three cleaning devices but is constructed the same way. The methanol reactor is filled with pills of catalyst material. This material catalyze the methanol synthesis when the syngas passes. This process is exothermic. It is not know exactly which catalysts the reactors contains.
To have an optimal methanol synthesis the temperature is really important. Therefore an air-cooled jacket around the methanol reactor is installed. A heat blower makes it possible to adjust the temperature for the methanol reactor separately. This also secures that the convection on the methanol reactors surface increases because of the air stream. 6 different thermoelements monitor the temperatures in the reactor. Inlet- outlet and blower temperature is measured as well as the temperature 3 places on the reactor surface.

Figure 3.16: The methanol reactor

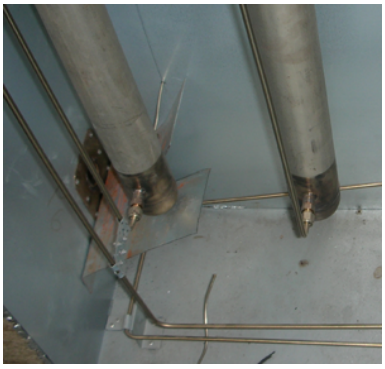

Figure 3.17: The metal sheet for better mix of heat flows in the oven.

It was seen in the test run, that the difference in temperature in the top and the bottom of the oven was about 15 °C. A piece metal sheet was inserted at the entry of the lower heat blower next to the Cl guard (see figure 3.17. This metal sheet gives a better mix of the heat in the oven. After this modification the difference in temperature was about 2 °C.

3.3.13 Gas mixer

Because the cleaning devices did not work properly (see section 3.4), the test with different flows was made with bottled gas. To obtain the proper gas for the testing, a gas mixer was used. The gas mixer recieves gas feeds from the 5 wanted gases N_2, CO, CO_2, CH_4 and H_2. These gas containers, except N_2, is fixed on a platform with metal chains. N_2 comes from a larger container outside and is delivered with a rubber hose. The flow from each container is registered with 5 flow meters and adjusted with needle valves. The 5 different gas feeds is mixed in a buffer container on the back of the gas mixer. A pressure switch and a electromagnetic valve opens and closes for the gas flow to the buffer container depending on the pressure within the buffer container. To ensure supply, the pressure from the gas containers needs to be higher than the pressure in the buffer container. The gas from the buffer container is choked to just less than 1 baro before going through the gas meter before the compressor because the gas meter cannot tolerate high pressures.

Figure 3.18: The front of the gas mixer

Figure 3.19: The back of the gas mixer

It is almost impossible to adjust the gas mixer to the proper gas mix with the needle valves and the 5 different flow meters. An outlet before the buffer container enables the use of the gas analysis to tune the gas composition to the desired mix. This makes the adjustment much easier, but it is still dificult to get exactly the wanted composition.

3.4 Practical

The practical aspects of the project is described in this section. Unfortunately many practical problems delayed the time scheduled and therefore made it impossible to fulfil the original plan for this project.

3.4.1 DME reactor

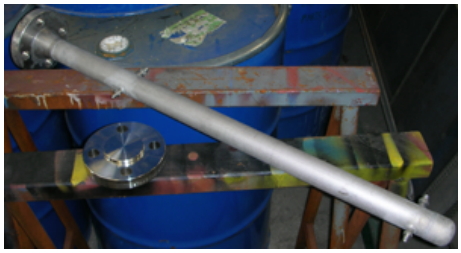

Figure 3.20: The DME reactor

To produce DME it was necessary to get an extra reactor because it was not certain that a mixture of methanol and DME catalysator pills in one reactor would work. The plan was to produce methanol in the first reactor and then DME in the second reactor (sec. 2.4)

Because the operational pressure is around 40 baro the welding on the DME reactor needs to be specially certified. DTU do not have this kind of certification so this job was done outside of DTU. A stainless steel tube and a flange was bought at Sandvik Materials Technology and send to C.E Andersen Machinery Factory for certificated welding.

3.4.2 DME catalyst pills

To produce DME it was all-important to have some DME catalyst pills. These were to be delivered by Haldor Topsøe but this process was unfortunately delayed and it was uncertain if the pills would be received before the paper had to be turned in. But after many mails and conversations the catalyst pills arrived 3 weeks before our report deadline. Sadly the pills were never used because other problems occurred.

3.4.3 The Viking gasifier

The first time the new cleaning devices were to be tested, the Viking gasifier had a operational stop because of some instability. This caused the time schedule to move about an extra week.

After these problems was fixed the cleaning devices were to be tested with syngas directly from the Viking gasifier. But it turned out that the gas feed from the gasifier was not present. The rubber hose that leads the syngas to the cleaning devices was checked, but the hose had no leakage. Then it was checked if the gasifier could deliver enough pressure to lead the gas to the cleaning devices. This was not the problem either. Finally it was realized that the valve that controlled the gas flow from the gasifier was clogged. Another valve was found to lead the syngas to the cleaning devices and this worked.

A gas analysis of the syngas was made. Unfortunately the syngas contained oxygen. This is a problem because the syngas is flammable and will be pressurized and heated in the facility. The test of the cleaning devices was cancelled once more because the source of the oxygen had to be located. First the rubber hose that leads the syngas from the gasifier to the cleaning devices was changed to make sure that it was leak-free. This was however an unlikely source of the oxygen because the gasifier delivers the syngas with some positive pressure.

Next the cleaning devices where checked. When there where negative pressure in the system the oxygen amount was rising which meant that the cleaning devices had a leak. Foam and traceable gas was used to find the leak. Two leaks was found in the washing tower, one in the CO_2 scrubber and one at a thermoelement. These leaks were errors in some weldings to fixate a grid inside the cleaning devices. The first leakage was welded again and the two others was fixed with aluminum tape due to lack of time. The thermoelement was tightened.

But these repairs did not remove the oxygen from the gas so the oxygen could only enter somewhere in the gasifier. It turned out that a flexible pipe section was leaking, which meant that the oxygen could enter. This pipe section is flexible to allow for heat expansion. The flexible pipe section was cut out and a inflexible pipe section was welded on instead. In order to keep the flexible properties, a heat exchanger was unbolted at the top and allowed to move in the longitudinal direction of the pipe. The top was still fixed in the other directions.

The reason why the flexible pipe section was leaking, was that when the gasifier is shut down it will slowly cool down which makes some water from the syngas condense. This water combined with ammonia and different salts from the syngas made the stainless steel pipe section corrode. This is showed on Figure 3.21

Figure 3.21: The corroded pipe section

3.4.4 Gas pump

During the tests to find the leaks the gas pump (see Figure 3.11) to increase the pressure after the first flow meter and before the compressor, stopped working. This pump had been cleaned and tested before use. The pump could not deliver enough pressure, so the sealing was changed to a stiffer one, because the current sealing had moved a little bit. This new sealing solve the problem, but after 10 minutes the pump burned out. This meant the experiments had to be done without this gas pump because it was not possible to get another one before deadline. This meant that the flow through the facility was limited.

3.4.5 Cleaning devices

The CO_2 scrubber quickly stopped working (described in section 3.5.1). It was know from tests that the reaction between CO_2 and potassium hydroxide formed water. The idea was that heating the gas would evaporate this water, and prevent a paste of potassium hydroxide and water to form. But when the CO_2 scrubber was dismantled is was clear that this did not work. The potassium hydroxide had become liquid and floated through the grid to hold it in place. At the bottom of the CO_2 scrubber, the heater had dried the substance to a solid block. The syngas enters above this block and no more CO_2 was removed from the gas. Figure 3.23 shows the bottom of the scrubber. In the middle the thermoelement to monitor temperatures can be seen.

The NH_3 washing tower is connected to a buffer tank with a pump that leads the water away from the facility in into the drain. See Figure 3.9.

This pump is controlled by a floating device that is activated when the buffer container is filled with water. During the first test with syngas directly from the gasifier a malfunction in the washing tower caused the gas meter and the first activated carbon filter to become flooded. The floating device was suspected to have caused the flood and the buffer tank was tilted so the water easily could activate the pump. The gas meter was dried and the activated carbon exchanged.
Demister and sleeve in the top of the washing tower was supposed to prevent little drops of water to travel further in the system. If these blocked the tower, water could be pulled up from the tank through a little hose originally installed to even out pressure. The sleeve was removed to be sure the tower is not blocked.

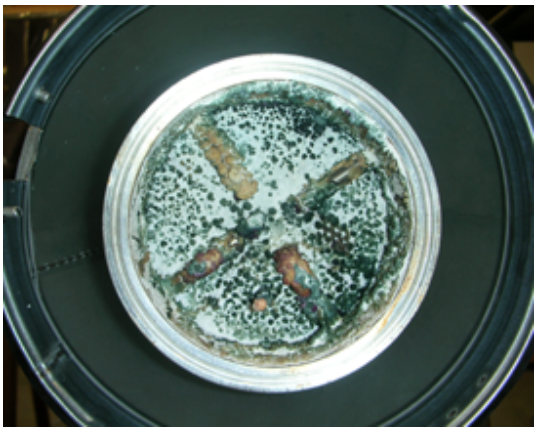

Figure 3.22: The grid in the CO_2 scrubber

Figure 3.23: The block in the bottom of the CO_2 scrubber

During a later experiment, both of the activated carbon filters and the gas meter was flooded again. Further investigation showed that the brand new pump from Grundfos did not start every time although the floating device was activated.

The gas meter was dried after each flooding but was never tested to see if the reading were right. The manufacturer claimed that if it was properly dried it should still be accurate. Even so the N_2 buffer tank made the value of these measurement useless unless the compressor was adjusted very precisely. Therefore these reading are disregarded.

After each test stop the facility was flushed with nitrogen. This was necessary to avoid oxygen in the facility. This process was time demanding especially when done several times because of many different leakages not found all at the same time.

3.4.6 Carbon monoxide alert

When the gas mixer was used in the flow experiment it was discovered that the safety CO meter in the experimental workshop registered 25 ppm. The gas cylinder with CO was closed and then the pressure on the flow meter in the gas mixer dropped to zero which meant that there where a leak from the CO cylinder to the gas mixer. CO is very toxic so the workshop was vented with fresh air from the outside. Once again foam was used to find the leak. It turned out that the joint on the hose on the gas mixer was cracked, probably because it was tightened to much. The solution was to change to entire joint.

Figure 3.24: Cracked joint leaking CO

3.5 Experiments

We successfully made two sets of experiments. In the first experiment methanol was produced with syngas directly from the Viking gasifier. In the second experiment bottled gas was used to check the output with different flows. The experiments where made from the 6-8'th of june 2007.
All experiments were made with a facility pressure of 40 bar and synthesis temperature as close to 250 °C as possible. This setup gave the purest outcome in earlier experiments made by Henrik Iversen, with a methanol content in the liquid of about 88 %.[20]

3.5.1 The methanol experiment

In this experiment syngas directly from the Viking gasifier was let trough the different cleaning devices and into the facility. The gas composition from the Viking gasifier and after the cleaning devices is showed in Table 3.2.

Gas composition	CH_4	CO	CO_2	H_2	N_2
From the gasifier	2,38%	13,19%	17,91%	26,52%	40,0%
After the cleaning devices	2,93%	15,12%	1,94%	29,6%	50,21%

Table 3.2: The gas composition in percent from the Viking gasifier

The two different gas compositions shows that the cleaning devices worked and it was possible to get the desired gas composition from the Viking gasifier.
Unfortunately after about 5 minutes the CO_2 proportion was rising. The amount of CO_2 steadily went to the same level as in the gas from the Viking gasifier. This meant that something was wrong with the CO_2 scrubber. We had to stop the experiment. The good news was that there where some methanol in the methanol container which meant that it is possible to produce methanol directly from the Viking gasifier. There was produced 0,33 g methanol which is not much, but the experiment was stopped after only a few minutes.
The problems with the cleaning devices is described further in section 3.4.

The CO_2 scrubber could not be repaired within the time scheduled. It was then decided to try to produce methanol with syngas directly from the gasifier without removing the CO_2 from the gas. The reason why CO_2 is removed is because it is not part of the synthesis reaction, and will therefore result in poorer efficiency. Furthermore large concentrations of CO_2 would form water in the water-gas-shift reaction (reaction 1.4). Water is absorbed in the catalysts and limits the activity. This affect depends on the type of catalyst used [34]. It is not known how sensitive the catalysts supplied by HTAS are.

Gas composition	CH_4	CO	CO_2	H_2	$N2$
From the gasifier	1,59%	14,15%	17,16%	24,98%	42,3%
After the cleaning devices	1,55%	14,67%	13,58%	25,3%	45,1%

Table 3.3: The gas composition in percent from the Viking gasifier

During the experiment it was suddenly discovered that the gas meter and both the activated carbon filters where flooded. It was later discovered that a defective pump caused the flooding (see section 3.4.5 for more details). Immediate action had to be taken in order to save the compressor from the water. This meant that the experiments was disrupted and the accurate

duration of the experiment is not known. But in about 30 minutes only 2,87 grams of methanol was produced. In an earlier experiment about 14 grams was produced in about the same amount of time (App. C.1). But the outcome of these two experiments cannot be compared because the gas composition were very different.
The model reports poor outcome for this setup as well. But because the time is not known exactly it is difficult to conclude much other than it is possible to produce methanol with this composition, but it is very inefficient. Whether or not water blocking the catalysts played a part in the low outcome is difficult to say. But the model indicates that the water-gas-shift reaction consumed water, rather than producing it.

3.5.2 Flow experiment

The purpose of these experiments were to evaluate the assumption of chemical equilibrium in the reactors made in the model (section 2.1). Hopefully the result will show at which flows equilibrium can be assumed.

The gas mixer was adjusted to the proper gas mix and three test was made with different flows. Test 1 is made with the maximum flow the compressor could deliver (1,5 Nm^3/h). This flow is not particular high because the gas meter before the compressor cannot handle high pressures so the output from the gas mixer is choked. Since the gas meter measurements later was disregarded (see section 3.4.5), the gas meter could have been bypassed, and higher flows could have been used. Test 2 and 4 are chosen to get a wide span of measurements but still get reasonable outcome.

The gas composition is showed in table 3.5.

The three test duration was different because the gas was to have about the same volume of gas trough the facility.

The third experiment failed and was stopped before time. This is because about 35 min within the experiment the nitrogen supply failed making the gas mixture incorrect. This experiment is removed from the actual flow experiment.

Test no.	Flow	Duration	Residual gas	Condensed	Methanol/res. gas	Time in reactor
1	35%	40 min	0,888 m^3	20,01 g	22,53 g/m^3	9,19 sek
2	22%	60 min	0,846 m^3	30,62 g	36,19 g/m^3	14,3 sek
4	10%	90 min	0,684 m^3	26,14 g	38,22 g/m^3	26,6 sek

Table 3.4: The results from the flow experiment

It is assumed that 88% of the condensed liquid is methanol (see section 3.1.5).

The 3 experiments had different flows and duration. They are therefore compared by methanol production per volume residual gas. This is not affected by duration or flow and if equilibrium is not reached in the reactors the tests with lower flows should have more methanol produced per m^3 residual gas. The methanol per volume will be called the *compensated yield*.

The time in the reactor is calculated with the assumption that the catalyst pills takes up $\frac{2}{3}$ of the reactor volume, and the reactor volume therefore is $0,5L \cdot \frac{2}{3} = \frac{1}{6}$L. This might not be a

very valid assumption, but for comparison of the three experiments it is fine. But the calculated times can therefore not be compared with other studies.
The number of moles of methanol is calculated as

$$n_{met} = \frac{m_{met}}{M_{met}} \tag{5.1}$$

Where m_{met} is the mass of methanol from the experiment and M_{met} is the molar mass of methanol.
The number of moles of residual gas is found assuming ideal gas behavior.

$$n_{res.gas} = \frac{p_{exit} \cdot V_{res.gas}}{R \cdot T} \tag{5.2}$$

The volume of the gas can be found from the ideal gas equation.

$$V_{tot} = \frac{n_{tot} \cdot R \cdot T_{reac}}{p_{reac}} \tag{5.3}$$

With p_{reac} and T_{reac} being the pressure and temperature in the methanol reactor. The temperature is the mean of the measured temperatures at the outlet of the methanol reactor.
The time the gas was in the reactor can now be calculated from the experiment duration t_{exp}.

$$\dot{V} = \frac{V_{tot}}{t_{exp}} \tag{5.4}$$

$$t_{reac} = \frac{V_{reac}}{\dot{V}} \tag{5.5}$$

Table 3.4 shows that the longer time the gas was in contact with the catalysts the higher was the compensated yield. This is not very surprising, it takes time for the catalytic processes to reach equilibrium.
The compensated yield versus the time in the reactor is plotted to see if a tendency can be recognized.

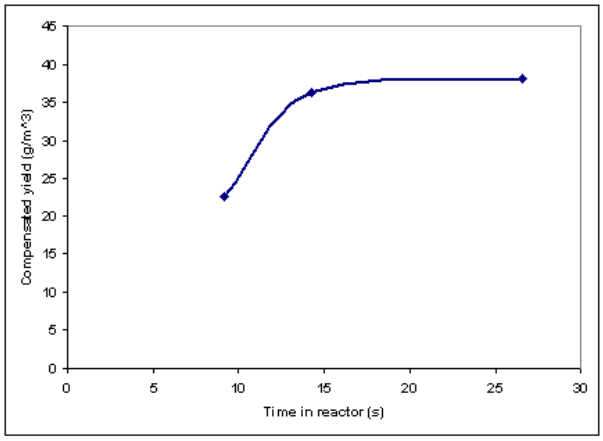

Figure 3.25: Compensated yield vs. time in reactor

Figure 3.25 shows that the experiments indicates that chemical equilibrium is obtained in the methanol reactor after approximately 19 seconds (remember that these time calculations not necessarily tell us how long the gas was in contact with the catalysts). This compares to a flow into the facility about 0,75 Nm^3/h.
A more accurate curve could be made from more experiments.

It is important to notice that other factors could have affected the increased outcome at the lower flows.
When the gas moves slower in the facility the pressure losses are smaller. The pressure is regulated at the facility entrance, and is kept at 40 bars throughout all 3 test. This could mean that at the low flow tests the pressure in the reactor could be a little higher. This is however not considered to be a very significant source of error (see section 3.6).
Other factors could be gas composition and temperature. As described in section 3.3.13 the fine tuning of the gas mixer is difficult, especially when the time is limited. The temperature is also difficult to adjust precisely. The heat blower controlling the temperature in the reactor only has temperature steps of 10 degrees.
Table 3.5 shows the differences in the composition and temperature during the test. These are the average values of the data supplied by the data collection. Composition in test 4 is a bit different than the 2 first. This is because the gas mixer failed in the 3. test run as mentioned earlier. The difference in temperatures is caused by the alternating flows because the methanol synthesis is exothermic. Less flow means less synthesis reactions and therefore lower temperatures.

Test no.	H_2	CO	CO_2	CH_4	N_2	Temp
1	39,52 %	23,75 %	2,66 %	2,22 %	31,85 %	256,89 °C
2	39,75 %	22,49 %	2,81 %	2,02 %	30,94 %	256,23 °C
4	36,70 %	21,51 %	1,92 %	2,44 %	37,44 %	250,82 °C

Table 3.5: Gas composition in the flow experiments

If the 3 compositions are inserted in the model, and all other parameters are kept the same it can give an idea as to how much the differences might affect the outcome. Table 3.6 shows the differences in outcome, using test 2 as reference.

Parameter	Test 1	Test 2	Test 4
Composition	+ 3,87 %	-	- 17,41 %
Temperature	-2,10 %	-	+ 18,22 %

Table 3.6: Gas composition in the flow experiments

Fortunately the differences in temperature and gas composition seems to almost cancel out each other. It could appear as the outcome from test 1 and 3 should be a little higher than from test 2. But there is nothing conclusive to say because of the many factors in play.

The condensation process could also affect the outcome of the flow experiment. When the flow is lower the speed of the molecules are smaller. This gives better conditions for condensation. This would mean that more methanol should come from tests with lower flows. Whether the condensation column is affected by different flows is evaluated in section 3.6

3.5.3 Comparison with model

The methanol experiments (section 3.5.1) are not compared with the model. This is because the CO_2 scrubber broke before the experiment could even start. The experiment with high CO_2 concentration is not compared with the model because nothing can be concluded about it, other than the gas composition used gives a very low outcome.

The flow experiments are very interesting because these will show validity of the chemical equilibrium assumption. Values for gas composition and synthesis temperature are found in table 3.5. When comparing with actual experiments the volume of the residual gas and the experiment duration is used instead of flow to calculate how much syngas went through the facility. This is done because these are the two most precise measurements. Values are found in table 3.4.

Test no.	Experiment	Model	Deviation
1	17,62 g	68,56 g	289,1 %
2	26,95 g	64,15 g	138,0 %
4	23,0 g	50,65 g	120,2 %

Table 3.7: Methanol yield from flow experiment

Table 3.7 clearly shows that the model yields substantially higher results than the actual test. The model deviates much more when the flows are high. This is because chemical equilibrium is assumed in the model no matter what the flow is. The flow experiment showed that the synthesis reactions are far from equilibrium when flows are high (figure 3.25). The chemical equilibrium assumption only seems to be valid when flows are lower than 0,75 Nm^3/h. But if reactions in test 4 should be very near equilibrium, then why does the model deviate with more than 100 %?
To answer this question every assumption and possible sources of error are examined.

3.6 Sources of error

In order to review the differences between the experiments and the model, all the possible sources of error are listed and evaluated.

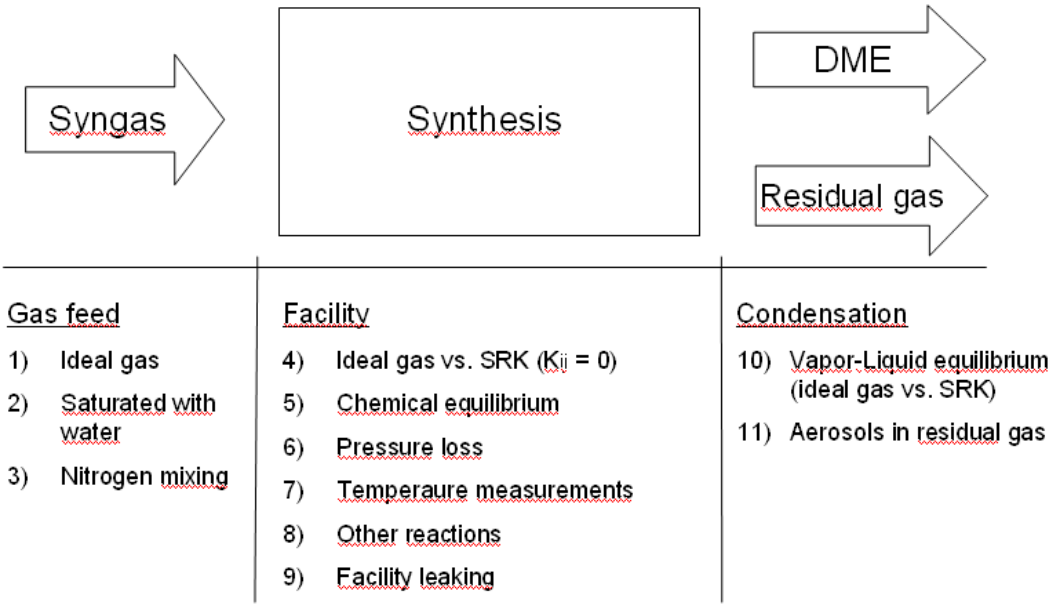

Figure 3.26: Sources of error in model and facility

1. The ideal gas assumptions is used to determine the molar fractions from the volume measurements y_i = vol %. This neglects the volume of the molecules. The assumption should

be good as the pressure is atmospheric.

2. As the gas is cooled with water in the NH_3 it is saturated with water. The assumption is not made in the calculations of flow experiments as the bottled gas contains no water.

3. As mentioned in section 3.3.8 a little N_2 from the buffer tank will mix into the syngas feed. The volume of the buffer tank is 20 L and the pressure is 40 bar. With measurements of the gas composition from the buffer tank and the time of the experiments it is estimated how much the gas composition has changed. From this conclusion it is concluded that the increase in N_2 can be neglected.

4. Section **??** compares the two equations of state. Readings from figure 2.10 at 250 °C and 50 bar gives an error + 3,5 %

5. Figure 3.25 shows that chemical equilibrium is not attained when flows are high. But at the lowest flow in the flow experiment the it looks like chemical equilibrium is reached.

6. Loss of pressure in the pipes of the facility could lead to lower pressures in the methanol reactor. When calculated for high flow with methods from the literature [20] it is found that the pressure loss can be neglected.

7. The temperature inside the methanol reactor is not measured directly. The temperature measured at the reactor outlet is used in the model. But the temperature at the surface of the catalysts where the exothermic synthesis reaction takes place could easily be higher. This will be investigated further down in this section.

8. Other reactions than the ones used in the model could take place within the facility. In experiments made by Henrik Iversen the liquid outcome contained about 9% (based on mass) of substances other than water and methanol. There is however no way to evaluate the effects of these reactions.

9. The facility was pressure tested over night and concluded leak-free (see section 3.2.1)

10. The differences between the ideal gas equation and SRK is evaluated in section 2.3.5. The error is found to be + 1.3 % at condensation temperatures of 20 °C.

11. Will all the condensed gas settle as drops or will some leave as aerosols in the residual gas? If the velocity of the aerosols are less than 0.2 m/s and the flight time is above 3 sec. gravitation should assure no aerosols in the residual gas[36]. Calculations gives much lower velocities and much longer flight time which means the residual gas should be free from aerosols.

Of the listed errors possible, it seems that the most plausible explanation for the large deviations of the model, is the temperature used as input for the synthesis (error no. 7). The affects of this temperature is tested, using the flow experiment no. 4 as reference, since this is most likely to have reached equilibrium.

3.27 shows that the methanol outcome of the model is very sensitive to changes in temperature. If the temperature input of the model is increased 20 °C, the deviation decreases from 120 % to less than 10 %. As mentioned the temperature used as input is measured at the methanol reactor outlet. The other temperature measurements indicate than temperatures inside the reactor could be higher.

MR 1-3 are surface temperatures of the methanol reactor at the top, middle and at the bottom of the reactor. The surface temperature at the middle of the reactor is higher than the air blown

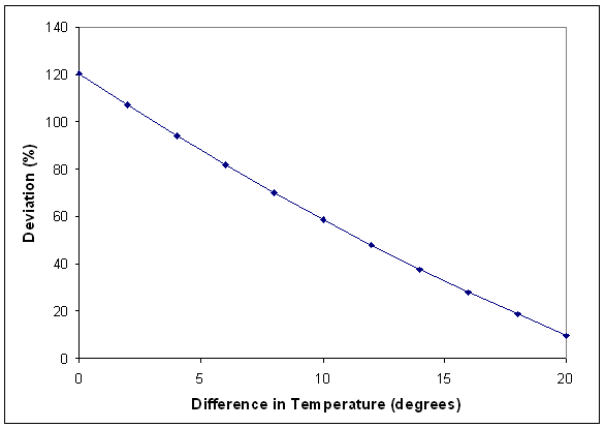

Figure 3.27: Deviation as function of increased temperature in model

Measurement	Inlet	Outlet	Air	MR 1	MR 2	MR 3
Temperature (°C)	241,6	251,8	255,3	250,0	257,4	255,6

Table 3.8: Average temperatures of methanol reactor

in by the heat blower. Knowing that the reactions in the reactor are exothermic, this indicates that temperatures are even higher inside the reactor.
Other experiments with synthesis of hydrocarbons has shown that the temperature on the surface of the catalysts can be higher than the gas temperatures. The exothermic reactions takes place on the surface of the catalysts, and all the heat is absorbed by the catalyst and then emitted to the gas by heat transfer[37].
Methods of calculations found in the literature [20] indicates that if the surface temperature of the reactor is 254,3 (°C) (average of measurements) then the temperature at the center axis of the reactor is 269,1 (°C). The calculations are based on a number of assumptions and simplifications. But all together there are several strong indications that the temperature input of the model should be higher than the outlet measurement. Increasing this temperature drastically decrease the deviation of the model.
If the temperature inside the reactor in fact is higher then the difference will be lower with lower flows, because fewer reactions will increase the temperature. This means that the effects of the flow experiments (fig. 3.25) is not just because equilibrium is reached, but also because the temperature differences are lower.
Further investigations are needed before anything conclusive can be said about the input temperature of the model, but this is beyond the scope of this report.

3.7 Future solutions

In section 3.4 the different practical issues are described. Modification needs to be made before the facility steadily can produce methanol from gasified biomass and in the future DME.

With regard to methanol production only a few alterations is needed.

3.7.1 CO_2 scrubber

The new CO_2 scrubber is different from the old one but it still uses potassium hydroxide to remove all the CO_2 from the syngas. Instead of having the potassium hydroxide on pill form and heating these pills, the scrubber works by having the syngas bubbling trough a recirculating wet solution of potassium hydroxide. In this way the CO_2 is removed from the syngas without having the aforementioned problem with the potassium hydroxide (cf. section 3.4). To recirculate this wet solution a pump is used. The solution is kept in a buffer tank (the one previously used for the washing tower).

3.7.2 NH_3 washing tower

Because of the mentioned problem in section 3.4 a hose pump is installed. The pump leads the ammonia water in the drain without having a buffer tank. It is not the best solution to put ammonia into the drain but with the quantities we operate with this should not be a problem.

3.7.3 Small gas pump

In the first experiment the gas pump before the main compressor broke down. This is replaced with a new one. This new compressor can only deliver 1 baro of pressure, but this should be enough to get the desired flow through the system. It should be installed before the CO_2 scrubber in order to get positive pressure for the bubbling.

3.7.4 Extra buffer tank

It might be a good idea to have a extra buffer tank with pure nitrogen for safety. This buffer tank should normally be closed, but if some experiments run out of control, there is always pure nitrogen to stop the unwanted reactions. The present N_2 buffer tank obtains a mixture of N_2 and syngas because of changing pressure from the compressor, and it cannot be closed because it is needed to secure constant pressure after the compressor.

3.7.5 Development of model

It is suggested in section 3.6 that the the main source of error is the synthesis temperature used as input in the model. The temperature is measured outside the reactor and it is then assumed that this is the temperature of the catalysts. It would be interesting the develop the model to include calculations of these temperatures.

3.7.6 DME production

To produce DME more modifications are needed. This is the condensation column and perhaps the installation of a DME reactor.
DME production could theoretical be produced in two ways.

1. Two reactors with different catalysts pills.
2. One reactor with mixed pills.

The 2. solution is easier realized because no extra reactor needs to be installed in the oven, although this means flows must be lowered.

The theoretic model indicates that the 2. solution has a higher efficiency. But the model does not take the activity of the catalysts pills into account (see section 2.4).

The first solution might however be a safer choice because the literature underpins the method and with two separate reactors the temperature can be set for optimal conditions for each reaction.

The literature reports different synthesis temperature for methanol and DME. If the optimal temperature for DME synthesis is much higher than for methanol this could have effect on which solution is better.
It is previously seen that the temperature is very important for the output of the methanol process (see section 3.6).

In practical terms the DME reactor is produced so the critical components for the 1. solution is available.

It is not decided in this report which solution will be used, because much more study and experiments is needed to make a qualified decision.
Will the 2. solution be better because the temperature can be regulated to the optimum for each synthesis, or will the increased equilibrium yield of the 1. solution be better?
It is likely that the desired flow must be included in the decision. Low flows points towards the first solution, because equilibrium (and hence higher yield) is more likely to be reached. The 2. solution gives the possibility of obtaining high activity and therefore high reaction rates, which is favorable at high flows.

3.7.7 The DME condensation column

DME is a gas at normal temperature and pressure. Storage tanks must be pressurized to handle liquid DME.

Based on the model (see section 2.3.5) the DME condensation process can be evaluated and possible design suggestions of a condensation column can be made.

The calculations made in the section 2.3.5 shows that the partial pressure is decisive for at which temperature DME is condensed. With the gas composition from the Viking gasifier, calculations of the DME condensation suggests temperatures around -50 °C if approx. 80 % is to be condensed. Increasing the partial pressure of DME increases the condensation temperature as well.

To produce almost pure DME the methanol and water in the gas needs to be removed. Especially the water needs to be removed before the DME condensation to avoid freezing and thereby blocking the pipes.

In the current facility the methanol condensation process takes place at about 25 °C which mean that 91% is condensed (cf. figure 2.8) and a little higher percentage of water. An idea is that the condensation process could be done in two steps. First condensation of methanol and water in one column and then condensation of DME in another column.
To get most of the methanol and water condensed, the temperature for this process needs to be around a couple of °C. The thought is therefore to use a combined freezer/refrigerator, where the methanol and water condensation takes place in the refrigerator and the DME condense process takes place in the freezer (see figure 3.28). The pipe can go through the wall and be fitted to the refrigerator and the freezer. Two different containers can contain the condensed water methanol mixture and the DME.

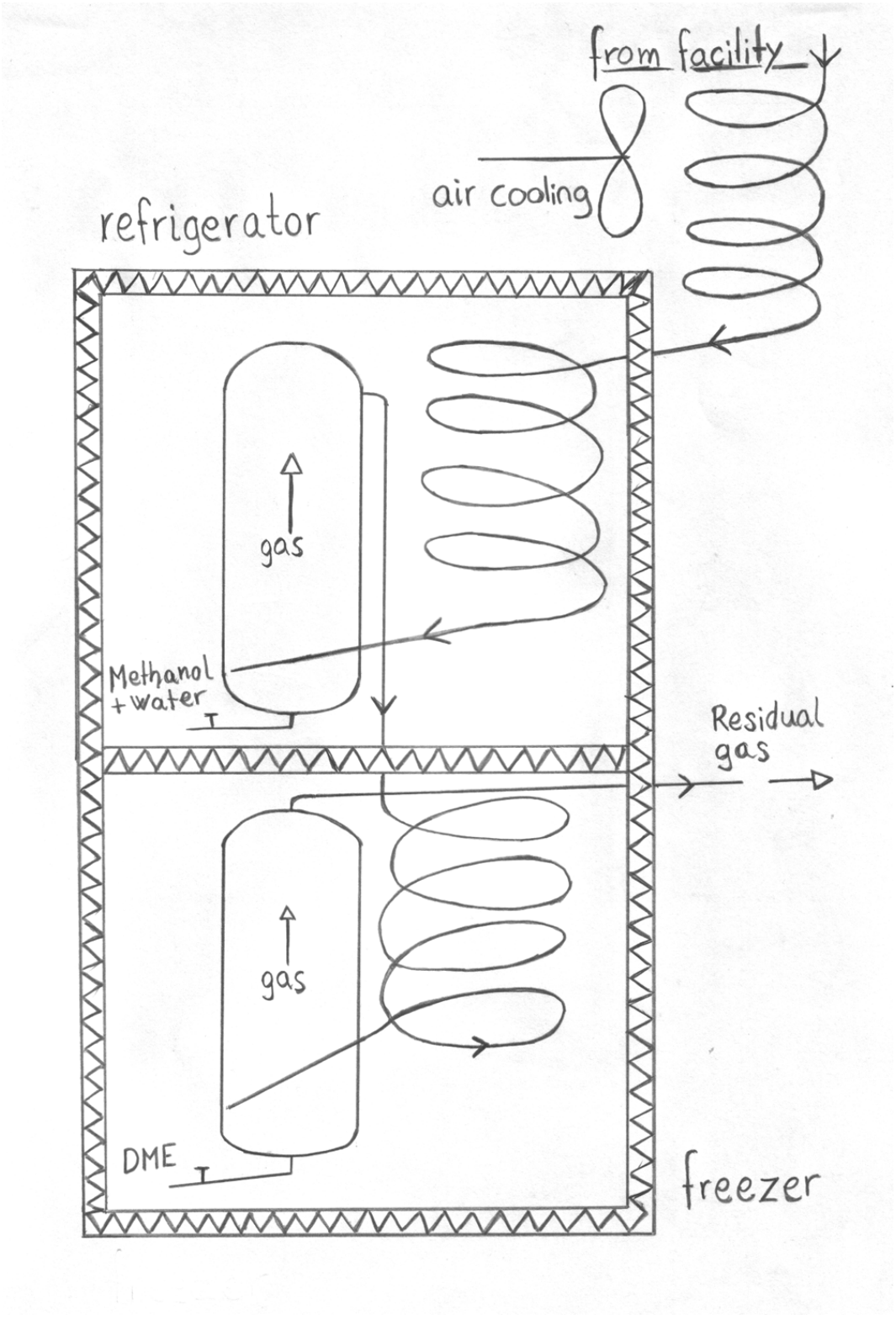

Figure 3.28: A schematic drawing of the condensation column

It is important to make sure that the freezer/refrigerator has sufficient capacity to cool the gasses. The gas is cooled to atmospheric temperature before entering the refrigerator.
The refrigerator provides the right temperature for the methanol and water condensation, but the freezer can only deliver about -25 °C. To lower the temperature further dry ice could be used which is about -70 °C. Small amount of dry ice are easily kept in the freezer during experiments. The solution with dry ice is a good solution for demonstration, but not as a more permanent solution.

Calculations shows (see figure 3.29) that some CO_2 also is condensed at temperatures about -50 °C. The percentage of CO_2 is much lower than the DME percentage. But it is necessary to be aware of this if the focus is to condense pure DME. The students behind the Ecocar do not think the CO_2 content will affect the engine of the Ecocar.

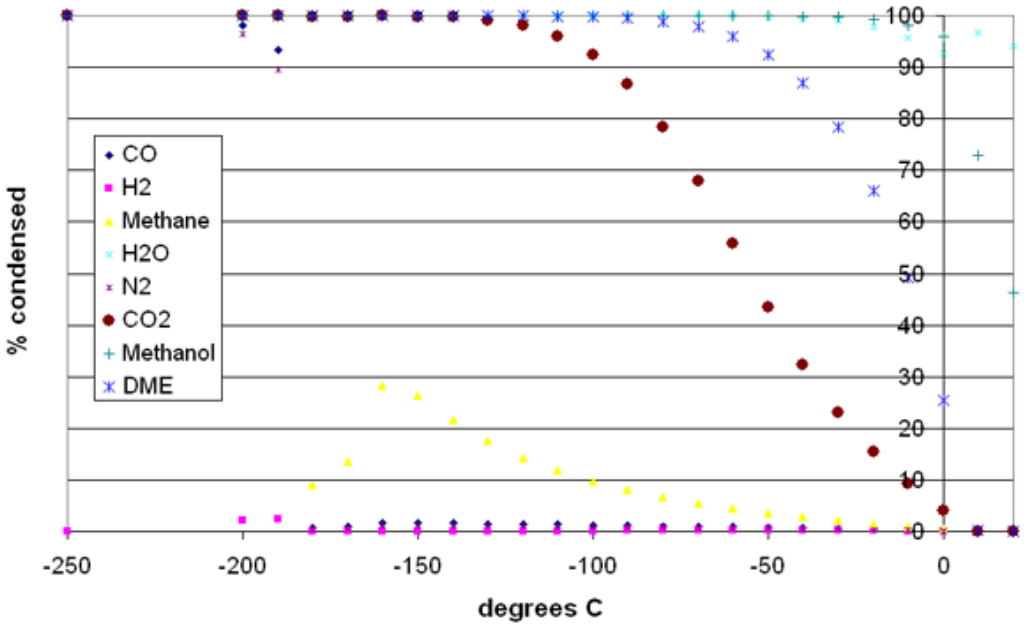

Figure 3.29: A overview of the condense process with all the components. For gas composition see App. B.2

Calculations are made for two other gasifiers, that has other gas compositions. These gasifiers are the Carbo V and the Güssing. The efficiencies and how clean the gas is, is not considered. Only the composition of gas is used to investigate the condensation process.

Güssing is a circulation fluid bed gasifier, type FICFB (fast internal circulating fluidised bed) located in Austria. It uses only steam in the gasifying process which results in small amount of nitrogen in the gas. A typical gas composition from the Güssing gasifier is seen in figure 3.30. The high CH_4 content could be lowered with steam reforming before used in the synthesis facility. This is not considered in this calculation.

The Carbo V is a pressurized entrained flow gasifier. Pure oxygen and steam is added which results in small amount of nitrogen and metan in the syngas. A typical gas composition from the Güssing gasifier is seen in figure 3.31

These two compositions are assumed saturated with water at 10 °C and CO_2 content is lowered to 4,0 % (as if the gas had been through the cleaning devices of the facility) before used in the theoretical model to get the gas composition for the condensation process (see figure 3.32 and 3.33). It should be noted that these compositions have very high DME contents. They are

Component	Composition
CO	26%
CO_2	19%
H_2	40%
N_2	2.5%
CH_4	10%
C_2H_4	2.5%

Figure 3.30: The gas composition in percent from the Güssing gasifier

Component	Composition
CO	39.3%
CO_2	20.4%
H_2	40.1%
N_2	0.2%
CH_4	0.1%

Figure 3.31: The gas composition in percent from the Carbo V gasifier

calculated with the mixed pills model with a synthesis temperature of 260 °C (see section 2.4 for evaluation of the mixed pills model and temperature). Furthermore a pressure of 50 bar is used in the model instead of 40 bar. This is done to get as high contents of DME possible to evaluate effects on the condensation column.

Component	Composition
CO	3,08%
CO_2	21,19%
H_2	27,61%
H_2O	2,22%
N_2	6,08%
Methane	23,56%
Methanol	1,3%
DME	14,96%

Figure 3.32: The gas composition for the condense process in percent from the Güssing gasifier

Component	Composition
CO	9,45%
CO_2	42,23%
H_2	14,47%
H_2O	0,76%
N_2	0,54%
Methane	0,27%
Methanol	1,1%
DME	31,18%

Figure 3.33: The gas composition for the condense process in percent from the Carbo V gasifier

Calculations of the condense process is made with the model and the SRK equation of state (see figure 3.34).

These calculations show that more DME in the gas means that the DME condensation process takes place at higher temperatures. In figure 2.9 the condensation process for a realistic gas composition for the syngas from the Viking gasifier is seen. It is clear that solutions with more DME in the gas is desired because the condense process would be much easier and less expensive. At -10 °C the syngas from the Viking gasifier has 9% DME condensed, Güssing has 80% and Carbo V has 95%.

In figure 3.34 it is seen that the data from the SRK equation of state has higher values than the ideal gas equation of state when there is much DME in the gas. Earlier in the report it is seen that the ideal gas equation of state has higher values than the SRK equation of state when there is little amounts of DME in the gas (see figure 2.9). It is a interesting perspective, that the theoretic better equation of state indicates that more DME is condensed. This should of course be checked with experiments, but the method has been verified by Georgios Kontogeorgis from the IVC-SEP research group.

With DME contents at this level a condensation column different from the refrigerator/freezer solution can be used. Acceptable percentages are condensed at 0 °C. Hence problems with ice can be avoided. Although this means that the DME must be separated from water and methanol afterwards (e.g. by lowering the pressure, because DME is a gas at normal temperature and pressure).

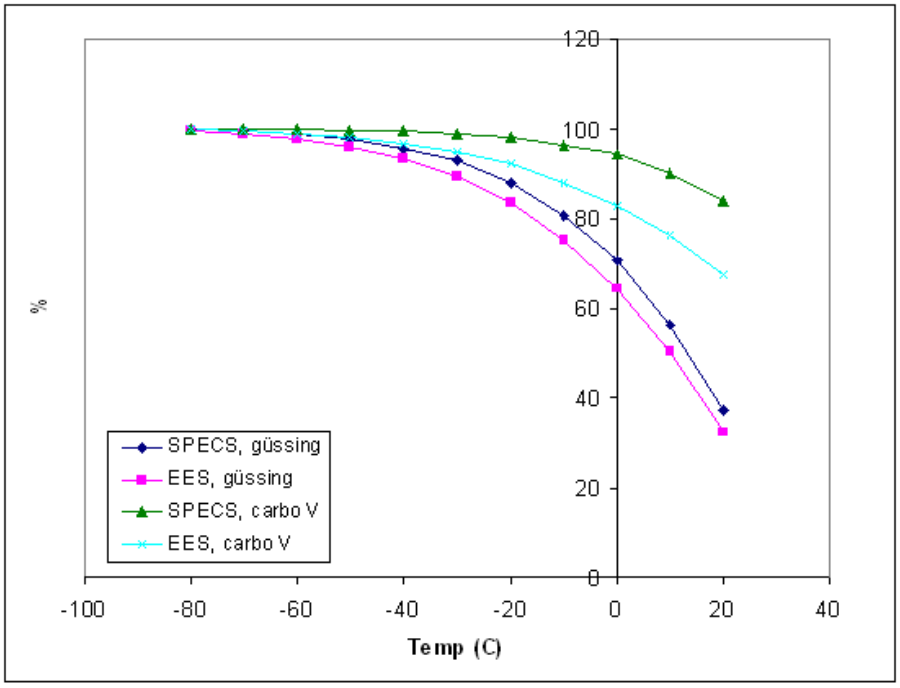

Figure 3.34: The theoretic condensation process for the gas composition from the Güssing and Carbo V gasifiers

3.7.8 Oxygen enrichment of the Viking gasifier

Higher DME content is desirable and therefore possibilities of oxygen enrichment of the Viking gasifier is considered. This would lower the content of the inert N_2 in the syngas, and thereby result in higher yields.
A possible gas composition for the Viking gasifier, using air enriched to 80% oxygen (instead of atmospheric air), is calculated by an equilibrium gasifier model made by Jens Holm. This gas composition is however just a estimate. When operated with enriched air, water vapor must be added to the gasifier in order to control the temperature. This is not accounted for in the gasifier model. Therefore the biomass used as input in the model was assumed very wet. The gas composition is given as volume % on dry basis.
Once again the gas is assumed saturated with water at 10 °C and the CO_2 content is lowered to 4 %.

Gas composition	CH_4	CO	CO_2	H_2	N_2
From the gasifier model	2,41 %	18,69 %	34,19 %	38,46 %	6,25 %
Input in model of this work	3,52 %	27,31 %	4,0 %	56,19 %	8,98 %

Table 3.9: Estimated gas composition from oxygen enriched Viking gasifier

Oxygen enrichment costs energy, and whether or not it would be beneficial to enrich air for the Viking gasifier is beyond the scope of this project.

Figure 3.35 indicates that if the Viking gasifier is oxygen enriched 85% of the DME can be condensed with a freezer solution. In the suggested refrigerator/freezer condensation column about 50% of the DME would condense with the water and methanol in the refrigerator.

Another advantage of oxygen enrichment is the possibility to recirculate the residual gas and

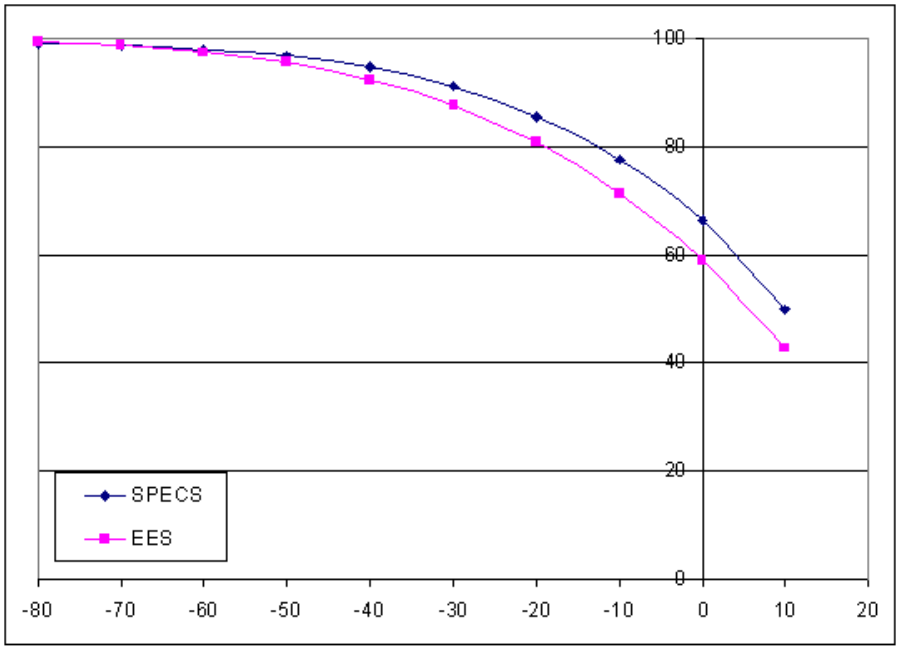

Figure 3.35: The theoretic condensation process for oxygen enriched Viking gasifier

thereby increasing the fuel production efficiency. This possibility is not reviewed in this report.

3.8 Future experiments

Producing DME from gasified biomass is the top priority. Efficiency is not important only proving the concept. Especially because bio DME production has not been found in the literature.

It would also be interesting to use experiments to examine the limitations of the models. The model is only valid within certain intervals. For instance does the lack of activity calculations mean that the model cannot be used at low temperatures. It would be interesting to establish in which intervals the model is valid. The different experiments described are interesting for both methanol and DME.

1. Yield versus reactor temperature. What are the optimal temperatures for methanol and DME synthesis?
2. Yield versus CO_2 content. How much is needed to speed up the methanol synthesis? Does the catalysts loose activity when CO_2 concentrations are high?
3. Effects of water on catalyst activity. How big is the effect of active site blocking?
4. Investigating the effect of changing the H_2/CO ratio using bottled gas.
5. Experiments with simulated enriched gasifier gas composition using bottled gas.

Beyond these experiments a experiment with different pressure could be made, but this test is pretty much covered previously [20].

The temperature test is important to evaluate if DME should be produced with separate reactors or mixed pills. If the temperature for optimal methanol and DME production is to far apart,

the solution with to reactors seems better (cf. section 2.4). But this experiments cannot be done without having to reactors, therefore a literature study must decide how large the difference is between optimum methanol and DME process temperature. The experiment is however still interesting to verify model and literature study.

Calculations has showed that much cooling is needed to condense DME, when the amount of DME in the gas is small. Therefore solutions towards more DME in the gas is interesting. But before trying to solve this problem it is necessary to make practical tests to ensure the effect on the condensation process with more DME in the gas. These experiments should be done from bottle gas, because it is fairly easy and then the gas composition could be totally controlled and the desired parameters could be checked.

Chapter 4

Conclusion

Experiments
Methanol was successfully produced directly from gasified biomass from the Viking gasifier. DME production was not tested because of practical obstacles and limited time. Improved cleaning devices and another condensation column is needed to produce DME.

Many practical problems arose during the project. These problems delayed the entire project. This shows that unforeseen things can easily happen during experiments and that external factors can affect the time schedule.

The CO_2 scrubber with pills of potassium hydroxide did not work as intended. Water is created in the reaction between the CO_2 and the potassium hydroxide. Heating the gas prior to the reaction was supposed to evaporate this water. This did not work. Instead the potassium hydroxide became liquid and floated to the bottom of the scrubber, where it had no effect.

It is possible to produce methanol without removing the CO_2. This is however very ineffective. The production decreases about 80% with 14 % CO_2 in the gas instead of 2 %.

Experiments showed that chemical equilibrium in the methanol reactor is not reached with flows higher than 0,75 Nm^3/h.

Theoretic model
The prevalent theory is basis for the created models of the methanol and DME production. The model has been verified by a literature study and compared to practical experiments.
The created model has large deviations from the experimental results.

An investigation indicates that it is the measured temperature of the methanol synthesis and not the model, that is the main source of error.

The model uses the ideal gas equation of state which is verified with the theoretic better Soave-Redlich-Kwong (SRK) equation of state. The ideal gas equation is a good assumption for the used gas composition, different operating temperatures and pressures. Even in the two phase area the ideal gas equation has acceptable deviation from the SRK equation of state compared to other sources of error.

Literature
It is concluded from the literature study that DME has many interesting perspectives.

DME is versatile, it can be used for many different things and can be produced in various ways.

The main purposes for DME is as aerosol propellant, in gas turbines, for cooking, heating, to produce olefins and as engine fuel.

Bio DME (DME produced from biomass) has many interesting properties as diesel engine fuel. It has a minimum of emissions, is CO_2 neutral and have the best well to wheel efficiency compared with the other alternative bio fuels.

There are some problems with implementing DME as a diesel engine fuel. Especially the distribution net and engine lubrication are problems that needs to be solved.

Project perspectives

With the model and the literature study it has been possible to evaluate the important parameters in order to further develop the methanol facility to produce DME. The model is used to evaluate the condensation process for DME. The amount of DME in the gas after synthesis is so small that the gas must cooled to below -50 °C if more than 80% to be condensed.

Solutions to increase the percentage of DME in the gas is interesting, because then the condensation process takes place at higher temperatures.
In the literature examples of such solutions was found. Oxygen enrichments of the Viking gasifier could lower the amount of nitrogen in the gas and thereby increasing the partial pressure of DME. If this is practical possible 85% DME could be condensed at -25 °C.

Bibliography

[1] Ni Weidou, Tan Lijian, Fang Dewei (Tsinghua University) , *Rational Cognition of DME Market in China*, www.aboutdme.org

[2] Dansk Energi and Cowi, *Anvendelse af biomasse i transportsektoren*, DTU **2006**

[3] D.W. Gill and H. Ofner, *DME as an Automotive Fuel*, 9 th IEA workshop, **2001**

[4] Teknologirådet, *Morgendagens transportbrændstoffer. Danske perspektiver*, **2006**

[5] Nils Elam, *Automotive Fuels Survey: Raw Materials and Conversion. vol. 1*, IEA/AFIS, **1996**

[6] Professor Spencer C. Sorenson, *Engine Principles and Vehicles*, DTU **2006**

[7] Peter Ahlvik and Åke Brandberg, *WELL-TO-WHEEL EFFICIENCY For alternative fuels fromnatural gas or biomass*, Ecotraffic, Swedish National Road Administration, **2001**

[8] Visit at IRD A/S, january **2007**

[9] Carlo N. Hamelinck, André P.C. Faaij, Herman den Uil and Harold Boerrigter, *Production of FT transportation fuels from biomass; technical options, process analysis and optimisation, and development potential*, Sciencedirect **2003**

[10] Hubert de Mestier du Bourg, *FUTURE PROSPECTIVE OF DME*, 23rd World Gas Conference, Amsterdam **2006**

[11] Totaro Ohno, *New Clean Fuel DME*, DeWitt Global Methanol and MTBE Conference, **2006**

[12] HUANG Zhen, *An Overview of DME Activities in China*, 2nd International DME Conference, **2006**

[13] Jim McCandless, *DME as an automotive fuel: Technical, Economic and Social perspektives*, Energy Frontiers Conference, **2001**

[14] Arun Basu, Mike Gradassi, Ron Sills, Theo Fleisch and Raj Puri, *Use of DME as a Gas Turbine Fuel*, BP Exploration, **2001**

[15] Robert H. Williams, *TOWARD A GLOBAL CLEAN COOKING FUEL INITIATIVE*, 2nd International DME Conference in London **2006**

[16] Troy A. Semelsberger, Rodney L. Borup and Howard L. Greene, *Dimethyl ether (DME) as an alternative fuel*, Journal of Power Sources - Elsevier, **2005**

[17] J. Wu, Z. Huang, X. Qiao, J. Lu, L. Zhang and J. Zhang, *Combustion and Emission Characteristics of a Turbocharged Diesel Engine Fuelled with Dimethyl Ether*, **2006**

[18] From the DTU eco cars homepage, http://www.ecocar.dk/, **2007**

[19] Henrik Landälv, Volvo Powertrain Corporation, *Heavy Duty DME vehicles*, **2005**

[20] Henrik Laudal Iversen, *Produktion af flydende biobrændsler udfra biomasse*, DTU **2006**

[21] P.L. Spath and D.C. Dayton, *Preliminary Screening — Technical and Economic Assessment of Synthesis Gas to Fuels and Chemicals with Emphasis on the Potential for Biomass-Derived Syngas*, **2003**

[22] Raymond Chang, *General Chemistry*, McGraw-Hill, **2006**

[23] J.D. Seader, Ernest J. Henley, *SEPARATION PROCESS PRINCIPLES*, John Wiley & Sons, INC., **1998**

[24] Walas, *APhase Equilibria in Chemical Engineering*, Betterworth-Heinemann **1985**

[25] D.P. Tassios, *Applied Chemical Engineering Thermodynamics*, Springer-Verlag, **1993**

[26] Chorng H. Twu*, John E. Coon, and David Bluck, *A Comparison of the Peng-Robinson and Soave-Redlich-Kwong Equations of State Using a New Zero-Pressure-Based Mixing Rule for the Prediction of High Pressure and High Temperature Phase Equilibria*, Simulation Sciences Inc.

[27] Conversations with Kaj Thomsen and Georgios Kontogeorgis , *IVC-SEP research group witin chemical engineering*

[28] H. Knapp, R. Döring, L. Dellrich, U. Plöcker, J.M. Prausnite, *Vapor - Liquid Equilibria for mixtures of low boiling substances*, Dechema

[29] Robert C. Reid, John M. Prausnitz and Bruce E. Poling, *The Properties of Gases and Liquids* 4.th edt., **1987**

[30] Poul Scheel Larsen, *TEKNISK TERMODYNAMIK*, DTU-tryk **2005**

[31] NASA Thermo build, http://cea.grc.nasa.gov/, **2005**

[32] Guangxin Jia, Yisheng Tan and Yizhuo Han, *A Comparative Study on the Thermodynamics of Dimethyl Ether Synthesis from CO Hydrogenation and CO_2 Hydrogenation*, **2006**

[33] C. Mas, E. Dinjus, H. Ederer, E. Henrich and C. Renk, *Dehydration of methanol to Dimethylether*

[34] Javier Ereña, Raúl Garoña, José M. Arandes, Andrés T. Aguayo, Javier Bilbao, *Effect of operating conditions on the synthesis of dimethyl ether over a $CuO - ZnO - Al_2O_3/NaHZSM - 5$ bifunctional catalyst*, **2005**

[35] AIRLOQ notes from FLSmith

[36] Conversation with Joachim Paul, Professor, DTU

[37] Conversations with Anker Degn Jensen, lecturer at DTU and co-supervisor on this project

Appendix A

Biofuels

A.0.1 Estimation of bio diesel production efficiency

Nils Elam, *Automotive Fuels Survey: Raw Materials and Conversion. vol. 1*, IEA/AFIS, **1996** [5]

This report states that the production of biodiesel from rape (RME) yields:
47,8 GJ/hectare biodiesel
28,2 GJ/hectare oilcake
43 GJ/hectare rape straw

$$\frac{47,8}{47,8+28,2+43} \cdot 100\% = 40,17\% \tag{0.1}$$

The table 1.3 is created from data from the swedish well-to-wheel report [7]. The production efficiency is multiplied with a distribution efficiency and a powertrain efficiency to get the well-to-wheel efficiency. The powertrain efficiency is 0.176 for diesel cycle engines and 0.149 for otto cycle engines (gasoline).

Appendix B

Theoretic model

B.0.2 SPECS

The SPECS program is developed by the IVC-SEP research group within technical chemistry from DTU. (cf. Figure B.1)

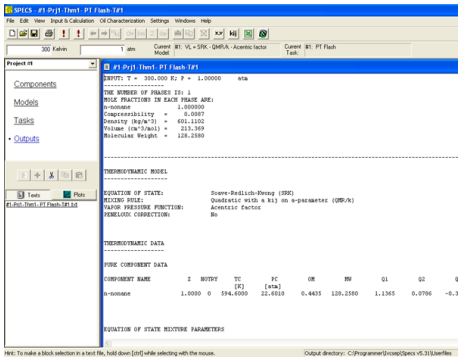

Figure B.1: Screen shot from the SPECS program

In SPECS it is possible to chose which equation of state and what mixing rule to use. The Specs program can also calculate the fugacity coefficient of the different components in the system.

The composition of the gas plays a major role at which temperature the condensation process takes place. Besides the physical properties of the components it is the partial pressure that determines at which temperature the different components is condensed. That means it is important to have as much DME in the gas as possible because then the condense process takes place at higher temperatures and less energy is needed to cool the gas.

Calculations of probable gas compositions was made with the EES simulation. SPECS was then used to calculate what temperatures was needed to condense certain percentages of either DME or methanol.

Two different compositions was chosen to evaluate the different parameters in this process. One calculated from *mixed pills* and one from *separate synthesis* (see section 2.4)

Figure B.4 and B.4 shows that more DME in the gas means the condensation process takes place at higher temperatures.

Component	Per cent
CO	11,53
H2	30,45
CH4	1,69
H2O	0,14
N2	44,8
CO2	6,55
Methanol	0,17
DME	4,67

Figure B.2: Composition 1

Component	Per cent
CO	2,57
H2	22,21
CH4	1,96
H2O	1,06
N2	51,94
CO2	10,42
Methanol	0,70
DME	9,14

Figure B.3: Composition 2

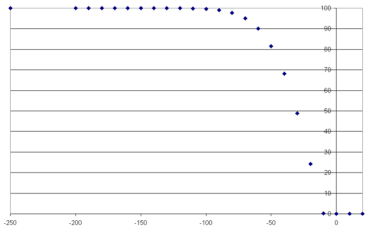

Figure B.4: Condensed with composition 1

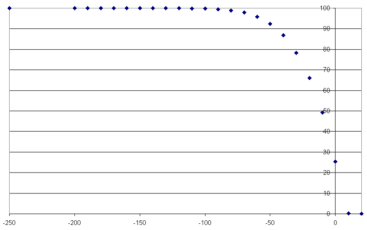

Figure B.5: Condensed with composition 2

From figure B.6 it can be seen that higher pressure means that a higher percentage will condense.

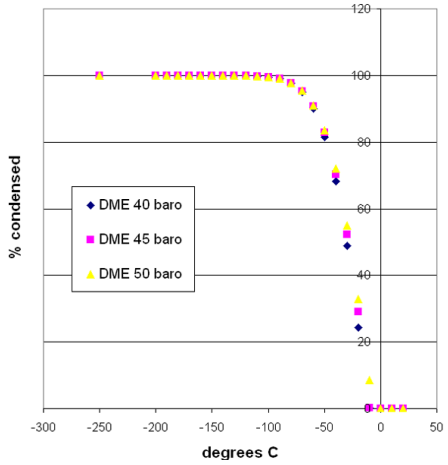

Figure B.6: In the temperature ranges where DME is condensed, larger pressure raises the percentage

At these very low temperatures the calculations shows that CO_2 will condense as well, however at lower percentages (figure B.7).

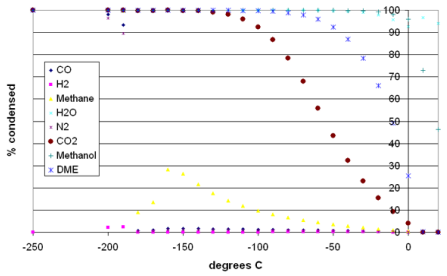

Figure B.7: The condense process for all the components

B.0.3 NASA Verification

THERMODYNAMIC FUNCTIONS CALCULATED FROM COEFFICIENTS FOR CH3OH

T	Cp	H-H298	S	-(G-H298)/T	H	delta Hf	log K
deg-K	J/mol-K	kJ/mol	J/mol-K	J/mol-K	kJ/mol	kJ/mol	
0	0.	-11.435	0.	INFINITE	-212.375	-190.046	INFINITE
500	59.683	10.424	266.158	245.310	-190.516	-207.690	14.0012
505	60.077	10.723	266.754	245.520	-190.217	-207.835	13.7863
510	60.468	11.025	267.348	245.731	-189.915	-207.978	13.5754
515	60.858	11.328	267.939	245.943	-189.612	-208.120	13.3686
520	61.246	11.633	268.529	246.158	-189.307	-208.260	13.1655
525	61.633	11.940	269.117	246.374	-189.000	-208.400	12.9662
530	62.017	12.250	269.703	246.591	-188.690	-208.538	12.7706
535	62.400	12.561	270.287	246.810	-188.379	-208.676	12.5784
540	62.781	12.874	270.870	247.030	-188.066	-208.812	12.3897

THERMODYNAMIC FUNCTIONS CALCULATED FROM COEFFICIENTS FOR CH3OCH3

T	Cp	H-H298	S	-(G-H298)/T	H	delta Hf	log K
deg-K	J/mol-K	kJ/mol	J/mol-K	J/mol-K	kJ/mol	kJ/mol	
0	0.	-14.354	0.	INFINITE	-198.464	-166.613	INFINITE
500	92.921	16.022	307.813	275.769	-168.088	-193.511	6.4742
505	93.565	16.488	308.741	276.091	-167.622	-193.708	6.2739
510	94.207	16.958	309.666	276.415	-167.152	-193.903	6.0774
515	94.845	17.430	310.588	276.742	-166.680	-194.097	5.8845
520	95.480	17.906	311.508	277.072	-166.204	-194.289	5.6951
525	96.112	18.385	312.424	277.405	-165.725	-194.479	5.5092
530	96.740	18.867	313.338	277.739	-165.243	-194.667	5.3265
535	97.365	19.353	314.250	278.076	-164.757	-194.853	5.1472
540	97.987	19.841	315.158	278.415	-164.269	-195.038	4.9709

THERMODYNAMIC FUNCTIONS CALCULATED FROM COEFFICIENTS FOR CO

T	Cp	H-H298	S	-(G-H298)/T	H	delta Hf	log K
deg-K	J/mol-K	kJ/mol	J/mol-K	J/mol-K	kJ/mol	kJ/mol	
0	0.	-8.671	0.	INFINITE	-119.206	-113.813	INFINITE
500	29.794	5.931	212.837	200.975	-104.604	-110.013	16.2370
505	29.822	6.080	213.133	201.094	-104.455	-110.016	16.1232
510	29.851	6.229	213.427	201.213	-104.306	-110.018	16.0117
515	29.881	6.378	213.719	201.333	-104.157	-110.022	15.9023
520	29.910	6.528	214.007	201.454	-104.007	-110.026	15.7950
525	29.941	6.677	214.294	201.575	-103.858	-110.030	15.6897
530	29.971	6.827	214.578	201.696	-103.708	-110.035	15.5864
535	30.003	6.977	214.859	201.818	-103.558	-110.041	15.4851
540	30.034	7.127	215.139	201.940	-103.408	-110.047	15.3856

THERMODYNAMIC FUNCTIONS CALCULATED FROM COEFFICIENTS FOR CO2

T	Cp	H-H298	S	-(G-H298)/T	H	delta Hf	log K
deg-K	J/mol-K	kJ/mol	J/mol-K	J/mol-K	kJ/mol	kJ/mol	
0	0.	-9.365	0.	INFINITE	-402.875	-393.142	INFINITE
500	44.624	8.307	234.898	218.284	-385.203	-393.655	41.2565
505	44.772	8.530	235.342	218.451	-384.980	-393.660	40.8493
510	44.918	8.755	235.784	218.618	-384.755	-393.666	40.4502
515	45.063	8.980	236.223	218.787	-384.530	-393.672	40.0587
520	45.207	9.205	236.659	218.957	-384.305	-393.678	39.6748
525	45.349	9.432	237.093	219.128	-384.078	-393.684	39.2982
530	45.489	9.659	237.523	219.299	-383.851	-393.690	38.9287
535	45.629	9.887	237.951	219.471	-383.623	-393.696	38.5660
540	45.766	10.115	238.376	219.645	-383.395	-393.703	38.2101

THERMODYNAMIC FUNCTIONS CALCULATED FROM COEFFICIENTS FOR H2O

T	Cp	H-H298	S	-(G-H298)/T	H	delta Hf	log K
deg-K	J/mol-K	kJ/mol	J/mol-K	J/mol-K	kJ/mol	kJ/mol	
0	0.	-9.904	0.	INFINITE	-251.730	-238.922	INFINITE
500	35.225	6.925	206.529	192.680	-234.901	-243.827	22.8831
505	35.277	7.101	206.880	192.819	-234.725	-243.874	22.6309
510	35.330	7.278	207.228	192.958	-234.548	-243.922	22.3835
515	35.383	7.454	207.573	193.099	-234.372	-243.970	22.1410
520	35.436	7.631	207.915	193.239	-234.195	-244.017	21.9030
525	35.490	7.809	208.254	193.381	-234.017	-244.064	21.6695
530	35.544	7.986	208.591	193.523	-233.840	-244.112	21.4404
535	35.598	8.164	208.925	193.665	-233.662	-244.159	21.2156
540	35.653	8.342	209.257	193.808	-233.484	-244.205	20.9948

THERMODYNAMIC FUNCTIONS CALCULATED FROM COEFFICIENTS FOR H2

T	Cp	H-H298	S	-(G-H298)/T	H	delta Hf	log K
deg-K	J/mol-K	kJ/mol	J/mol-K	J/mol-K	kJ/mol	kJ/mol	
0	0.	-8.468	0.	INFINITE	-8.468	0	INFINITE
500	29.254	5.883	145.740	133.975	5.883	0	0
505	29.256	6.029	146.031	134.093	6.029	0	0
510	29.258	6.175	146.319	134.211	6.175	0	0
515	29.260	6.321	146.605	134.330	6.321	0	0
520	29.263	6.468	146.888	134.450	6.468	0	0
525	29.265	6.614	147.168	134.570	6.614	0	0
530	29.268	6.760	147.445	134.690	6.760	0	0
535	29.271	6.907	147.720	134.810	6.907	0	0
540	29.273	7.053	147.992	134.931	7.053	0	0

B.1 Fugacity coefficients in the condense process at 40 baro

Component	Composition	Specs	Fugacity	% diversion fror
Co	0.0257	-0.0058	0.994217	
H2	0.2221	0.0678	1.070151	7.015125
Methane	0.0196	-0.0777	0.925242	7.47580
H2o	0.0106	-0.4027	0.668513	33.1487
N2	0.5194	0.0013	1.001301	0.130084
Co2	0.1042	-0.1833	0.832518	16.74816
Methanol	0.007	-0.5195	0.594818	40.51821
DME	0.0914	-0.3675	0.692463	30.75366

Figure B.8: The fugacity coef. at 10° C

Component	Composition	Specs	Fugacity	% diversion from 1
Co	0.0257	-0.0103	0.989753	1.024713665
H2	0.2221	0.074	1.076807	7.68068055
Methane	0.0196	-0.0893	0.914571	8.542883893
H2o	0.0106	-0.4478	0.639032	36.09675223
N2	0.5194	-0.0023	0.997703	0.229735703
Co2	0.1042	-0.2074	0.812695	18.73054928
Methanol	0.007	-0.5832	0.55811	44.18904446
DME	0.0914	-0.4135	0.661332	33.86684656

Figure B.9: The fugacity coef. at 0° C

Component	Composition	Specs	Fugacity	% diversion fron
Co	0.0257	-0.0156	0.984521	1.547895
H2	0.2221	0.0813	1.084696	8.469625
Methane	0.0196	-0.1028	0.902307	9.769258
H2o	0.0106	-0.5	0.606531	39.34693
N2	0.5194	-0.0066	0.993422	0.657826
Co2	0.1042	-0.2354	0.790255	20.97453
Methanol	0.007	-0.6572	0.518301	48.16994
DME	0.0914	-0.4667	0.627068	37.29318

Figure B.10: The fugacity coef. at −10° C

Component	Composition	Specs	Fugacity	% diversion from 1
Co	0.0257	-0.0219	0.978338	2.166193603
H2	0.2221	0.0899	1.094065	9.406487175
Methane	0.0196	-0.1185	0.888252	11.17481843
H2o	0.0106	-0.5609	0.570695	42.9304793
N2	0.5194	-0.0116	0.988467	1.15329794
Co2	0.1042	-0.2681	0.764831	23.51687059
Methanol	0.007	-0.7437	0.475352	52.46481441
DME	0.0914	-0.5288	0.589312	41.06882804

Figure B.11: The fugacity coef. at −20° C

Component	Composition	Specs	Fugacity	% diversion fron
Co	0.0257	-0.0292	0.971222	2.87777
H2	0.2221	0.1002	1.105392	10.53919
Methane	0.0196	-0.137	0.87197	12.80297
H2o	0.0106	-0.6323	0.531368	46.86317
N2	0.5194	-0.0176	0.982554	1.744602
Co2	0.1042	-0.3066	0.735945	26.405
Methanol	0.007	-0.8459	0.429171	57.08290
DME	0.0914	-0.6021	0.54766	45.23396

Figure B.12: The fugacity coef. at −30° C

Component	Composition	Specs	Fugacity	% diversion from 1
Co	0.0257	-0.038	0.962713	3.728705911
H2	0.2221	0.1128	1.119408	11.9408029
Methane	0.0196	-0.1588	0.853167	14.68330247
H2o	0.0106	-0.7173	0.488068	51.19317371
N2	0.5194	-0.0245	0.975798	2.420231108
Co2	0.1042	-0.3525	0.702929	29.70714302
Methanol	0.007	-0.9678	0.379918	62.00820612
DME	0.0914	-0.6893	0.501927	49.80727048

Figure B.13: The fugacity coef. at −40° C

Component	Composition	Specs	Fugacity	% diversion fron
Co	0.0257	-0.0483	0.952848	4.715211
H2	0.2221	0.1285	1.137121	13.71214
Methane	0.0196	-0.1849	0.831187	16.88126
H2o	0.0106	-0.8198	0.44052	55.94802
N2	0.5194	-0.0328	0.967732	3.226791
Co2	0.1042	-0.4078	0.665112	33.48881
Methanol	0.007	-11.154	0	
DME	0.0914	-0.7946	0.451762	54.82380

Figure B.14: The fugacity coef. at −50° C

Component	Composition	Specs	Fugacity	% diversion from 1
Co	0.0257	-0.0606	0.9412	5.880035565
H2	0.2221	0.1486	1.160209	16.02088129
Methane	0.0196	-0.2165	0.805333	19.46674651
H2o	0.0106	-0.9454	0.388524	61.14758698
N2	0.5194	-0.0424	0.958486	4.151369064
Co2	0.1042	-0.4756	0.621512	37.84879627
Methanol	0.007	-12.971	0	100
DME	0.0914	-0.9239	0.396968	60.30321564

Figure B.15: The fugacity coef. at −60° C

Component	Composition	Specs	Fugacity	% diversion fron
Co	0.0257	-0.0751	0.927651	7.234928
H2	0.2221	0.1751	1.191365	19.13653
Methane	0.0196	-0.2554	0.774607	22.53934
H2o	0.0106	-11.033	0	
N2	0.5194	-0.0537	0.947716	5.228362
Co2	0.1042	-0.5605	0.570924	42.90764
Methanol	0.007	-15.264	0	
DME	0.0914	-10.864	0	

Figure B.16: The fugacity coef. at -70° C

Component	Composition	Specs	Fugacity	% diversion from 1
Co	0.0257	-0.0924	0.91174	8.825961956
H2	0.2221	0.2122	1.236395	23.63951394
Methane	0.0196	-0.3043	0.73764	26.23604586
H2o	0.0106	-13.087	0	100
N2	0.5194	-0.0666	0.935569	6.443064576
Co2	0.1042	-0.67	0.511709	48.82914222
Methanol	0.007	-18.258	0	100
DME	0.0914	-12.974	0	100

Figure B.17: The fugacity coef. at -80° C

Component	Composition	Specs	Fugacity	% diversion from
Co	0.0257	-0.112	0.894044	10.595574
H2	0.2221	0.2684	1.30787	30.787018
Methane	0.0196	-0.3682	0.691979	30.802122
H2o	0.0106	-15.920	0	1
N2	0.5194	-0.0803	0.922839	7.716054
Co2	0.1042	-0.819	0.440872	55.912769
Methanol	0.007	-22.402	0	1
DME	0.0914	-15.875	0	1

Figure B.18: The fugacity coef. at -90° C

Component	Composition	Specs	Fugacity	% diversion from 1
Co	0.0257	-0.1312	0.877042	12.29576516
H2	0.2221	0.3697	1.4473	44.73003594
Methane	0.0196	-0.458	0.632547	36.74525238
H2o	0.0106	-20.350	0	100
N2	0.5194	-0.0899	0.914023	8.597741704
Co2	0.1042	-10.453	0	100
Methanol	0.007	-28.903	0	100
DME	0.0914	-20369.	0	100

Figure B.19: The fugacity coef. at -100° C

B.2 Fugacity coefficients in the gaseous phase

The compositions mix1 and mix2 originates from the typical gas composition from the Viking gasifier defined by Henrik Iversen. This composition is assumed saturated with water at 10 degrees C and the CO_2 content is lowered to 4 %. This composition is used as input in the 2 different DME models. Separate reactors gives mix1 and mixed pills gives mix2 as results after synthesis.

Composition	Mix 1 (%)	Mix 2 (%)
Co2	11.53	2.57
H2	30.45	22.21
Methane	1.69	1.96
H2O	0.14	1.06
N2	44.8	51.94
CO2	6.55	10.42
Methanol	0.17	0.7
DME	4.67	9.14

Figure B.20: The gas compositions

	% divertion from 1	% divertion from 1	% divertion fro
Co2	1.887593998	2.132417895	2.377830
H2	1.857032304	2.08136445	2.316421
Methane	0.672249521	0.772972124	0.863708
H2O	5.000637031	5.57836927	6.152588
N2	1.938550533	2.193715733	2.439275
CO2	0.657826784	0.727341972	0.786887
Methanol	4.170536873	4.638952687	5.095588
DME	2.009534219	2.224876281	2.429988
Total deviation	18.19396126	20.35001041	22.46228

Figure B.21: The coef. at 220° C Mix 1

	% divertion from 1	% divertion from 1	% divertion from 1
Co2	1.918164862	2.163062217	2.408548031
H2	1.714532233	1.928357188	2.152846421
Methane	0.904062177	1.025219732	1.156637921
H2O	3.940269952	4.400251817	4.848516386
N2	1.948744898	2.203935616	2.449519644
CO2	0.159872068	0.169855582	0.179838097
Methanol	2.858353553	3.188074308	3.497377322
DME	1.044506743	1.15329794	1.252095235
Total deviation	14.48850649	16.2320544	17.94537906

Figure B.22: The coef. at 250° C Mix 1

	% divertion from 1	% divertion from 1	% divertion fro
Co2	1.928357188	2.173279034	2.418789
H2	1.602707762	1.806116518	2.009932
Methane	1.075744972	1.217350116	1.359153
H2O	3.081522597	3.449113946	3.805692
N2	1.938550533	2.193715733	2.439275
CO2	0.220242178	0.250312761	0.290420
Methanol	1.832992541	2.03892695	2.234653
DME	0.29955045	0.309519996	0.319488
Total deviation	11.97966822	13.43833505	14.87740

Figure B.23: The coef. at 280° C Mix 1

	40 baro	45 baro	50 baro
	% divertion from 1	% divertion from 1	% divertion from 1
Co2	2.04054007	2.295960563	2.56227612
H2	2.234601396	2.521259414	2.798440841
Methane	0.41084165	0.471106232	0.531406985
H2O	6.56460957	7.327647043	8.075261177
N2	2.122205164	2.38806837	2.664889695
CO2	1.281715163	1.429681588	1.56758348
Methanol	6.13381671	6.835179686	7.512806527
DME	3.622749222	4.036281668	4.42892744
Total deviation	24.41107895	27.30518456	30.14159226

Figure B.24: The coef. at 220° C Mix 2

	% divertion from 1	% divertion from 1	% divertion fro
Co2	2.050744634	2.30619067	2.5725328
H2	2.030336526	2.285731478	2.5315120
Methane	0.682317249	0.772972124	0.8737954
H2O	5.275736097	5.889447091	6.49918
N2	2.101782765	2.377830075	2.644358
CO2	0.687624966	0.757119302	0.826565
Methanol	4.51490271	5.029132565	5.5405930
DME	2.420231108	2.683341126	2.9457417
Total deviation	19.76367606	22.10176443	24.434280

Figure B.25: The coef. at 250° C Mix 2

	% divertion from 1	% divertion	% divertion from 1
Co2	2.04054007	2.2959606	2.56228
H2	1.857032304	2.0813645	2.31642
Methane	0.883883383	0.9949167	1.11618
H2O	4.237594025	4.7342661	5.21888
N2	2.08136445	2.3368871	2.60331
CO2	0.219758177	0.2397122	0.24969
Methanol	3.226791335	3.6034718	3.95948
DME	1.469101831	1.6266252	1.77407
Total deviation	16.01606558	17.913204	19.8003

Figure B.26: The coef. at 280° C Mix 2

B.3 Comparison between SRK and PR equation of state

T	DME	% Liquid frac		% condens	
20	1.2E-05	0.0012	0.000827	1E-06	2.12505E-
10	1.1E-05	0.0011	0.00112	1E-06	2.63812E-
0	1.4E-05	0.0014	0.001303	2E-06	3.90621E-
-10	0.02015	2.0152	0.002661	0.0054	0.1148275
-20	0.68862	68.8621	0.016496	1.1359	24.324394
-30	0.72439	72.4391	0.03147	2.2797	48.814956
-40	0.70727	70.7267	0.045008	3.1833	68.16418
-50	0.66712	66.7124	0.057095	3.8089	81.561980
-60	0.61226	61.2256	0.068715	4.2071	90.088160

Figure B.27: The PR equation of state Mix 1

T	DME	% Liquid frac		% condensed	
20	1.4E-05	0.0014	0.00072	1E-06	2.15846E-05
10	1.2E-05	0.0012	0.001054	1E-06	2.70835E-05
0	1.3E-05	0.0013	0.001255	2E-06	3.49358E-05
-10	0.02023	2.023	0.00255	0.0052	0.110463597
-20	0.67246	67.2459	0.014929	1.0039	21.49708867
-30	0.71747	71.7473	0.029899	2.1452	45.93517179
-40	0.70318	70.3176	0.043746	3.0761	65.86967301
-50	0.66482	66.4816	0.056137	3.7321	79.91600812
-60	0.61153	61.1529	0.067968	4.1564	89.00300444

Figure B.28: The SRK equation of state Mix 1

B.4 Calculation of Carbo V gasifier composition

	Composition
CO	9.45
H2	14.47
Methane	0.27
H2O	0.76
N2	0.54
CO2	42.23
Methano	1.1
DME	31.18

Figure B.29: The Carbo V gas compositions in percent

T	with kij	with out kij	% divercity with	% divercity without kij
20	26.134	26.14761	83.81650696	83.86019246
10	28.111	28.11969	90.15768535	90.18500985
0	29.344	29.34779	94.11038586	94.12376699
-10	30.091	30.09343	96.50895264	96.51517295
-20	30.539	30.53961	97.94491657	97.94614241
-30	30.806	30.80558	98.80054067	98.79916795
-40	30.965	30.9639	99.309058	99.30692628
-50	31.058	31.05766	99.60963378	99.60764155
-60	31.113	31.11262	99.78569543	99.78390232
-70	31.145	31.14427	99.88648013	99.88542042
-80	31.162	31.16188	99.94252145	99.94189752

Figure B.30: Percent condensed DME with and without k_{ij}

B.5 Calculation of Güssing gasifier composition

	Composition
CO	3.08
H2	27.61
Methane	23.56
H2O	2.22
N2	6.08
CO2	21.19
Methanol	1.3
DME	14.96

Figure B.31: The Güssing gas compositions in percent

T	with kij	with out kij	% divercity with kij	% divercity without kij
20	6.093648	5.5536335	40.73294315	37.12321854
10	8.66399	8.4499811	57.91437231	56.48383058
0	10.65941	10.539404	71.25271786	70.45055861
-10	12.14318	12.070139	81.17099124	80.68274433
-20	13.19199	13.147739	88.1817465	87.88595908
-30	13.89497	13.869651	92.88080893	92.71157415
-40	14.34183	14.328637	95.86781968	95.7796561
-50	14.61371	14.606935	97.68522888	97.63994188
-60	14.77261	14.769187	98.74739358	98.72451083
-70	14.86258	14.860723	99.34881622	99.33638574
-80	14.91188	14.910749	99.67837311	99.67078171

Figure B.32: Percent condensed DME with and without k_{ij}

B.6 Comparison between SRK and the model for methanol condensation

	Composition
CO	17.74
H2	28.44
Methane	1.48
H2O	0.11
N2	41.5
CO2	5.63
Methanol	5.1

Figure B.33: The gas composition to be compared

T	with kij	with out kij
50	68.077	67.263013
45	74.584	73.862994
40	79.928	79.304171
35	84.286	83.755167
30	87.81	87.366642
25	90.637	90.271253
20	92.885	92.586739
15	94.652	94.41368
10	96.028	95.839085
5	98.039	96.94011
0	97.893	97.77996
-5	98.498	98.411729
-10	98.945	98.879357
-15	99.271	99.223734
-20	99.506	99.470629

Figure B.34: Percent condensed methanol with and without k_{ij}

B.7 Methanol condensation process with different pressures

There is 5.705% methanol i the gas.

T	Methanol	% condensed
30	5.08498	89.132
25	5.22888	91.6543
20	5.34315	93.6573
15	5.43306	95.2334
10	5.5031	96.4611
5	5.55696	97.405
0	5.59788	98.1224
-5	5.62862	98.6612
-10	5.65137	99.06
-15	5.66798	99.3511

Figure B.35: 40 baro

T	Methanol	% condensed
30	5.13166	89.9503
25	5.26384	92.2671
20	5.36911	94.1123
15	5.45204	95.566
10	5.51672	96.6997
5	5.56662	97.5745
0	5.6046	98.2402
-5	5.63328	98.7428
-10	5.65444	99.1138
-15	5.66993	99.3854

Figure B.36: 45 baro

T	Methanol	% condensed
30	5.16833	90.593
25	5.29128	92.7481
20	5.38935	94.4671
15	5.46673	95.8234
10	5.52727	96.8847
5	5.57406	97.7049
0	5.60974	98.3303
-5	5.63672	98.8032
-10	5.65679	99.155
-15	5.67147	99.4122

Figure B.37: 50 baro

B.8 Amount of liquid at different pressures

T	Fraction_g	Fraction_l	% liquid
20	0.000827	0.999173	0.0827
10	0.00112	0.99888	0.112
0	0.001303	0.998697	0.1303
-10	0.002661	0.997339	0.2661
-20	0.016496	0.983504	1.6496
-30	0.03147	0.96853	3.147
-40	0.045008	0.954992	4.5008
-50	0.057095	0.942905	5.7095
-60	0.068715	0.931285	6.8715
-70	0.080541	0.919459	8.0541
-80	0.092156	0.907844	9.2156
-90	0.102288	0.897712	10.2288
-100	0.109997	0.890003	10.9997
-110	0.115249	0.884751	11.5249
-120	0.118605	0.881395	11.8605
-130	0.120787	0.879213	12.0787
-140	0.122437	0.877563	12.2437
-150	0.123984	0.876016	12.3984

Figure B.38: % liquid in the gas at 40 baro

T	Fraction_g	Fraction_l	% liquid
20	0.000908	0.999092	0.0908
10	0.001163	0.998837	0.1163
0	0.002162	0.997838	0.2162
-10	0.007408	0.992592	0.7408
-20	0.02196	0.97804	2.196
-30	0.036388	0.963612	3.6388
-40	0.049329	0.950671	4.9329
-50	0.061158	0.938842	6.1158
-60	0.072689	0.927311	7.2689
-70	0.084245	0.915755	8.4245
-80	0.095221	0.904779	9.5221
-90	0.104547	0.895453	10.4547
-100	0.11159	0.88841	11.159
-110	0.116429	0.883571	11.6429
-120	0.119573	0.880427	11.9573
-130	0.121626	0.878374	12.1626
-140	0.123077	0.876923	12.3077
-150	0.124089	0.875911	12.4089

Figure B.39: % liquid in the gas at 50 baro

B.9 Condense process with all the components mix 1

Mix 1 references to the gas composition described in B.20

T	Co	H2	Methane	H2o	N2	Co2	Methanol	DME
20	0	1.82E-07	0	0.0897	9E-08	2E-05	0.00111	1E-06
10	0	2.33E-07	0	0.1139	1E-07	2E-05	0.00237	2E-06
0	8.9E-06	1.62E-05	9E-06	0.1238	3E-05	0.0019	0.08826	0.0022
-10	0.00225	0.002185	0.0014	0.1101	0.0078	0.0681	0.15019	0.3988
-20	0.01342	0.011955	0.0075	0.1255	0.0465	0.2934	0.16362	1.5342
-30	0.02563	0.020767	0.0147	0.134	0.0882	0.6172	0.16783	2.5705
-40	0.03712	0.026973	0.0227	0.1375	0.1266	1.0524	0.16923	3.3604
-50	0.04811	0.030946	0.0316	0.139	0.1625	1.629	0.16973	3.9049
-60	0.05937	0.033299	0.0423	0.1396	0.1984	2.3736	0.16991	4.2524
-70	0.07124	0.034279	0.0556	0.1399	0.2352	3.2617	0.16997	4.4567
-80	0.08324	0.033699	0.0717	0.14	0.2711	4.1854	0.16999	4.567
-90	0.09445	0.03149	0.0907	0.14	0.303	5.0025	0.16999	4.6225
-100	0.1044	0.028009	0.1129	0.14	0.3294	5.6252	0.17	4.6491
-110	0.11344	0.023845	0.1391	0.14	0.3512	6.044	0.17	4.6613
-120	0.1223	0.019586	0.1713	0.14	0.371	6.2964	0.17	4.6666
-130	0.13181	0.015617	0.2119	0.14	0.3909	6.4336	0.17	4.6688
-140	0.14208	0.01216	0.262	0.14	0.4114	6.5005	0.16999	4.6696
-150	0.1504	0.009294	0.3146	0.14	0.4254	6.5294	0.17	4.6698
-160	0.14068	0.007204	0.319	0.14	0.3928	6.5385	0.17	4.6699
-170	0.09318	0.005965	0.1992	0.14	0.265	6.5328	0.17	4.6695

Figure B.40: Amount condensed

T	Co	H2	Methane	H2o	N2	Co2	Methanol	DME
20	0	5.96E-07	0	64.048	2E-07	0.0003	0.65499	3E-05
10	0	7.64E-07	0	81.357	3E-07	0.0004	1.39676	3E-05
0	7.7E-05	5.33E-05	0.0006	88.425	7E-05	0.0286	51.9152	0.0474
-10	0.01949	0.007177	0.0819	78.669	0.0174	1.0399	88.3448	8.5388
-20	0.11637	0.039261	0.4413	89.642	0.1037	4.4793	96.2494	32.852
-30	0.22227	0.068199	0.872	95.708	0.1968	9.4231	98.7206	55.042
-40	0.3219	0.088582	1.3409	98.221	0.2826	16.067	99.5488	71.957
-50	0.41729	0.101629	1.8691	99.277	0.3628	24.87	99.8422	83.616
-60	0.51488	0.109356	2.5028	99.724	0.4429	36.238	99.9474	91.058
-70	0.61785	0.112576	3.2875	99.903	0.525	49.797	99.9839	95.432
-80	0.72196	0.110669	4.2438	99.968	0.6052	63.899	99.9933	97.794
-90	0.81915	0.103414	5.369	99.992	0.6764	76.374	99.9961	98.983
-100	0.9055	0.091984	6.6782	100	0.7352	85.882	99.9978	99.553
-110	0.98384	0.078308	8.2306	99.996	0.784	92.274	99.9988	99.814
-120	1.0607	0.064322	10.138	99.997	0.8281	96.129	99.9982	99.928
-130	1.14316	0.051287	12.538	100	0.8726	98.223	99.998	99.974
-140	1.23226	0.039934	15.5	100	0.9184	99.244	99.9964	99.99
-150	1.30439	0.030523	18.614	99.998	0.9496	99.685	100.001	99.996
-160	1.2201	0.023659	18.877	99.997	0.8769	99.824	100	99.998
-170	0.80812	0.019591	11.789	100	0.5915	99.737	100.001	99.99

Figure B.41: % condensed

B.10 Condense process with all the components mix 2

Mix 2 references to the gas composition described in B.20

T	Co	H2	Methane	H2o	N2	Co2	Methanol	DME
20	4E-06	3.1E-05	1.9E-05	0.9922	6.4E-05	0.00452	0.32592	0.00334
10	7.8E-06	5.4E-05	4E-05	1.01974	0.00014	0.01041	0.51277	0.01144
0	0.0023	0.00796	0.00712	0.97917	0.04174	0.4208	0.67384	2.32407
-10	0.0062	0.01949	0.01835	1.01123	0.11215	0.96664	0.69043	4.50003
-20	0.00957	0.02745	0.02922	1.03328	0.17234	1.59951	0.69761	6.03379
-30	0.01271	0.03287	0.0408	1.04511	0.2269	2.38888	0.70078	7.15736
-40	0.01571	0.03624	0.05377	1.05108	0.27798	3.36604	0.70212	7.93848
-50	0.01871	0.03799	0.06889	1.05392	0.32774	4.53004	0.70268	8.44994
-60	0.02173	0.03827	0.08683	1.05518	0.37634	5.81265	0.7029	8.76342
-70	0.02463	0.037	0.10787	1.05571	0.42153	7.07682	0.70298	8.94328
-80	0.02729	0.03424	0.13206	1.0559	0.46032	8.17737	0.703	9.04063
-90	0.02959	0.03035	0.15978	1.05597	0.49148	9.02966	0.703	9.09079
-100	0.03162	0.02586	0.19223	1.05599	0.5161	9.62447	0.70299	9.11552
-110	0.03354	0.02125	0.23155	1.056	0.537	10.0016	0.703	9.12698
-120	0.0356	0.01692	0.28089	1.056	0.55746	10.2191	0.70299	9.132
-130	0.03796	0.01308	0.34414	1.05599	0.5804	10.3325	0.70299	9.13398
-140	0.04074	0.00984	0.42432	1.056	0.60699	10.3854	0.70301	9.13469
-150	0.04356	0.00724	0.51609	1.05599	0.63152	10.4072	0.703	9.13491
-160	0.04263	0.00549	0.55379	1.05601	0.60731	10.414	0.70301	9.13496
-170	0.02464	0.00591	0.26728	1.05599	0.3682	10.3997	0.70301	9.13396

Figure B.42: Amount condensed

T	Co	H2	Methane	H2o	N2	Co2	Methanol	DME
20	0.00016	0.00014	0.00095	93.9582	0.00012	0.04341	46.3612	0.03658
10	0.0003	0.00024	0.00206	96.5663	0.00028	0.09987	72.9404	0.12515
0	0.08949	0.03584	0.36315	92.7246	0.08035	4.03842	95.8521	25.4275
-10	0.24158	0.08776	0.93612	95.7602	0.21587	9.27674	98.2119	49.2345
-20	0.37326	0.12361	1.49088	97.8485	0.33174	15.3504	99.2339	66.0153
-30	0.49544	0.14798	2.08187	98.969	0.43676	22.9259	99.6843	78.3081
-40	0.61259	0.16316	2.74314	99.5338	0.53509	32.3036	99.8755	86.8542
-50	0.72959	0.17105	3.5146	99.8031	0.63087	43.4745	99.9552	92.4502
-60	0.84714	0.17229	4.4302	99.9226	0.72443	55.7836	99.9856	95.8799
-70	0.96039	0.16658	5.50344	99.9728	0.81142	67.9157	99.9965	97.8477
-80	1.06381	0.15415	6.73757	99.9907	0.88609	78.4776	99.9998	98.9128
-90	1.15356	0.13665	8.1522	99.997	0.94606	86.657	100.001	99.4616
-100	1.23278	0.11643	9.80785	99.9989	0.99345	92.3654	99.999	99.7321
-110	1.30773	0.0957	11.8136	99.9997	1.03368	95.9845	99.9998	99.8576
-120	1.38782	0.07618	14.3309	99.9999	1.07307	98.0717	99.9993	99.9125
-130	1.48007	0.05888	17.558	99.9991	1.11723	99.1599	99.9992	99.9341
-140	1.58837	0.0443	21.6491	99.9998	1.16841	99.6683	100.001	99.9419
-150	1.69821	0.03262	26.3313	99.9992	1.21562	99.8771	99.9996	99.9443
-160	1.6618	0.02474	28.2545	100.001	1.16903	99.9424	100.001	99.9448
-170	0.96053	0.0266	13.6368	99.9994	0.70877	99.8055	100.001	99.9339

Figure B.43: % condensed

Appendix C

Experiments

C.1 Test run

A test run was made to ensure that the facility has no leakages and it still could produce methanol from bottle gas. The output was not analyzed but it was flammable which should be good enough. (cf. brandtest under measuremnets!!!!)

C.1.1 Nitrogen test

Temperature settings: Heat blower_ in = 370 C, maximum air flow, Heat blower_cl = 350 C, maximum air flow Blæser_met = 270 C, level 5 air flow, Heat blower_låg = 110 C, level 6 air flow

These settings gave the correct temperature for purest methanol production(cf. henriks indstillinger!!!!!)

The pressure before the facility was 45 baro.

Facility pressure = 40 bar, T_oven 240 C

Flow = 30 p_in = 235 mbaro p-out = 0,008 baro

The start of the experiment: Volume meter before the compressor = 6,231 m^3, Volume meter on the residual gas = 0,771 m^3

The end of the experiment: Volume meter before the compressor = 6,714 m^3, Volume meter on the residual gas = 1,363 m^3

Time = 35 min 58,38 sek

C.1.2 Methanol test from bottle gas d. 29/3

Gas composition: CH4 = 1,88 % H2 = 36,0 % CO2 = 1,96 % CO = 22,3 %

Temperature settings: Heat blower_ind = 370 C, maximum air flow Blæser_cl = 320 C, maxi-

mum air flow, Heat blower_met = 250 C, maximum air flow, Heat blower_lid = 120 C, level 6 air flow

The start of the experiment: Volume meter before the compressor = 7,656 m^3, Volume meter on the residual gas = 2,446 m^3

he end of the experiment: Volume meter before the compressor = 8,258 m^3, Volume meter on the residual gas = 3,023 m^3

Time = 30 min 09,53 sek

Total methanol outcome: 14,60 g

C.2 Data collection

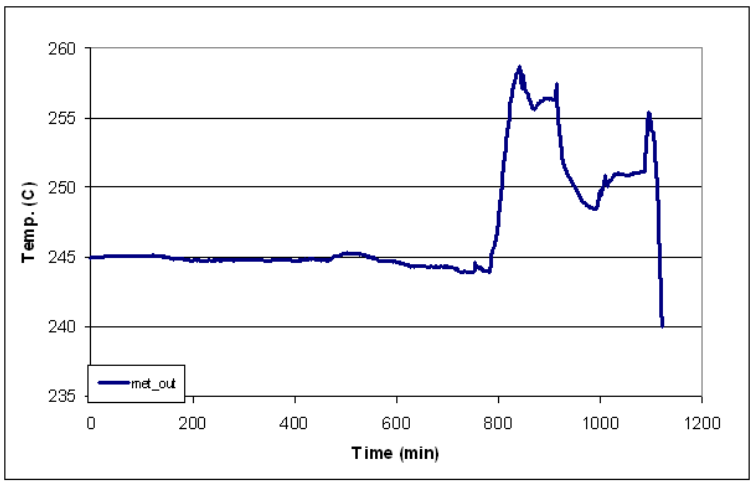

Figure C.1: The data from the methanol experiment

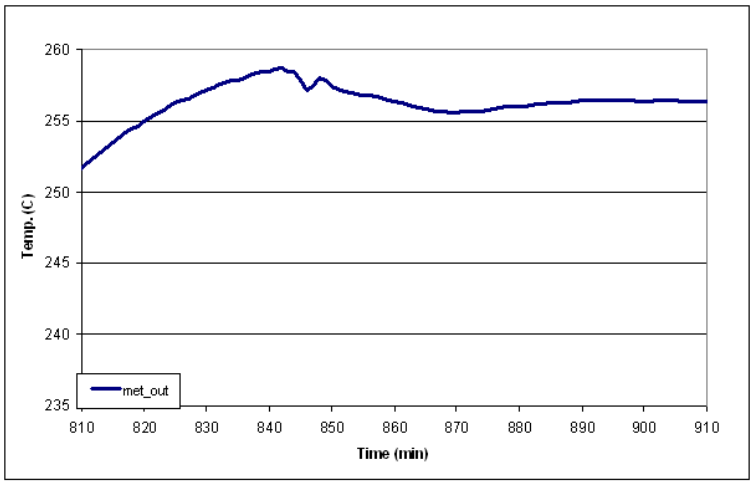

Figure C.2: The data from the flow experiment 1 + 2

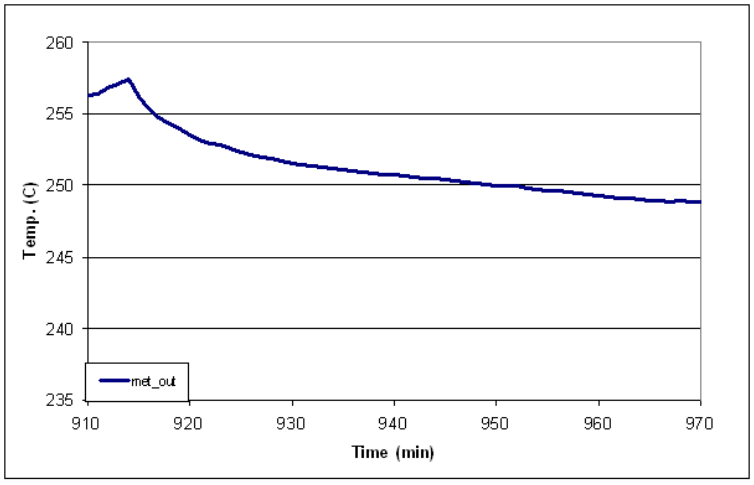

Figure C.3: The data from the flow experiment 3

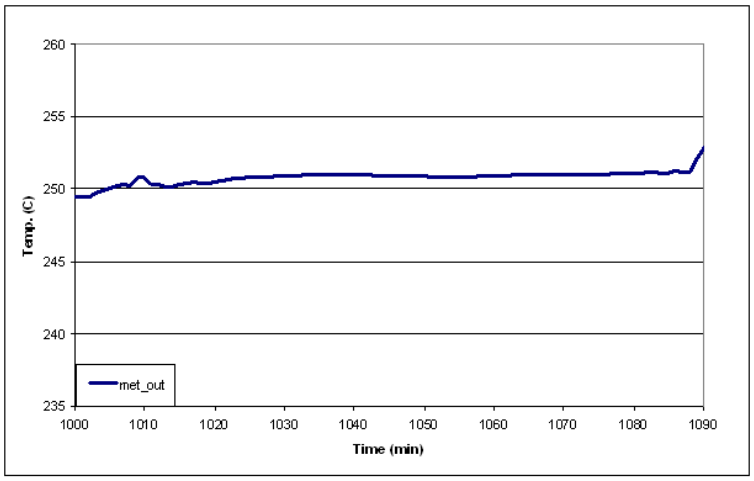

Figure C.4: The data from the flow experiment 4

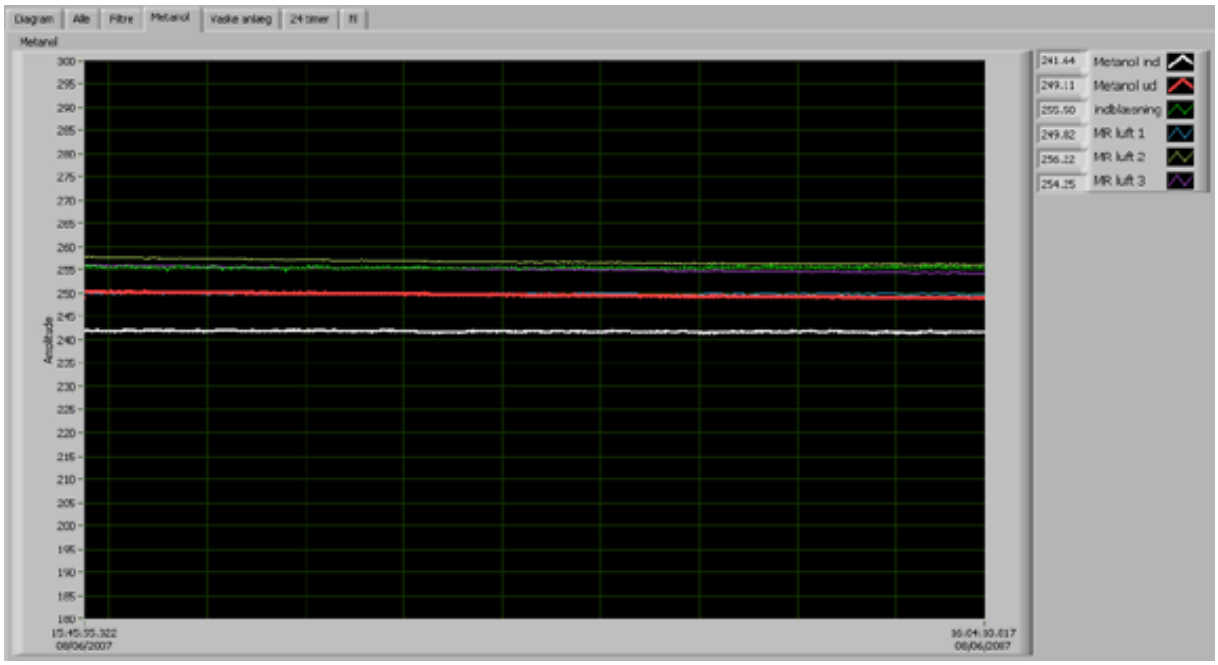

Figure C.5: Monitoring of the temperature

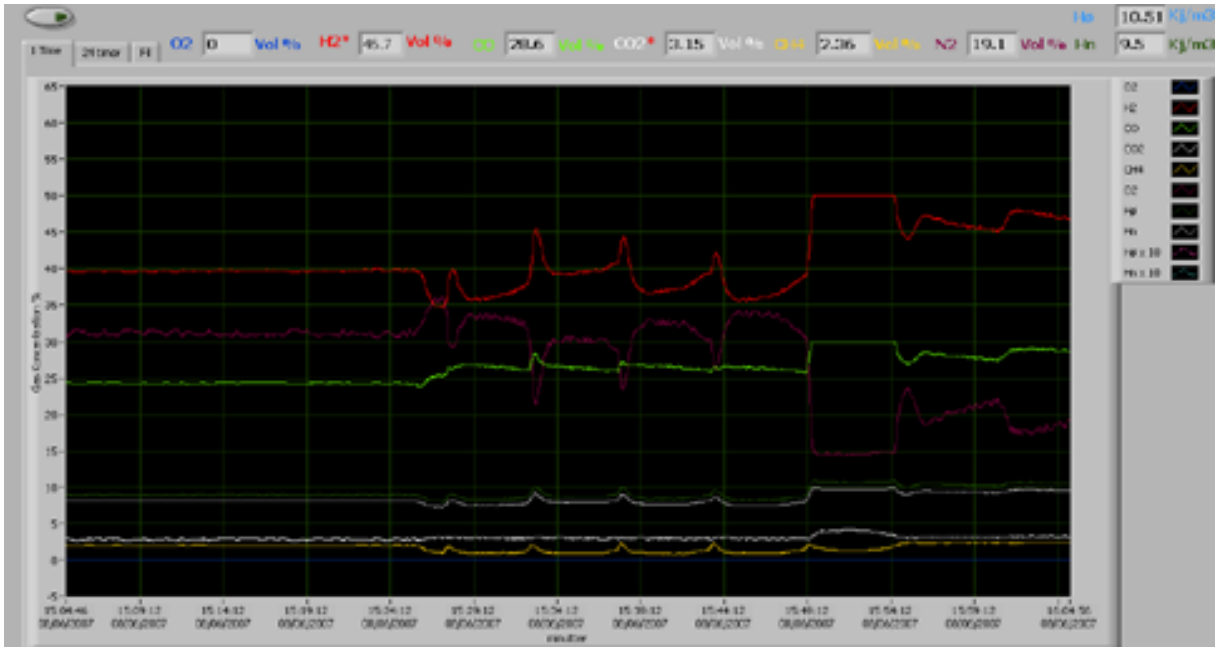

Figure C.6: Monitoring of the gas composition

C.3 Table of thermoelements

Name	Description
Top of oven	Temp. of the air in the top of the oven
Oven entre	Temp. of the injected air from a heat blower
Bottom of oven	Temp. of the air in the bottom of the oven
Top of Cl	Temp. of the gas opposite to the entry to the Cl reactor
Bottom of Cl	Temp. of the gas opposite to the exit to the Cl reactor
Top of sulphur	Temp. of the gas opposite to the entry to the sulphur reactor
Bottom of sulphur	Temp. of the gas opposite to the exit to the sulphur reactor
Top of LSK	Temp. of the gas opposite to the entry to the LSK reactor
Bottom of LSK	Temp. of the gas opposite to the exit to the LSK reactor
Top of the methanol	Temp. of the gas opposite to the entry to the methanol reactor
Bottom of the methanol	Temp. of the gas opposite to the exit to the methanol reactor
Metal jacket 1	Surface temp. of the top of the methanol reactor
Metal jacket 2	Surface temp. of the center of the methanol reactor
Metal jacket 3	Surface temp. of the bottom of the methanol reactor
Methanol container	Temp. in the top of the methanol container
Out of the compressor	Temp. on the outside of the gas outlet on the compressor
Entre of the syngas	Temp. from gasifier trough the rubber hose
Bottom of the CO_2	Temp. after passing the Leisner burner
Top of the CO_2	Temp. after the CO_2 cleaning process
Top of the NH_3 device	Temp. after the NH_3 cleaning process
Gas meter	Temp. in the gas meter before the compressor
Top of the carbon filters	Temp. before the tar and sulphur cleaning process
Bottom of the carbon filters	Temp. before the tar and sulphur cleaning process

Table C.1: Overview all the temperature measurements

Appendix D

Source code

D.1 Source code for the model

hej

Appendix B. Methanol/DME production based on the Two-Stage Gasifier

ISI Journal Paper

Clausen LR, Elmegaard B, Ahrenfeldt J, Henriksen U. "Thermodynamic analysis of small-scale DME and methanol plants based on the efficient Two-stage gasifier". Submitted to Energy (manuscript number: EGY-D-11-00180), 2011.

THERMODYNAMIC ANALYSIS OF SMALL-SCALE DME AND METHANOL PLANTS BASED ON THE EFFICIENT TWO-STAGE GASIFIER

Lasse R. Clausen [a, *], Brian Elmegaard [a], Jesper Ahrenfeldt [b], Ulrik Henriksen [b]

[a] Section of Thermal Energy Systems, Department of Mechanical Engineering, The Technical University of Denmark (DTU), Nils Koppels Allé Bld. 403, DK-2800 Kgs. Lyngby, Denmark

[b] Biosystems Division, Risø National Laboratory for Sustainable Energy, The Technical University of Denmark (DTU), Frederiksborgvej 399, DK-4000 Roskilde, Denmark

Received: xx

Abstract

Models of DME and methanol synthesis plants have been designed by combining the features of the simulation tools DNA and Aspen Plus. The plants produce DME or methanol by catalytic conversion of a syngas generated by gasification of woody biomass. Electricity is co-produced in the plants by a gas engine utilizing the unconverted syngas. A two-stage gasifier with a cold gas efficiency of 93% is used, but because of the design of this type of gasifier, the plants have to be of small scale (5 MWth biomass input). The plant models show energy efficiencies from biomass to DME/methanol + electricity of 51-58% (LHV), which shows to be 6-8%-points lower than efficiencies achievable on large-scale plants based on torrefied biomass pellets. By using waste heat from the plants for district heating, the total energy efficiencies become 87-88%.

Keywords: biorefinery, dimethyl ether, DME, methanol, Two-Stage Gasifier, syngas.

1. Introduction

The CO_2 emissions of the transportation sector can be reduced by increasing the use of biofuels – especially when the biofuels are produced from lignocellulosic biomass [1]. Dimethyl ether (DME) and methanol are two such biofuels. DME is a diesel-like fuel that can be produced from biomass in processes very similar to methanol production processes. Combustion of DME produces lower emissions of NO_x than combustion of diesel, with no particulate matter or SO_x in the flue gas [2], however it also requires storage pressures in excess of 5 bar to maintain a liquid state, which is similar to LPG.

Two DME and two methanol synthesis plant configurations, based on syngas from gasification of wood chips, are investigated in this paper:

- The DME-OT and MeOH-OT plants uses once through synthesis and the unconverted syngas is combusted in a gas engine to produce electricity.
- The DME-RC and MeOH-RC plants use recycling of some of the unconverted syngas to the DME/methanol reactor to maximize DME/methanol production. All the electricity produced by the gas engine is used on-site.

Production of methanol from biomass is very well investigated in the literature (e.g., [3,4]), and DME production from biomass has also been reported in the literature (e.g., [5,6]). Small-scale tri-generation of liquid fuel, electricity and heat based on an efficient two-stage gasifier has however not been presented in the literature. The small-scale production enables the use of the energy efficient Two-Stage Gasifier [7,8] and enhances the possibility of utilizing a district heating co-production. The economy of small-scale production of liquid fuel cannot compete with large-scale

* Corresponding author. Fax: +45 45884325, email: lrc@mek.dtu.dk

production [9,10][1], but the co-production of district heating in the small-scale plants will improve the economy of these plants.
This paper documents the design of two DME and two methanol plants using the modeling tool DNA [11,12] for the steam dryer and gasifier modeling and Aspen Plus for the downstream modeling. Thermodynamic performance of the plant configurations are presented and compared with the performance of large-scale plants.

2. Design of the DME and methanol plants

A simplified process flow sheet of the DME and methanol plant designs is shown in Fig. 1 and detailed process flow sheets can be seen in Fig. 3-Fig. 6. Plant design aspects related to feedstock preparation, gasification, syngas conditioning, DME/methanol synthesis and separation are described next and are followed by a discussion of electricity and heat production in the plants. Important process design parameters used in the modeling are shown in Table 1.

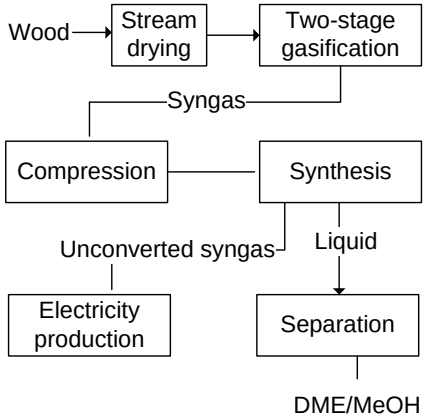

Fig. 1. Simplified flow sheet of the DME and methanol plant models

Steam drying

The wet wood chips are dried in co-flow with superheated steam by using a screw conveyer design. The methanol/DME reactor and the gas engine exhaust supply the heat needed to superheat the steam.

Gasification

A two-stage gasifier at atmospheric pressure is used for gasifying the dried wood chips. The gasifier is an updated design of the one described in [7,8]. In the first stage, the dried wood chips, together with the steam surplus from the steam dryer, are heated/pyrolyzed in a closed screw conveyer by passing the hot syngas from the gasifier on the outside surface of the closed screw conveyer[2]. In order to lower the tar content, the pyrolysis gas is partially oxidized by adding air. In the second stage, the partially oxidized gas passes through a downdraft fixed bed, where the gasification reactions occur. The bed consists of coke from the pyrolysis stage. After this stage, the tar content in the gas is almost zero [7][3]. The composition of the syngas is calculated by assuming

[1] Small-scale plants will have lower biomass transportation cost than large-scale plants, but economy of scale more than outweighs this.

[2] The heat consumption in the pyrolysis unit for the pyrolysis of dry wood is calculated based on measured temperatures of inputs and outputs and measured syngas composition – the heat loss to the surroundings is not included. The heat consumption for pyrolysis of dry wood (0% water) was estimated to be 952 kJ/kg-(dry wood) or 5.2% of the LHV (heating from 115°C to 630°C).

[3] Only naphthalene could be measured and the content was <0.1 mg/Nm^3 [7].

chemical equilibrium at a temperature slightly above the gasifier exit temperature[4]. In the methanol plants the H_2/CO ratio of the syngas is set to 2 by adjusting the biomass water content (42.5 mass% water), and in the DME plants the H_2/CO ratio is reduced to 1.5 by removing steam from the steam dryer loop. A H_2/CO ratio of 1 is optimal for DME synthesis (Eq. 4), but a ratio of 1.5 is estimated to be the lowest achievable ratio that the gasifier can produce, due to soot formation in the partial oxidation at lower steam contents.
The two-stage gasification concept has been demonstrated in plants with 75 kWth [7] and 700 kWth biomass input. Because of the design of the pyrolysis stage (heat is transferred from gas to solid), it is not considered possible to scale up the gasifier to more than some MWth [8][5]. Therefore, the biomass input for the modeled gasifier is set to 5 MWth (dry).

Gas cleaning
Gas cleaning of biomass syngas for DME/methanol synthesis includes cyclones and filters for particle removal, a water wash to remove NH_3 and HCl, and guard beds placed just before the synthesis reactor to remove sulfur and other impurities [13,14]. The guard beds consist of ZnO filters to remove H_2S, and active carbon filters to remove traces of NH_3, HCl, HCN, CS_2, and COS [14]. Guard beds are used to remove sulfur because the sulfur content in biomass syngas is very low[6]. Measurements on a two-stage gasifier with 75 kWth input showed only 0.93 ppm of COS and 0.5-1 ppm of H_2S in the raw gas [15]. This is most likely due to the coke bed in the gasifier acting as an active carbon filter. The gas cleaning does not comprise tar removal because the tar content in the syngas is almost zero. The gas cleaning steps are not included in the modeling.

Synthesis of DME and methanol
The cooled syngas is sent to an intercooled compressor before it enters the DME/methanol synthesis reactor. Both reactors are boiling water reactors (BWR) because these reactor types are preferred over slurry/liquid phase reactors at small-scale [16,17]. The chemical reaction equations producing DME and methanol are showed in Eqs. 1-5. The product gas composition is calculated by assuming an approach to chemical equilibrium at the reactor operating temperature and pressure (approach temperatures in Table 1).

Methanol synthesis reaction (from CO and H_2):

$4H_2 + 2CO \leftrightarrow 2CH_3OH$	-181.6 kJ	(1)

Methanol dehydration:

$2CH_3OH \leftrightarrow CH_3OCH_3 + H_2O$	-23.4 kJ	(2)

Water gas shift reaction:

$CO + H_2O \leftrightarrow CO_2 + H_2$	-41.0 kJ	(3)

Direct DME synthesis reactions, (1)+(2) (+(3)):

$3H_2 + 3CO \leftrightarrow CH_3OCH_3 + CO_2$	-246.0 kJ	(4)
$4H_2 + 2CO \leftrightarrow CH_3OCH_3 + H_2O$	-205.0 kJ	(5)

[4] In order to match measured data for the methane content, the model adds 0.67 mole% to the methane content calculated by chemical equilibrium.
[5] The reference states a size of 3-10 MWth biomass input.
[6] At a sulfur content of 0.02-0.1 mass% (dry biomass), the sulfur concentration in the dry gas becomes 55-275 ppm (H_2S+COS).

The reactor product gas is cooled to 40°C (methanol) or -50°C (DME) in order to condense the methanol/DME. A gas-liquid separator then separates the liquid from the unconverted syngas. In the RC plants, about 76-79% of the unconverted syngas is recycled to the synthesis reactor, and the remaining 21-24% is used for power production. The recycle ratio has been optimized together with the synthesis pressure to yield the highest fuel production. Regarding the OT plants, the synthesis pressure was set to 40 bar in the DME-OT plant [17] and the synthesis pressure in the MeOH-OT plant was then adjusted to give the same fuel production as the DME-OT plant (96 bar). This was done to simplify the comparison of the OT plants.
Because the syngas from the Two-Stage Gasifier only consists of 56-57 mole% H_2+CO, the syngas conversions are lower than what would be achieved in large-scale plants using oxygen blown gasification and CO_2 removal (Fig. 2). The syngas conversions are lowered from 86% to 64% for methanol synthesis (96 bar, 220°C), and from 85% to 64% for DME synthesis (40 bar, 240°C). The reduction in syngas conversion, due to the inert content, can however be compensated for by increasing the synthesis pressure (Fig. 2)[7]. The relatively low operating temperatures of 220°C and 240°C are suggested by [17] to compensate for the high inert content in the syngas. This however results in higher costs for catalytic material compared to large-scale plants operating at 250-280°C (DME synthesis) [5,18].

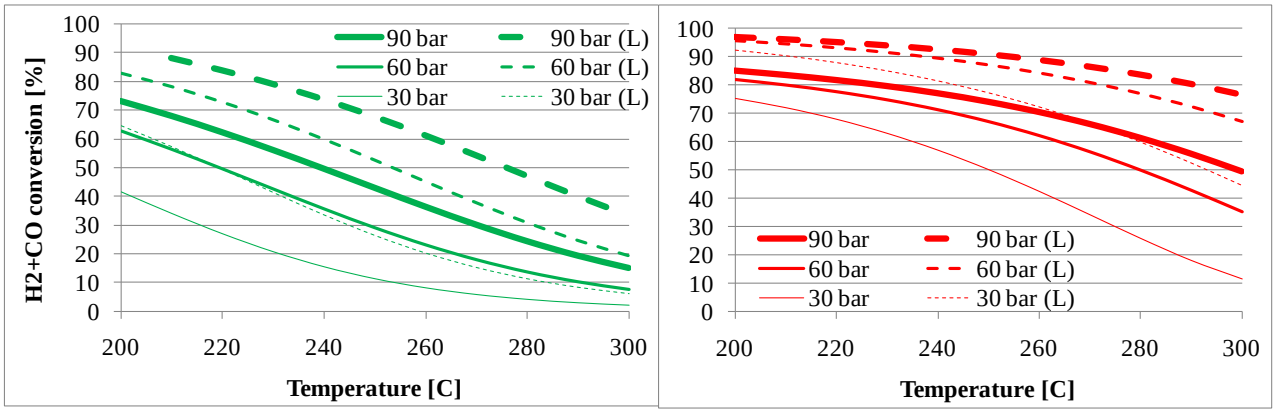

Fig. 2. Syngas conversions (H_2+CO) for methanol synthesis (left) and DME synthesis (right) at different synthesis temperatures and pressures. The solid lines are for the syngas from the Two-Stage Gasifier (composition in Table 2 for DME and Table 4 for methanol), and the dashed lines marked (L) are for a typical syngas used in a large-scale plant (methanol: 64.7% H_2, 32.3% CO, 3% CO_2. DME: 48.5% H_2, 48.5% CO, 3% CO_2 (mole%)). The syngas conversions are calculated with the approach temperatures listed in Table 1.

Separation

The liquid stream from the gas-liquid separator is distilled by fractional distillation in a topping column in order to remove the absorbed gasses (CO_2). The CO_2-rich stream from the column is sent to the gas engine. The resulting crude methanol product contains 2-5% water and the crude DME product contains 9-18% water and 10-14% methanol. The crude liquid fuel products are sent to central upgrading/purification because this is considered too costly at this small-scale. If additional distillation columns were added to the plants, the heat demand for the reboilers could be supplied by plant waste heat.

[7] For methanol synthesis at 220°C, the syngas conversion at 96 bar corresponds to the syngas conversion at 45 bar in a large-scale plant. For DME synthesis at 240°C, the syngas conversion at 40 bar corresponds to the syngas conversion at 13 bar in a large-scale plant. The syngas conversion is 64% in all cases.

Power production

The unconverted syngas that is not recycled to the synthesis reactor is heated by the gas engine exhaust before being expanded through a turbine to 2 bar[8]. The gas is then combusted with air in a turbocharged gas engine. Gas engine operation on syngas is described in [7]. Because the unconverted syngas from the DME plant contains some DME (0.4 mole%), which is a diesel fuel, the operation of the gas engine may need to be adjusted. More simple plant designs could be obtained if the expander turbines were removed[9].

District heating production

District heating is produced in order to improve the overall energy conversion efficiency for the plants. The main sources for district heating are syngas cooling, compressor intercooling and gas engine cooling. In the detailed flow sheets (Fig. 3 to Fig. 6), all the sources for district heating in the plants can be seen.

Table 1
Process design parameters used in the modeling.

Feedstock	Wet wood chips. Dry composition (mass%): 48.8% C, 43.9% O, 6.2% H, 0.17% N, 0.02% S, 0.91% Ash [7]. LHV = 18.3 MJ/kg-dry [7]. Moisture content = 42.5 mass%
Steam dryer	T_{exit} = 115°C. $T_{superheat}$ = 200°C. Dry wood moisture content = 2 mass%[a].
Gasifier	P = 1 bar. Carbon conversion = 99% [7]. Heat loss = 3% of the biomass thermal input (dry). T_{exit} = 730°C. $T_{equilibrium}$ = 750°C.
Compressors	$\eta_{polytropic}$ = 80%, $\eta_{mechanical}$ = 94%. $\eta_{electrical}$ = 100% [19][b]. Syngas compressor: 5 stages with intercooling to 40°C.
DME/MeOH synthesis	BWR reactor. Chemical equilibrium at reactor outlet temperature and pressure. Reactor outlet temperatures: 240°C (DME) and 220°C (MeOH) [17]. Reactor pressures: 40.0 bar (DME-OT), 44.7 bar (DME-RC), 96.0 bar (MeOH-OT), 95.0 bar (MeOH-RC). The approach temperatures used are: 15°C for the methanol reaction (1) and the water gas shift reaction (3), 100°C for the methanol dehydration reaction (2) [17].
Cooling	COP = 1.2 (cooling at -50°C)
Expander / turbine	$\eta_{isentropic}$ = 70%, $\eta_{mechanical}$ = 94%.
Gas engine	38% of the chemical energy in the gas (LHV) is converted to electricity. Excess air ratio (λ) = 2. $T_{exhaust}$ = 400°C. Turbocharger: p = 2 bar, $\eta_{is,\ compressor}$ = 75%, $\eta_{is,\ turbine}$ = 78%, $\eta_{mechanical}$ = 94%.
Heat exchangers	ΔT_{min} = 10°C (gas-liq) or 30°C (gas-gas). In pyrolysis stage: ΔT_{min} = 100°C (gas-solid).
District heating	$T_{water,\ supply}$ = 80°C, $T_{water,\ return}$ = 30°C

[a] The model of the steam dryer is based on measured data for a steam dryer of the same configuration and 700 kWth wood chips input.
[b] The polytropic efficiency of the syngas compressor may be lower than 80%, because of the small scale. If the efficiency was 70%, the power consumption of the compressor in the MeOH-OT would be 101 kWe higher (17% higher), resulting in a 2%-points lower net electricity output (Fig. 7).

[8] The MeOH-RC plant also uses waste heat from the gasification section to heat the gas before the expander because not enough waste heat is available in the gas engine exhaust.
[9] Removing the expander turbine would lower the number of heat exchangers required, but would also result in a reduction of the net power production of 2-3%-points for the OT plants (Fig. 7) and an estimated reduction of the fuel production in the RC plants of 4-6%-points (Fig. 7).

3. Results

The results from the simulation of the DME and methanol plants are presented in the following. In the flow sheets in Fig. 3 to Fig. 6, some of the important thermodynamic parameters are shown together with electricity production/consumption and heat transfer in the plants. In Table 2 to Table 5, the composition of specific streams in the flow sheets are shown.

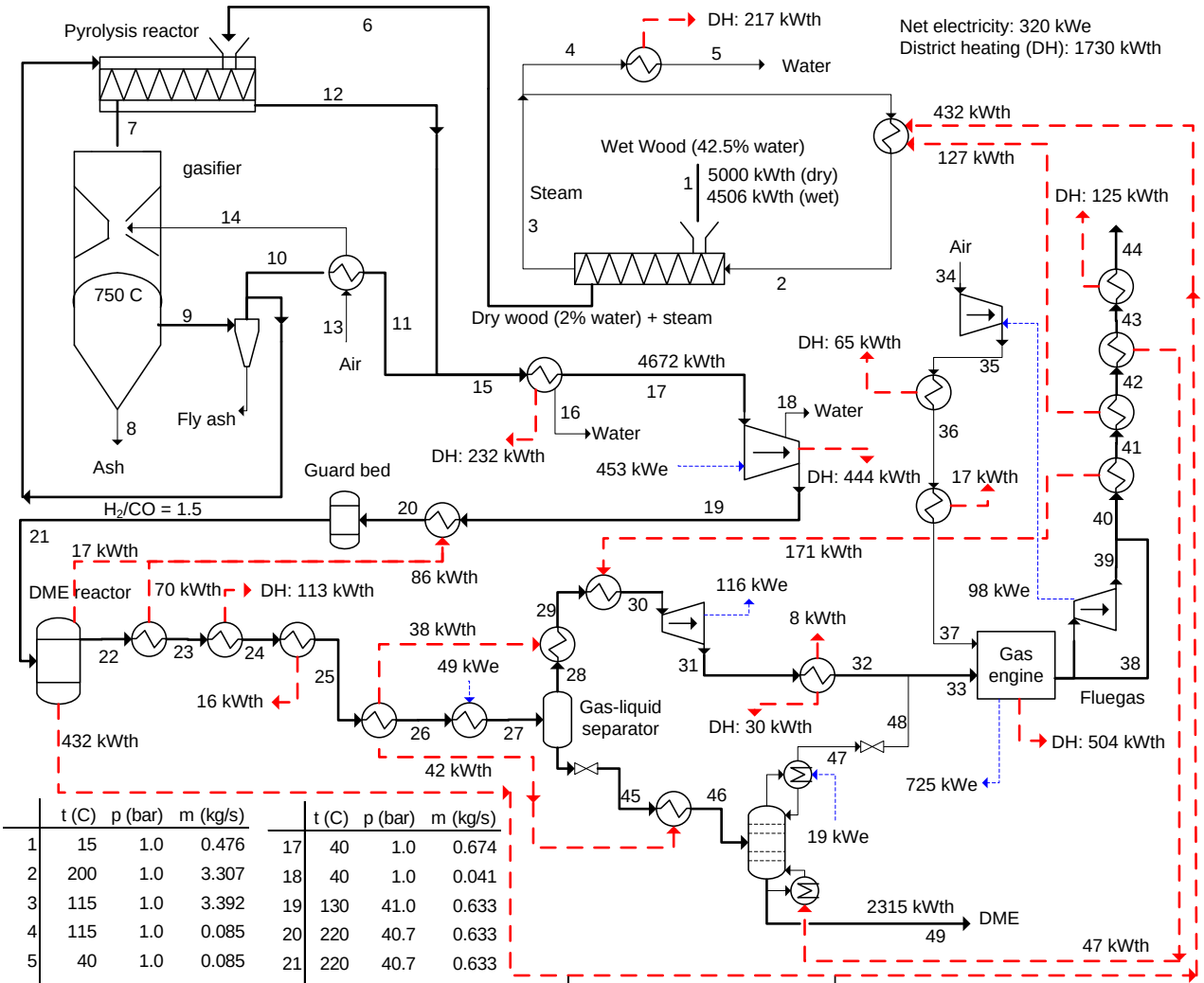

	t (C)	p (bar)	m (kg/s)
1	15	1.0	0.476
2	200	1.0	3.307
3	115	1.0	3.392
4	115	1.0	0.085
5	40	1.0	0.085
6	115	1.0	0.391
7	630	1.0	0.391
8	730	1.0	0.004
9	730	1.0	0.707
10	730	1.0	0.223
11	80	1.0	0.223
12	230	1.0	0.484
13	15	1.0	0.320
14	700	1.0	0.320
15	183	1.0	0.707
16	40	1.0	0.033

	t (C)	p (bar)	m (kg/s)
17	40	1.0	0.674
18	40	1.0	0.041
19	130	41.0	0.633
20	220	40.7	0.633
21	220	40.7	0.633
22	240	40.0	0.633
23	160	39.8	0.633
24	40	39.4	0.633
25	25	39.4	0.633
26	-23	39.3	0.633
27	-50	39.2	0.633
28	-50	38.5	0.412
29	15	38.3	0.412
30	314	37.5	0.412
31	95	2.0	0.412
32	25	2.0	0.412

	t (C)	p (bar)	m (kg/s)
33	11	2.0	0.547
34	15	1.0	1.089
35	99	2.0	1.089
36	40	2.0	1.089
37	25	2.0	1.089
38	400	1.9	0.401
39	325	1.0	1.235
40	344	1.0	1.636
41	250	1.0	1.636
42	178	1.0	1.636

	t (C)	p (bar)	m (kg/s)
43	152	1.0	1.636
44	80	1.0	1.636
45	-52	10.0	0.221
46	-16	10.0	0.221
47	-41	10.0	0.136
48	-56	2.0	0.136
49	51	10.0	0.086

Fig. 3. Flow sheet of the DME-OT plant model, showing mass flows, electricity consumption/production and heat transfer.

Table 2
Stream compositions for the DME-OT plant (stream numbers refer to Fig. 3)

	Gasifier exit	Reactor inlet	Reactor outlet[a]	To expander	To distil-lation	CO_2 to engine	Gas to engine[b]	DME[c]
Stream number	9	21	22	30	46[d]	48	33	49[d]
Mass flow (kg/s)	0.707	0.633	0.633	0.412	0.221	0.136	0.547	0.086
Flow (mole/s)	34.2	30.1	22.8	17.6	5.18	3.14	20.7	2.04
Mole frac (%)								
H_2	30.0	34.1	20.2	26.1	0.20	0.33	22.2	0.00
CO	20.4	23.2	7.3	9.3	0.35	0.58	8.0	0.00
CO_2	11.0	12.5	23.8	13.7	58.0	95.7	26.1	0.00
H_2O	12.4	0.42	0.84	0.00	3.7	0.00	0.00	9.3
CH_4	0.76	0.87	1.1	1.4	0.30	0.49	1.3	0.00
N_2	25.1	28.5	37.7	48.4	1.7	2.7	41.4	0.00
Ar	0.30	0.34	0.45	0.56	0.06	0.09	0.49	0.00
CH_3OH	-	-	0.92	0.00	4.1	0.00	0.00	10.3
CH_3OCH_3	-	-	7.6	0.48	31.7	0.05	0.41	80.4

[a] The syngas conversion in the DME reactor is 64% (55% H_2-conversion and 76% CO-conversion).
[b] The energy content in the gas to the engine is 7.8 MJ/m^3 (LHV).
[c] The flow of methanol-equivalent is 3.49 mole/s (1 mole of DME is 2 mole methanol-equivalent).
[d] Liquid.

Table 3
Stream compositions for the DME-RC plant (stream numbers refer to Fig. 4)

	Gasifier exit	After compressor	Reactor inlet	Reactor outlet[a]	Recycle gas[b]	To distil-lation	CO_2 to engine	Gas to engine[c]	DME[d]
Stream number	9	19	22	23	31	48[e]	50	35	51[e]
Mass flow (kg/s)	0.707	0.633	1.733	1.733	1.100	0.278	0.164	0.519	0.114
Flow (mole/s)	34.2	30.1	74.5	65.5	44.4	6.71	3.80	18.1	2.91
Mole frac (%)									
H_2	30.0	34.1	25.8	18.0	20.1	0.13	0.23	15.9	0.00
CO	20.4	23.2	12.6	4.9	5.4	0.17	0.30	4.3	0.00
CO_2	11.0	12.5	12.5	16.8	12.5	54.2	95.7	29.9	0.00
H_2O	12.4	0.39	0.16	0.79	0.00	7.6	0.00	0.00	17.6
CH_4	0.76	0.87	1.3	1.5	1.7	0.32	0.56	1.4	0.00
N_2	25.1	28.6	46.8	53.3	59.2	1.7	3.0	47.4	0.00
Ar	0.30	0.34	0.54	0.62	0.68	0.06	0.11	0.56	0.00
CH_3OH	-	-	0.00	0.61	0.00	5.9	0.00	0.00	13.6
CH_3OCH_3	-	-	0.28	3.5	0.47	29.8	0.05	0.38	68.7

[a] The syngas conversion in the DME reactor is 48% (39% H_2-conversion and 66% CO-conversion).
[b] 76% of the unconverted syngas is recycled, resulting in a reactor inlet mole flow that is 2.5 times higher than the feed flow.
[c] The energy content in the gas to the engine is 5.8 MJ/m^3 (LHV).
[d] The flow of methanol-equivalent is 4.39 mole/s (1 mole of DME is 2 mole methanol-equivalent).
[e] Liquid.

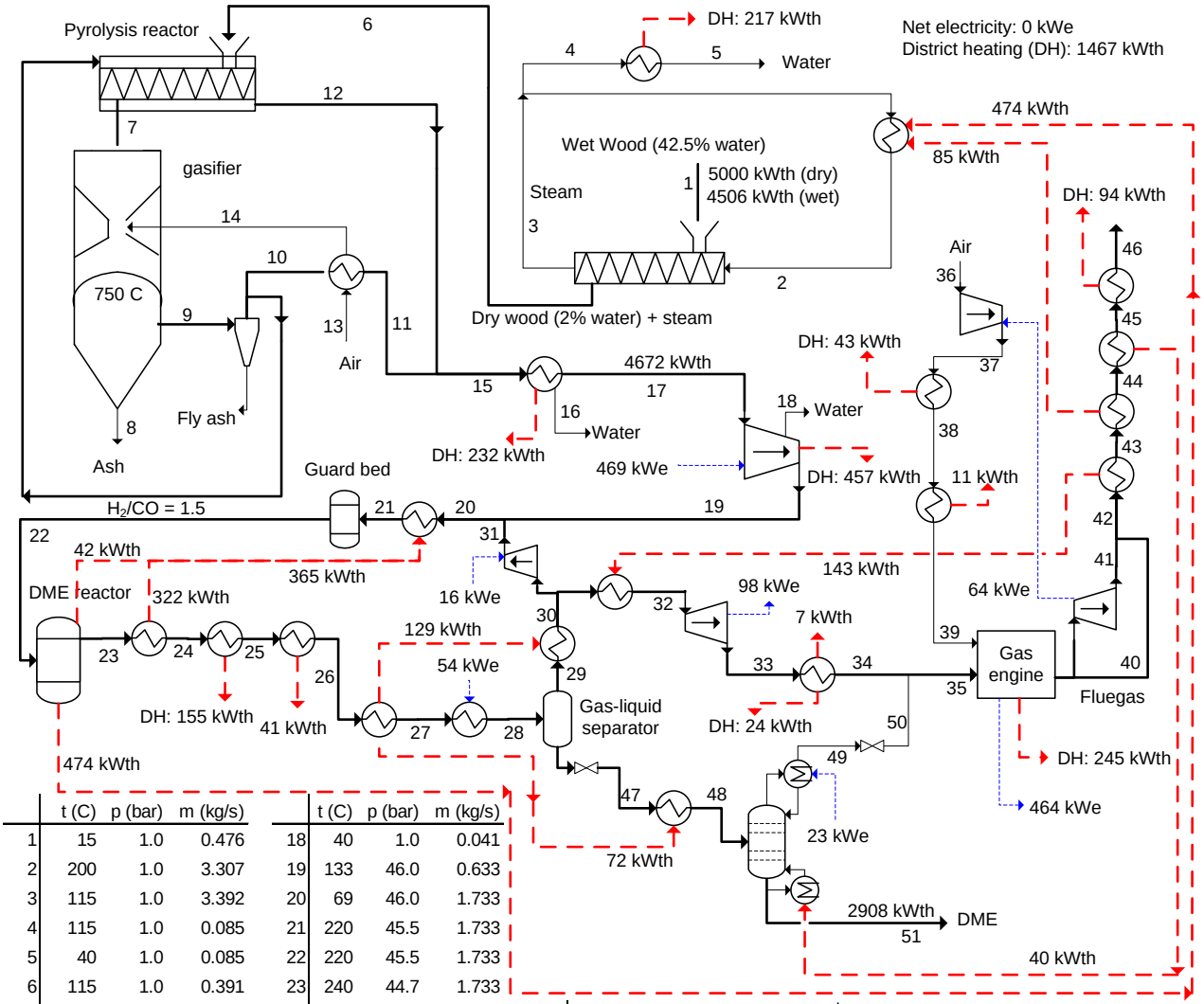

	t (C)	p (bar)	m (kg/s)
1	15	1.0	0.476
2	200	1.0	3.307
3	115	1.0	3.392
4	115	1.0	0.085
5	40	1.0	0.085
6	115	1.0	0.391
7	630	1.0	0.391
8	730	1.0	0.004
9	730	1.0	0.707
10	730	1.0	0.223
11	80	1.0	0.223
12	230	1.0	0.484
13	15	1.0	0.320
14	700	1.0	0.320
15	183	1.0	0.707
16	40	1.0	0.033
17	40	1.0	0.674

	t (C)	p (bar)	m (kg/s)
18	40	1.0	0.041
19	133	46.0	0.633
20	69	46.0	1.733
21	220	45.5	1.733
22	220	45.5	1.733
23	240	44.7	1.733
24	99	44.2	1.733
25	40	43.9	1.733
26	25	43.9	1.733
27	-37	43.8	1.733
28	-50	43.7	1.733
29	-50	42.9	1.454
30	15	42.7	1.454
31	26	47.7	1.100
32	321	41.7	0.355
33	93	2.0	0.355
34	25	2.0	0.355

	t (C)	p (bar)	m (kg/s)
35	6	2.0	0.519
36	15	1.0	0.713
37	99	2.0	0.713
38	40	2.0	0.713
39	25	2.0	0.713
40	400	1.9	0.411
41	326	1.0	0.821
42	351	1.0	1.232
43	246	1.0	1.232
44	182	1.0	1.232

	t (C)	p (bar)	m (kg/s)
45	152	1.0	1.232
46	80	1.0	1.232
47	-51	10.0	0.278
48	-5	10.0	0.278
49	-41	10.0	0.164
50	-56	2.0	0.164
51	54	10.0	0.114

Fig. 4. Flow sheet of the DME-RC plant model, showing mass flows, electricity consumption/production and heat transfer.

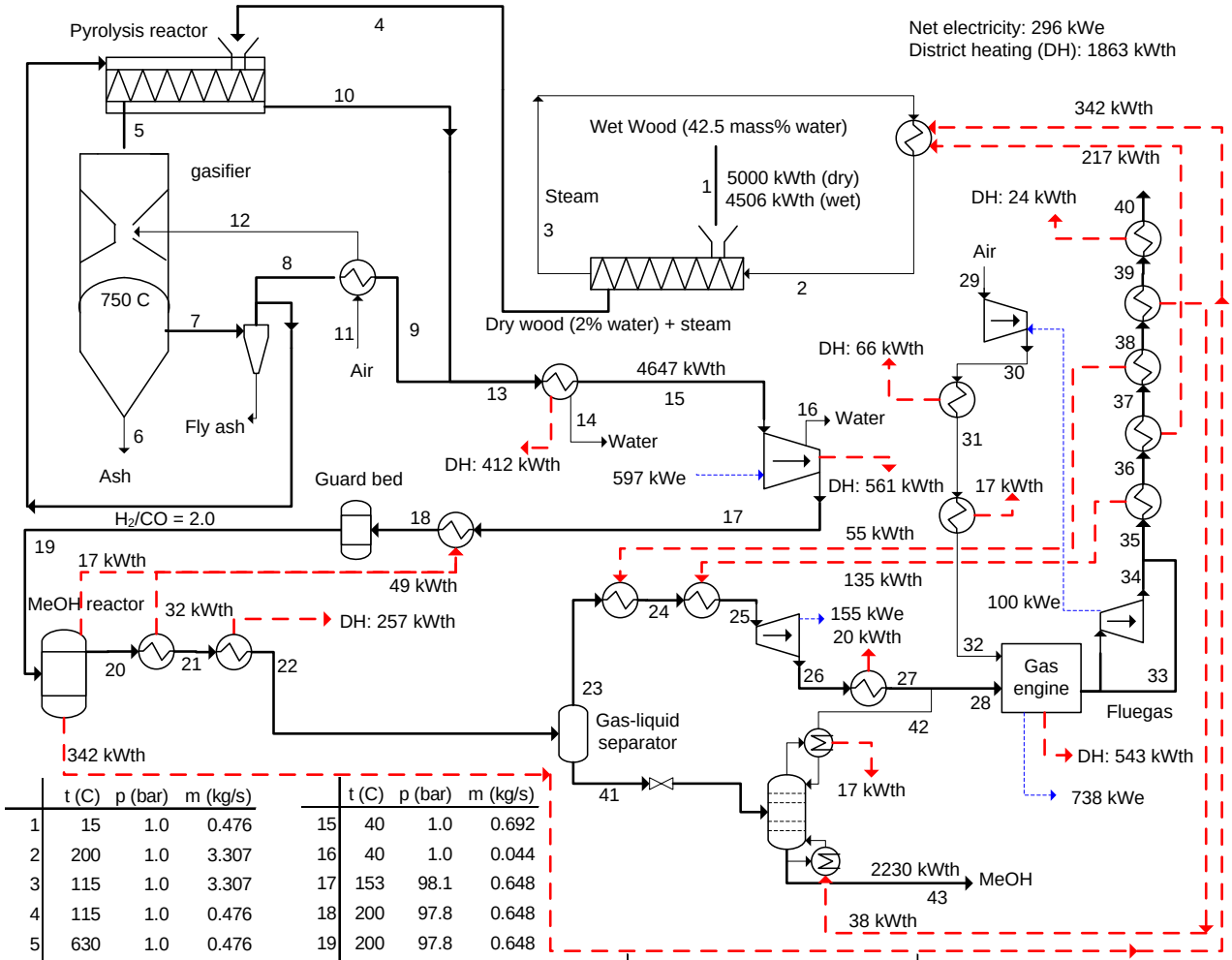

	t (C)	p (bar)	m (kg/s)
1	15	1.0	0.476
2	200	1.0	3.307
3	115	1.0	3.307
4	115	1.0	0.476
5	630	1.0	0.476
6	730	1.0	0.004
7	730	1.0	0.784
8	730	1.0	0.209
9	80	1.0	0.209
10	236	1.0	0.575
11	15	1.0	0.313
12	700	1.0	0.313
13	195	1.0	0.784
14	40	1.0	0.092

	t (C)	p (bar)	m (kg/s)
15	40	1.0	0.692
16	40	1.0	0.044
17	153	98.1	0.648
18	200	97.8	0.648
19	200	97.8	0.648
20	220	96.0	0.648
21	183	95.8	0.648
22	40	94.8	0.648
23	40	93.0	0.509
24	117	92.5	0.509
25	313	91.3	0.509
26	58	2.0	0.509
27	25	2.0	0.509
28	25	2.0	0.535

	t (C)	p (bar)	m (kg/s)
29	15	1.0	1.104
30	99	2.0	1.104
31	40	2.0	1.104
32	25	2.0	1.104
33	400	1.9	0.384
34	325	1.0	1.255
35	343	1.0	1.639
36	269	1.0	1.639

	t (C)	p (bar)	m (kg/s)
37	147	1.0	1.639
38	116	1.0	1.639
39	94	1.0	1.639
40	80	1.0	1.639
41	40	93.0	0.139
42	25	2.0	0.026
43	83	2.0	0.113

Fig. 5. Flow sheet of the MeOH-OT plant model, showing mass flows, electricity consumption/production and heat transfer.

Table 4
Stream compositions for the MeOH-OT plant (stream numbers refer to Fig. 5)

	Gasifier exit	Reactor inlet	Reactor outlet[a]	To expander	To distil-lation	CO_2 to engine	Gas to engine[b]	MeOH[c]
Stream number	7	19	20	25	41[d]	42	28	43[d]
Mass flow (kg/s)	0.784	0.648	0.648	0.509	0.139	0.026	0.535	0.113
Flow (mole/s)	38.7	31.1	23.7	19.5	4.19	0.63	20.2	3.57
Mole frac (%)								
H_2	29.9	37.1	17.5	21.2	0.15	0.99	20.6	0.00
CO	14.9	18.6	8.8	10.6	0.13	0.85	10.3	0.00
CO_2	12.8	15.9	20.9	22.7	12.7	85.4	24.6	0.00
H_2O	19.7	0.24	0.32	0.01	1.8	0.00	0.01	2.1
CH_4	0.71	0.88	1.2	1.4	0.08	0.53	1.4	0.00
N_2	21.7	27.0	35.4	42.9	0.52	3.5	41.6	0.00
Ar	0.26	0.32	0.42	0.51	0.02	0.13	0.49	0.00
CH_3OH	-	-	15.6	0.77	84.6	8.6	1.0	97.9

[a] The syngas conversion in the methanol reactor is 64% (64% H_2-conversion and 64% CO-conversion).
[b] The energy content in the gas to the engine is 7.8 MJ/m^3 (LHV).
[c] The flow of methanol is 3.49 mole/s.
[d] Liquid.

Table 5
Stream compositions for the MeOH-RC plant (stream numbers refer to Fig. 6)

	Gasifier exit	After compressor	Reactor inlet	Reactor outlet[a]	Recycle gas[b]	To distil-lation	CO_2 to engine	Gas to engine[c]	MeOH[d]
Stream number	7	18	21	22	26	43[e]	44	31	45[e]
Mass flow (kg/s)	0.784	0.648	2.391	2.391	1.743	0.180	0.035	0.504	0.145
Flow (mole/s)	38.7	31.1	92.5	83.3	61.3	5.45	0.83	17.3	4.62
Mole frac (%)									
H_2	29.9	37.1	21.3	12.5	13.3	0.09	0.58	12.7	0.00
CO	14.9	18.6	11.6	7.5	8.1	0.09	0.59	7.7	0.00
CO_2	12.8	15.9	21.8	24.0	24.8	13.1	85.8	27.7	0.00
H_2O	19.7	0.24	0.09	0.29	0.01	4.2	0.00	0.01	4.9
CH_4	0.71	0.88	1.4	1.5	1.6	0.09	0.57	1.6	0.00
N_2	21.7	27.0	42.7	47.4	50.7	0.57	3.7	48.5	0.00
Ar	0.26	0.32	0.50	0.56	0.60	0.02	0.14	0.58	0.00
CH_3OH	-	-	0.52	6.1	0.78	81.8	8.6	1.2	95.1

[a] The syngas conversion in the methanol reactor is 45% (47% H_2-conversion and 42% CO-conversion).
[b] 79% of the unconverted syngas is recycled, resulting in a reactor inlet mole flow that is 3.0 times higher than the feed flow.
[c] The energy content in the gas to the engine is 5.9 MJ/m^3 (LHV).
[d] The flow of methanol is 4.39 mole/s.
[e] Liquid.

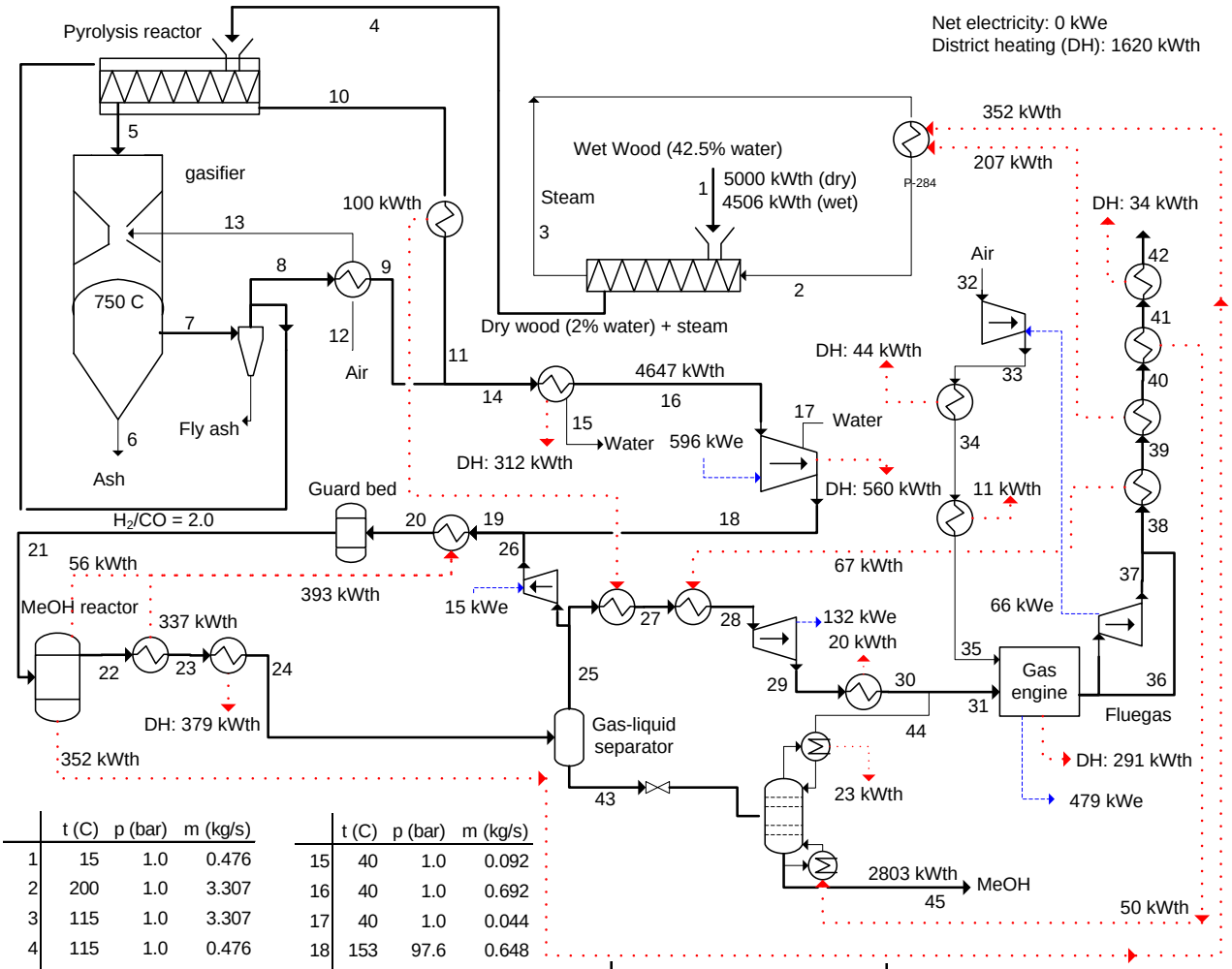

	t (C)	p (bar)	m (kg/s)
1	15	1.0	0.476
2	200	1.0	3.307
3	115	1.0	3.307
4	115	1.0	0.476
5	630	1.0	0.476
6	730	1.0	0.004
7	730	1.0	0.784
8	730	1.0	0.209
9	80	1.0	0.209
10	236	1.0	0.575
11	127	1.0	0.575
12	15	1.0	0.313
13	700	1.0	0.313
14	114	1.0	0.784

	t (C)	p (bar)	m (kg/s)
15	40	1.0	0.092
16	40	1.0	0.692
17	40	1.0	0.044
18	153	97.6	0.648
19	80	97.6	2.391
20	200	96.8	2.391
21	200	96.8	2.391
22	220	95.0	2.391
23	110	94.3	2.391
24	40	93.8	2.391
25	40	92.0	2.211
26	47	99.0	1.743
27	206	90.9	0.469
28	320	90.2	0.469

	t (C)	p (bar)	m (kg/s)
29	64	2.0	0.469
30	25	2.0	0.469
31	25	2.0	0.504
32	15	1.0	0.730
33	99	2.0	0.730
34	40	2.0	0.730
35	25	2.0	0.730
36	400	1.9	0.389
37	326	1.0	0.844

	t (C)	p (bar)	m (kg/s)
38	350	1.0	1.233
39	301	1.0	1.233
40	145	1.0	1.233
41	106	1.0	1.233
42	80	1.0	1.233
43	40	92.0	0.180
44	25	2.0	0.035
45	84	2.0	0.145

Fig. 6. Flow sheet of the MeOH-RC plant model, showing mass flows, electricity consumption/production and heat transfer.

Fig. 3 to Fig. 6 shows that the 5000 kWth biomass input can be converted to a maximum of 2803 kWth of methanol or 2908 kWth of DME in the RC plants - with no net electricity production, but with a heat production of 1620 kWth (MeOH) or 1467 kWth (DME) (see Fig. 7 for corresponding energy efficiencies). If once-through synthesis is used to simplify the synthesis process, the fuel production drops to 2230 kWth of methanol or 2315 kWth of DME, but the net electricity production and the heat production increases to 296 kWe and 1863 kWth (MeOH) or 320 kWe and 1730 kWth (DME). These values show that the DME plants produce more fuel than the methanol plants on an energy basis, but if the fuel production is compared on a methanol-equivalence basis

(two moles methanol is used to produce one mole DME), the fuel production is actually the same for the OT plants and the RC plants respectively (Table 2 to Table 5)[10].
The lower net electricity production by the MeOH-OT plant compared with the DME-OT plant is due to the higher synthesis pressure in the methanol plants (96 bar vs. 40 bar for the OT plants), resulting in a higher syngas compressor duty. The difference in syngas compressor duty is however almost completely compensated for by the electricity consumption for refrigeration needed in the DME plants, and by a higher gross electricity production in the methanol plants.
The higher heat production by the OT plants compared with the RC plants is due to the higher waste heat production by the gas engine, and the higher heat production by the methanol plants compared with the DME plants is because of: 1. the compressor intercooling due to the higher synthesis pressure, and 2. the cooling of the syngas from the methanol/DME reactor due to the condensation of methanol when cooling to 40°C.
Because the performance of the DME/methanol plants showed to be very similar when comparing OT plants and RC plants respectively, it is difficult to conclude that one type is better than the other. However, because the design of the synthesis loop is more complex in the DME plants and a refrigeration plant is needed in the synthesis loop and for the topping column, a methanol plant may be more suited for small-scale production[11]. If the RC plants are compared with the OT plants, Fig. 7 shows that the fuels effective efficiencies (FEE) are 5%-points higher for the RC plants[12], which means that the RC plants should be preferred because they produce DME/methanol more efficiently. The added cost for the synthesis loop and the larger DME/methanol reactor (2.5-3 times higher mole flow, see Table 3 and Table 5) may however make the RC plants less attractive than the OT plants.

[10] Equal fuel production for the OT plants was an input to the modeling. The reason why the energy content of the produced DME is higher than the energy content of the produced methanol is that LHV for methanol includes the heat of vaporization because methanol is liquid at standard conditions ($LHV_{methanol}$ = 638.1 MJ/kmole, LHV_{DME} = 1328 MJ/kmole).
[11] The fact that a higher synthesis pressure is used in the methanol plants may have a negative economic impact on the methanol plants, because of a higher syngas compressor cost, and perhaps higher costs for the synthesis section.
[12] If the FEE's were calculated with an electric efficiency of 30-31% instead of 50%, the FEE's for the OT plants would be the same as the FEE's for the RC plants (56% and 58%).

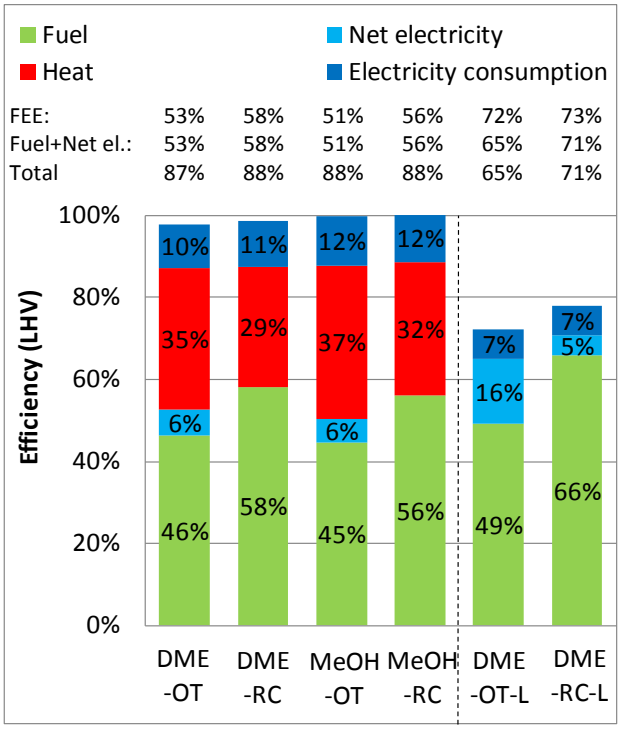

Fig. 7. Energy efficiencies for the conversion of biomass to DME/methanol and electricity for the four small-scale plants compared with two large-scale DME plants from [20] (the reference gives the fuel efficiency for the DME-OT-L plant to 48% instead of 49%. 49% is the correct value). FEE = fuels effective efficiency, defined as $\frac{\text{fuel}}{\text{biomass} - \frac{\text{net electricity}}{50\%}}$ where the fraction $\frac{\text{net electricity}}{50\%}$ corresponds to the amount of biomass that would be used in a stand-alone BIGCC power plant with an efficiency of 50% [5] to produce the same amount of electricity. Electricity consumption + net electricity = gross electricity production.

3.1 Comparison with large-scale DME plants

In Fig. 7, the energy efficiencies for the DME and methanol plants are compared with energy efficiencies for two large-scale DME plants. The large-scale plants are based on pressurized oxygen-blown entrained flow gasification of torrefied biomass and are reported in [20]. These plants do not produce district heating like the small-scale plants, but this could of course be implemented, if a significant heat demand was present near the plants.

Fig. 7 shows that the small-scale plants produce MeOH/DME + electricity at efficiencies of 51-58% while the large-scale plants achieve 65-71% from torrefied biomass, but only 59-64% from untreated biomass (90% efficiency of the torrefaction process) [20]. The large-scale plants are therefore 6-8%-points better than the small-scale plants when the basis is untreated biomass[13].

One of the reasons for the lower efficiencies achieved for the small-scale plants is the high electricity consumption of the plants (10-12% vs. 7%), due to the high syngas compressor duty - because of air-blown gasification at atmospheric pressure. The air-blown gasifier is however very energy efficient – achieving a cold gas efficiency of 93% (Fig. 8) while the gasifier used in the large-scale plants only has a cold gas efficiency of 81% (Fig. 8, 81=73/90).

The reason why this does not result in higher fuel efficiencies for the small-scale plants, is that the high electricity consumption is covered by a gas engine operating on unconverted syngas –

[13] The efficiencies stated for torrefied biomass could also be achieved from untreated biomass if the torrefaction process was done on-site and the volatile gasses was feed to the gasifier – e.g. as a chemical quench as suggested by [21]. Such a plant would however have higher biomass transportation and storage costs because torrefied biomass pellets are very energy dense and can be stored outside [20]. It is unclear which of the two plant types that has the best plant economy.

meaning that a certain amount of unconverted syngas must be supplied to the engine. In the large-scale plants, waste heat is also used for electricity production why no unconverted syngas is needed to cover the (low) electricity consumption. In the DME-RC plant, 24% of the input chemical energy is used for electricity production, while only 1% is used in large-scale DME-RC plant. This clearly eliminates the higher flow of chemical energy in the small-scale plants after gasification (93% vs. 73%, Fig. 8).
If less unconverted syngas was needed by the gas engine or external electricity was supplied to the small-scale plants, it would however be difficult to increase the fuel production much, because of the high level of inerts in the syngas.

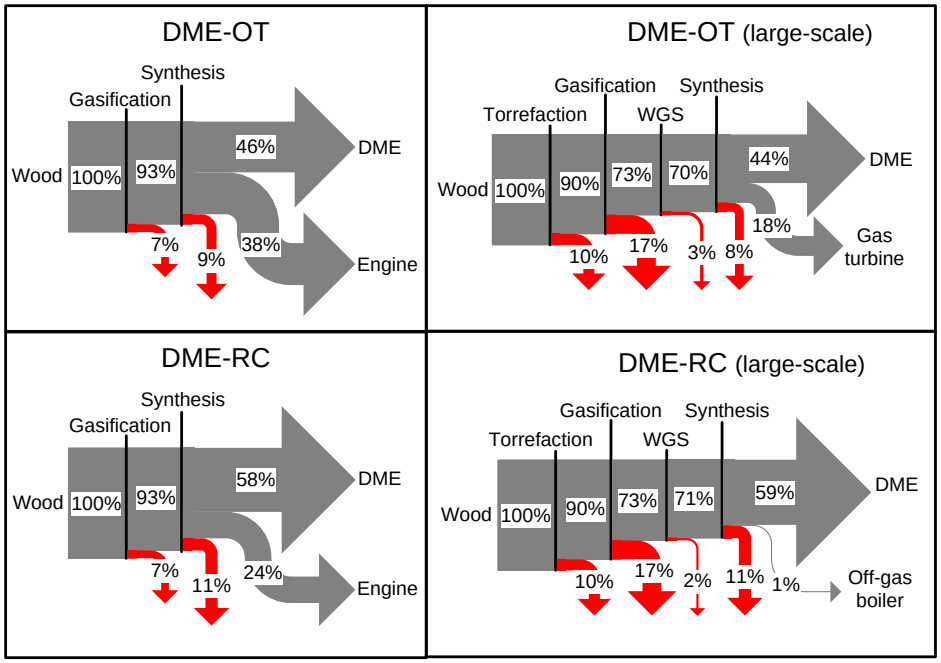

Fig. 8. Chemical energy streams (LHV, dry) in the small-scale DME plants compared with two large-scale DME plants from [20]. The figure includes conversion heat losses. The conversion heat losses (excluding the torrefaction heat loss) are in the large-scale DME plants used by a steam plant to produce electricity. In the small-scale DME plants, the conversion heat losses are used internally in the gasifier and for steam drying of biomass. The torrefaction process does not occur in the large-scale DME plants, but decentralized. WGS = water gas shift.

4. Conclusion

Synthesis of DME or methanol from syngas generated by the efficient Two-Stage Gasifier showed to give energy efficiencies from biomass to methanol/DME + electricity of 51-53% (LHV) for once through synthesis, and 56-58% (LHV) for RC synthesis. There was almost no difference between the energy performance of the methanol plants and the DME plants, when comparing the fuel production on a methanol-equivalence basis. Besides producing liquid fuel and electricity, the plants also produced district heating, which increased the total energy efficiency of the plants to 87-88% (LHV).
The energy efficiencies achieved for biomass to methanol/DME + electricity were 6-8%-points lower than what could be achieved by large-scale DME plants. The main reason for this difference showed to be the use of air-blown gasification at atmospheric pressure in the small-scale plants, because this results in high syngas compressor duties and high inert content in the synthesis reactor. However, the use of a gas engine operating on unconverted syngas to cover the on-site electricity consumption also limits how much of the syngas that can be converted to liquid fuel.

The reason why the difference between the small-scale and the large-scale plants showed not to be greater, was the high cold gas efficiency of the gasifier used in the small-scale plants.

Acknowledgements
For financial support, the authors would like to thank the Danish Energy Research Programme (Energiforskningsprogrammet - EFP). The Danish Energy Research Programme had no influence on the research presented in this article, or the writing of the article.

References

[1] JRC, Eucar, Concawe. Well-to-wheels analysis of future automotive fuels and powertrains in the European context. Report, version 2C, 2007, http://ies.jrc.ec.europa.eu/jec-research-collaboration/downloads-jec.html, accessed 12/15/2010.

[2] International DME association (IDA). DME - Clean Fuel for Transportation. http://www.aboutdme.org/index.asp?bid=219, accessed 12/15/2010.

[3] Sues A, Juraščík M, Ptasinski K. Exergetic evaluation of 5 biowastes-to-biofuels routes via gasification. Energy 2010;35(2):996-1007

[4] Hamelinck CN, Faaij APC. Future prospects for production of methanol and hydrogen from biomass, report NWS-E-2001-49. Utrecht, The Netherlands: Utrecht University, Copernicus Institute, 2001. http://www.mtholyoke.edu/courses/tmillett/course/geog_304B/e2001-49.pdf, accessed 12/15/2010.

[5] Larson ED, Jin H, Celik FE. Large-scale gasification-based coproduction of fuels and electricity from switchgrass. Biofuels, Biorprod. Bioref. 2009;3:174–194.

[6] Pettersson K, Harveya S. CO2 emission balances for different black liquor gasification biorefinery concepts for production of electricity or second-generation liquid biofuels. Energy 2010;35(2):1101-1106.

[7] Ahrenfeldt J, Henriksen U, Jensen TK, Gøbel B, Wiese L, Kather A, Egsgaard H. Validation of a Continuous Combined Heat and Power (CHP) Operation of a Two-Stage Biomass Gasifier. Energy & Fuels 2006;20(6):2672-2680.

[8] Bentzen JD, Hummelshøj RM, Henriksen U, Gøbel B, Ahrenfelt J, Elmegaard B. Upscale of the two-stage gasification process. In: procedings of 2. World Conference and Technology Exhibition on Biomass for Energy and Industry, Florence & WIP-Munich, Rome, 2004. http://orbit.dtu.dk/getResource?recordId=155745&objectId=1&versionId=1, accessed 12/15/2010.

[9] Boerrigter H. Economy of Biomass-to-Liquids (BTL) plants, report: ECN-C--06-019. Petten, The Netherlands: ECN, 2006. http://www.ecn.nl/publications/, accessed 12/15/2010.

[10] Larson ED, Williams RH, Jin H. Fuels and electricity from biomass with CO2 capture and storage. In: proceedings of the 8th International Conference on Greenhouse Gas Control Technologies, Trondheim, Norway, June 2006, http://www.princeton.edu/pei/energy/publications/, accessed 12/15/2010.

[11] Elmegaard B, Houbak N. DNA – A General Energy System Simulation Tool. In: J. Amundsen et al., editors. SIMS 2005, 46th Conference on Simulation and Modeling, Trondheim, Norway. Tapir Academic Press, 2005. p. 43-52.

[12] Homepage of the thermodynamic simulation tool DNA. http://orbit.dtu.dk/query?record=231251. Technical University of Denmark (DTU). Accessed 12/15/2010.

[13] van der Drift A, Boerrigter H. Synthesis gas from biomass, report: ECN-C--06-001. Petten, The Netherlands: ECN, 2006. http://www.ecn.nl/publications/, accessed 12/15/2010.

[14] Boerrigter H, Calis HP, Slort DJ, Bodenstaff H, Kaandorp AJ, Kaandorp AJ, den Uil H, Rabou LPLM. Gas Cleaning for Integrated Biomass Gasification (BG) and Fischer-Tropsch (FT) Systems, report: ECN-C--04-056. Petten, The Netherlands: ECN, 2006. http://www.ecn.nl/publications/, accessed 12/15/2010.

[15] Iversen HL, Henriksen U, Ahrenfeldt J, Bentzen JD. D25 Performance characteristics of SOFC membranes at two stage gasifier (confidential), report (EU project no.: 502759). Technical University of Denmark (DTU), 2006.

[16] Hansen JB, Nielsen PEH (Haldor Topsøe). Methanol Synthesis. Section 13.13 in "Handbook of Heterogeneous Catalysis", Wiley-VCH, 2008, online ISBN: 9783527610044, http://onlinelibrary.wiley.com/doi/10.1002/9783527610044.hetcat0148/abstract, accessed 12/15/2010.

[17] Personal communication with John Bøgild Hansen (Senior Scientist & Adviser to Chairman, Company Mangement) and Poul Erik Højlund Nielsen (department manager of science & innovation, R&D) about methanol synthesis, and Finn Joensen about DME synthesis, Haldor Topsøe A/S, 2010.

[18] Lee S, Cho W, Song T, Ra Y (R & D Division, Korea Gas Corporation (KOGAS)). Scale up study of DME direct synthesis technology. In: proceedings of the 24th World Gas Conference, 2009, http://www.igu.org/html/wgc2009/papers/docs/wgcFinal00745.pdf, accessed 12/15/2010.

[19] Kreutz TG, Larson ED, Liu G, Williams RH. Fischer-Tropsch Fuels from Coal and Biomass, report. Princeton, New Jersey: Princeton Environmental Institute, Princeton University, 2008. http://www.princeton.edu/pei/energy/publications, accessed 12/15/2010.

[20] Clausen LR, Elmegaard B, Houbak N. Technoeconomic analysis of a low CO2 emission dimethyl ether (DME) plant based on gasification of torrefied biomass. Energy 2010;35(12):4831-4842.

[21] Prins MJ, Ptasinski KJ, Janssen FJJG. More efficient biomass gasification via torrefaction. Energy 2006;31(15):3458–3470.

Appendix C. DME production based on entrained flow gasification of biomass

ISI Journal Paper

Clausen LR, Elmegaard B, Houbak N. "Technoeconomic analysis of a low CO2 emission dimethyl ether (DME) plant based on gasification of torrefied biomass". Energy 2010;35(12):4831-4842.

Energy 35 (2010) 4831–4842

Contents lists available at ScienceDirect

Energy

journal homepage: www.elsevier.com/locate/energy

Technoeconomic analysis of a low CO_2 emission dimethyl ether (DME) plant based on gasification of torrefied biomass

Lasse R. Clausen [a,*], Brian Elmegaard [a], Niels Houbak [b]

[a] Section of Thermal Energy Systems, Department of Mechanical Engineering, The Technical University of Denmark (DTU), Nils Koppels Allé Bld. 403, Room 211, DK-2800 Kgs. Lyngby, Denmark
[b] DONG Energy A/S, A.C. Meyers Vænge 9, DK-2450 Copenhagen, Denmark

ARTICLE INFO

Article history:
Received 30 March 2010
Received in revised form
18 August 2010
Accepted 2 September 2010
Available online 18 October 2010

Keywords:
Biorefinery
Biofuel
Torrefication
Gasification
Syngas
CO_2 capture

ABSTRACT

Two models of a dimethyl ether (DME) fuel production plant were designed and analyzed in DNA and Aspen Plus. The plants produce DME by either recycle (RC) or once through (OT) catalytic conversion of a syngas generated by gasification of torrefied woody biomass. Torrefication is a mild pyrolysis process that takes place at 200–300 °C. Torrefied biomass has properties similar to coal, which enables the use of commercially available coal gasification processing equipment. The DME plants are designed with focus on lowering the total CO_2 emissions from the plants; this includes e.g. a recycle of a CO_2 rich stream to a CO_2 capture plant, which is used in the conditioning of the syngas.

The plant models predict energy efficiencies from torrefied biomass to DME of 66% (RC) and 48% (OT) (LHV). If the exported electricity is included, the efficiencies are 71% (RC) and 64% (OT). When accounting for energy loss in torrefaction, the total efficiencies are reduced to 64% (RC) and 58% (OT). The two plants produce DME at an estimated cost of \$11.9/GJ_{LHV} (RC) and \$12.9/GJ_{LHV} (OT). If a credit is given for storing the CO_2 captured, the future costs may become as low as \$5.4/GJ_{LHV} (RC) and \$3.1/GJ_{LHV} (OT).

1. Introduction

One of the ways of reducing the CO_2 emissions from the transportation sector is by increasing the use of biofuels in vehicular applications. Dimethyl ether (DME) is a diesel-like fuel that can be produced from biomass in processes very similar to methanol production processes. Combustion of DME produces lower emissions of NO_x than combustion of diesel, with no particulate matter or SO_x in the exhaust [1], however, it also requires storage pressures in excess of 5 bar to maintain a liquid state (this pressure is similar to LPG). Other "advanced" or "second generation" biofuels include methanol, Fischer–Tropsch diesel and gasoline, hydrogen and ethanol. Like DME and methanol, Fischer–Tropsch fuels and hydrogen are also produced by catalytic conversion of a syngas.[1] Ethanol could also be produced by catalytic conversion of a syngas (at research stage), but is typically produced by biological fermentation. Of these fuels, only hydrogen can be produced at a higher biomass to fuel energy efficiency than methanol and DME. Ethanol (produced from fermentation of cellulosic biomass) and Fischer–Tropsch fuels have lower biomass to fuel energy efficiency than methanol and DME [2]. The advantage of Fischer–Tropsch diesel and gasoline – as well as methanol and ethanol blended in gasoline – is that these fuels can be used in existing vehicle power trains, while hydrogen, DME and neat ethanol and methanol require new or modified vehicle power trains.

The relative low cost needed to implement DME as a transportation fuel, together with its potential for energy efficient production and low emissions (including low well-to-wheel greenhouse gas emissions) when used in an internal combustion engine, makes DME attractive as a diesel substitute [2].

Two DME production plants, based on syngas from gasification of torrefied wood pellets, are investigated in this paper.

- The OT (once through) plant uses once through synthesis and the unconverted syngas is used for electricity production in a combined cycle.
- The recycle (RC) plant recycles unconverted syngas to the DME reactor to maximize DME production.

* Corresponding author. Tel.: +45 20712778; fax: +45 45884325.
E-mail address: lrc@mek.dtu.dk (L.R. Clausen).

[1] For hydrogen, the catalytic conversion occurs in a WGS reactor, where steam reacts with CO to produce hydrogen. Hydrogen can also be produced by fermentation.

0360-5442/$ – see front matter © 2010 Elsevier Ltd. All rights reserved.
doi:10.1016/j.energy.2010.09.004

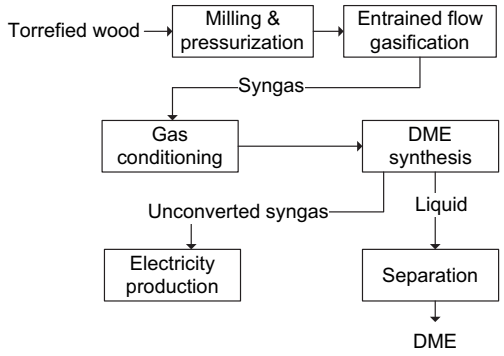

Fig. 1. Simplified flow sheet of the DME plant models.

Both plants uses CO_2 capture to condition the syngas for DME synthesis and the captured CO_2 is sent to underground storage. The plants are designed with focus on lowering the total CO_2 emission from the plants, even though the feedstock used is biomass. Capturing and storing CO_2 from a biomass plant gives a negative greenhouse effect, and can be an interesting concept, if a credit is given for storing CO_2 generated from biomass. The concept of receiving a credit for storing CO_2 generated from biomass has been investigated before (e.g., in [3]), but a study of the thermodynamics and economics of a biomass-based liquid fuel plant, where the focus in the design of the plant, was lowering the total CO_2 emission from the plant is not presented in the literature.

The DME plants modeled are of large-scale (>2000 tonnes per day) because of the better economics compared to small-scale production of DME [3,4]. Larger-scale plants, however, have higher feedstock transportation costs, which increase the attractiveness of torrefied wood pellets as a feedstock instead of conventional wood pellets. Torrefication of biomass also makes it possible to use commercially available coal gasification processing equipment.[2]

Production of DME from biomass has been investigated before (e.g., [5,6]). In [6] the feedstock used is black liquor and in [5] the feedstock used is switchgrass.

This paper documents the design of two DME plants using DNA[3] [7,8] and Aspen Plus modeling tools. Thermodynamic and economic performance of the plant configurations are presented and discussed.

1.1. Torrefication of biomass

Torrefaction of biomass is a mild pyrolysis process, taking place at 200–300 °C. The process alters the properties of biomass in a number of ways, including increased energy density, improved grindability/pulverization, better pelletization behavior, and higher resistance to biodegradation and spontaneous heating. This conversion process enables torrefied biomass to achieve properties very similar to coal, and therefore allows the altered biomass feedstock to be handled and processed using conventional coal preparation methods. Additionally, torrefied biomass can be stored in outdoor environments and the electricity consumption for milling and pelletization is significantly lower than that of wood [9,10].

[2] See the Gasification World Database [11] for a list of commercial gasification plants.

[3] Because of DNA's excellent solids handling, DNA was used to model the gasifier. The rest of the modeling was done with Aspen Plus.

Table 1
Process design parameters used in the modeling.

Feedstock	Torrefied wood pellets, composition (mass%): 49.19% C, 40.14% O, 5.63% H, 3.00% H_2O, 0.29% N, 0.06% S, 0.04% Cl, 1.65% Ash [9,13]. LHV = 19.9 MJ/kg [9]
Pretreatment	Power consumption for milling = 0.29% of the thermal input (LHV)[a]
Pressurizing and feeding	Pressurizing: CO_2/biomass mass-ratio = 6.0%. Feeding: CO_2/biomass mass-ratio = 12.0%
Gasifier	P_{exit} = 45 bar [12]. ΔP = 1.2 bar. Temperature before gas quench = 1300 °C[b]. Temperature after gas quench = 900 °C. Steam/biomass = 2.9 mass%. Carbon conversion = 100%[c]. Heat loss: 2.7% of the thermal input is lost to surroundings and 1% of the thermal input is used to generate steam[d].
Air separation unit	O_2 purity = 99.6 mole%. Electricity consumption = 1.0 MWe/(kg-O_2/s) [23]
Water gas shift (WGS) reactor	Pressure drop = 2 bar. Steam/carbon mole-ratios = 0.41 (RC) or 0.47 (OT)
DME synthesis	Liquid-phase reactor. Reactor outlet: T = 280 °C[e], P = 56 bar (RC) or 51 bar (OT). $\Delta P_{reactor}$ = 2.6 bar.
Distillation	Number of stages in distillation columns: 20 (topping column), 30 (DME column). P = 9.0 bar (topping column), 6.8 bar (DME column).
Cooling	COP = 1.2
Heat exchangers	ΔT_{min} = 10 °C (gas–liq) or 30 °C (gas–gas).
Steam plant	$\eta_{isentropic}$ for turbines in the RC plant: IP1 (55 bar, 600 °C[f]) = 86%, IP2 (9 bar, 600 °C[f]) = 88%, LP (2.0 bar, 383 °C. Outlet: 0.042 bar, vapor fraction = 1.00) = 89%[g]. $\eta_{isentropic}$ for turbines in the OT plant: HP (180 bar[f], 600 °C[f]) = 82%, IP1 (55 bar, 600 °C[f]) = 85%, IP2 (16 bar, 600 °C[f]) = 89%, LP (2.0 bar, 311 °C. Outlet: 0.042 bar, vapor fraction = 0.97) = 88%[g]. $\eta_{mechanical,\ turbine}$ = 98%[g]. $\eta_{electrical}$ = 98.6%[g]. $T_{Condensing}$ = 30 °C (0.042 bar).
Gas turbine	Air compressor: pressure ratio = 19.5 [g], $\eta_{polytropic}$ = 87%[g]. Turbine: TIT = 1370 °C[g], $\eta_{isentropic}$ = 89.8%[g]. $\eta_{mechanical}$ = 98.7%[g]. $\eta_{electrical}$ = 98.6%[g]
Compressors	$\eta_{polytropic}$ = 80% (4 stage CO_2 compression from 1 to 150 bar) [24], 85% (3 stage O_2 compression from 1 to 46 bar), 80% (syngas compressors)[g]. $\eta_{mechanical}$ = 94%[g]. $\eta_{electrical}$ = 100%

[a] [15]. In [9] the power consumption for milling torrefied biomass and bituminous coal are determined experimentally to be the same (1% of the thermal input). It is assumed that the size of the mill used in the experiments is the reason for the higher value (heavy-duty cutting mill, 1.5 kWe).

[b] In [13], 1300 °C is used for entrained flow gasification of torrefied biomass. Addition of silica or clay to the biomass to make the gasifier slagging at this relatively low temperature is probably needed [13], but these compounds are not added in the modeling.

[c] 95% is used in [15] for an entrained flow coal-slurry gasifier, but because the gasifier used in this study is dry fed, the carbon conversion is more than 99% (99,5% is a typical figure) [25]. The extensive use of slag recycle (fly ash is also recycled back to the gasifier) because of the low ash content in biomass increases this figure to almost 100%.

[d] [25] (for a coal gasifier). The 2.7% includes the heat loss from the gas cooler placed after the gasifier. In [25] 2% of the thermal input is used to generate steam. The figure is reduced to 1% because the gasification temperature is lowered from 1500–1600 °C to 1300 °C.

[e] A low temperature moves the chemical equilibrium towards DME, but slows down the chemical reactions, on the other hand, a too high temperature causes catalyst deactivation: "In practice, a reactor operating temperature of 250–280 °C balances kinetic, equilibrium, and catalyst activity considerations" [21].

[f] The integrated steam cycles are modeled as generic cycles. Commercial steam turbines for 600 °C are not available at these low pressures (e.g. the Siemens SST 900 steam turbine can have inlet conditions of maximum 585 °C and 165 bar).

[g] [15]. Note for gas turbine: the gas turbine is a natural gas fired gas turbine (GE 7FB) that is fitted to use syngas. In [15], simulations of the gas turbine operating on syngas show that the $m_{air\ compressor}/m_{turbine}$ ratio can be 0.91 – in this paper the ratio is 0.94. This high ratio is a result of the composition of the unconverted syngas (contains 80 mole% H_2). Typically, the TIT would be de-rated by 20–30 °C when operating on syngas (compared to natural gas) or up to 50 °C when operating on hydrogen. It is however assumed (as suggested in [15]) that the historic increase in TIT will continue, why the TIT of 1370 °C has not been de-rated.

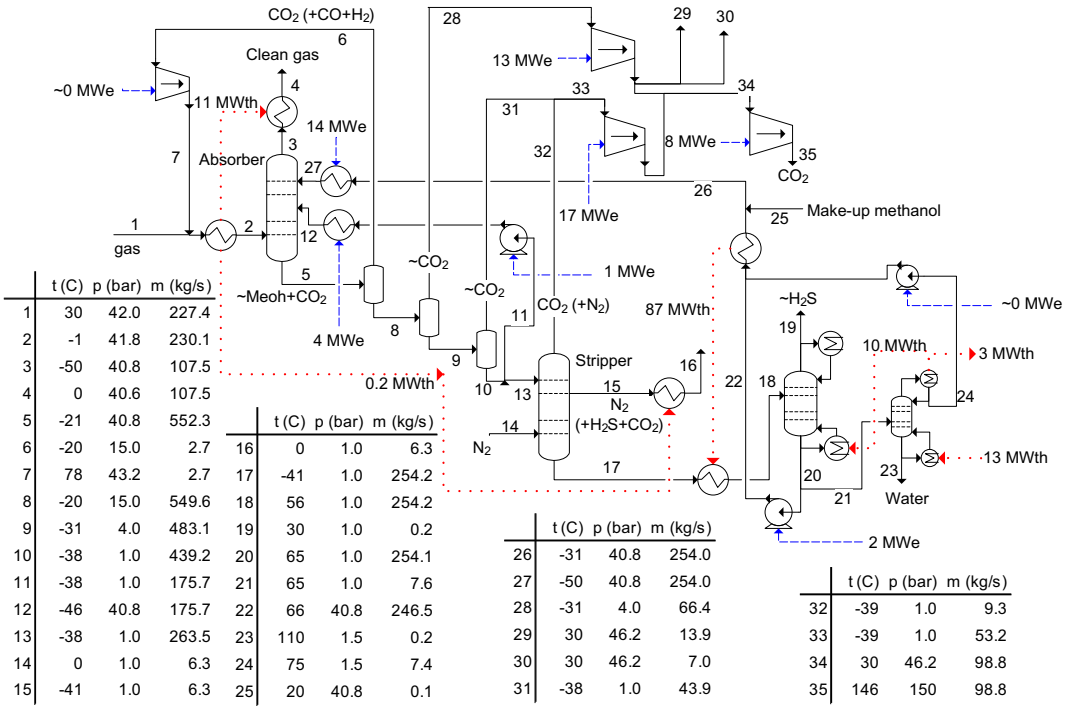

	t (C)	p (bar)	m (kg/s)
1	30	42.0	227.4
2	-1	41.8	230.1
3	-50	40.8	107.5
4	0	40.6	107.5
5	-21	40.8	552.3
6	-20	15.0	2.7
7	78	43.2	2.7
8	-20	15.0	549.6
9	-31	4.0	483.1
10	-38	1.0	439.2
11	-38	1.0	175.7
12	-46	40.8	175.7
13	-38	1.0	263.5
14	0	1.0	6.3
15	-41	1.0	6.3

	t (C)	p (bar)	m (kg/s)
16	0	1.0	6.3
17	-41	1.0	254.2
18	56	1.0	254.2
19	30	1.0	0.2
20	65	1.0	254.1
21	65	1.0	7.6
22	66	40.8	246.5
23	110	1.5	0.2
24	75	1.5	7.4
25	20	40.8	0.1

	t (C)	p (bar)	m (kg/s)
26	-31	40.8	254.0
27	-50	40.8	254.0
28	-31	4.0	66.4
29	30	46.2	13.9
30	30	46.2	7.0
31	-38	1.0	43.9

	t (C)	p (bar)	m (kg/s)
32	-39	1.0	9.3
33	-39	1.0	53.2
34	30	46.2	98.8
35	146	150	98.8

Fig. 2. Flow sheet of the acid gas removal (AGR) step incl. CO_2 compression, showing mass flows, electricity consumption and heat transfer. The numbers are valid for the RC plant.

2. Design of the DME plant

A simplified process flow sheet of the DME plant design is shown in Fig. 1 and detailed process flow sheets are shown in Figs. 5 and 6. Plant design aspects related to feedstock preparation, gasification, syngas conditioning, DME synthesis and distillation are described next and are followed by a discussion of electricity co-production in the two plants and the commercial status of the process components used. Important process design parameters used in the modeling are shown in Table 1.

2.1. Pretreatment and feeding

The pretreatment and feeding of torrefied wood pellets are assumed to be accomplished with existing commercial coal technology [9,10]. The torrefied biomass is milled to powder and the powder is pressurized with lock hoppers and fed to the gasifier with pneumatic feeders, both using CO_2 from the carbon capture process downstream.

2.2. Gasification

A commercial, dry-fed, slagging[4] entrained flow coal gasifier from Shell is used for gasifying the torrefied wood powder. The gasifier is oxygen blown, pressurized to 45 bar and steam moderated [12]. The oxygen supply is provided by a cryogenic air separation unit. A gas quench using about 200 °C recycled syngas downstream of the dry solids removal lowers the temperature of the syngas from 1300 °C to 900 °C. The composition of the syngas is calculated by assuming chemical equilibrium at 1300 °C (composition given in Tables 2 and 3).

2.3. Gas cooling and water gas shift

The syngas is further cooled to 200–275 °C by generating superheated steam for primarily the integrated steam cycle.[5] A sulfur tolerant[6] water gas shift (WGS) reactor adjusts the H_2/CO ratio to 1 (RC plant) or 1.6 (OT plant). In the RC plant, the H_2/CO ratio is adjusted to 1, to optimize DME synthesis according to Eq. (1) [5]. In the OT plant, the H_2/CO ratio is set to 1.6 to increase the amount of CO_2 captured in the downstream conditioning and thereby minimizing the CO_2 emissions from the plant. After the WGS reactor, the gas is cooled to 30 °C prior to the acid gas removal (ACR) step.

2.4. Gas cleaning incl. Carbon Capture and Storage (CCS)

Gas cleaning of biomass syngas for DME synthesis includes cyclones and filters for particle removal placed just after the high temperature syngas cooler, an AGR step and guard beds[7] placed just before the synthesis reactor [15,16]. The AGR step is done with a chilled methanol process similar to the Rectisol process [17,18], and it removes sulfur components (H_2S and COS[8]), CO_2 and other species such as NH_3 and HCl in one absorber (Fig. 2). By using only one absorber, some of the sulfur components will be removed and stored with the CO_2. This is an option because the sulfur content in biomass syngas is very low (~250 ppm of $H_2S + COS$). The sulfur components that are not stored with the CO_2 are sent to the off-gas boiler or gas turbine. The captured CO_2 is compressed to 150 bar for underground storage. The $H_2S + COS$ content in the syngas after

[4] Because of the low ash content in biomass a slag recycle is needed to make the gasifier slagging [13]. Also see note b below Table 1.

[5] Steam is superheated to 600 °C in the gas cooling (at 55 bar (RC) or 180 bar (OT)). In [12] it is stated that only a "mild superheat" can be used in the gas cooling, but in [14] steam at 125 bar is superheated to 566 °C.

[6] e.g. Haldor Topsoe produces such catalysts [19].

[7] ZnO and active carbon filters.

[8] Sulfur is only modeled as H_2S.

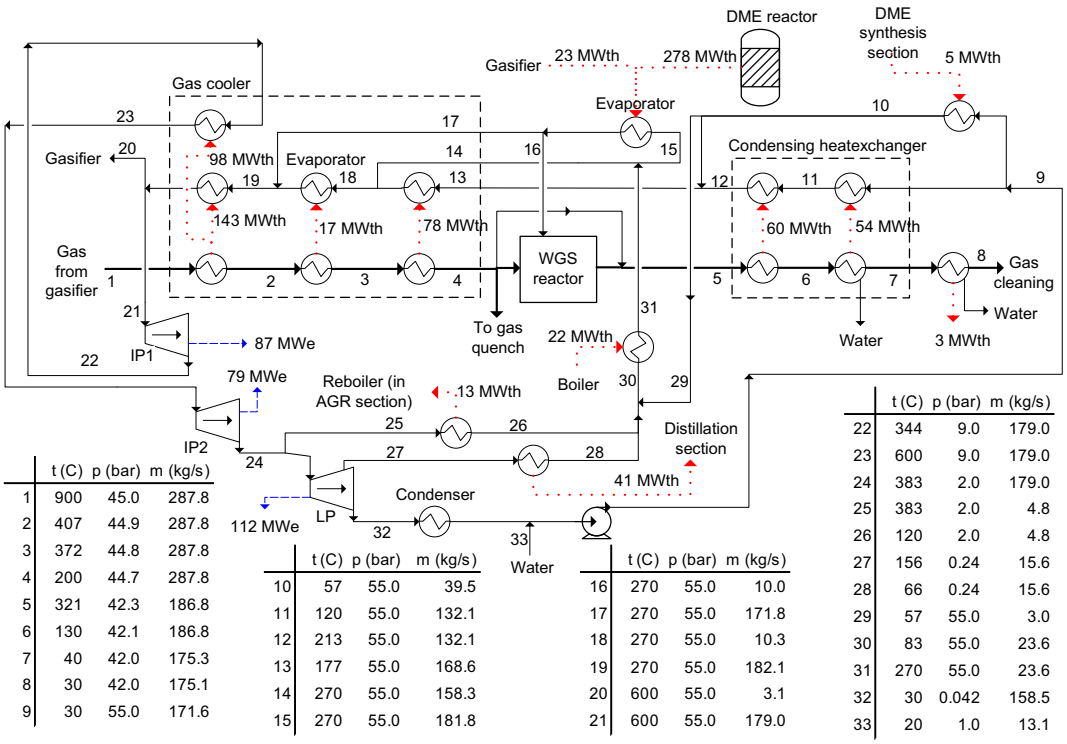

	t (C)	p (bar)	m (kg/s)
1	900	45.0	287.8
2	407	44.9	287.8
3	372	44.8	287.8
4	200	44.7	287.8
5	321	42.3	186.8
6	130	42.1	186.8
7	40	42.0	175.3
8	30	42.0	175.1
9	30	55.0	171.6

	t (C)	p (bar)	m (kg/s)
10	57	55.0	39.5
11	120	55.0	132.1
12	213	55.0	132.1
13	177	55.0	168.6
14	270	55.0	158.3
15	270	55.0	181.8

	t (C)	p (bar)	m (kg/s)
16	270	55.0	10.0
17	270	55.0	171.8
18	270	55.0	10.3
19	270	55.0	182.1
20	600	55.0	3.1
21	600	55.0	179.0

	t (C)	p (bar)	m (kg/s)
22	344	9.0	179.0
23	600	9.0	179.0
24	383	2.0	179.0
25	383	2.0	4.8
26	120	2.0	4.8
27	156	0.24	15.6
28	66	0.24	15.6
29	57	55.0	3.0
30	83	55.0	23.6
31	270	55.0	23.6
32	30	0.042	158.5
33	20	1.0	13.1

Fig. 3. Flow sheet of the power production part in the RC plant, showing mass flows, electricity production and heat transfer.

AGR is about 0.1 ppm[9] [20] and the CO_2 content is 0.1 mole% (RC) or 3 mole% (OT).[10]

The energy input for the AGR process is primarily electricity to power a cooling plant, but electricity is also used to run pumps that pressurize the methanol solvent.

2.5. Synthesis of DME

The syngas is compressed to 55–60 bar before entering the synthesis reactor. The reactor is modeled as a liquid-phase reactor operating at 280 °C, where the product gas is assumed to be in chemical equilibrium.[11] Besides the production of DME (Eqs. (1) and (2)) in the reactor, methanol is also produced in small quantities (Eq. (3)), and promoted by a high H_2/CO ratio. The reactor operating temperature is maintained at 280 °C by a water-jacketed cooler that generates saturated steam at 270 °C (55 bar). The reactor product gas is cooled to −37 °C (RC)[12] or −50 °C (OT) in order to dissolve most of the CO_2 in the liquid DME and a gas-liquid separator separates the liquid from the unconverted syngas. In the RC plant, 95% of the unconverted syngas is recycled to the synthesis reactor and the remaining 5% is sent to an off-gas boiler that augments the steam generation for electricity co-production in the Rankine power cycle. In the OT plant, the unconverted syngas is sent to a combined cycle.

In both the RC and the OT plant, the DME reactor pressure and temperature, and the cooling temperature before the gas-liquid separator have been optimized to improve the conversion efficiencies of biomass to DME and electricity. In both plants, the DME reactor temperature is kept as high as possible (280 °C) to ensure a more efficient conversion of the waste heat to electricity. In the RC plant, the reactor pressure (56 bar) and the cooling temperature (−37 °C) have been optimized to lower the combined electricity consumption of the syngas compressor and the cooling plant. In the OT plant the cooling temperature is set at −50 °C to dissolve most of the CO_2 in the liquid DME, while the reactor pressure (53 bar) is set so that the right amount of unconverted syngas is available for the gas turbine (see the section below about the power production).

$$3H_2 + 3CO \leftrightarrow CH_3OCH_3 + CO_2 \quad (1)$$

$$4H_2 + 2CO \leftrightarrow CH_3OCH_3 + H_2O \quad (2)$$

$$4H_2 + 2CO \leftrightarrow 2CH_3OH \quad (3)$$

2.6. Distillation

The liquid stream from the gas-liquid separator is distilled by fractional distillation in two columns. The first column is a topping column separating the absorbed gasses from the liquids. The gas from the topping column consisting mainly of CO_2 is compressed and recycled back to the AGR mentioned earlier. The second column separates the water and methanol from the DME. The DME liquid product achieves a purity of 99.99 mole%. The water is either sent to waste water treatment or evaporated and injected into the gasifier. The methanol is in the OT plant sent to

[9] The simulations show even lower sulfur content, but it is not known if this is credible.

[10] Some CO_2 is left in the syngas to ensure catalyst activity in the DME reactor [21]. In the RC plant, the CO_2 will be supplied by the recycled unconverted syngas.

[11] Assuming chemical equilibrium at 280 °C and 56 bar corresponds to a CO conversion of 81% (RC plant). In practice, chemical equilibrium will not be obtained. The Japanese slurry phase reactor (similar to the liquid-phase reactor) by JFE has achieved 55–64% CO conversion (depending on catalyst loading) at a 100 t/day pilot plant operating at 260 °C and 50 bar and $H_2/CO = 1$ [22]. The consequences of assuming chemical equilibrium are discussed in Section 3.1.

[12] As mentioned in the paragraph about gas cleaning some CO_2 is needed in the recycled unconverted syngas. When the stream is cooled to −37 °C, the right amount of CO_2 is kept in the gas phase.

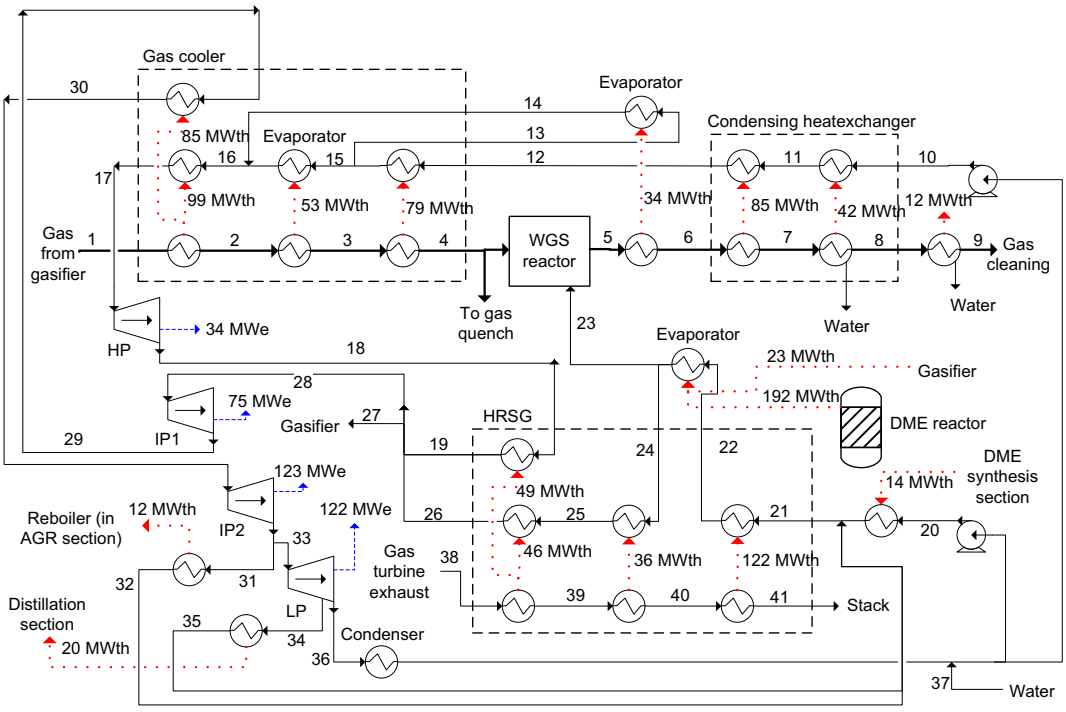

	t (C)	p (bar)	m (kg/s)
1	900	45.0	300.7
2	542	44.9	300.7
3	437	44.8	300.7
4	275	44.7	300.7
5	465	42.3	200.8
6	367	42.2	200.8
7	124	42.1	200.8
8	63	42.0	191.1
9	30	42.0	190.2
10	30	180.0	112.2
11	114	180.0	112.2

	t (C)	p (bar)	m (kg/s)
12	265	180.0	112.2
13	357	180.0	44.3
14	357	180.0	44.3
15	357	180.0	67.9
16	357	180.0	112.2
17	600	180.0	112.2
18	413	55.0	112.2
19	600	55.0	112.2
20	30	55.0	115.5
21	61	55.0	128.5

	t (C)	p (bar)	m (kg/s)
22	270	55.0	128.5
23	270	55.0	24.0
24	270	55.0	104.5
25	413	55.0	104.5
26	600	55.0	104.5
27	600	55.0	3.1
28	600	55.0	213.6
29	418	16.0	213.6
30	600	16.0	213.6
31	311	2.0	4.7

	t (C)	p (bar)	m (kg/s)
32	120	2.0	4.7
33	311	2.0	208.8
34	85	0.18	8.3
35	58	0.18	8.3
36	30	0.042	200.5
37	20	1.0	27.1
38	646	1.1	395.1
39	446	1.0	395.1
40	367	1.0	395.1
41	90	1.0	395.1

Fig. 4. Flow sheet of the power production part in the OT plant, showing mass flows, electricity production and heat transfer.

a dehydration reactor to produce DME, which is then recycled back to the topping column. In the RC plant, the methanol is instead recycled back to the synthesis reactor, because the mass flow of methanol is considered too low to make the dehydration reactor feasible.

2.7. Power production in the RC plant

An integrated steam cycle with reheat utilizes waste heat from mainly the DME reactor and the syngas coolers, to produce electricity (Fig. 3). Waste heat from the DME reactor is used to generate steam and the temperature of the reactor limits the steam pressure to 55 bar. Preheating of the water to the DME reactor and superheating of the steam from the DME reactor is mainly done with waste heat from the syngas coolers.

2.8. Power production in the OT plant

Besides power production from a steam cycle, power is in this plant also produced by a gas turbine utilizing unconverted syngas from the DME reactor. A heat recovery steam generator (HRSG) uses the exhaust from the gas turbine to produce steam for the steam cycle. Two pressure levels and double reheat is used in the steam cycle (Fig. 4). Steam at 180 bar is generated by the gas coolers placed after the gasifier, and steam at 55 bar is generated by waste heat from the DME reactor and the HRSG. The steam is reheated at 55 bar and 16 bar.

2.9. Status of process components used

It is assumed that commercial coal processing equipment (for milling, pressurization, feeding and gasification) can be used for torrefied biomass [9,10]. This needs to be verified by experiments and demonstrated at commercial scale, which to the author's knowledge has not been done. The liquid-phase DME reactor has only been demonstrated at pilot scale for DME synthesis, but is commercially available for Fischer–Tropsch synthesis, and has been demonstrated at commercial scale for methanol synthesis [5]. Commercial gas turbines and steam turbines are only available at specific sizes, and typically, the plant size would be fixed by the size of the gas turbine used. In this paper this has not been done. The size of the plant is based on two gasification trains, each at maximum size [12]. Commercial steam turbines are also only available for specific steam pressures and temperatures. However, in order to ease

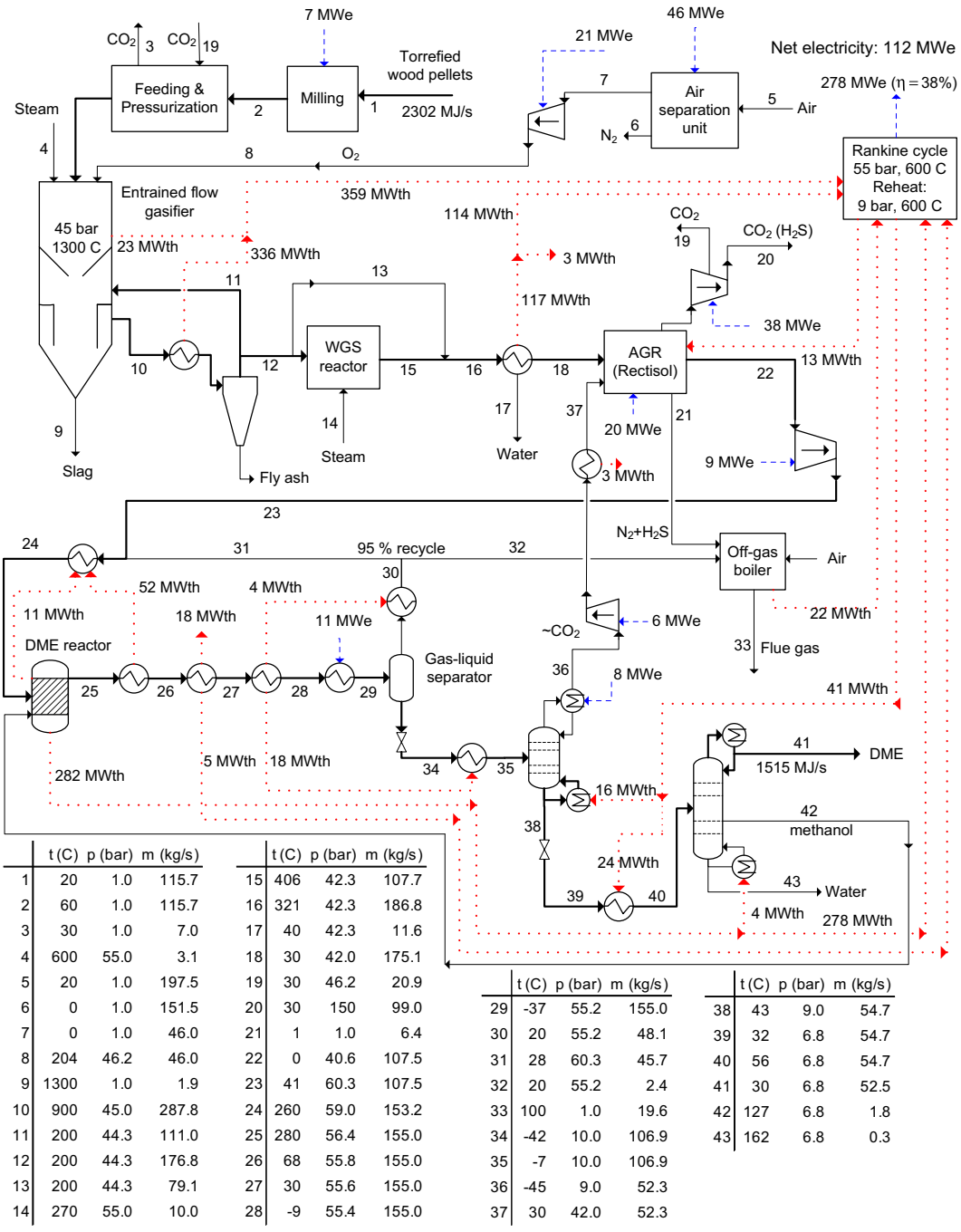

	t (C)	p (bar)	m (kg/s)
1	20	1.0	115.7
2	60	1.0	115.7
3	30	1.0	7.0
4	600	55.0	3.1
5	20	1.0	197.5
6	0	1.0	151.5
7	0	1.0	46.0
8	204	46.2	46.0
9	1300	1.0	1.9
10	900	45.0	287.8
11	200	44.3	111.0
12	200	44.3	176.8
13	200	44.3	79.1
14	270	55.0	10.0

	t (C)	p (bar)	m (kg/s)
15	406	42.3	107.7
16	321	42.3	186.8
17	40	42.3	11.6
18	30	42.0	175.1
19	30	46.2	20.9
20	30	150	99.0
21	1	1.0	6.4
22	0	40.6	107.5
23	41	60.3	107.5
24	260	59.0	153.2
25	280	56.4	155.0
26	68	55.8	155.0
27	30	55.6	155.0
28	-9	55.4	155.0

	t (C)	p (bar)	m (kg/s)
29	-37	55.2	155.0
30	20	55.2	48.1
31	28	60.3	45.7
32	20	55.2	2.4
33	100	1.0	19.6
34	-42	10.0	106.9
35	-7	10.0	106.9
36	-45	9.0	52.3
37	30	42.0	52.3

	t (C)	p (bar)	m (kg/s)
38	43	9.0	54.7
39	32	6.8	54.7
40	56	6.8	54.7
41	30	6.8	52.5
42	127	6.8	1.8
43	162	6.8	0.3

Fig. 5. Flow sheet of the recycle (RC) DME plant model, showing mass flows, electricity consumption/production and heat transfer.

the modeling of the integrated steam cycle a generic steam cycle has been modeled, using superheat and reheat temperatures of 600 °C (Table 1). Components used for WGS, gas cleaning, CO_2 capture and compression, distillation are commercially available [5].

The modeling input values are based on best commercially available technology, only the values used for: the steam superheating temperature (600 °C), HP steam pressure in the OT plant (180 bar) and the gas turbine TIT (1370 °C) can be considered progressive (see comments at Table 1). The assumption of chemical equilibrium in the DME synthesis is very progressive and the consequences of this assumption are discussed in Section 3.1.

3. Results

3.1. Process simulation results

The results from the simulation of the two DME plants are presented in the following. In the flow sheets in Figs. 5 and 6, some of the important thermodynamic parameters are shown together with electricity production/consumption and heat transfer in the plants. In Tables 2 and 3, the composition of specific streams in the flow sheets is shown.

Important energy efficiencies for the DME plants are shown in Fig. 7. It can be seen, for the RC plant, that 66% of the input chemical energy in the torrefied wood is converted to chemical

Table 2
Stream composition for the RC plant (stream numbers refer to Fig. 5).

	Gasifier exit	WGS outlet	AGR inlet	AGR outlet	Reactor inlet	Reactor outlet	Recycle gas	To distillation	Recycle CO_2	DME
Stream number	12	15	18 + 37	22	24 + 42	25	31	34[a]	37	41[a]
Mass flow (kg/s)	176.8	107.9	227.4	107.5	155.0	155.0	45.7	106.9	52.3	52.6
Flow (kmole/s)	8.66	5.35	9.81	7.08	9.24	4.67	2.10	2.46	1.24	1.14
Mole frac (%)										
H_2	29.1	44.0	35.7	49.4	45.5	16.2	33.7	0.57	1.1	0.00
CO	50.9	27.7	35.7	49.4	45.5	17.0	33.6	2.2	4.3	0.00
CO_2	7.4	24.6	27.7	0.10	3.0	30.0	12.8	45.4	90.0	0.00
H_2O	12.3	3.4	0.12	0.00	0.09	0.56	0.00	1.1	0.00	0.10
CH_4	0.04	0.03	0.25	0.35	0.93	1.8	2.9	0.86	1.7	0.00
H_2S	0.03	0.02	0.02	0.00	0.00	0.00	0.00	0.00	0.00	0.00
N_2	0.14	0.12	0.28	0.39	2.8	5.4	10.8	0.65	1.3	0.00
Ar	0.07	0.06	0.25	0.34	1.5	2.9	5.2	0.75	1.5	0.00
CH_3OH	–	–	0.00	0.00	0.55	1.1	0.00	2.1	0.00	0.00
CH_3OCH_3	–	–	0.01	0.00	0.25	25.0	1.1	46.4	0.09	99.9

[a] Liquid.

energy stored in the output DME. If the torrefication process – that occurs outside the plant – is accounted for, the efficiency drops to 59%. In [5] energy efficiencies of biomass to DME are reported to be 52% (RC) and 24% (OT), if the net electricity production is included the efficiencies are 61% (RC) 55% (OT) [5]. The gasifier used in [5] is an oxygen-blown, pressurized fluid bed gasifier that produces a gas with a high concentration of CH_4 (7 mole% after AGR [26]), because of this a high conversion efficiency from biomass to DME is difficult to achieve.[13] JFE reports the natural gas to DME efficiency to be 71% [22] and the coal to DME efficiency to be 66% [27]. Since the cold gas efficiency of the Shell gasifier operated on torrefied biomass is similar to the cold gas efficiency of the same gasifier operated on coal (see below), the coal to DME efficiency should be similar to the torrefied biomass to DME efficiency.

The biomass to DME efficiency of 66% for the RC plant is mainly achieved because only a small fraction of the syngas in the RC plant is not converted to DME, but sent to the off-gas boiler (Fig. 8). This is possible because the syngas contains very few inerts, but also because CO_2, which is a by-product of DME production (Eq. (1)), is dissolved in the condensed DME, and therefore does not accumulate in the synthesis loop.

The input chemical energy in the torrefied wood that is not converted to DME is converted to thermal energy in the plants and used to produce electricity in the integrated steam cycle or gas turbine. Fig. 8 shows in which components that chemical energy is converted to thermal energy. Only small amounts of thermal energy is not used for electricity production, but directly removed by cooling water (see flow sheets in Figs. 5 and 6). The thermal energy released in the gasifier, WGS reactor, DME reactor and the off-gas boiler is converted to electricity in the integrated steam cycle with an efficiency of 38% (RC) or 40% (OT). The thermal energy released in the gas turbine combustor is converted to electricity with an efficiency of 60%.[14] The chemical energy in the torrefied biomass input that is not converted to DME or electricity is lost in the form of waste heat mainly in the condenser of the integrated steam plant. In order to improve the total energy efficiency of the plant, the steam plant could produce district heating instead. This would however result in a small reduction in power production.

From Fig. 8 the cold gas efficiency of the gasifier can be seen to be 81% (73%/90%), which is similar to the efficiency of the same Shell gasifier operated on coal (81–83% [12]). The cold gas efficiency of the oxygen-blown, pressurized fluid bed gasifier reported in [5] is also similar (80% for switchgrass [5]).

The assumption of chemical equilibrium in the DME synthesis reactor results in a CO conversion of 81% (per pass) in the RC plant. If a CO conversion of 60% (as suggested in footnote 11) was assumed, the recycle gas flow would double, but the reactor inlet mole flow would only increase from 9.24 kmol/s to ~12 kmol/s. The higher flow increases the duty of the recycle compressor and the cooling need in the synthesis loop, but the effect on the net electricity production would only be modest. The total biomass to DME conversion efficiency would drop slightly, but could be kept constant by raising the recycle ratio from 95% to 97%.

The effect of lowering the syngas conversion in the DME reactor would be greater in the OT plant: it is estimated that the unconverted syngas flow to the gas turbine would increase with ~70%, and this would lower the biomass to DME conversion efficiency from 48% to 35% but raise the DME to net electricity conversion efficiency from 16% to 24%.

3.2. Cost estimation

3.2.1. Plant investments

The investments for the two DME plants are estimated based on component cost estimates given in Table 4. In Fig. 9 the cost distribution between different plant areas is shown for both the RC and the OT plant. It is seen that the gasification part is very cost intensive, accounting for 38–41% of the investment. The figure also shows that the OT plant is slightly more expensive than the RC plant, mostly due to the added cost of the gas turbine and HRSG, which is not outbalanced by what is saved on the DME synthesis area.

[13] Because the biomass to DME conversion efficiency in [5] is limited by especially the high CH_4 concentration in the syngas, and this creates a great amount of purge gas from the DME reactor in the RC plant, it is more appropriate to compare the RC plant in [5] with the OT plant in this paper: The (torrefied) biomass to DME efficiencies are: 48% (OT) and 52% ([5]). The (torrefied) biomass to electricity (gross) efficiencies are 23% (OT) and 16% ([5]). If a mild recirculation of unconverted syngas was incorporated in the OT plant, a torrefied biomass to DME efficiency of 52% could be achieved, with an expected drop in gross electricity efficiency from 23% to 20%. The higher gross electricity production in the modified OT plant compared to the RC plant in [5] (20% vs. 16%) is due to a more efficient waste heat recovery system in the modified OT plant (e.g. double reheat).

[14] The gas turbine is only used in the OT plant. The net efficiency of the gas turbine is 38%. The 60% efficiency is calculated by assuming that 40% (the efficiency of the complete steam cycle in the OT plant) of the heat transferred in the HRSG is converted to electricity. Because the steam pressure in the HRSG is 55 bar, while the HP steam in the OT plant is 180 bar, it may be more correct to use the steam cycle efficiency of the RC plant (38%), which is also based on steam at 55 bar. If this is done, the efficiency is reduced from 60% to 58%.

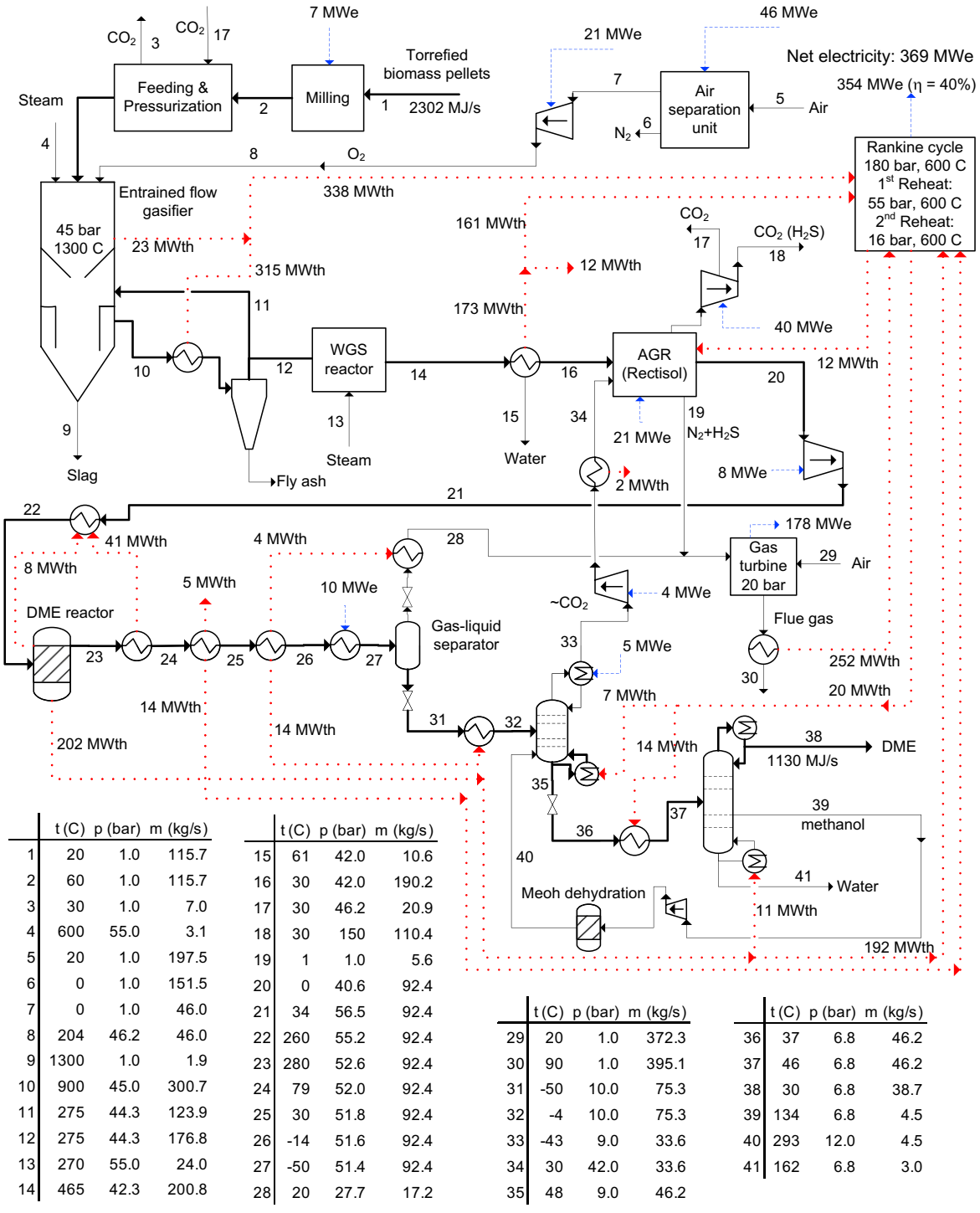

	t (C)	p (bar)	m (kg/s)
1	20	1.0	115.7
2	60	1.0	115.7
3	30	1.0	7.0
4	600	55.0	3.1
5	20	1.0	197.5
6	0	1.0	151.5
7	0	1.0	46.0
8	204	46.2	46.0
9	1300	1.0	1.9
10	900	45.0	300.7
11	275	44.3	123.9
12	275	44.3	176.8
13	270	55.0	24.0
14	465	42.3	200.8

	t (C)	p (bar)	m (kg/s)
15	61	42.0	10.6
16	30	42.0	190.2
17	30	46.2	20.9
18	30	150	110.4
19	1	1.0	5.6
20	0	40.6	92.4
21	34	56.5	92.4
22	260	55.2	92.4
23	280	52.6	92.4
24	79	52.0	92.4
25	30	51.8	92.4
26	-14	51.6	92.4
27	-50	51.4	92.4
28	20	27.7	17.2

	t (C)	p (bar)	m (kg/s)
29	20	1.0	372.3
30	90	1.0	395.1
31	-50	10.0	75.3
32	-4	10.0	75.3
33	-43	9.0	33.6
34	30	42.0	33.6
35	48	9.0	46.2

	t (C)	p (bar)	m (kg/s)
36	37	6.8	46.2
37	46	6.8	46.2
38	30	6.8	38.7
39	134	6.8	4.5
40	293	12.0	4.5
41	162	6.8	3.0

Fig. 6. Flow sheet of the once through (OT) DME plant model, showing mass flows, electricity consumption/production and heat transfer.

Similar plant costs are reported in [5] (per MWth biomass input) for RC and OT DME plants, but in this reference, the cost for the RC plant is higher than the cost for the OT plant due to high cost of the DME synthesis part in the RC plant.[15]

3.2.2. *Levelized cost calculation*

To calculate the cost of the produced DME, a 20-year levelized cost calculation is carried out for both DME plants (Table 5). The levelized costs are calculated with a capacity factor of 90% and with no credit for the CO_2 stored. The results show a lower cost for the RC plant than the OT plant. Levelized costs reported in [5] for OT and RC DME plants without CCS are \$16.9/GJ_{LHV} (OT) and \$13.8/GJ_{LHV} (RC). The difference between these costs and the costs calculated in this paper is mainly due to a lower credit for the electricity co-production in [5],[16] but the higher conversion efficiencies

[15] The cost is scaled with the DME reactor mole flow, which is more than five times the mole flow in the OT case [26].

[16] An electricity price of 40 \$/MWh is assumed in [5]. The capital charge rate and O&M rate are the same as used in this paper, but the biomass cost used in [5] is lower.

Table 3
Stream composition for the OT plant (stream numbers refer to Fig. 6).

	Gasifier exit	WGS outlet	AGR inlet	Reactor inlet	Reactor outlet	Gas to gas turbine	Recycle CO_2	Methanol	Dehyd. methanol	DME
Stream number	12	14	16 + 34	22	23	28	34	39	40	38[a]
Mass flow (kg/s)	176.8	200.8	223.8	92.4	92.4	17.2	33.6	4.5	4.5	38.7
Flow (kmole/s)	8.66	9.83	10.02	7.08	3.73	1.98	0.77	0.16	0.16	0.83
Mole frac (%)										
H_2	29.1	43.2	42.5	60.2	42.6	79.7	1.5	0.00	0.00	0.00
CO	50.9	26.2	25.8	36.5	6.3	11.5	1.1	0.00	0.00	0.00
CO_2	7.4	24.3	31.3	3.0	23.8	7.3	97.1	0.00	0.00	0.01
H_2O	12.3	6.0	0.12	0.00	3.1	0.00	0.00	29.6	56.9	0.09
CH_4	0.04	0.03	0.04	0.06	0.11	0.16	0.10	0.00	0.00	0.00
H_2S	0.03	0.02	0.02	0.00	0.00	0.00	0.00	0.00	0.00	0.00
N_2	0.14	0.12	0.12	0.17	0.33	0.59	0.05	0.00	0.00	0.00
Ar	0.07	0.06	0.06	0.09	0.17	0.29	0.08	0.00	0.00	0.00
CH_3OH	–	–	0.00	0.00	2.4	0.00	0.00	69.4	14.7	0.00
CH_3OCH_3	–	–	0.01	0.00	21.2	0.45	0.11	1.0	28.4	99.9

[a] Liquid.

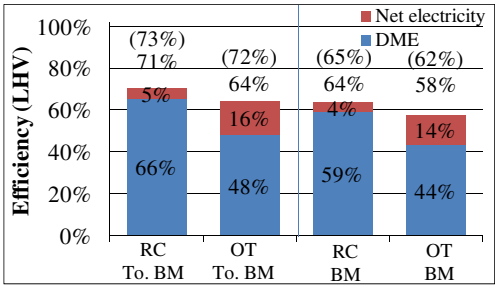

Fig. 7. Energy efficiencies for the conversion of torrefied or untreated biomass to DME and electricity for the two plants. An energy efficiency of torrefication of 90% is assumed. The numbers in parentheses are the fuels effective efficiencies, defined as $\frac{DME}{biomass^{\frac{electricity}{50\%}}}$ where the fraction $\frac{electricity}{50\%}$ corresponds to the amount of biomass that would be used in a stand-alone BIGCC power plant with an efficiency of 50% [5], to produce the same amount of electricity.

achieved in this paper also plays a role. Levelized cost reported in [15] for coal and biomass based Fischer–Tropsch production (CTL, CBTL and BTL) are \$12.2/GJ_{LHV} to \$27.7/GJ_{LHV}[17] for OT and RC plants with CCS. The \$27.7/GJ_{LHV} is for the biomass based Fischer–Tropsch plant (BTL).

If a credit is given for storing the CO_2 captured in the DME plants, since the CO_2 is of recent photosynthetic origin (bio-CO_2), the plant economics become even more competitive, as seen in Fig. 10. At a credit of \$100/ton-CO_2, the levelized cost of DME becomes \$5.4/GJ_{LHV} (RC) and \$3.1/GJ_{LHV} (OT). From Fig. 10 it is also seen that above a CO_2 credit of about \$27/ton-CO_2 the OT plant has a lower DME production cost than the RC plant. It should be noted that that the figure is generated by conservatively assuming all other costs constant. This will, however, not be the case because an increase in the GHG emission cost (=the credit for bio-CO_2 storage) will cause an increase in electricity and biomass prices. In [3], the increase in income from coproduct electricity (when the GHG emission cost is increased) more than offsets the increase in biomass cost. The effect of increasing the income from coproduct electricity for the two DME plants can be seen in Fig. 11. This figure clearly shows how important the income from coproduct electricity is for the economy of the OT plant, because the net electricity production is more than three times the net electricity production of the RC plant.

[17] The capital charge rate, O&M rate and electricity sale price are the same as used in this paper. The biomass and coal cost are 1.8 and 5.5 \$/GJ_{LHV}.

Since torrefied biomass pellets are not commercially available, the assumed price of \$4.6/GJ_{LHV} [29] is uncertain. In Fig. 12, the relation between the price of torrefied biomass pellets and the DME production cost is shown.

If no credit was given for bio-CO_2 storage, the plants could achieve lower DME production cost, and higher energy efficiencies, by venting the CO_2 instead of compressing and storing the CO_2. If the RC plant vented the CO_2, the levelized cost of DME would be reduced from \$11.9/GJ_{LHV} to \$10.7/GJ_{LHV}, and the total energy efficiency would increase from 71% to 73%. The effect of venting the CO_2 from the OT plant would be even greater, because more energy consuming process changes were made, to lower the plant CO_2 emissions.

3.3. Carbon analysis

Since the feedstock for the DME production is biomass, it is not considered a problem – concerning the greenhouse effect – to vent CO_2 from the plants. However, since CO_2 is captured in order to condition the syngas, the pure CO_2 stream can be compressed and stored with little extra cost. Storing CO_2 that is of recent photosynthetic origin (bio-CO_2), gives a negative greenhouse effect and might be economic in the future, if CO_2 captured from the atmosphere is rewarded, in the same way as emission of CO_2 is taxed. If not, some of the biomass could be substituted by coal – matching the amount of CO_2 captured (this is investigated in [15]).

In the designed plants, the torrefied biomass mass flow contains 56.9 kg/s of carbon and the DME product contains 47% (RC) or 34% (OT) of this carbon (Fig. 13). The carbon in the product DME will (if used as a fuel) eventually be oxidized and the CO_2 will most likely be vented to the atmosphere. Almost all of the remaining carbon is captured in the syngas conditioning (55% (RC) or 61% (OT)) but small amounts of carbon are vented as CO_2 in either, the flue gas from the GT/boiler or from the pressurizing of the biomass feed. The total CO_2 emission from the plants is therefore 3% (RC) and 10% (OT) of the input carbon in the torrefied biomass. Accounting for the torrefication process, which occurs outside the plant, the emissions become about 22% (RC) and 28% (OT) of the input carbon in the untreated biomass.

A number of measures were taken to minimize the CO_2 emissions from the plants.

1. Recycling a CO_2-containing gas stream from the distillation section to the CO_2 capture step (contains 24% (RC) or 16% (OT) of the input carbon in the torrefied biomass).

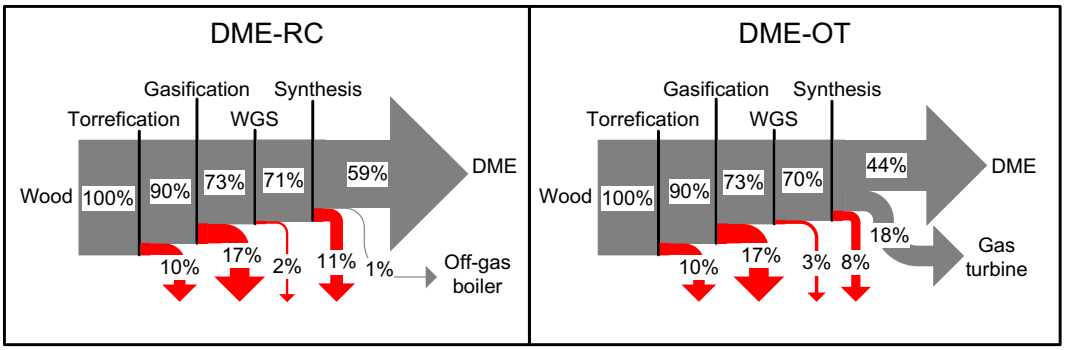

Fig. 8. Chemical energy streams (LHV) in the two DME plants, including conversion heat losses. The torrefication process does not occur in the DME plants, but decentralized. The conversion heat losses (excluding the torrefication heat loss) are used by the integrated steam plant to produce electricity.

Table 4
Investment estimates for plant areas and components in the DME plants.

Plant area/ component	Reference size	Reference cost (million 2007 $)	Scaling exponent	Overall installation factor	Source
Air separation unit	52.0 kg-O_2/s	141	0.5	1	[23]
Gasification island[a]	68.5 kg-feed/s	395	0.7	1	[12]
Water gas shift reactor	815 MW_{LHV} biomass	3.36	0.67	1.16	[15]
AGR (Rectisol)	2.48 kmole/s feed gas	28.8	0.63	1.55	[15]
CO_2 compression to 150 bar	13 MWe	9.52	0.67	1.32	[15]
CO_2 transport and storage	113 kg-CO_2/s	110	0.66	1.32	[28]
Compressors	10 MWe	6.3	0.67	1.32	[15]
DME reactor	2.91 kmole/s feed gas	21.0	0.65	1.52	[26]
Cooling plant	3.3 MWe	1.7	0.7	1.32	
Distillation	6.75 kg/s DME	28.4	0.65	1.52	[26]
Steam turbines and condenser	275 MWe	66.7	0.67	1.16	[15]
Heat exchangers	355 MWth	52	1	1.49	[15]
Off-gas boiler	355 MWth	52	1	1.49	
Gas turbine	266 MWe	73.2	0.75	1.27	[15]

The cost for a specific size component is calculated in this way: cost = reference cost × (size/reference size)$^{\text{scaling exponent}}$ × overall installation factor.
The overall installation factor includes balance of plant (BOP) costs and indirect costs such as engineering, contingency and startup costs. For some components these costs are, however, included in the reference cost. All costs are adjusted to 2007 $ by using the CEPCI (Chemical Engineering Plant Cost Index (data for 2000–2007 in [15])).
[a] The reference size basis chosen is mass flow instead of energy flow. This means that the cost might be overestimated because the dried coal LHV used in the reference is 24.84 MJ/kg and the LHV of torrefied wood pellets is 19.9 MJ/kg.

Table 5
Twenty-year levelized production costs for DME.

	Price/rate	RC	OT
		Levelized cost in $/GJ-DME	
Capital charges	15.4% of plant investment [15]	4.9	7.2
O&M	4% of plant investment [15]	1.3	1.9
Torrefied biomass pellets	4.6$/$GJ_{LHV}$ [29]	6.9	9.3
Electricity sales	At 60$/MWh [15]	−1.2	−5.4
Credit for bio-CO_2 storage		0	0
DME ($/$GJ_{LHV}$)		11.9	12.9

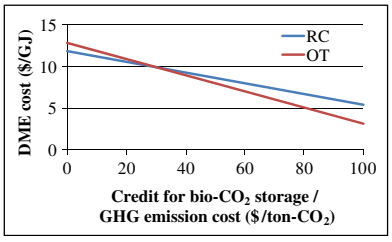

Fig. 10. DME production cost as a function of the credit given for bio-CO_2 storage.

2. Cooling the product stream from the DME reactor to below −35 °C in order to dissolve CO_2 in the liquid that is sent to the distillation section (80% (RC) or 83% (OT) of the CO_2 in the stream is dissolved in the liquid).
3. Having an H_2/CO ratio of 1.6 instead of 1 in the OT plant, which lowers the amount of carbon left in the unconverted syngas, that is combusted and vented (the H_2/CO ratio in the unconverted syngas is 6.6).

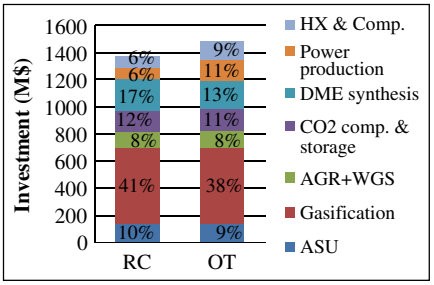

Fig. 9. Cost distribution between different plant areas for the two DME plants.

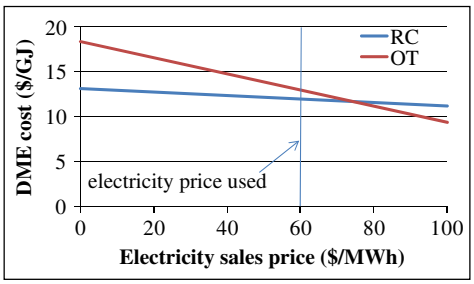

Fig. 11. DME production cost as a function of the electricity sales price.

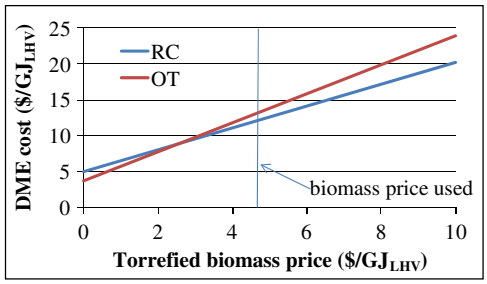

Fig. 12. DME production cost as a function of the price of torrefied biomass pellets.

the N_2 content of the biomass is important. The N_2 content of the torrefied wood used is 0.29 mass%, but the N_2 content in other biomasses can be higher. If for instance a torrefied grass is used with a N_2 content of 1.2 mass%, the inert fraction in the product gas from the DME reactor would be increased from 10 to 23 mole %. This would still be a feasible option but would increase the size/cost of the DME reactor.

4. Conclusion

The paper documents the thermodynamics and economics of two DME plants based on gasification of torrefied wood pellets,

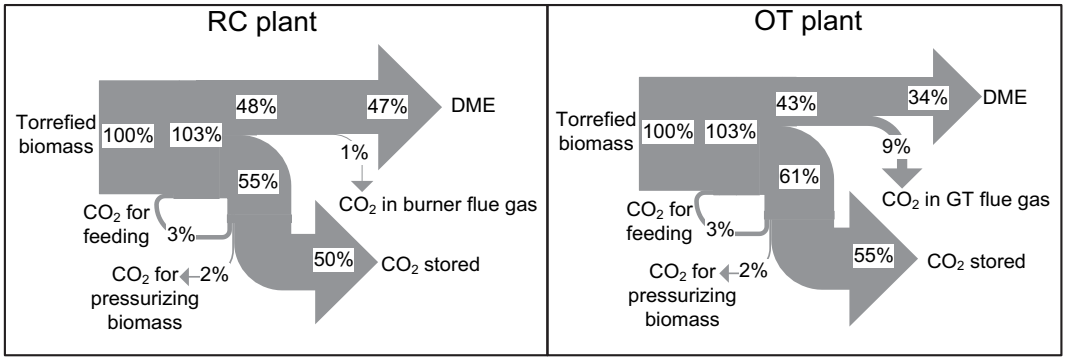

Fig. 13. Carbon flows in the two DME plants.

The costs of doing these measures are as follows.

1. 6 MWe (RC) or 4 MWe (OT) to compress the CO_2-containing gas stream.
2. For the RC plant: most likely nothing, because CO_2 is typically removed before recycling the gas stream to the DME reactor, in order to keep the size/cost of the reactor as low as possible. For the OT plant: some of the 11 MWe used to cool the gas stream could be saved.
3. By increasing the H_2/CO ratio from 1 to 1.6 in the OT plant, more heat will be released in the WGS reactor (Fig. 8) and therefore less in the GT combustion chamber. Even though the waste heat from the WGS reactor is used to produce electricity, it is more efficient to release the heat in the GT. Besides this, the conversion rate in the DME reactor is also lowered, which is compensated for by increasing the reactor pressure. Also, more methanol is produced in the DME reactor, which increases the need for (or increases the benefit of adding) the methanol dehydration step.

Doing the recycle of the CO_2 containing gas stream in the RC plant is only possible if the inert fraction (sum of N_2, Argon and CH_4) in the gas from the gasifier is very low. For the plants modeled, the inert fraction in the gas is 0.24 mole%. The inert fraction in the syngas leaving the AGR step has however risen to 1.1 mole%, because of the recycle of the CO_2 stream. The inert fraction in the product gas from the DME reactor is even higher (10 mole%). In the simulations, all the N_2 originates from the biomass[18], and because more than half of the inert fraction is N_2, where the focus in the design of the plants was lowering the CO_2 emissions from the plants. It is shown that CO_2 emissions can be reduced to about 3% (RC) and 10% (OT) of the input carbon in the torrefied biomass. Accounting for the torrefication process, which occurs outside the plant, the emissions become 22% (RC) and 28% (OT) of the input carbon in the untreated biomass. The plants achieve total energy efficiencies of 71% (RC) and 64% (OT) from torrefied biomass to DME and net electricity, but if the torrefication process is taken into account, the total energy efficiencies from untreated biomass to DME and net electricity are 64% (RC) and 58% (OT). The two plants produce DME at an estimated cost of \$11.9/GJ_{LHV} (RC) and \$12.9/GJ_{LHV} (OT) and if a credit is given for storing the CO_2 captured, the cost become as low as \$5.4/GJ_{LHV} (RC) and \$3.1/GJ_{LHV} (OT) (at \$100/ton-CO_2).

[18] It was assumed that the 0. mole% of inerts in the oxygen from the ASU is argon. This was done to show where the inerts in the downstream processing originated: argon from the ASU and nitrogen from the biomass. In practice, some nitrogen will also be present in the oxygen from the ASU.

References

[1] International DME association (IDA). DME – clean fuel for transportation, http://www.aboutdme.org/index.asp?bid=219.
[2] Eucar, Concawe, JRC. Well-to-wheels analysis of future automotive fuels and powertrains in the European context, version 2C. Eucar, Concawe, JRC, http://ies.jrc.ec.europa.eu/WTW; 2007.
[3] Larson ED, Williams RH, Jin H. Fuels and electricity from biomass with CO_2 capture and storage. In: Proceedings of the eighth international conference on greenhouse gas control technologies, Trondheim, Norway; June 2006.
[4] Boerrigter H. Economy of biomass-to-liquids (BTL) plants. Report: ECN-C–06-019. Petten, The Netherlands: ECN, http://www.ecn.nl/publications/; 2006.
[5] Larson ED, Jin H, Celik FE. Large-scale gasification-based coproduction of fuels and electricity from switchgrass. Biofuels Bioprod Bioref 2009;3:174–94.
[6] Pettersson K, Harveya S. CO_2 emission balances for different black liquor gasification biorefinery concepts for production of electricity or second-generation liquid biofuels. Energy 2010;35(2):1101–6.
[7] Elmegaard B, Houbak N. DNA – a general energy system simulation tool. In: Amundsen J, et al., editors. SIMS 2005, 46th conference on simulation and modeling, Trondheim, Norway. Tapir Academic Press; 2005. p. 43–52.
[8] Homepage of the thermodynamic simulation tool DNA, http://orbit.dtu.dk/query?record=231251.
[9] Kiel JHA, Verhoeff F, Gerhauser H, Meuleman B. BO_2-technology for biomass upgrading into solid fuel – pilot-scale testing and market implementation. In:

Proceedings for the 16th European biomass conference and exhibition, Valencia, Spain; 2008, p. 48–53. http://www.ecn.nl/publications/.
[10] Bergman PCA, Boersma AR, Kiel JHA, Prins MJ, Ptasinski KJ, Janssen FJJG. Torrefaction for entrained-flow gasification of biomass. Report: ECN-C–05-067. Petten, The Netherlands: ECN, http://www.ecn.nl/publications/; 2005.
[11] The National Energy Technology Laboratory (NETL). Gasification World Database 2007, http://www.netl.doe.gov/technologies/coalpower/gasification/database/database.html; 2007.
[12] van der Ploeg HJ, Chhoa T, Zuideveld PL. The shell coal gasification process for the US industry. In: Proceedings for the gasification technology conference, Washington DC, USA; 2004.
[13] van der Drift A, Boerrigter H, Coda B, Cieplik MK, Hemmes K. Entrained flow gasification of biomass; ash behaviour, feeding issues, system analyses. Report: ECN-C–04-039. Petten, The Netherlands: ECN, http://www.ecn.nl/publications/; 2004.
[14] The National Energy Technology Laboratory (NETL). Shell gasifier IGCC base cases. Report: PED-IGCC-98-002, http://www.netl.doe.gov/technologies/coalpower/gasification/pubs/pdf/system/shell3x_.pdf; 1998 (revised in 2000).
[15] Kreutz TG, Larson ED, Liu G, Williams RH. Fischer–Tropsch fuels from coal and biomass. Report. Princeton, New Jersey: Princeton Environmental Institute, Princeton University, http://www.princeton.edu/pei/energy/publications; 2008.
[16] van der Drift A, Boerrigter H. Synthesis gas from biomass. Report: ECN-C-06-001. Petten, The Netherlands: ECN, http://www.ecn.nl/publications/; 2006.
[17] Linde Engineering. Rectisol wash, http://www.linde-le.com/process_plants/hydrogen_syngas_plants/gas_processing/rectisol_wash.php.
[18] Lurgi GmbH. The rectisol process, http://www.lurgi.com/website/fileadmin/user_upload/1_PDF/1_Broshures_Flyer/englisch/0308e_Rectisol.pdf.
[19] Haldor Topsoe. Sulphur tolerant shift conversion, http://www.topsoe.com/Business_areas/Gasification-based/Processes/Sour_shift.aspx.
[20] Linde Engineering. Rectisol wash, http://www.linde-engineering.com/process_plants/hydrogen_syngas_plants/gas_processing/rectisol_wash.php [accessed 28.01.09].
[21] Larson ED, Tingjin R. Synthetic fuel production by indirect coal liquefaction. Energy Sustain Dev 2003;7(4):79–102.
[22] Yagi H, Ohno Y, Inoue N, Okuyama K, Aoki S. Slurry phase reactor technology for DME direct synthesis. Int J Chem React Eng 2010;8:A109.
[23] Andersson K, Johnsson F. Process evaluation of an 865 MW_e lignite fired O_2/CO_2 power plant. Energy Convers Manage 2006;47(18–19):3487–98.
[24] Moore JJ, Nored M, Brun K. Novel concepts for the compression of large volumes of carbon dioxide. Paper sent to Oil and Gas Journal in 2007, but a published version cannot be found. Southwest Research Institute. http://www.netl.doe.gov/technologies/coalpower/turbines/refshelf/papers/42650%20SwRI%20for%20Oil%20&%20Gas%20Journal.pdf.
[25] Shell. Coal gasification brochure. The shell coal gasification process – for sustainable utilisation of coal, http://www.shell.com/static/globalsolutions/downloads/innovation/coal_gasification_brochure.pdf; 2006.
[26] Larson ED, Jin H, Celik FE. Supporting information to: Large-scale gasification-based coproduction of fuels and electricity from switchgrass. Biofuels Bioprod Bioref 2009;3:174–94, http://www.princeton.edu/pei/energy/publications.
[27] Ohno Y. New clean fuel DME. Presentation at the DeWitt Global Methanol & MTBE Conference in Bangkok in 2007, http://www.methanol.org/pdf/Ohno_DME_Dev_Co.pdf.
[28] Ogden JM. Conceptual design of optimized fossil energy systems with capture and sequestration of carbon dioxide. Report UCD-ITSRR-04-34. University of California Davis, Institute of Transportation Studies; 2004.
[29] Uslu A, Faaij APC, Bergman PCA. Pre-treatment technologies, and their effect on international bioenergy supply chain logistics. Techno-economic evaluation of torrefaction, fast pyrolysis and pelletization. Energy 2008;33(8):1206–23.

Appendix D. Modification of the Entrained Flow Reactor for Gasification Experiments

Report

Weigang Lin. Report: Modification of the Entrained Flow Reactor for Gasification Experiments

18th January. 2011, DTU no. 50442

Final report - EFP06 – Produktion af methanol/DME ud fra biomasse

Report: Modification of the Entrained Flow Reactor for Gasification Experiments

Weigang Lin

Department of Chemical and Biochemical Engineering
Technical University of Denmark
Søltofts Plads, Building 229, DK-2800 Lyngby, Denmark

Content

Introduction

The CHEC high temperature entrained flow reactor was constructed to perform experiments with combustion, ash transformation and pyrolysis of solid fuels in a suspension flow reactor mode. Detailed descriptions of the reactor design and on how to conduct experiments on the reactor can be seen in references 1 to 3. In the present project, the reactor is used to perform experiments on biomass gasification at entrained flow gasifier conditions. To make the reactor setup suitable for gasification experiments with severe reducing conditions inside the reactor, the following factors were considered:

1. Possibility for injection of steam to the reactor
2. Simultaneous sampling of gaseous products , char + ash, tar and soot
3. Safety of the system when operated at reducing conditions

Thus, the modifications were focused in these three areas, which are described in the following sections.

Implementation of the steam injection system

The steam injection system consists of four parts: a reciprocating water pump, an externally heated steam generator, a heated pipeline and an injection probe. A photo of the pump and steam generator and a schematic view of the steam injection system are shown in Figure 1 and 2.

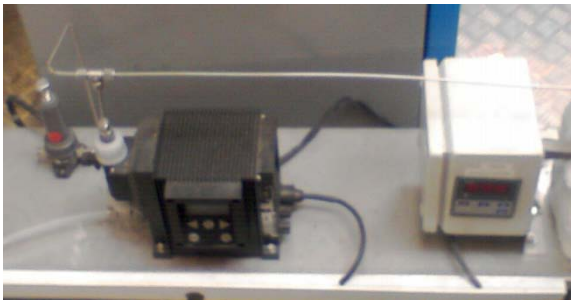

Figure 1. Photo of pump and steam generator system

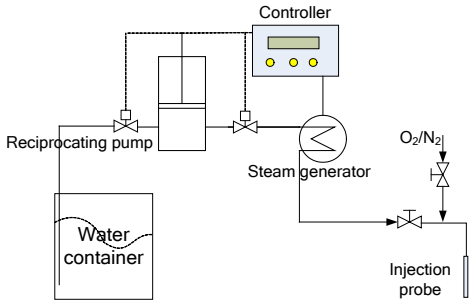

Figure 2. Schematic of steam injection system

The reciprocating water pump has a maximum capacity of 2.5l/h. When the setting of water feed rate is lower than 5% of the full capacity, the water feeding become unstable with pulses. The steam injection probe is made of ¼" stainless steel tube with one end closed. Three holes were drilled on the side of the tube to inject the mixture of steam and air (O_2/N_2). The probe is inserted to the upper part of the preheating section through an O-ring void in the vicinity of the inner wall of the heated ceramic tube. The temperature of the location of injection in the reactor preheater section is estimated to be about 300°C. The steam is injected tangentially to form a swirling flow, thus to avoid directly contacting the hot ceramic surface and causing damage by thermal stress. A photograph of the arrangement of installation of the steam injection probe at the reactor top is shown in Figure 3.

Figure 3. A photo of the arrangement of the steam injection probe on the top of the EFR

All pipelines from the steam generator to the injection probe (including part of the probe) were heated by heating tapes. In order ensure that no condensation of steam occurs, the temperature on the pipe surface was set to 110°C, which is at least 30°C higher than the dew point of the steam stream (Including O_2 and N_2), based on the calculation of dew point shown in Figure 4.

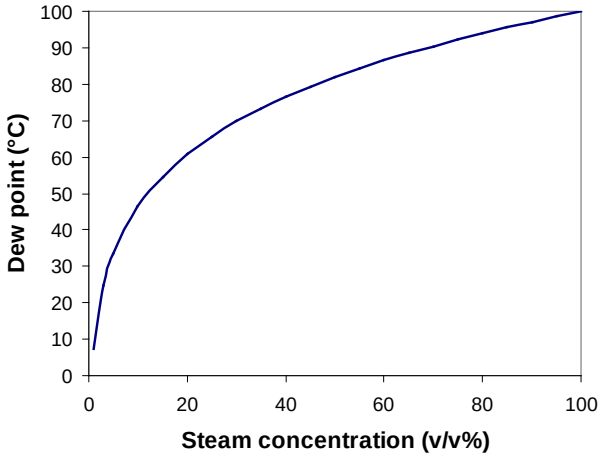

Figure 4. The dew point of different steam concentrations at atmospheric pressure in air

In addition, the reactor PLC system was connected to the steam injection system. If the reactor system is stopped unexpectedly, the power of the steam injection system will be switched off and the steam injection will be stopped.

Particle and gas sampling system

The previous combustion experiments particle sampling system applied a moveable water cooled probe with a fast quench of the burning fuel particles entering to the probe. During gasification experiments, the cooled probe cannot be used because of the presence of tar compounds. For previous high temperature pyrolysis experiments, a hot cyclone was designed to sample char particles. However, tar condensation in the unheated filter caused many problems. In addition, char, tar, soot and gas need to be sampled and measured simultaneously, any blockage of the sampling line is undesirable. Thus, a new sampling system was designed and constructed, which is described below.

A drawing of the main body of the new sampling system is shown in Figure 5. The system consists of three heated parts in sequence: a probe with a funnel form of the tip with a dimension illustrated in Figure 5, a cyclone and a filter. The length of the probe inside the reactor is 0.34 m, whose tip is located at the very bottom of the reactor tube. The probe tip is in a funnel form to have a high flow rate and to collect enough solid samples in a relatively short time at near iso-kinetic conditions at the probe tip. The three parts (probe, cyclone and filter) are electrically heated by heating tapes to a temperature higher than 350°C to avoid condensation of tar compounds on the inner surfaces of probe, cyclone and filter.

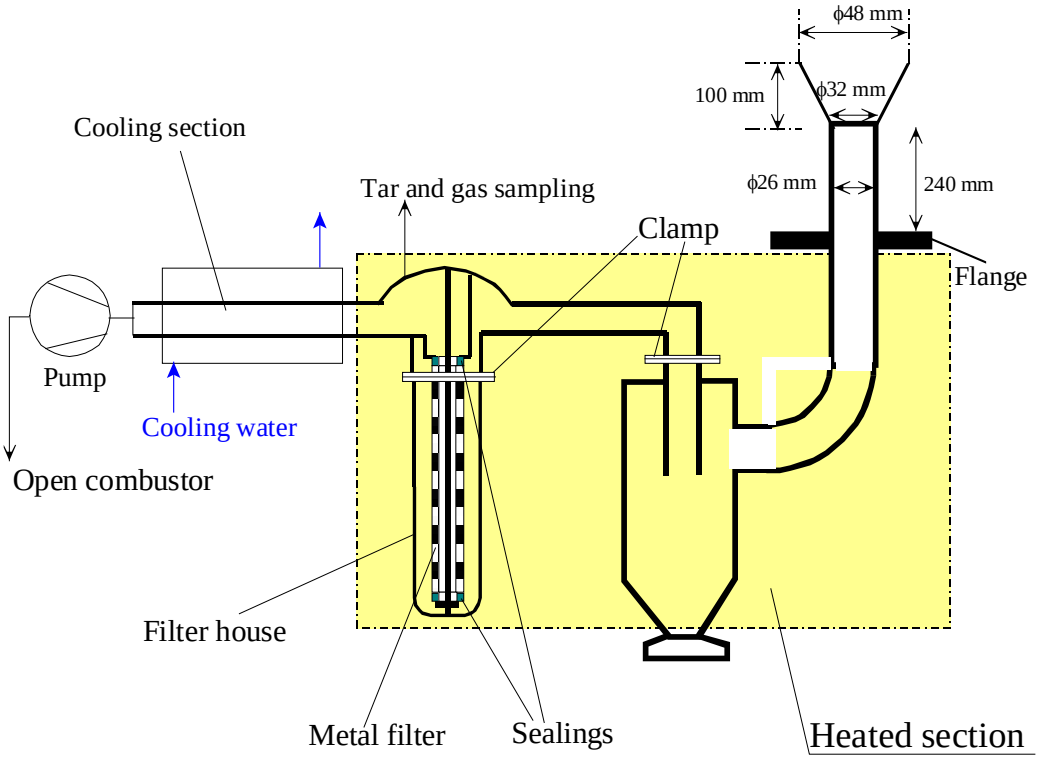

Figure 5. Illustration of the new sampling system

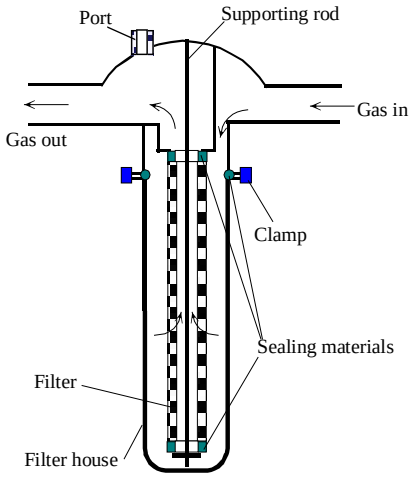

Figure 6. Structure of filter system

A problem to be solved for the high temperature filter is to prevent any leakage to the system from occurring. Sealing material which can stand high temperature must be used. After comparing different materials, graphite sealings are used in the assembly of the porous metal filter and the two parts of the filter house, which is tided by a clamp. The detail structure of the filter system is illustrated in Figure 6. On the top of the upper part of the filter house, a port is located, from which tar can be sampled. The gas sample can also be drawn from this port.

Tar is sampled by a method called “Solid Phase Absorption (SPA)”. A tube filled in 1 ml LC-NH2 absorbent is connected to an injection needle at one end of the LC-NH2 tube. The needle is inserted through the port. The other end of the LC-NH2 tube, is connected to either an injector or a tube followed by a needle valve, a pump and a flow meter. The tar containing gas is drawn by stroking the injector or by switching on the pump. When the gas passes the LC-NH2 tube, the tar compounds are absorbed on the surface of the absorbent. The amount of gas sampled is registered by the number of strokes or by the flow meter. The tar samples were sent to Risø, DTU and analyzed by a GC-MS.

Safety measures

Open burner

Since the produced gas from gasification contains high concentration of CO, H_2 and hydrocarbons, which are either poisonous or flammable, it is necessary to treat them before vented to the atmosphere. The easiest way for treatment is combustion, from which the products are CO_2 and water. Thus, an open burned was designed and constructed for combusting the producer gas. A schematic view of the system of combustion of the producer gas is shown in Figure 7.

In this system, a fan was installed to draw the producer gas to an open burner to burn out the combustible in the producer gas. The flue gas is then vented from the top of the open burner, which is illustrated by a photo in Figure 8 (a). The fan is controlled in such a way that the pressure in the reactor is kept to a slight under-pressure (from 0.3-0.5 mbar). The majority of the producer gas (except for the gas to the sampling system) first passes to a cooling section and a dust filter, which is a tube filled with activated carbon

particles used for capturing tar and dust before it enters the fan. In the late stage of the experimental work, the dust filter was not used because of a constant blockage of the filter, causing increased pressure in the reactor.

In order to avoid the risk of flame extinction in the open burner a methane fired Bunsen burner is installed in the open burner acting as a flame stabilizer, as well as an igniter. In addition, a flame detector is installed in the open burner to monitor the flames from the producer gas combustion and from the Bunsen burner (see Figure 9). When two flames are extinct, the flame detector (see Figure 9) will send a signal to the PLC system and the fuel feeder will be stopped and the methane supply line is be switched off simultaneously.

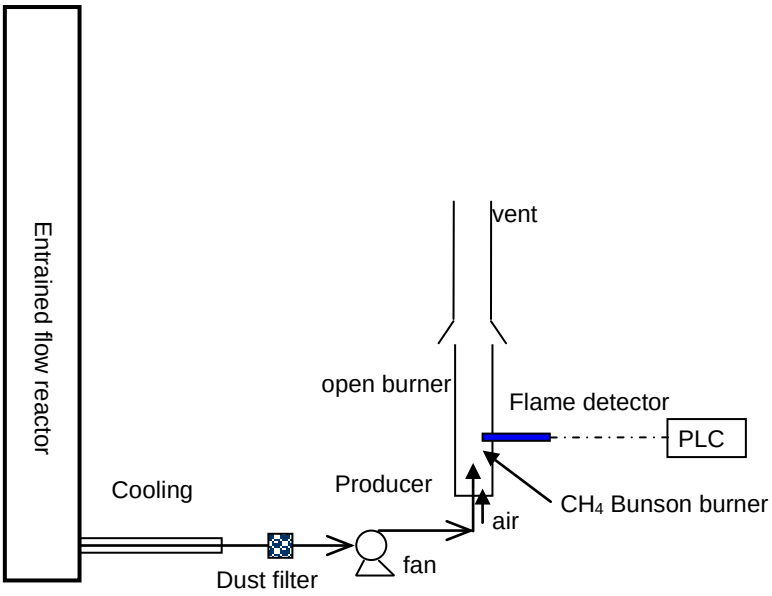

Figure 7. Illustration of the open burner system

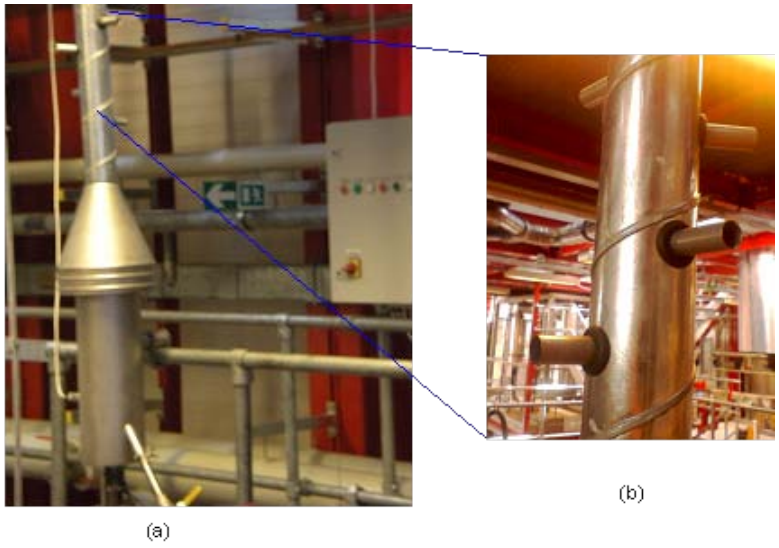

Figure 8. Photos of the open burner and exhaust pipeline (a) open burner; (b) details of the exhaust pipeline

During experiments, it was found that the temperature of the flue gas close to the connection between the metal pipe to the PVC pipe is too high (>70°C) when the feeding rate of biomass is higher than 800g/h. The PVC pipe could not stand such high temperature. It was also observed that the mixing between the high temperature flue gas and cold air sucked in is poor. To solve the problem several tubes were mounted horizontally on the exhaust pipeline (see Figure 8 (b)). Thus, most dilution air is sucked in from the tubes and forms a strong turbulence that enhances the mixing between the hot flue gas and the dilution air. After the tubes were installed in the exhaust pipe line, the gas temperature entering the PVC pipe decreased. However, the maximum feed rate of biomass is still limited to 1 kg/h, above which the gas temperature entering the PVC pipeline will be too high (>70°C). A heat exchanger will be needed if a fuel feed rate of the gasifier is higher than 1000g/h biomass or an equivalent fuel input power.

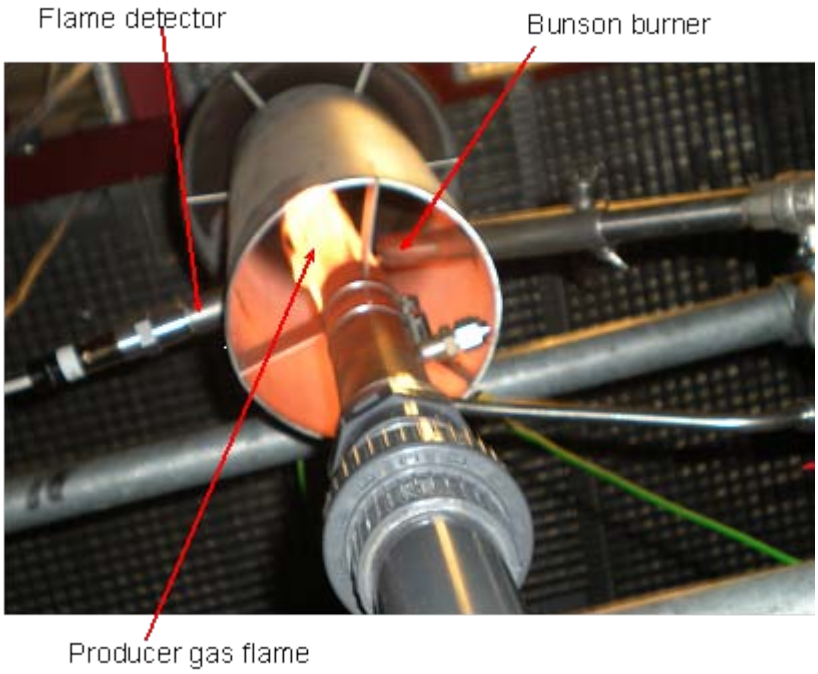

Figure 9. Illustration of the open burner with flame, flame detector and the Bunsen burner

Shell outside of the reactor

As mentioned previously, the gasifier was operated at a slightly under pressure to avoid a leakage of the producer gas, which is flammable and contains a high concentration of poisoning CO. The amount of leakage as a function of the reactor pressure was tested by measuring the outlet flow and comparing to the set inlet flow at various pressures inside the reactor. If the outlet flow is equal to the inlet flow, there is no leaking of the reactor. In case of the outlet flow is higher than the inlet flow; there is a leakage of surrounding air to the reactor. If the outlet flow is lower than the inlet flow, the gas inside the reactor is leaking out. The results of the leaking test are shown in Figure 10. It can be seen that the gas will be leaking out when the pressure inside the reactor is higher than approximately 0.15 mbar. It should be mentioned that this test was done at a condition without fuel feeding. Larger fluctuations of pressure inside the reactor were observed when fuel particles were fed to the reactor. The larger fluctuation of the reactor pressure may cause producer gas to leak out of the gasifier in some short time periods.

Actually, the CO alarm was triggered several times in the experimental hall when gasification of wood powder by using air as agent was performed. The CO concentration was as high as 17 v/v%, though the pressure in the gasifier was adjusted to <0.3 mbar. Triggering of the CO alarm leads to an interruption of the experimental work. So it was decided to conduct the initial experiments at low inlet O_2 concentration conditions, and this was obtained by mixing air with nitrogen. In this way, the producer gas was diluted and the product gas CO concentration was kept lower than 10%. At such conditions, no CO alarm was triggered.

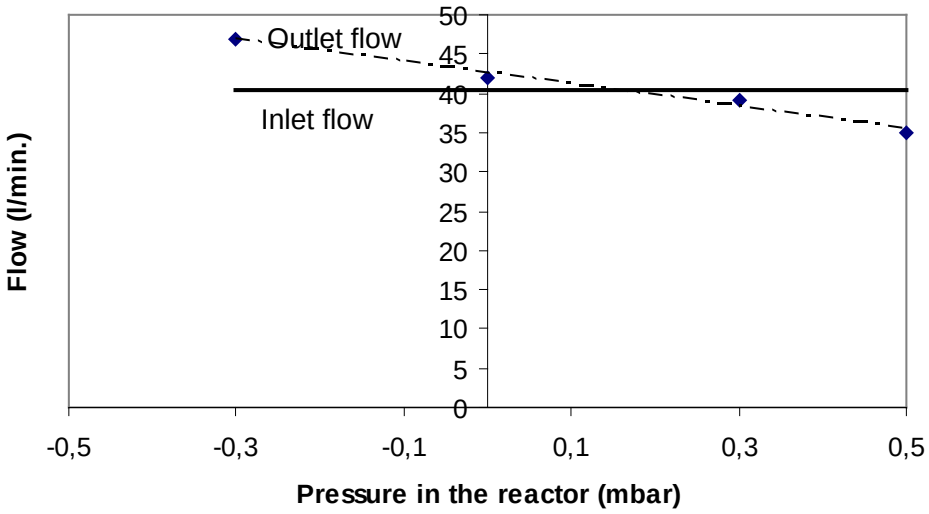

Figure 10. The inlet and outlet flow as a function of the pressure (in mbar) in the reactor

In order to be able to increase the inlet oxygen concentration, this short time leaking problem needs to be solved.

Figure 11. A photo of shell outside of the gasifier

Thus, a shell was installed outside the gasifier, which is connected to the vent system by two symmetric pipe-lines as shown in Figure 11. In this way, the small amount of gas leaking out caused by pressure fluctuations will be sucked out and there is no risk of the CO alarm being triggered.

Summary

Necessary modifications have been done to the entrained flow reactor to make it suitable for gasification experiments. The major modifications include steam injection, adequate solid and gas sampling of the product gas and modification of the safety system. The PI diagram of the entrained flow gasifier facility is shown in Figure 12.

The modification of the reactor setup included the following tasks:

1. Mounting of a steam injection system
2. Mounting of a new hot probe gas and particle sample extraction system making it possible to measure the content of tar, soot and char as well as the gas composition of the product flow from the gasifier.
3. Modification of the exhaust gas system to make a controlled combustion of the product gas
4. Modification of the facility PLC safety system to stop fuel feeding at high room CO level and if the exhaust flame was extinct.
5. Mounting of a gas shell around the reactor for the removal of gas leaking out of the reactor
6. Including a GC in the system to make measurements of light hydrocarbons possible.

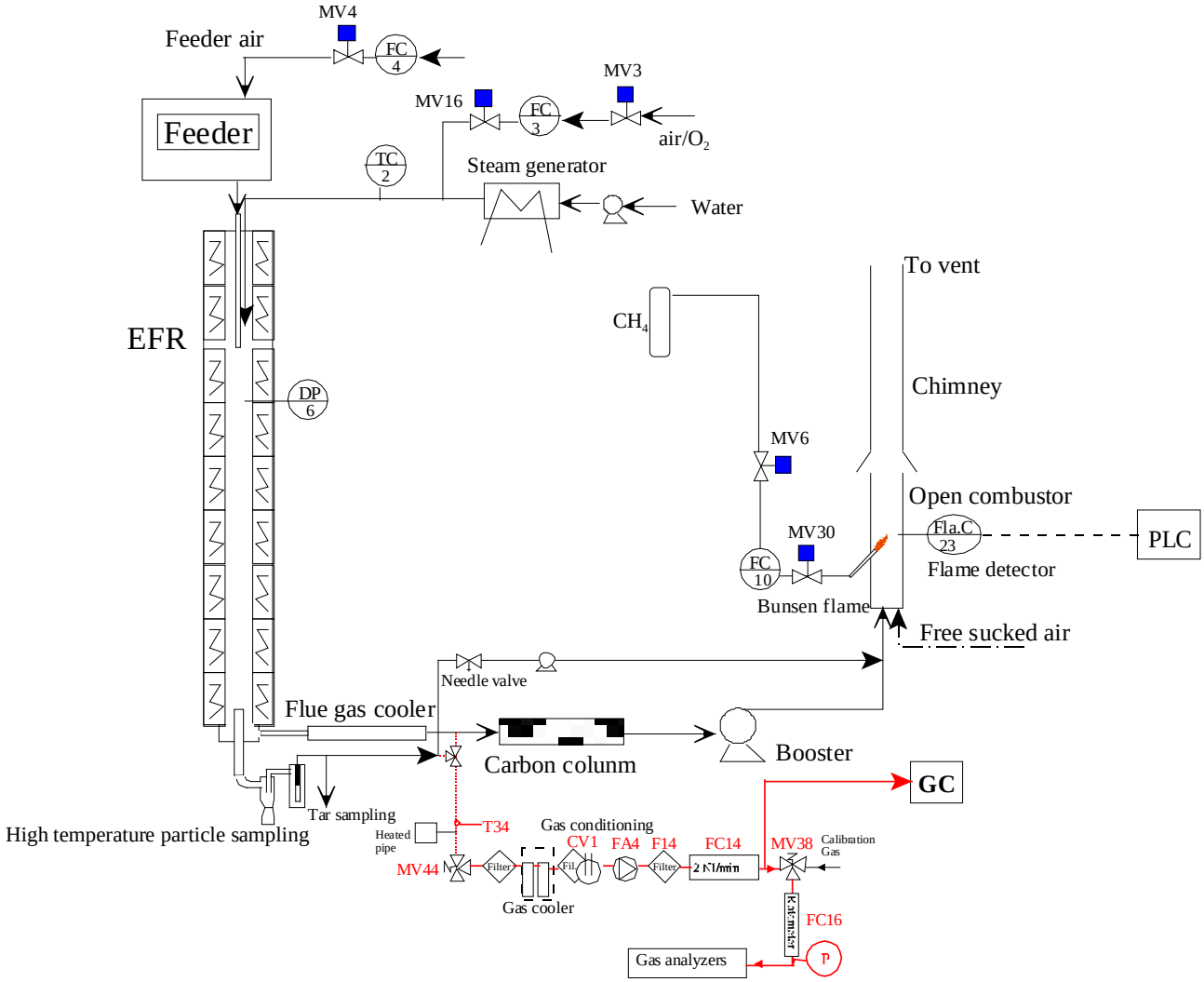

Figure 12. PI diagram of the entrained flow gasifier after modification

References

1. Peter Arendt Jensen, Jørn Hansen. Forsøgsanlæg til undersøgelse af faste brændsler ved høje temperaturer og lave opholdstider. Design, opbygning og indkøring af anlægget. CHEC report, **2001**. CHEC Rep. No. 0105
2. Jesper Jensen, Guilin Hu, Peter Arendt Jensen, Carsten Nørby, Jørn Hansen, Lars K. Hansen. Operation manual for Deposit Experiments on the Solid Fuel Flow reactor. Building 228-2, 045-3. **2004**. Internal KT/CHEC document – Can be found in CHECs disk K setup database.
3. Manual for experiments on the solid fuel flow reactor. **2003**. Internal KT/CHEC document – Can be found in CHECs disk K setup database.

Appendix E. Atmospheric pressure entrained flow gasification of biomass

Report

Ke Qin, Weigang Lin, Peter Arendt Jensen, Anker Degn Jensen. Report: Atmospheric pressure entrained flow gasification of biomass.

2011, DTU no. 50442

Final report - EFP06 – Produktion af methanol/DME ud fra biomasse

Report: Atmospheric pressure entrained flow gasification of biomass

Ke Qin, Weigang Lin, Peter Arendt Jensen, Anker Degn Jensen

Department of Chemical and Biochemical Engineering
Technical University of Denmark
Søltofts Plads, Building 229, DK-2800 Lyngby, Denmark

Content

1 Introduction

1.1 Background

Among the renewable energy sources biomass has a high potential [1], and biomass resources are a major component of strategies to mitigate global climate change. Plant growth "recycles" CO_2 from the atmosphere, and the use of biomass resources for energy and chemicals results in low net emissions of carbon dioxide. There is a world-wide interest in the use of biomass resources as feedstocks for producing power, fuels and chemicals [2]. Gasification is one of the key technologies for utilization of biomass, especially in the field of integrated gasification combined cycle (IGCC) and production of liquid fuels and chemicals [3][4]. Of several gasification methods, entrained flow gasifier has the advantage of a high gasification efficiency to produce a gas with low tar content and with the possibility to run at high pressure, which fits the pressure in a downstream synthesis process [5].

The present project investigates processes that can be used to produce liquid transport fuels from biomass [6]. Entrained flow gasification and liquid production integrated with a power plant has the advantage of a high conversion of fuel to liquid, and the residual energy can be applied for power and district heating in an IGCC plant. It may be possible to utilize a combination of coal, biomass and waste as fuel providing a large fuel flexibility in particular compared to fermentation based processes. It will also be possible to utilize hydrogen (and oxygen) from surplus windmill power to increase the H_2/CO ratio of the gas and thereby increase the liquid production and at the same time utilize the oxygen in the gasification process. The concept has a high flexibility, such that if liquid fuel production is not desired in a certain period, the gas produced can be used for efficient power production. The surplus CO_2 from the process will be provided in a high concentration stream, so it will also be relatively easy to carry out CO_2 sequestration in such a plant.

1.2 Objectives

Although gasification of coal in entrained flow gasifiers been studied extensively, systematic studies on gasification of biomass in entrained flow gasifier are scarce. In addition the fundamental processes taking place during biomass gasification at temperatures relevant to entrained flow gasifiers are not fully understood. In production of synthetic liquid fuels for transportation from biomass, it is important to control the syngas quality from gasification with respect to both the H_2/CO ratio and the amount of harmful impurities, such as tar [7][8]. In an entrained flow gasification plant, it is also important that the solid fuel can be completely converted to gas with a minimum consumption of oxygen. Gasification of biomass will be investigated under entrained flow reactor conditions with respect to main syngas composition ($CO/CO_2/H_2$), hydrocarbons, tar and soot, as a function of operating conditions. The measuring data will provide information on fuel conversion and gas composition as a function of fuel type and operating conditions such as temperature and oxygen and steam inlet content.

2 Experimental

2.1 Apparatus

All gasification experiments were conducted in the electrically heated entrained flow reactor placed at the Department of Chemical and Biochemical Engineering at DTU. The atmospheric pressure entrained flow reactor used for the gasification experiments is shown schematically in Figure 1. It has an inner diameter of 0.08 meter and a length of 2 meter. The reactor is externally heated by seven independent electric heating elements, which can be heated to a maximum temperature of 1500°C. A reasonably uniform temperature in the reactor can be realized, and so the influence of temperature and excess air ratio on the composition of the syngas can be studied independently. The heating element of preheater section A and reactor section 6 and 7 were broken, and could not be heated to the set point temperature. Besides the reactor, the complete facility includes equipments for fuel particle feeding, gas supply, solid particle sampling, gas sampling and analysis, liquid sampling, and flue gas treatment. The external high of the facility is 7

meters. An input of 5kW of pulverized solid fuel is normally fed to the reactor during experiments. The data acquisition is programmed by Labview. By this software, measuring data of feed rate, reactor pressure and gas compositions are stored in the computer.

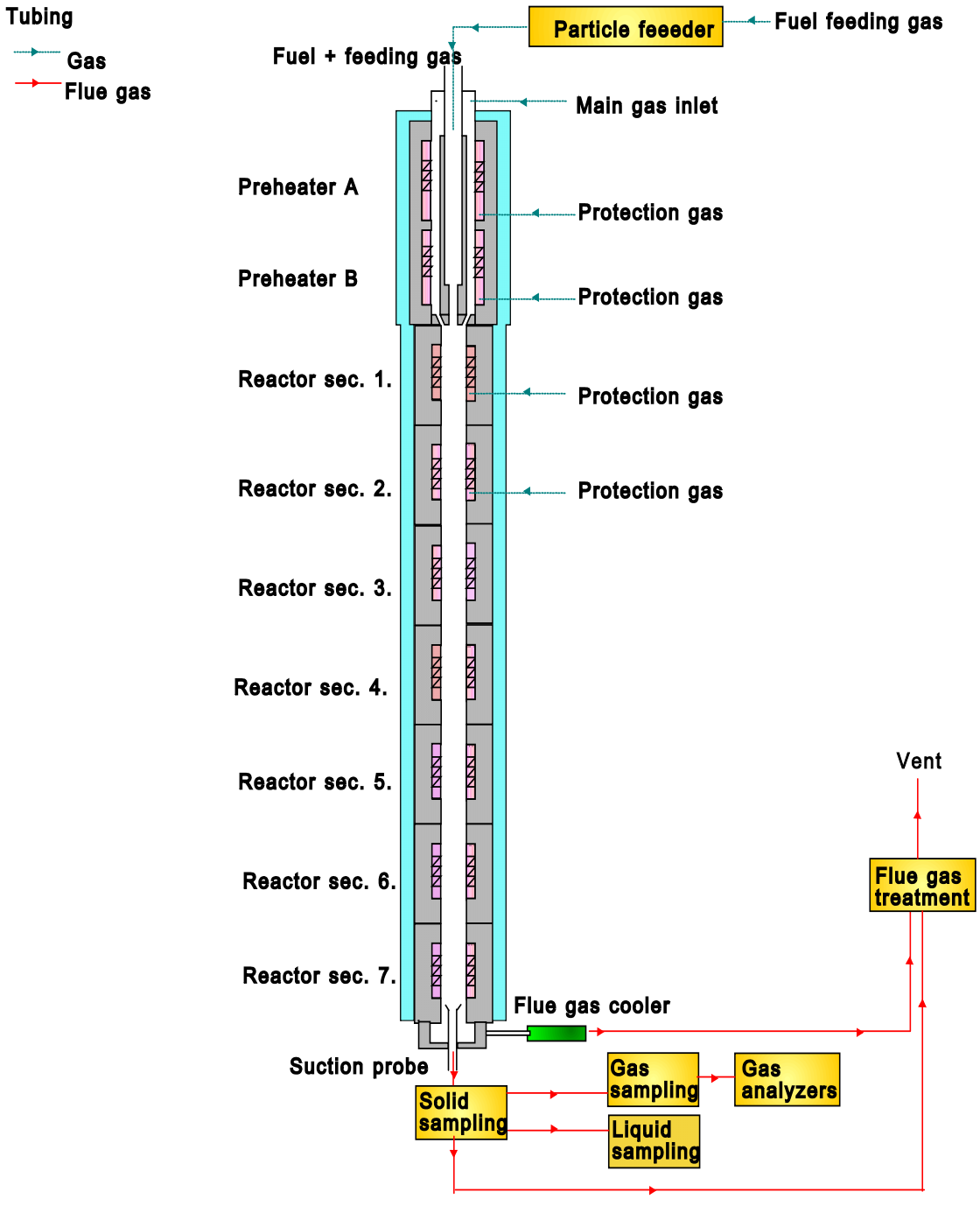

Figure 1 Sketch of experiment setup

The fuel particle feeding system is shown in Figure 2. It ensures a steady fuel supply for the reactor. The system is located in a pressure tight container so that the gas feeding flow the reactor can be controlled accurately. The solid fuel feeding flow is registered by the Labview program and measured by weighting of the silo and the strew feeder. In order to have a smooth fuel flow, a vibration table is used between the screw feeder and the injection tube to the reactor.

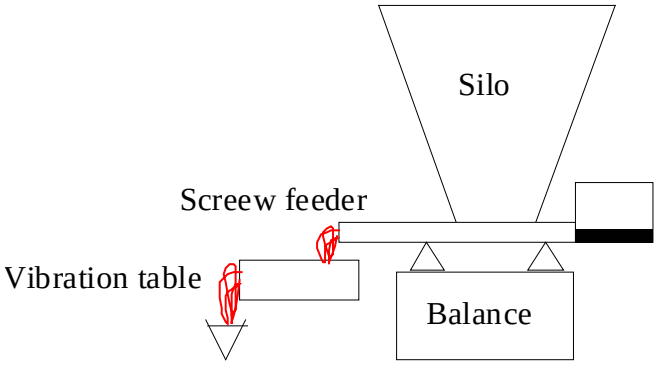

Figure 2 Sketch of fuel particle feeding system

The gas supply system controls the fuel feeding gas (air), the main gas supply (air, oxygen, nitrogen and steam) that is heated in the preheater, and protection gas (air for preheater section A and B, and reactor section 1 and 2). The gas supply system contains of mass flow meters and magnetic valves that make it possible to mix gas flows and direct gases to various purposes: the particle feeder (as feeding gas), the reactor (as main gas), and the reactor purge (as protection gas).

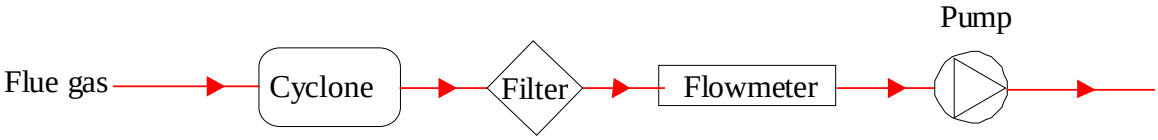

Figure 3 Sketch of solid particle sampling system

A simplified sketch of the solid particle sampling system is shown in Figure 3. It is made up of a cyclone, a filter, a flow meter and a pump. According to the principle of isokinetic sampling, the extraction flow is set at a calculated value. As soon as turning on the pump,

a solid sample is collected by the filter and cyclone at steady-state condition during the experiments.

The gas sampling and analysis system is shown in Figure 4. After the solid particle sampling system, the flue gas without solid particle is heated in order to prevent water condensation in the pipe. Water is then condensed in a gas cooler. The dry flue gas is analyzed by a NDIR gas analyzer and a new micro gas chromatography apparatus. Before the NDIR gas analyzer, the extraction flow is set at 1Nl/min. The concentration of CO and CO_2 is continuously measured by the NDIR gas analyzer. The CO is detected up to a maximum span of 20%. When CO and CO_2 reach a stable level, the micro GC was started. The micro GC is capable of measuring H_2, CO, CO_2 and hydrocarbons (C_2H_2, C_2H_4, C_2H_4O, C_3H_8). It takes approximate 6 minutes to analyze all gas components at a time. The calibration method for the micro GC is depicted in Appendix A.

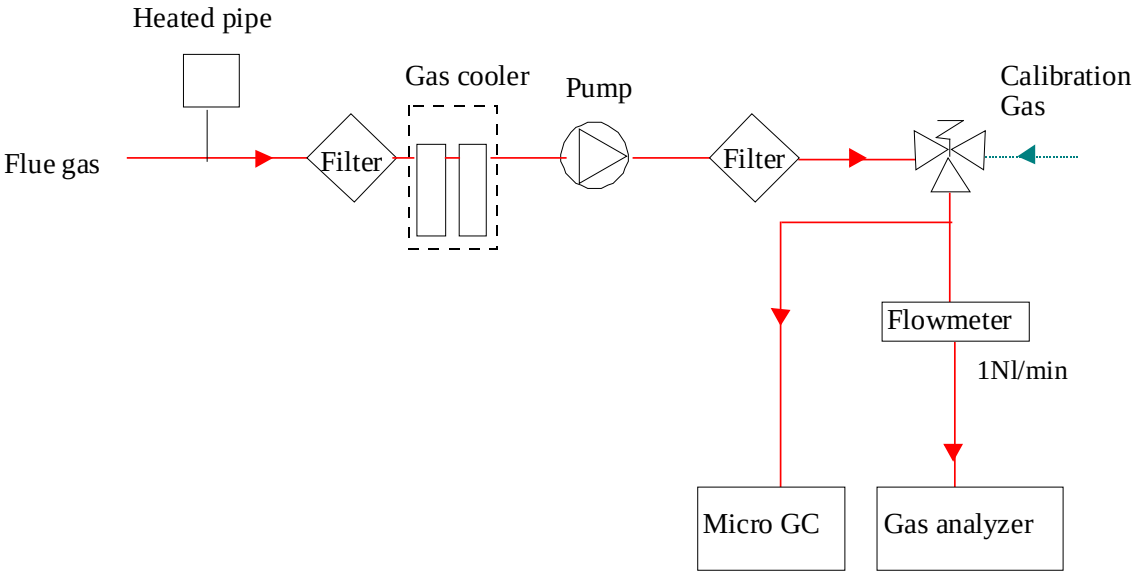

Figure 4 Sketch of gas sampling and analysis system

Liquid sampling is mainly applied to sample tar. Tar is sampled by a solid phase absorption method and analyzed at Risø.

The applied flue gas treatment system is shown in Figure 5. An open burner is used to burn the combustible component in the flue gas. The pilot burner is fed by CH_4, which ensures all combustible components to combust smoothly in the open burner.

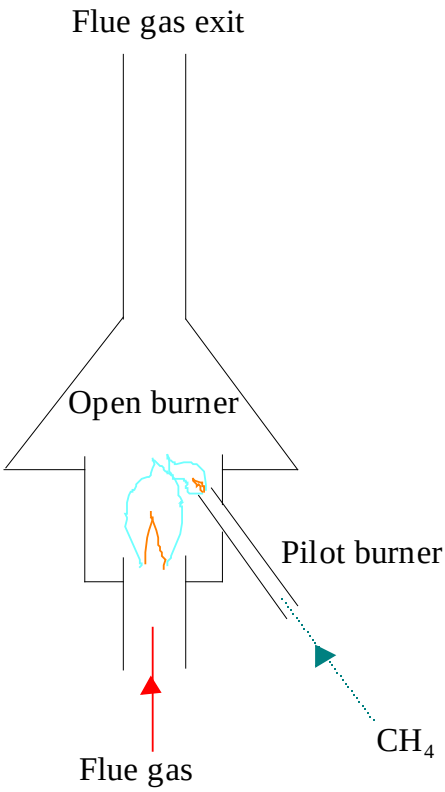

Figure 5 Sketch of flue gas treatment system

2.2 Fuels

Three fuels are used in the experiments: wood (beech saw dust), straw (pulverized wheat straw pellet) and coal (Columbian coal). The analyses of them are listed in Table 1. It is shown that the compositions of wood and straw are quite similar except for the ash content. An important difference between wood and straw is the high alkali content in straw, which may have a catalytic influence on the gasification processes [9]-[11].Comparing with coal, the content of volatile in biomass is higher, but the content of fixed carbon and the heating value are lower. The particle size distributions of the applied fuels are shown in Figure 6. The median diameter of the wood particles (280μm) is bigger than that of the straw particles (170μm).

Table 1 Proximate and ultimate analyses of fuels (on a delivered basis)

Fuel		Beech saw dust	Straw pellet	Columbian coal
Proximate analysis				
Moisture	wt. %	9.04	8.65	5.00
Ash	wt. %	0.61	4.76	9.6
Volatile	wt. %	76.70	69.87	34.9
Fixed carbon (by diff.)	wt. %	13.65	16.72	50.50
Lower Caloric Value	MJ/kg	16.44	15.76	28.19
Ultimate analysis				
Carbon	wt. %	45.05	42.88	68.9
Hydrogen	wt. %	5.76	5.65	4.61
Oxygen (by diff.)	wt. %	39.41	37.51	9.83
Nitrogen	wt. %	0.13	0.49	1.44
Sulphur	wt. %	0.01	0.06	0.62

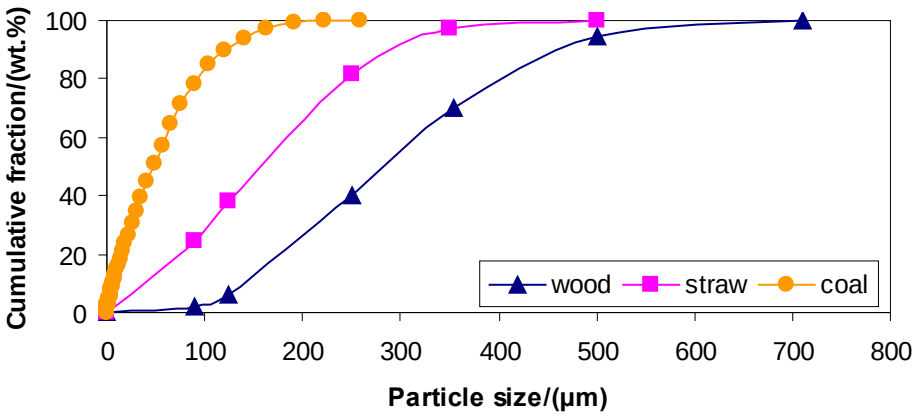

Figure 6 The particle size distributions of the applied fuels

2.3 Conditions

In Table 2 the operating conditions of the 40 experiments conducted at atmospheric pressure are list. The main experimental parameters varied are excess air ratio, oxygen concentration, temperature, steam/carbon ratio, and fuel type.

Experiments were conducted in the entrained flow reactor with excess air ratio from 0.1 to 0.9, oxygen concentration in the range of 2%-34%, temperature in the range of 1000-1350°C, steam/carbon ratio from 0.0 to 1.25, and typically used a fuel input from 0.5kg/h to 1.0kg/h. The reactor inlet gas consisted of air, oxygen nitrogen and steam.

Table 2 Operating conditions

NO.	data	excess air coefficient	oxygen concentration	steam/carbon ratio	temperature	biomass type	feed rate	effective residence time	total residence time
		λ	O_2	H_2O/C	T	-	-	$*t_{eff}$	$*t_{tot}$
		-	*%*	-	*°C*	-	*g/h*	*s*	*s*
1	Jan.2009	0.25	21	1.25	1350	coal	600	2.55	3.96
2	Jan.2009	0.25	21	0	1350	wood	1000	1.97	3.06
# 3	Jan.2009	0.25	21	1.25	1350	wood	1000	1.84	2.86
4	Jan.2009	0.25	29	1.25	1350	wood	1000	2.20	3.41
5	Aug. Sept. 2007	0.25	5	0	1350	wood	550	1.38	2.14
6	Aug. Sept. 2007	0.35	7	0	1350	wood	550	1.42	2.19
7	Aug. Sept. 2007	0.5	10	0	1350	wood	550	1.44	2.23
8	Aug. Sept. 2007	0.75	15	0	1350	wood	550	1.55	2.40
9	Aug. Sept. 2007	0.9	18	0	1350	wood	550	1.62	2.51
¤ 10	Aug. Sept. 2007	0.2	5	0	1350	wood	710	1.38	2.14
¤ 11	Aug. Sept. 2007	0.25	5	0.5	1350	wood	550	1.38	2.13
12	Aug. Sept. 2007	0.35	7	0.5	1350	wood	550	1.39	2.16
13	Aug. Sept. 2007	0.5	10	0.5	1350	wood	550	1.43	2.21
14	Aug. Sept. 2007	0.75	15	0.5	1350	wood	550	1.55	2.40
15	Aug. Sept. 2007	0.2	5	1	1350	wood	710	1.31	2.03
¤ 16	Aug. Sept. 2007	0.25	5	1	1350	wood	550	1.35	2.09
17	Aug. Sept. 2007	0.35	7	1	1350	wood	550	1.39	2.16
18	Dec. 2008	0.2	21	0	1350	wood	800	2.53	3.92
19	Dec. 2008	0.3	21	0	1350	wood	800	2.21	3.43
20	Dec. 2008	0.4	21	0	1350	wood	800	1.97	3.06
21	Dec. 2008	0.3	28	0	1350	wood	800	2.51	3.89
22	Dec. 2008	0.3	34	0	1350	wood	800	2.64	4.09
23	Dec. 2008	0.3	21	0	1200	wood	800	2.69	4.15
24	Aug. Sept. 2007	0.1	2	0	1200	wood	550	1.59	2.45
25	Aug. Sept. 2007	0.25	5	0	1200	wood	550	1.59	2.46
26	Aug. Sept. 2007	0.5	10	0	1200	wood	550	1.72	2.66
27	Aug. Sept. 2007	0.5	21	0	1200	wood	550	3.06	4.72
28	Aug. Sept. 2007	0.25	5	0.25	1200	wood	550	1.60	2.46
29	Aug. Sept. 2007	0.1	2	0.5	1200	wood	550	1.55	2.40
30	Aug. Sept. 2007	0.25	5	0.5	1200	wood	550	1.61	2.48
¤ 31	Aug. Sept. 2007	0.7	12	0	1000	wood	550	1.90	2.97
¤ 32	Aug. Sept. 2007	0.75	15	0	1000	wood	550	2.06	3.22
33	Aug. Sept. 2007	0.9	18	0	1000	wood	550	2.12	3.33
¤ 34	Aug. Sept. 2007	0.25	5	0.5	1000	wood	550	1.91	2.99
¤ 35	Aug. Sept. 2007	0.25	5	0	1350	straw	550	1.40	2.17
36	Aug. Sept. 2007	0.35	7	0	1350	straw	550	1.40	2.17
37	Aug. Sept. 2007	0.5	10	0	1350	straw	550	1.45	2.24
38	Aug. Sept. 2007	0.75	15	0	1350	straw	550	1.50	2.32
39	Aug. Sept. 2007	0.25	5	1	1350	straw	550	1.37	2.12
40	Aug. Sept. 2007	0.35	7	1	1350	straw	550	1.39	2.16

* For the present experiments, the last two electric heating elements (reactor section 5 and 6) are broken, so the effective reactor length is taken as 1.4m. The residence time is calculated as effective residence time (fuel flowed from rector section 1 to section 5) and total residence time (fuel flowed from rector section 1 to section 7).

Experiment done twice to test repeatability; ¤ Experiments in which tar measurement were made.

2.4 Experimental procedures

Before an experiment, at first, the Labview program is started to record input and output experimental data. Secondly, the NDIR gas analyzer is calibrated. Thirdly, the leak of the total system is tested. 10.87% oxygen is introduced to the system to make the leak test. If the measured oxygen concentration is more than the setting value, there is leak in the reactor system. Fourthly, the fuel feed rate is set at a particular value and the reactor is set to a desired temperature. After the atmospheric pressure reactor has been heated to the setting temperature, air, oxygen, nitrogen and steam are introduced. Fifthly, the gas sampling pipe is heated at 70°C, and the cyclone and the particle filter are heated to 400°C and 375°C respectively. At last, the pilot burner is ignited and the open burner is ready to combust the combustible components of the flue gas during the experiments.

To start an experiment, firstly, the CO detector is started to examine if the CO concentration in the surrounding air exceeds 25ppm. Secondly, the pump in the gas sampling system is started to extract flue gas for the NDIR gas analyzer to make real-time analyzes throughout the experimental process. Thirdly, biomass fuel is fed to the reactor by the screw feeder. Fourthly, the pump of the solid particle sampling system is started to collect solid samples for 20minutes and measure the components of the flue gas by the micro GC three times. The GC is started when the NDIR gas analyzer measure stable level of CO and CO_2. Every experimental condition last approximately 60 minutes in total.

After an experiment, the measuring data is treated. It is not possible to measure the flue gas flow directly. The total amount of flue gas is calculated by using N_2 as a tracer. The N_2 concentration in the flue gas is measured by micro GC. The concentration of each gas component in the flue gas can then be calculated. Appendix B describes this method in detail. The concentration of solid particles in the flue gas is also calculated. The details of this calculation are shown in appendix C.

2.5 Gasification processes and reactions

The solid fuels injected into the gasifier are transformed to gases by several processes that include drying, pyrolysis, partial oxidation (1), gasification of char and soot (2, 3 and 4) and gas phase reactions as the water shift reaction (5), the reaction of hydrocarbon with water (6) and the steam methane reformation reaction (7). Reaction (4) and (7) are mainly important at high pressure [5][12].

$$C + O_2 \leftrightarrow CO_2 \qquad \Delta H = -409.5 kJ/mol \qquad (1)$$

$$C + CO_2 \leftrightarrow 2CO \qquad \Delta H = +159.7 kJ/mol \qquad (2)$$

$$C + H_2O \leftrightarrow CO + H_2 \qquad \Delta H = +118.9 kJ/mol \qquad (3)$$

$$C + 2H_2 \leftrightarrow CH_4 \qquad \Delta H = -75.0 kJ/mol \qquad (4)$$

$$CO + H_2O \leftrightarrow CO_2 + H_2 \qquad \Delta H = -40.9 kJ/mol \qquad (5)$$

$$C_xH_y + xH_2O \leftrightarrow xCO + \frac{2x+y}{2} H_2 \qquad (6)$$

$$CH_4 + H_2O \leftrightarrow CO + 3H_2 \qquad \Delta H = +206.0 kJ/mol \qquad (7)$$

In full scale entrained flow gasifier, the oxidation reaction (1) provides the energy needed for the endothermic CO_2 and H_2O gasification reactions (2 and 3). In this study the energy for the gasification reactions are supplied by both the electrical heating and a partial oxidation of the fuel.

3 Thermodynamic equilibrium calculation

The thermodynamic equilibrium calculation is performed by Factsage. It is used to calculate the concentration of reaction products at chemical equilibrium conditions, according to the principle of Gibbs free energy minimization. Wood (with a composition as shown in Table 1) is used as fuel in the thermodynamic equilibrium calculations. Wood, oxygen and steam are the three input streams. The feeding rate of wood is fixed (1000g/h) for all calculations in this section. The inlet amount of oxygen and steam are changed to obtain different excess air ratio and steam/carbon molar ratio. The studied

ranges of excess air ratio, temperature, steam/carbon molar ratio and pressure are 0-1, 800-1600°C, 0-2, and 1-101atm respectively.

3.1 Effect of excess air ratio on products

The effect of excess air ratio on product yield is shown in Figure 7. 1350°C, 1200°C and no steam addition are selected, and lambda is in the range of 0 to 1. With no steam addition and lambda lower than 0.20, enough oxygen is not supplied for wood to be fully converted to gas products, and some carbon is formed. When lambda is higher than 0.2, wood can be completely converted to gas products. The yields of H_2 and CO decrease, while the yields of H_2O and CO_2 increase, and no CH_4 formation is observed when lambda is increased above 0.2 due to the promotion of oxidation.

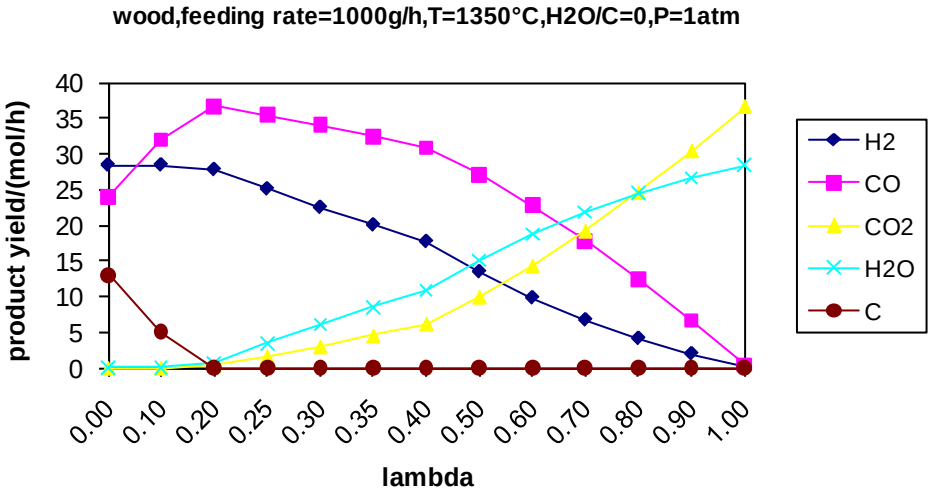

(a-1)

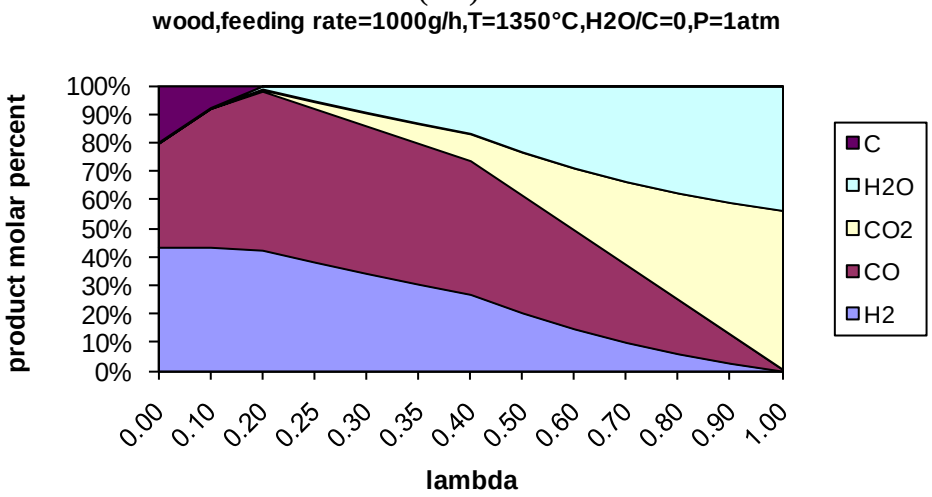

(a-2)

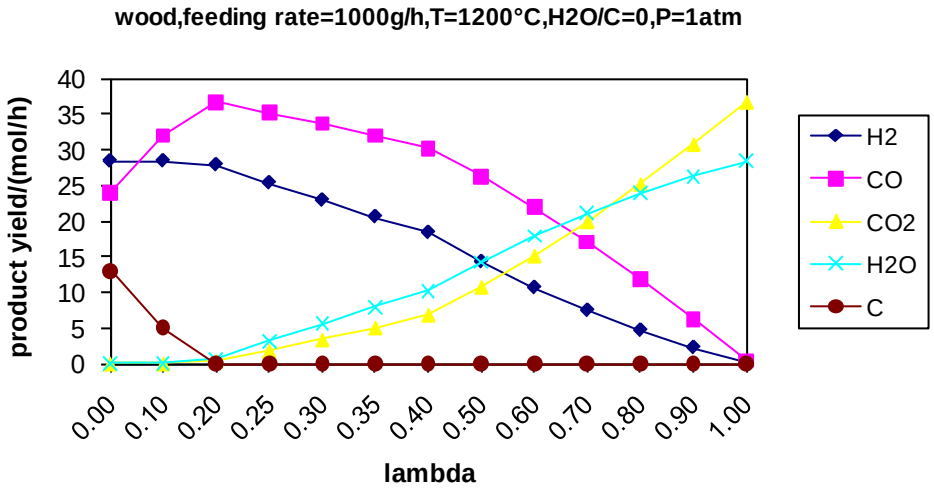

(b-1)

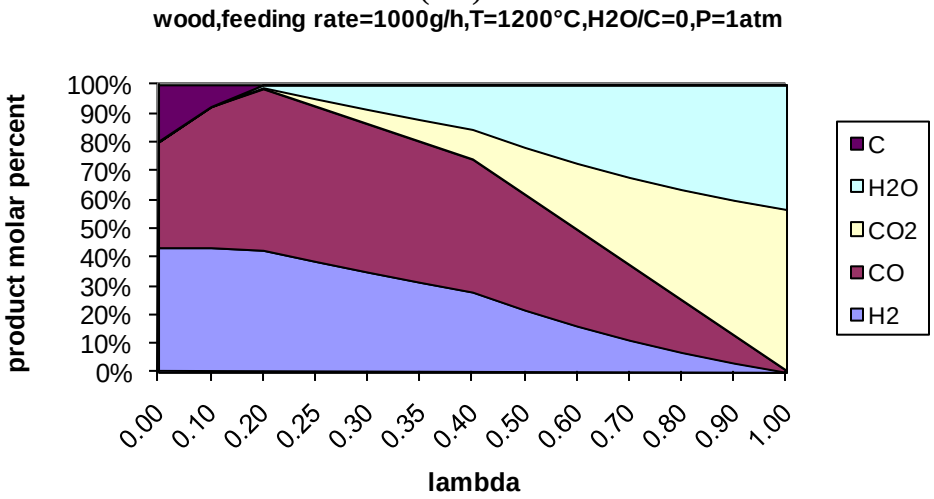

(b-2)

Figure 7 Effect of excess air ratio on product yield and percent

(a) T=1350°C (b) T=1200°C

3.2 Effect of temperature on products

The effect of temperature on product yield is shown in Figure 8. Lambda of 0.25 and 0.35 and no steam addition are selected. A temperature interval of 800°C to 1600°C is investigated. The yields of H_2 and CO_2 decrease a little, while the yields of CO and H_2O increase gradually with temperature increases because of the water gas shift reaction (4) that is exothermal and the increasing temperature suppresses the proceeding of this reaction [13][14]. The yield of CH_4 decreases from 800°C to 1000°C and no CH_4 is present above 1000°C.

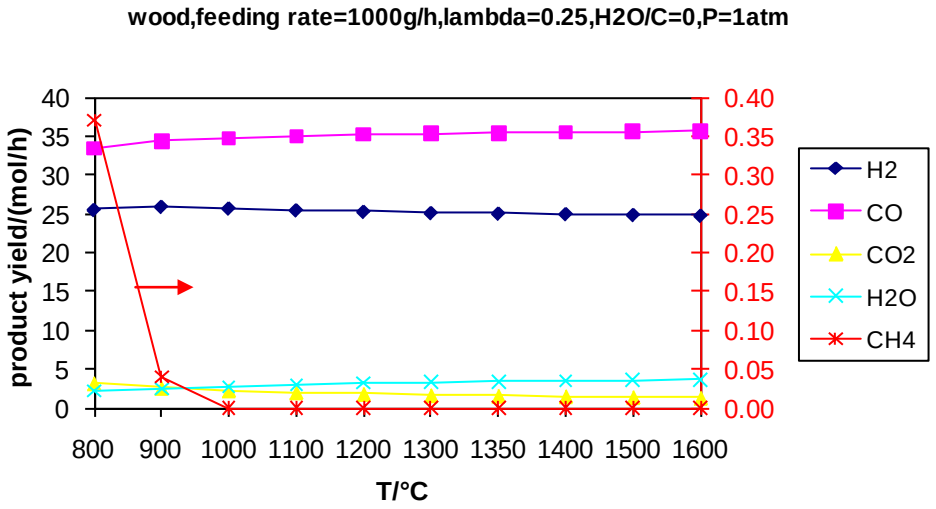
wood,feeding rate=1000g/h,lambda=0.25,H2O/C=0,P=1atm
product yield/(mol/h)
T/°C
H2
CO
CO2
H2O
CH4

(a-1)

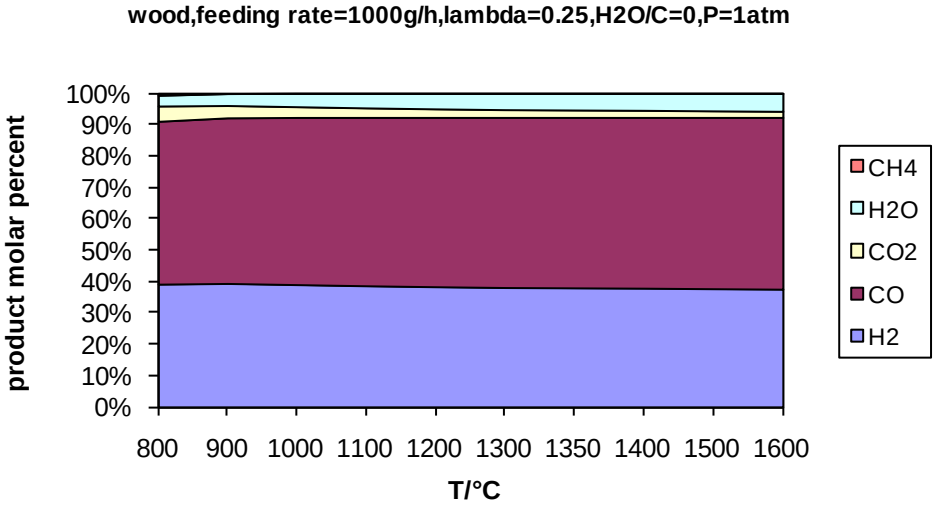
wood,feeding rate=1000g/h,lambda=0.25,H2O/C=0,P=1atm
product molar percent
T/°C
CH4
H2O
CO2
CO
H2

(a-2)

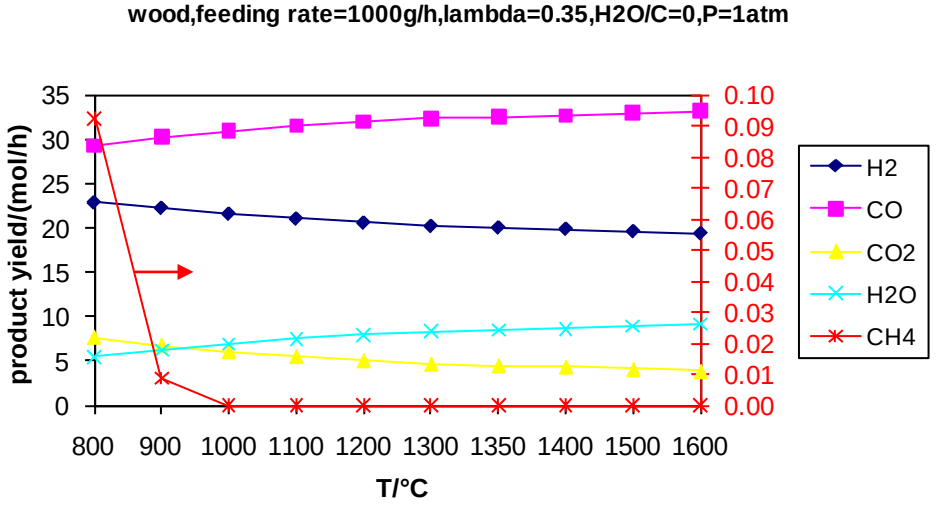
wood,feeding rate=1000g/h,lambda=0.35,H2O/C=0,P=1atm
product yield/(mol/h)
T/°C
H2
CO
CO2
H2O
CH4

(b-1)

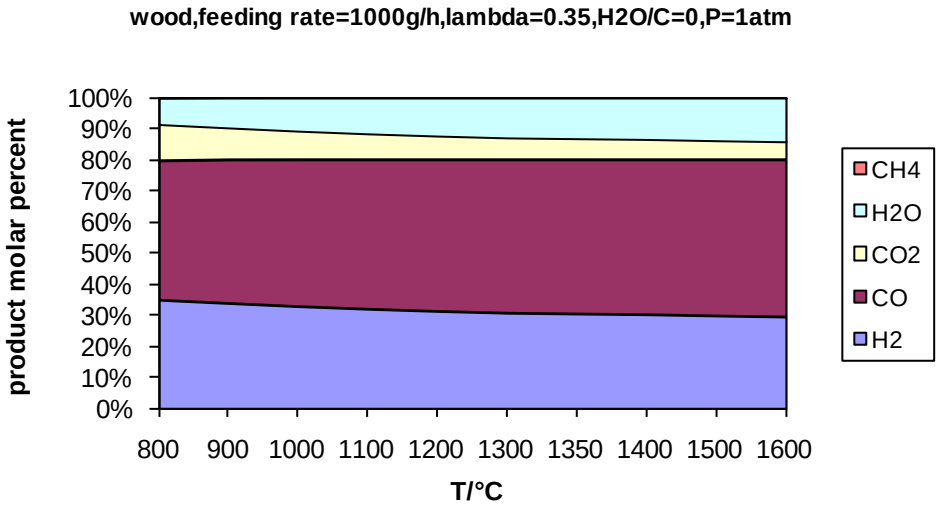

(b-2)

Figure 8 Effect of temperature on product yield and percent

(a) lambda=0.25 (b) lambda=0.35

3.3 Effect of steam/carbon molar ratio on products

The effect of steam/carbon molar ratio on product yield at the temperature of 1350°C and 1200°C is shown in Figure 9. The steam/carbon molar ratio is in the range of 0 to 2. The yields of H_2 and CO_2 increase, while CO yield decreases with increased H_2O/C ratio because the increased water content promotes the water gas shift reaction (4) [13][14]. The H_2O yield increases due to the increasing amount of steam addition.

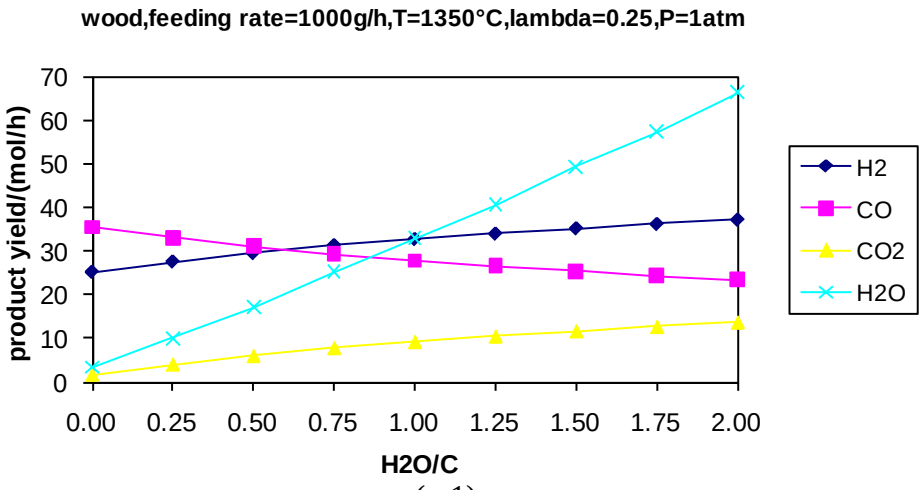

(a-1)

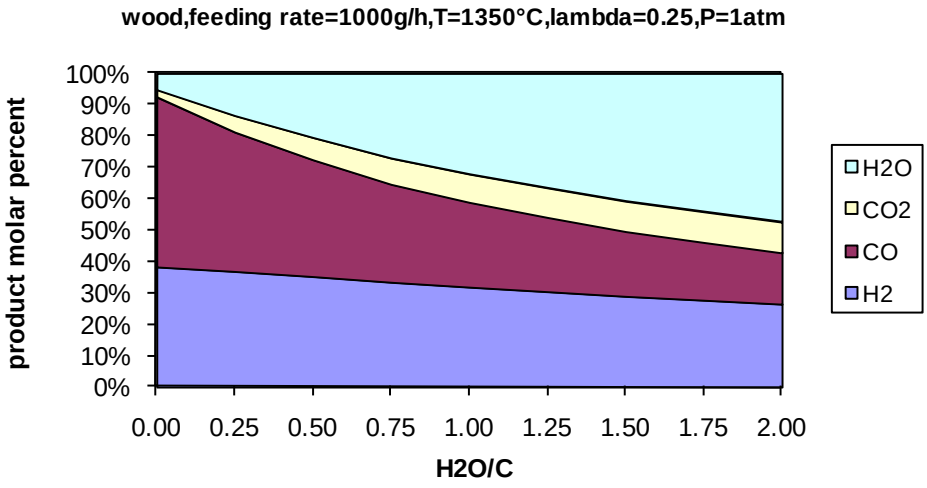

(a-2)

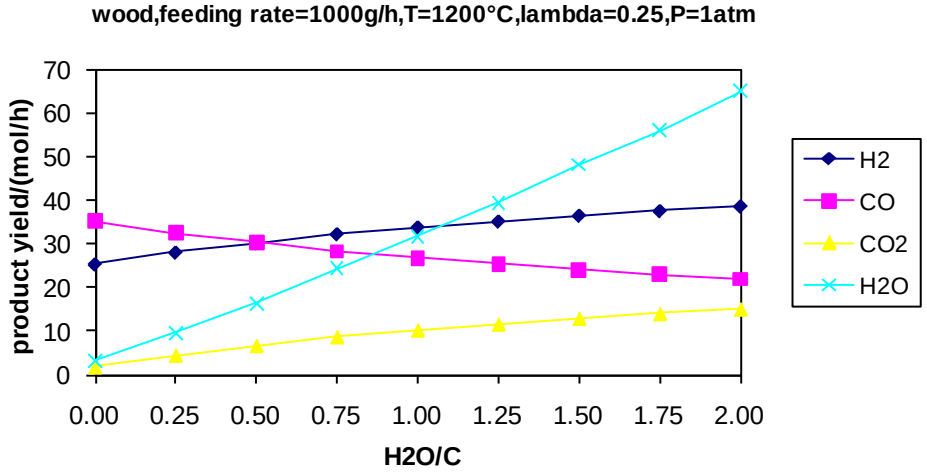

(b-1)

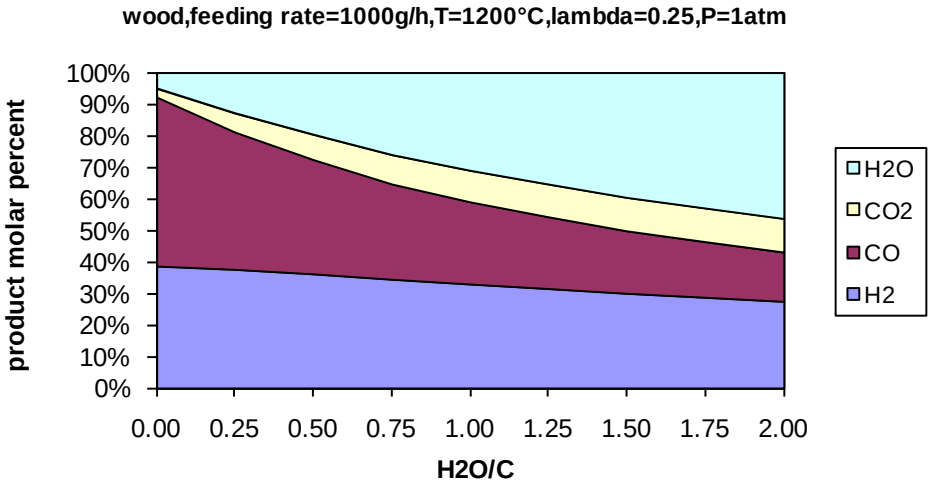

(b-2)

Figure 9 Effect of steam/carbon molar ratio on product yield and percent

(a) T=1350°C (b) T=1200°C

3.4 Effect of pressure on products

The effect of pressure on product yield is shown in Figure 10. Pressure is in the range of 1atm to 101atm. The yield of CH_4 increases a little with the increasing pressure due to the steam methane reformation reaction (7). The amounts of the other gaseous products nearly keep constant with pressure increases [13][14].

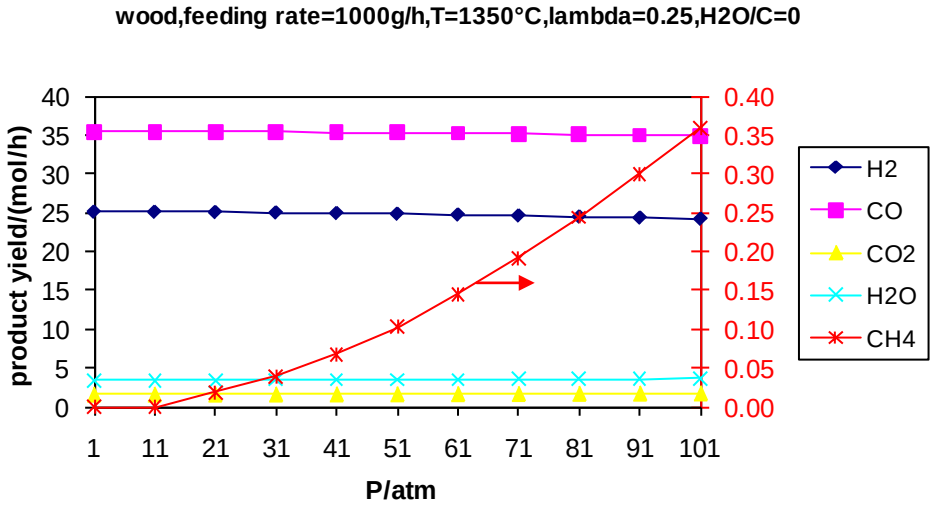

(a-1)

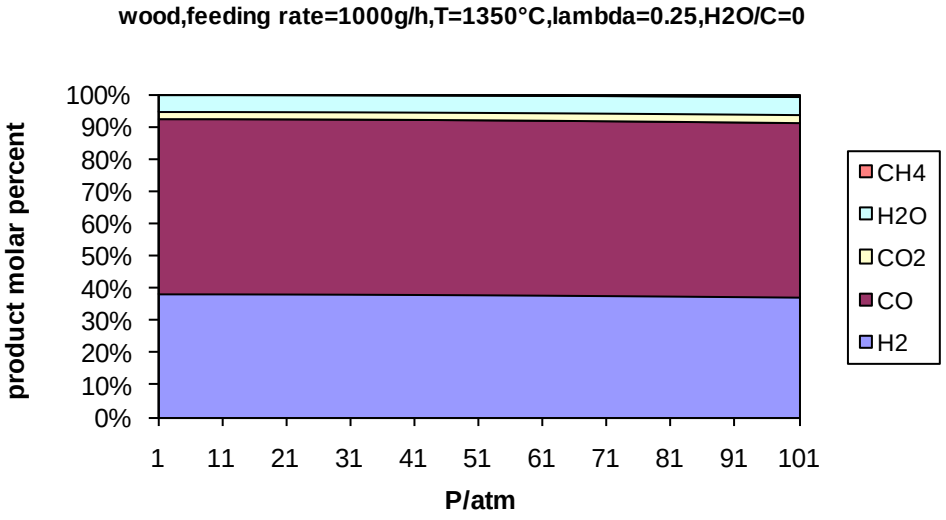

(a-2)

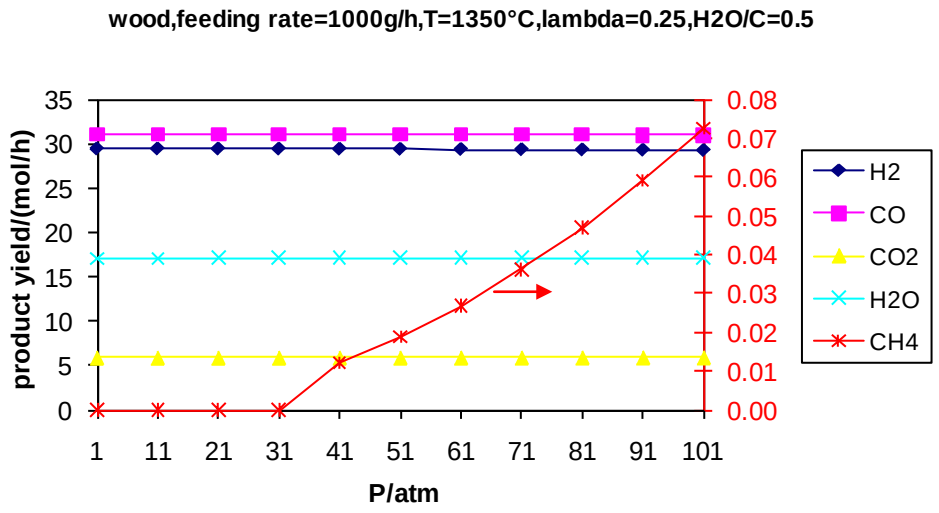

(b-1)

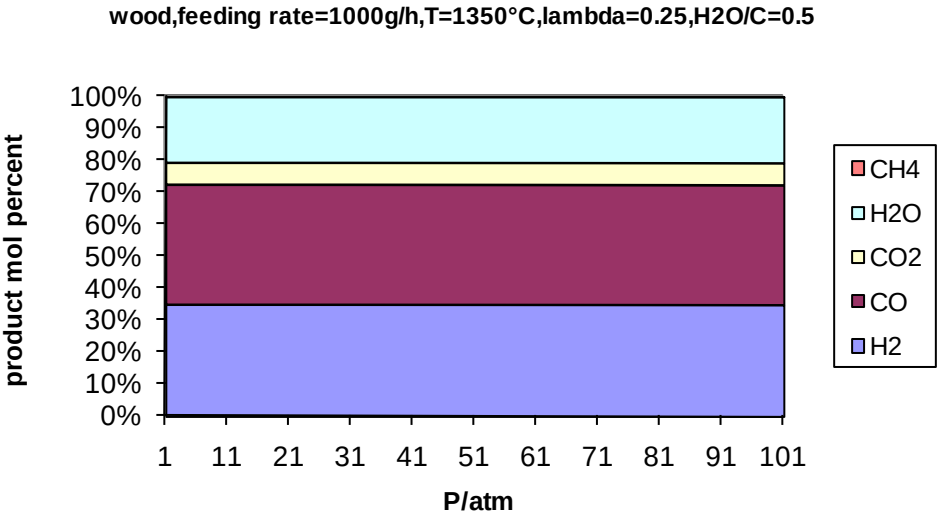

(b-2)

Figure 10 Effect of pressure on product yield and percent

(a) $H_2O/C=0$; (B) $H_2O/C=0.5$

4 Experiment results and discussion

The measurements conducted in this study on the entrained flow reactor exit gas included solid particle extraction, gas concentration of H_2, CO and CO_2, concentration of some hydrocarbon (C_xH_y includes CH_4, C_2H_4, C_3H_8, C_2H_4O by used of the Agilent 3000 micro GC) and in some of the experiments also tar concentration measurements were conducted.

In all experiments, the solid fuel was completely converted and no char particle was collected. However, in many of the experiments, some soot was observed in the exit gas.

4.1 Repeatability of experiment

The Repeatability of experiment is shown in Figure 11. From this figure, we can conclude that our experiments have good repeatability. The small errors of the gas products in the two experiments are caused by the errors of feeding rate, gas analyzer and micro GC. And the error of soot is mainly from different degree of the departure of isokinetic sampling.

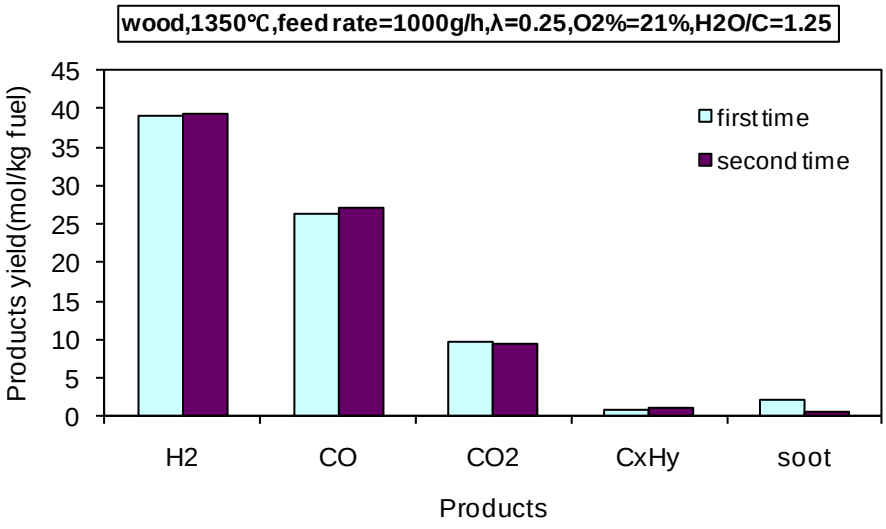

Figure 11 Repeatability of experiment (operating condition no. 3)

4.2 Mass balance

Based on the fuel composition and the measured product distribution (gas, hydrocarbon and soot measuring data), the carbon mass balances were calculated for all conducted experiments. The carbon balance is expressed as the outlet to inlet ratio. In the calculations, soot was assumed to be 100% carbon. It should be noticed that the amount of tar and char were not included in the mass balance calculations. In the biomass gasification experiments, the fuel was completely converted and no char was collected. The carbon balance results are shown in Figure 12. Almost all data fall between the two

horizontal lines from 0.9 to 1.1, which indicate that a reasonable mass balance closure was achieved. But at three conditions (no.1, 22, 34), there are large deviations. Experiment 1 was the only experiment in which coal fuel was used. In experiment 1, the large deviation of the carbon mass balance is caused by a significant amount of unconverted char that is not included in the calculation. At no.22, the deviation may be caused by a large departure from isokinetic sampling for the solid sample. In other words, the yield of soot has a large influence on the calculation of the carbon mass balance. Experiment 34 was performed at 1000°C and λ=0.25, this lead to a high fraction of carbon is missing probably due to the high tar levels and the unmeasured hydrocarbon yields at this temperature. The hydrogen and oxygen mass balance could not be closed since water yields were not determined.

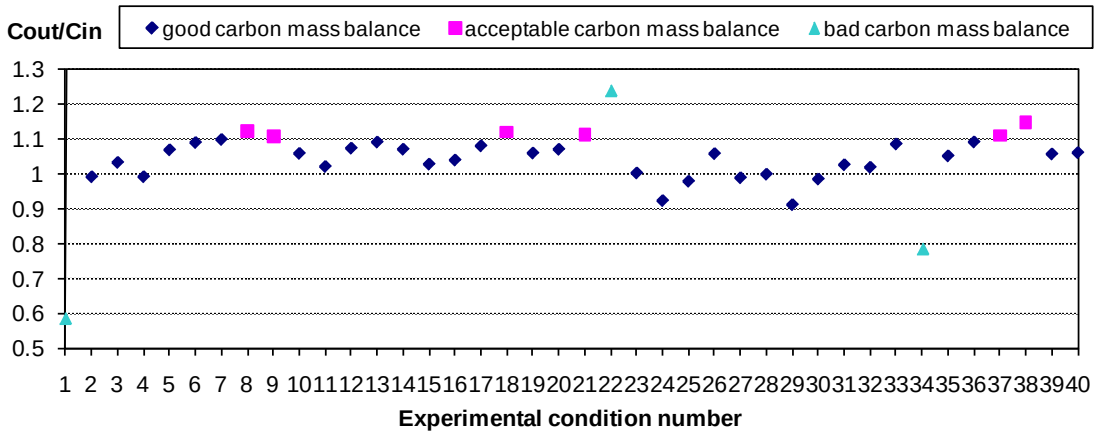

Figure 12 Carbon balances of experiments without steam addition

4.3 Soot and tar analysis

4.3.1 Soot analysis

A relatively large amount of soot is produced from wood and straw gasification at high temperature. To obtain basic characteristics of the soot several soot samples are examined by Scanning Electric Microscopy (SEM) and Simultaneous Thermal Analysis (STA) for their morphology and combustion reactivity.

4.3.1.1 Morphology of soot

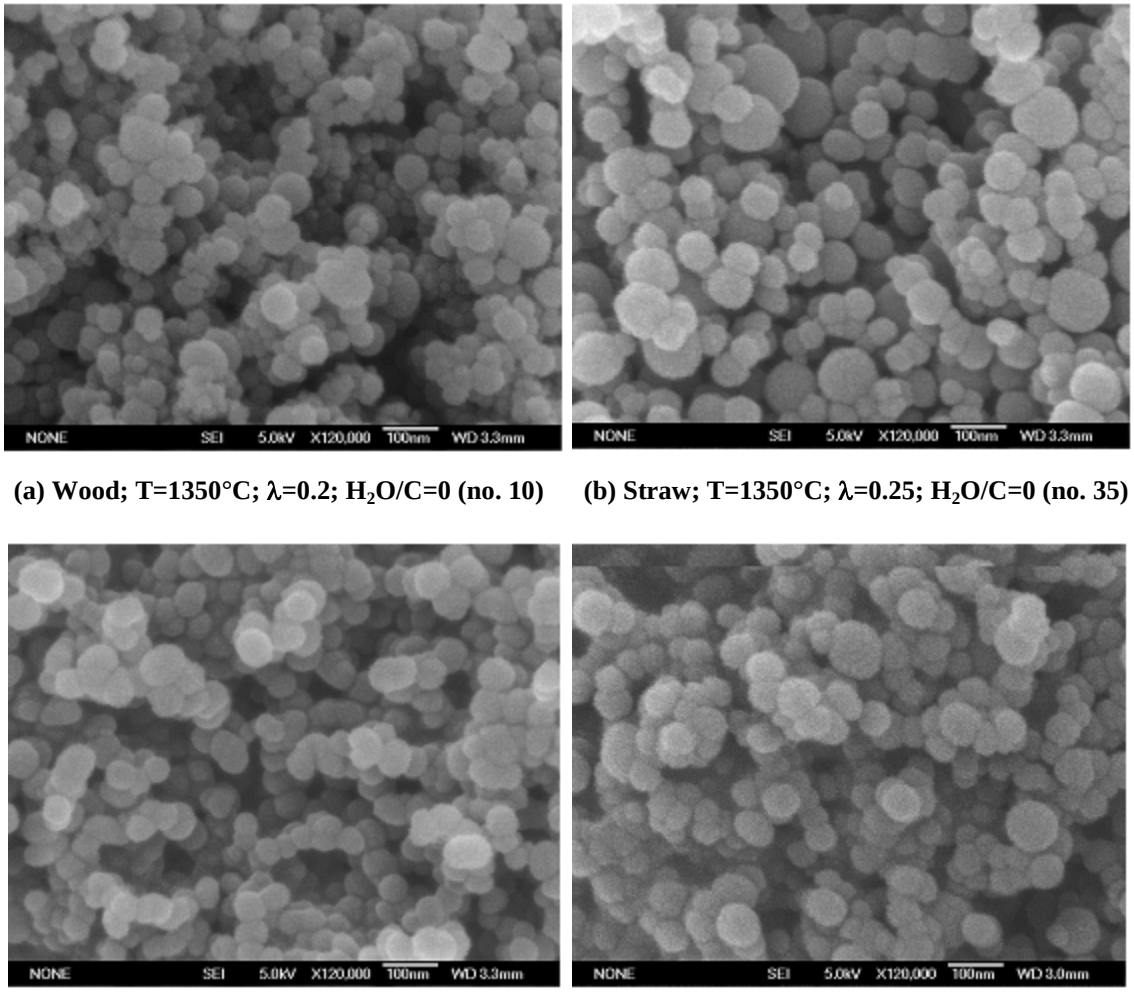

(a) Wood; T=1350°C; λ=0.2; H_2O/C=0 (no. 10) **(b) Straw; T=1350°C; λ=0.25; H_2O/C=0 (no. 35)**

(c) Wood; T=1350°C; λ=0.2; H_2O/C=1 (no. 15) **(d) Wood; T=1200°C; λ=0.25; H_2O/C=0.5 (no. 30)**

Figure 13 SEM images of soot sampled at different conditions

Figure 13 shows the SEM images of four soot samples from wood and straw gasification. In general, soot clusters consist of carbon spheres with a size range of 50-100 nm. No obvious difference can be observed of the morphology of the four samples.

4.3.1.2 Combustion reactivity of soot

The four samples are examined by a STA. The heating rates are kept at 20°C/min, and the samples are heated from room temperature to 900°C in air. The DSC signals as a function

of temperature for the four samples are presented in Figure 14, which can indicate the combustion reactivity of the soot samples qualitatively. The results show that soot from straw gasification at 1350°C has the highest reactivity while soot from wood gasification at 1200°C has the lowest reactivity. The reactivity of soot from wood gasification at 1350°C is in the middle. It seems that steam addition has little effect on the reactivity of the soot. It is presently not known why the 1200°C sample (wood, $H_2O/C=0$) has a larger reactivity than the other samples.

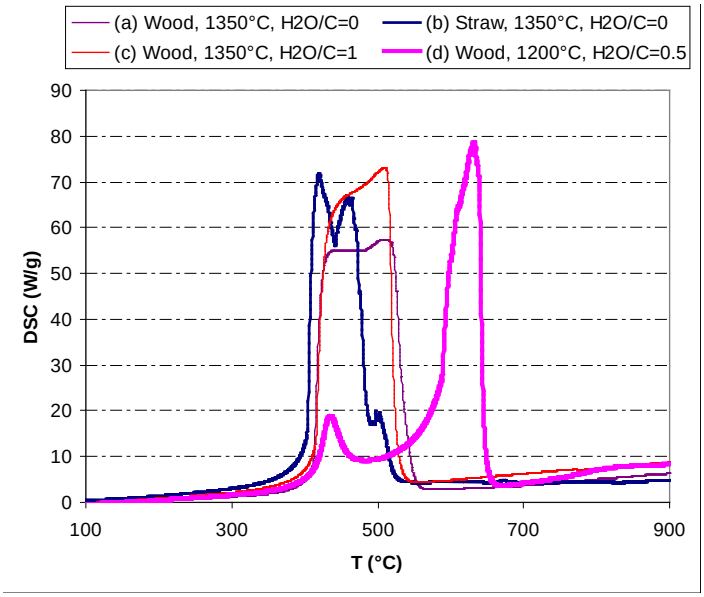

Figure 14 The combustion reactivity of the four soot samples

4.3.2 Tar analysis

The results of the tar analysis are shown in Table 3. The main characteristics of the detected tar compounds are listed in Table 4. It is obvious that the highest amount of tar is produced at low temperature (1000°C) and low excess air ratio (0.25). At this condition, the amount of tar obtained by the tar measurement and the carbon mass balance has the same trend but much different levels (in the tar measurement: 0.006%, carbon mass balance: 21.8%). So maybe the tar sampling method (SPA, solid phase absorption) is not suitable, and cannot collect all tar in the syngas.

Table 3 The tar compounds in different experimental conditions

Fuel		wood	wood	wood	straw	wood	wood	wood
	T (°C)	1350	1350	1350	1350	1000	1000	1000
Parameters	λ (-)	0.2	0.25	0.25	0.25	0.75	0.7	0.25
	H_2O/C (-)	0	0	1	0	0	0	0.5
Tar compounds		Content (mg/kg fuel)						
Phenol		0.005	0.000	0.009	0.158	0.000	0.017	0.010
Naphthalene		0.013	0.001	0.000	0.022	0.000	0.025	0.050
Acenaphthylene		0.039	0.001	0.000	0.000	0.000	0.180	3.582
Phenanthrene		0.000	0.000	0.002	0.121	0.045	0.719	8.872
Anthracene		0.002	0.021	0.005	0.004	0.002	0.003	0.001
Fluoranthene		0.041	0.126	0.022	0.017	0.001	0.208	3.653
Pyrene		0.254	0.126	0.219	0.017	0.001	1.308	10.054
Unknown		0.010	0.126	0.022	0.017	0.006	0.007	0.005
Total tar		0.364	0.401	0.280	0.357	0.057	2.468	26.228

Table 4 The main characteristics of the detected tar compounds

Name	formula	Molar weight (g/mole)	Structure
Phenol	C_6H_5OH	94	
Naphthalene	$C_{10}H_8$	128	
Acenaphthylene	$C_{12}H_8$	152	
Phenanthrene	$C_{14}H_{10}$	178	
Anthracene	$C_{14}H_{10}$	178	
Fluoranthene	$C_{16}H_{10}$	202	
Pyrene	$C_{16}H_{10}$	202	

At high temperature, and even at low excess air ratio, the amount of tar is small. With steam addition, at 1350°C, the tar yield is reduced nearly by a factor of two compared to the same condition without steam addition. Tar is formed during pyrolysis of solid fuel and consists of primarily heavy hydrocarbons. The lower tar yield at 1350ºC can be attributed to the heavy hydrocarbon chains being cracked at high temperatures and reacting with steam to form H_2, CO, and CO_2 [20][24][26]. The types of biomass have little influence on the yield of tar, but have some effect on the tar composition, which is probably due to the catalysis of the high alkali content in straw. In wood gasification, pyrene is the most abundant tar compound, and at lower temperature, phenanthrene and

acenaphthylene also appear as major compounds in the tar. In straw gasification tar, phenanthrene and phenol are the main compounds.

4.4 The yield and distribution of gasification products

4.4.1 Effect of excess air ratio on product yield and distribution

The influence of changes of the excess air ratio on the products composition where investigated by two methods. By changing the total inlet flow and by changing the oxygen content in the inlet flow. The excess air ratio (lambda, λ) is defined in equation 8.

(8)

The results of changing the excess air ratio from 0.2 to 0.4 by fixing the fuel feeding rate at 800 g/h and then changing the total gas inlet amount from 11 to 22 Nl/min are shown in Figures 15 and 16. The residence time was thereby changed from 3 to 4 seconds simultaneously. In another set of experimental data, shown in Figure 17 and 18, the change in lambda is obtained by changing the oxygen content in the inlet gas.

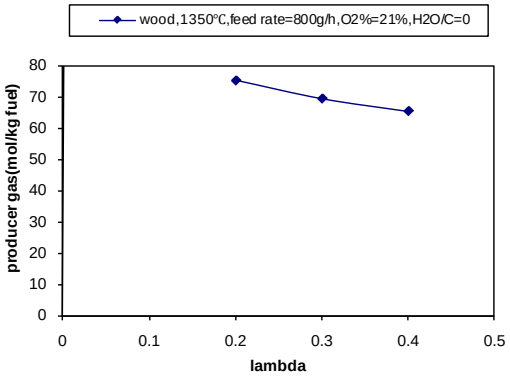

(a)

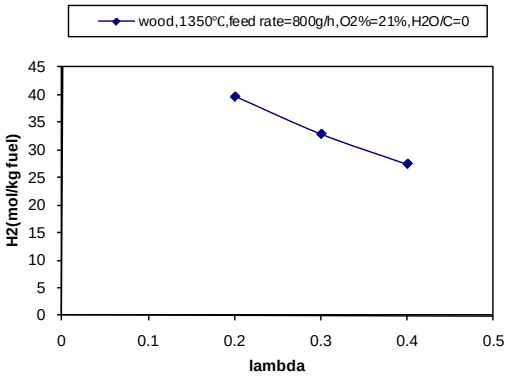

(b)

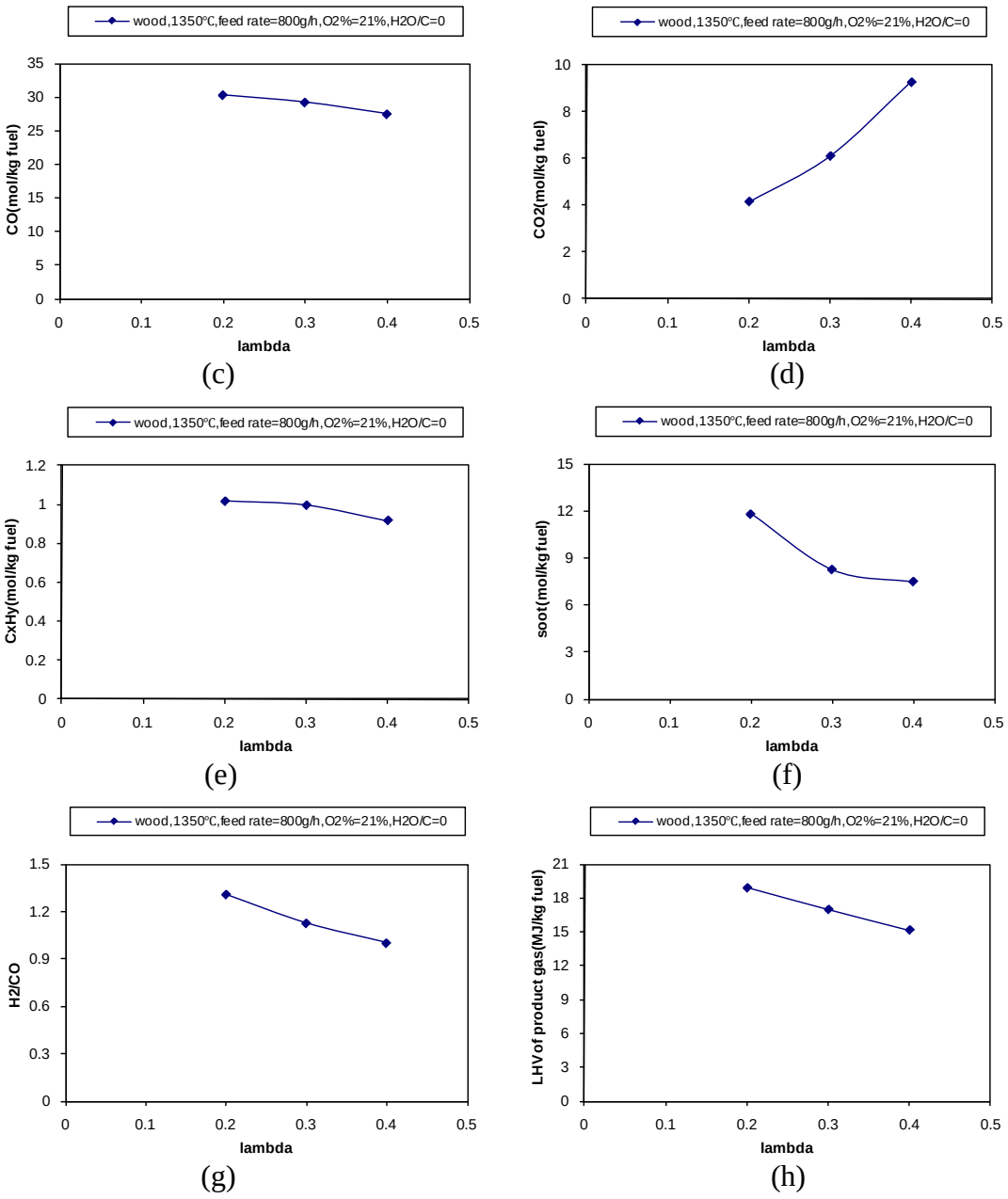

Figure 15 Effect of excess air ratio on product yield (fixing oxygen concentration)

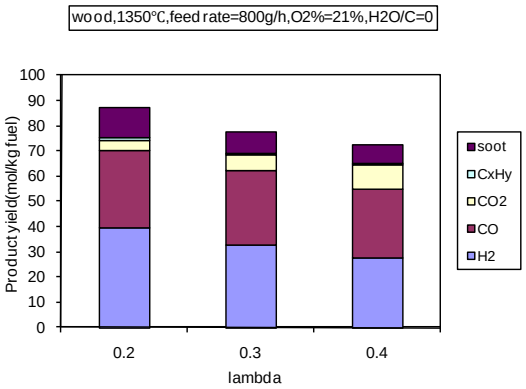

Figure 16 Effect of excess air ratio on product distribution (fixing oxygen concentration)

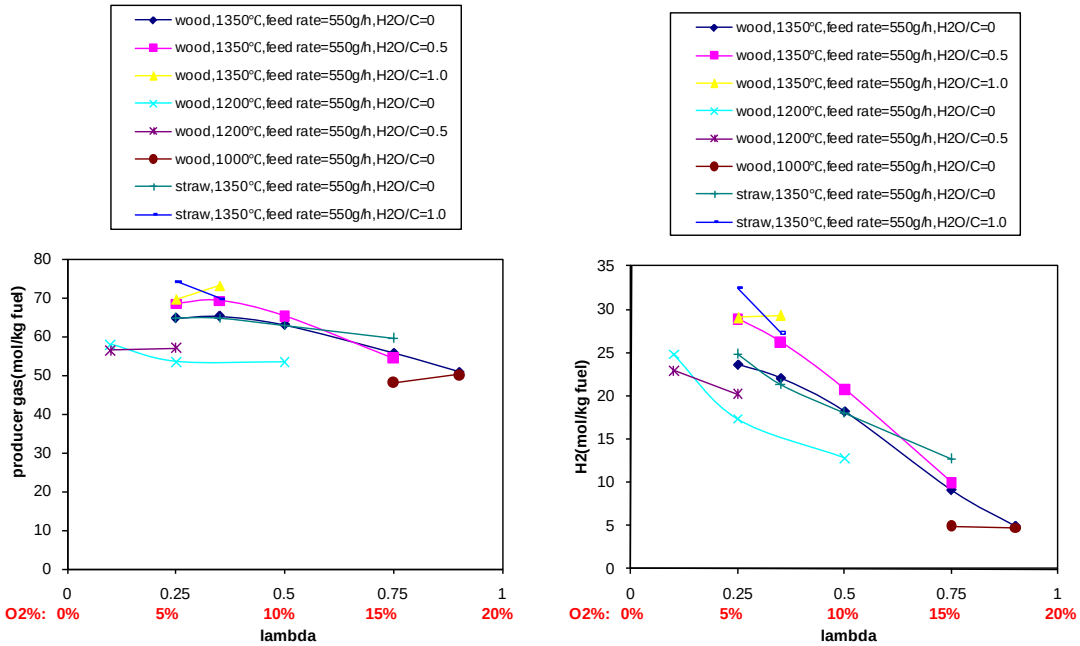

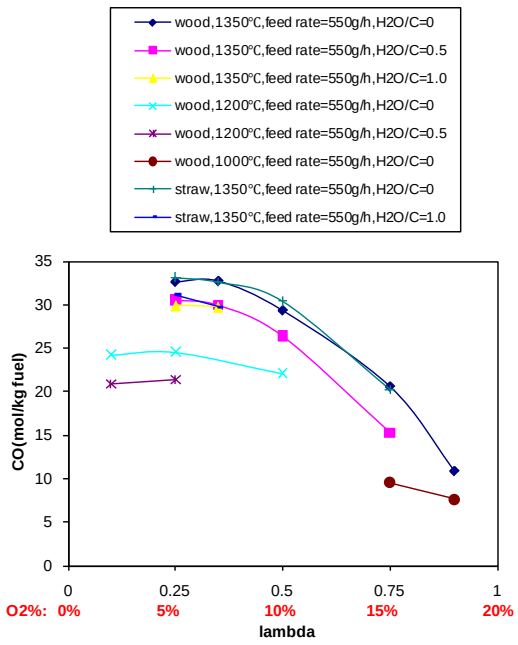
wood,1350℃,feed rate=550g/h,H2O/C=0
wood,1350℃,feed rate=550g/h,H2O/C=0.5
wood,1350℃,feed rate=550g/h,H2O/C=1.0
wood,1200℃,feed rate=550g/h,H2O/C=0
wood,1200℃,feed rate=550g/h,H2O/C=0.5
wood,1000℃,feed rate=550g/h,H2O/C=0
straw,1350℃,feed rate=550g/h,H2O/C=0
straw,1350℃,feed rate=550g/h,H2O/C=1.0
CO(mol/kg fuel)
0 5 10 15 20 25 30 35
0 0.25 0.5 0.75 1
O2%: 0% 5% 10% 15% 20%
lambda

(c)

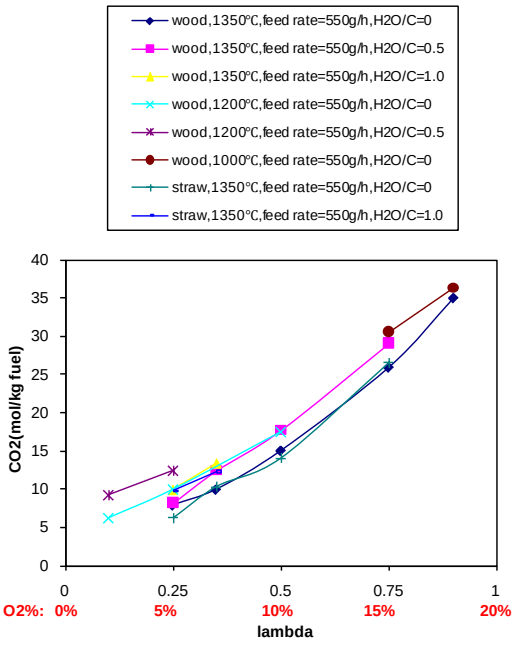
wood,1350℃,feed rate=550g/h,H2O/C=0
wood,1350℃,feed rate=550g/h,H2O/C=0.5
wood,1350℃,feed rate=550g/h,H2O/C=1.0
wood,1200℃,feed rate=550g/h,H2O/C=0
wood,1200℃,feed rate=550g/h,H2O/C=0.5
wood,1000℃,feed rate=550g/h,H2O/C=0
straw,1350℃,feed rate=550g/h,H2O/C=0
straw,1350℃,feed rate=550g/h,H2O/C=1.0
CO2(mol/kg fuel)
0 5 10 15 20 25 30 35 40
0 0.25 0.5 0.75 1
O2%: 0% 5% 10% 15% 20%
lambda

(d)

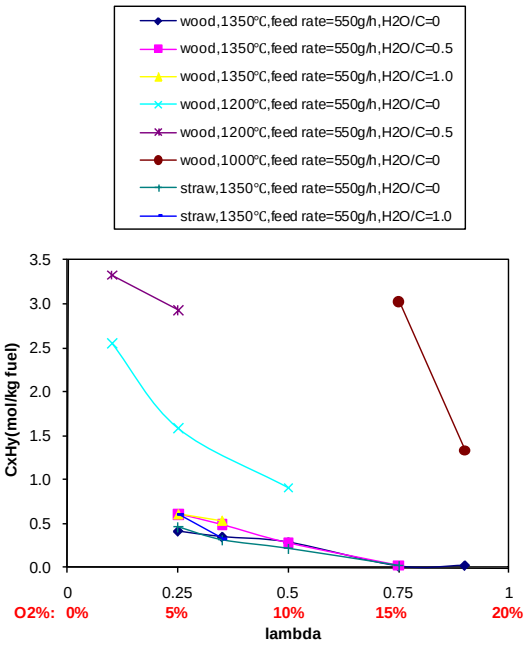
wood,1350℃,feed rate=550g/h,H2O/C=0
wood,1350℃,feed rate=550g/h,H2O/C=0.5
wood,1350℃,feed rate=550g/h,H2O/C=1.0
wood,1200℃,feed rate=550g/h,H2O/C=0
wood,1200℃,feed rate=550g/h,H2O/C=0.5
wood,1000℃,feed rate=550g/h,H2O/C=0
straw,1350℃,feed rate=550g/h,H2O/C=0
straw,1350℃,feed rate=550g/h,H2O/C=1.0
CxHy(mol/kg fuel)
0.0 0.5 1.0 1.5 2.0 2.5 3.0 3.5
0 0.25 0.5 0.75 1
O2%: 0% 5% 10% 15% 20%
lambda

(e)

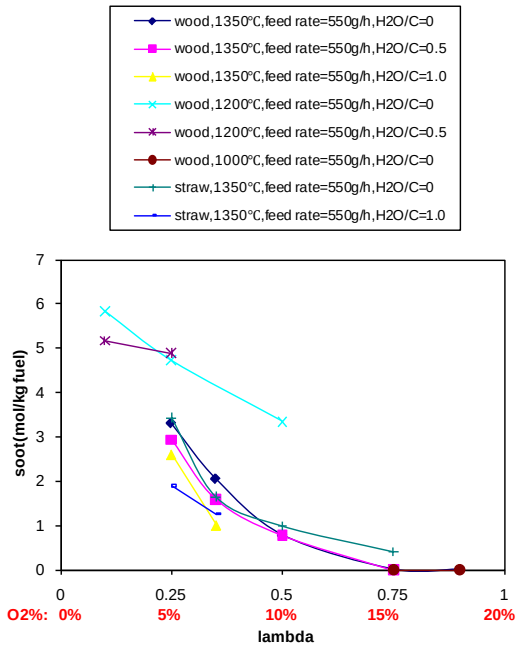
wood,1350℃,feed rate=550g/h,H2O/C=0
wood,1350℃,feed rate=550g/h,H2O/C=0.5
wood,1350℃,feed rate=550g/h,H2O/C=1.0
wood,1200℃,feed rate=550g/h,H2O/C=0
wood,1200℃,feed rate=550g/h,H2O/C=0.5
wood,1000℃,feed rate=550g/h,H2O/C=0
straw,1350℃,feed rate=550g/h,H2O/C=0
straw,1350℃,feed rate=550g/h,H2O/C=1.0
soot(mol/kg fuel)
0 1 2 3 4 5 6 7
0 0.25 0.5 0.75 1
O2%: 0% 5% 10% 15% 20%
lambda

(f)

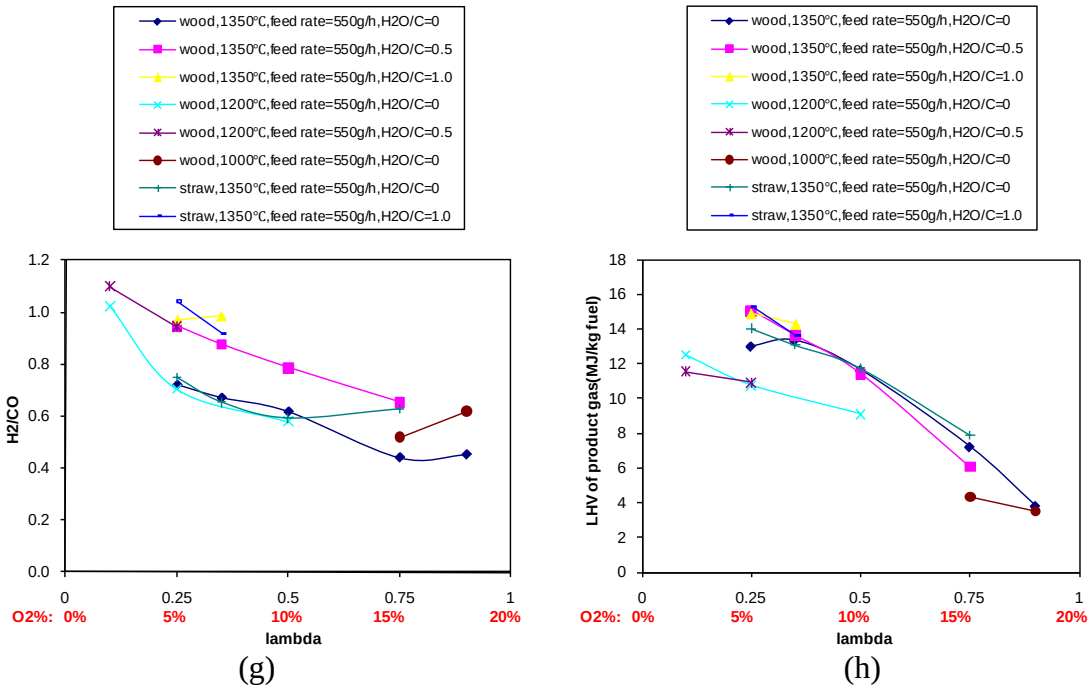

Figure 17 Effect of excess air ratio on product yield (fixing residence time)

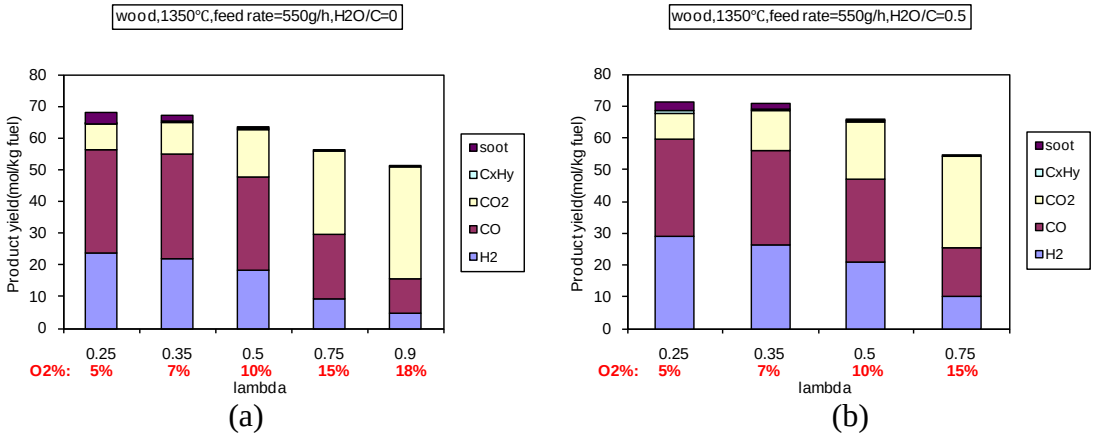

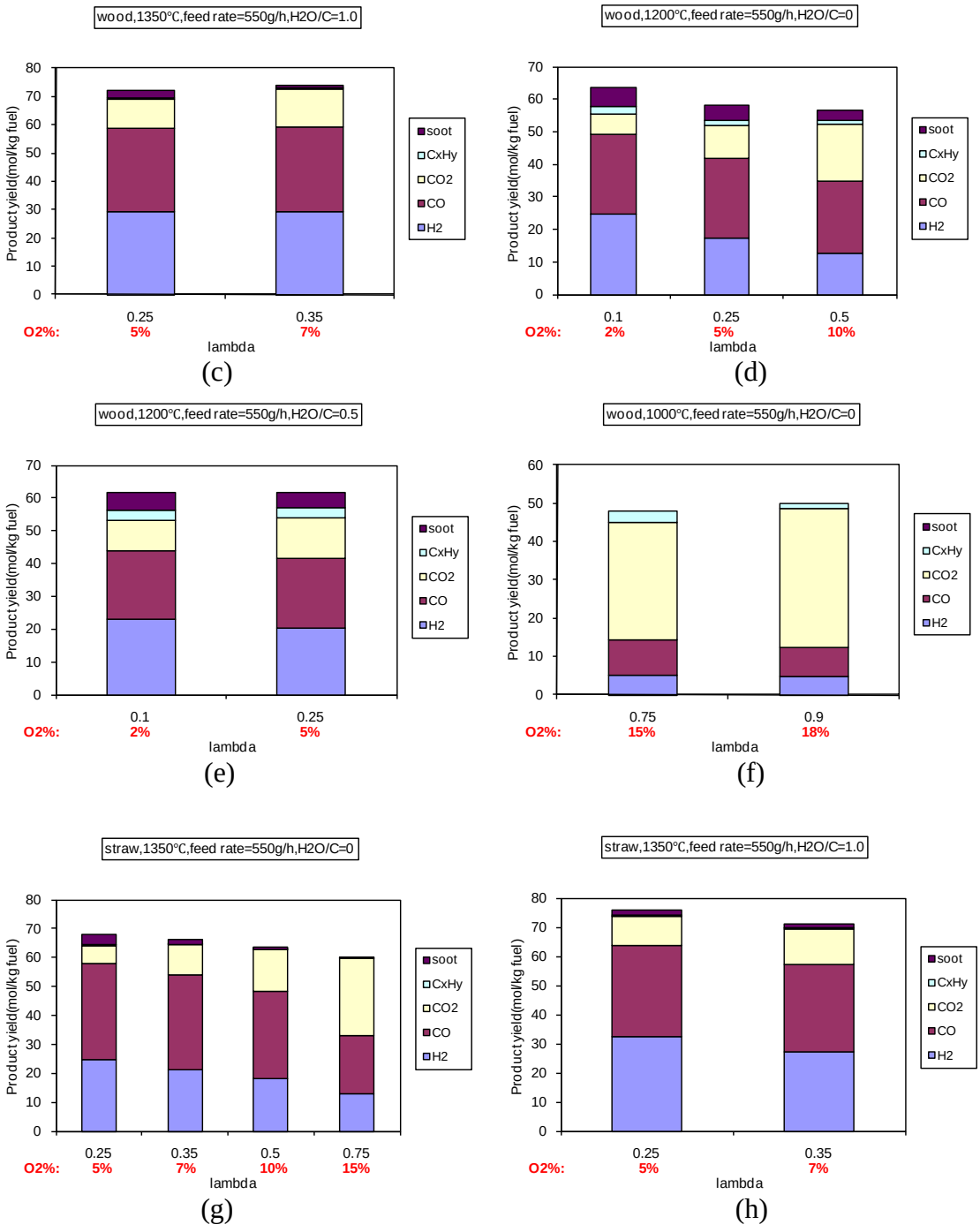

Figure 18 Effect of excess air ratio on product distribution (fixing residence time)

In general, the amount of producer gas which is defined as the sum of H_2, CO, CO_2 and C_xH_y (hydrocarbons up to C_3 species) decreases with increasing excess air ratio. An increased excess air ratio means that more oxygen is available for the combustion reactions [15]-[19]. With increasing excess air ratio, the yields of H_2, CO, C_xH_y, and soot

decrease, while the yields of CO_2 and H_2O increase. The decrease of the total amount of producer gas is cause by the conversion of H_2 to water [15][20]. It is observed that the amount of soot decreases with a rise in excess air ratio. As the excess air ratio increases, a larger part of the soot is combusted [21]. The H_2/CO ratio and the heating value (LHV) of the gas product decrease as the excess air ratio increases.

4.4.2 Effect of oxygen concentration on product yield and distribution

The change in oxygen concentration is mainly obtained by fixing the oxygen inlet flow and changing the nitrogen inlet flow. The effects of inlet oxygen concentration on product yields are shown in Figure 19 and 20. The reduced N_2 inlet flow at increased inlet oxygen concentration leads to some changes in fuel residence time from 1.4 s at 5 vol% oxygen up to 4.0 s at 34 vol% O_2. Some smaller changes in λ and feeding rates appear in the data shown in Figures 19 and 20, but those do probably not influence the results. A high inlet oxygen concentration will probably increase the temperature in the top of the reactor. The clearest tendency observed with increased inlet oxygen concentration is an increased product concentration of soot, C_xH_y and H_2 and a decreased concentration of CO_2. The reason for the large formation of soot at high oxygen inlet concentrations is presently not clear.

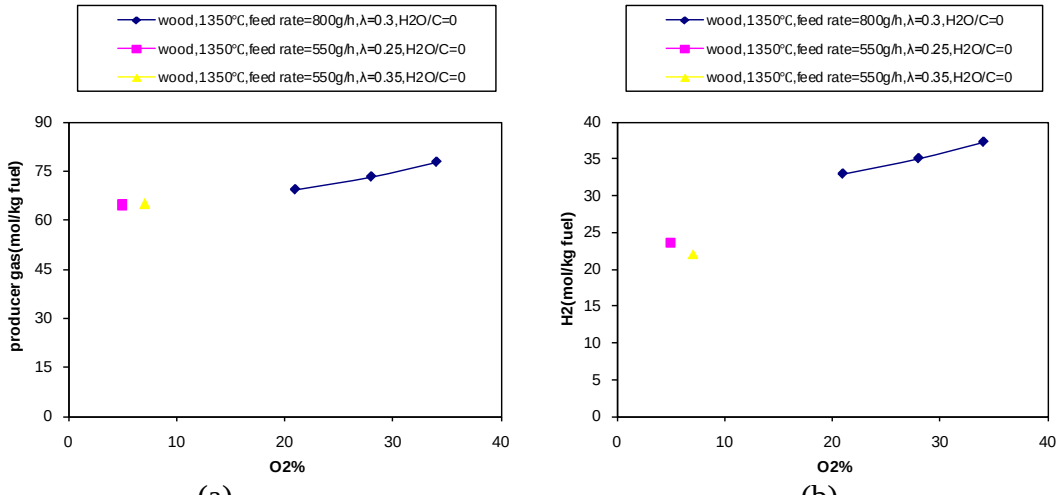

(a) (b)

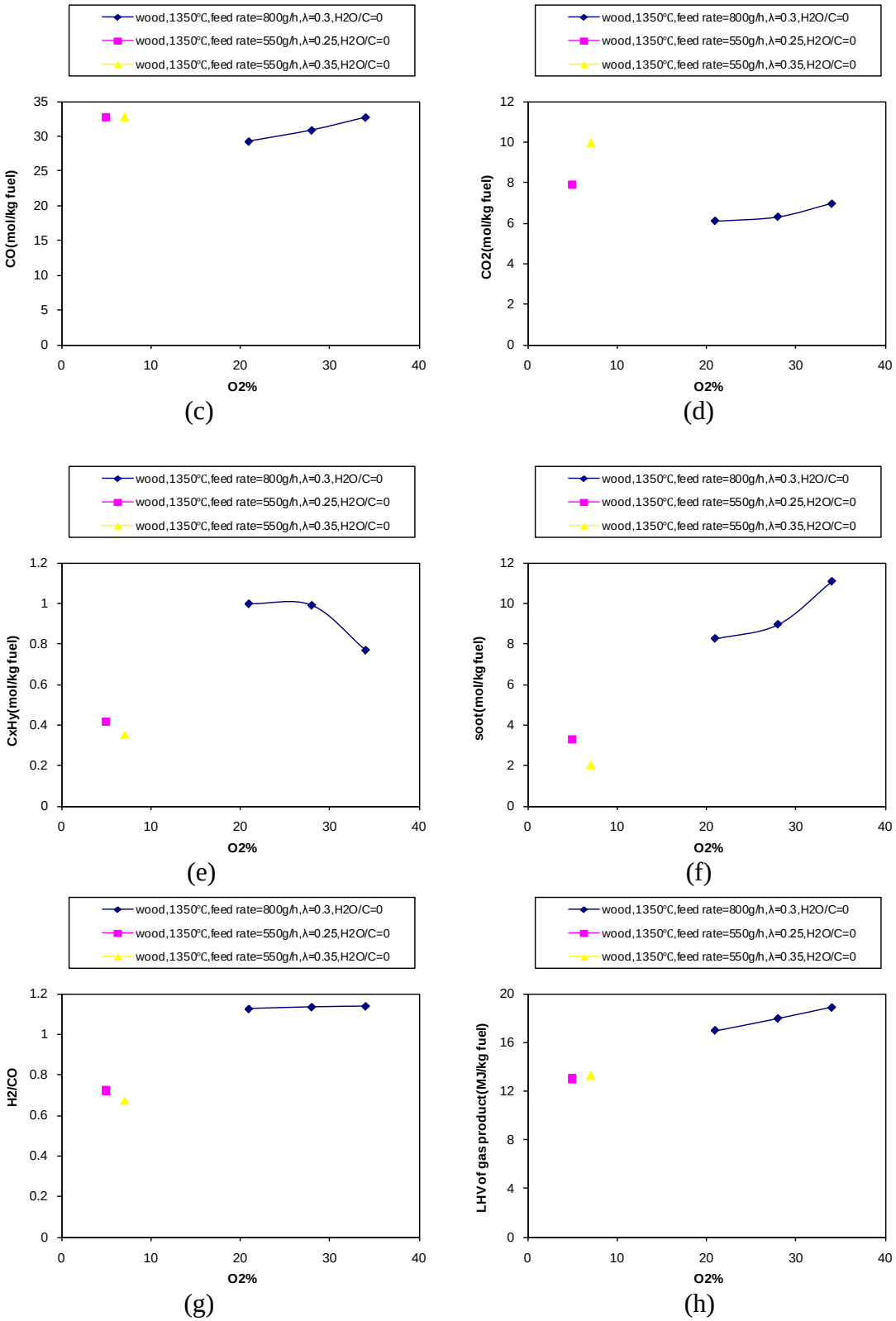

Figure 19 Effect of oxygen concentration on product yield

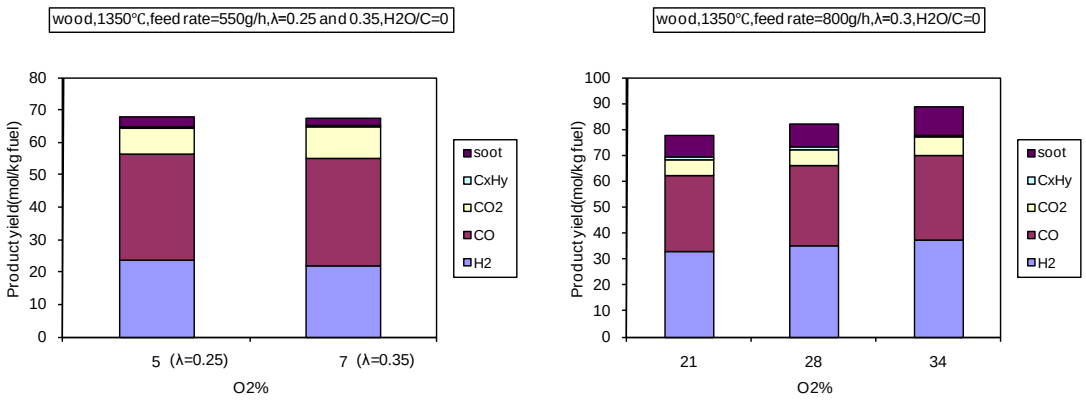

(a) (b)

Figure 20 Effect of oxygen concentration on product distribution

4.4.3 Effect of temperature on product yield and distribution

The effect of reactor set point temperature on product distribution is shown in Figure 21 and Figure 22. At lower lambda from 0.25 to 0.5, it can be seen that the amount of producer gas increases with increasing temperature. The increased gas formation is caused by the conversion of tar and larger hydrocarbons into lighter gaseous products. The H_2 and CO yields increase with increasing temperature, while the CO_2 and C_xH_y yields decrease [16]-[24]. From 1000°C to 1200°C, the soot yield increases, whereas from 1200°C to 1350°C, there is an opposite trend. Soot is formed at high temperature and an increasing temperature favors soot formation [21]. However, at higher temperature, soot has a higher reactivity for gasification with CO_2 and H_2O. As a result of the competition between formation and destruction of soot, the soot yield decreases above 1200°C. At higher temperature (1200°C and above), the H_2/CO ratio nearly keeps constant. The heating value (LHV) of the gas product increases in the range of 1000°C-1350°C.

At higher lambda from 0.75 to 0.9, the amount of producer gas remains unchanged as the temperature increases. Less tar and larger hydrocarbons are produced at higher lambda even at the lowest temperature (1000°C), so only a small amount of tar and larger hydrocarbons can be converted to lighter gaseous products and thereby increase producer gas yield. The yields of H_2 and CO increase with temperature, while CO_2 and C_xH_y yields decrease. There is no soot formation at lambda values above 0.7 because soot is

burnt at any temperature. The H_2/CO ratio and the heating value (LHV) of the gas product only change a little with temperature.

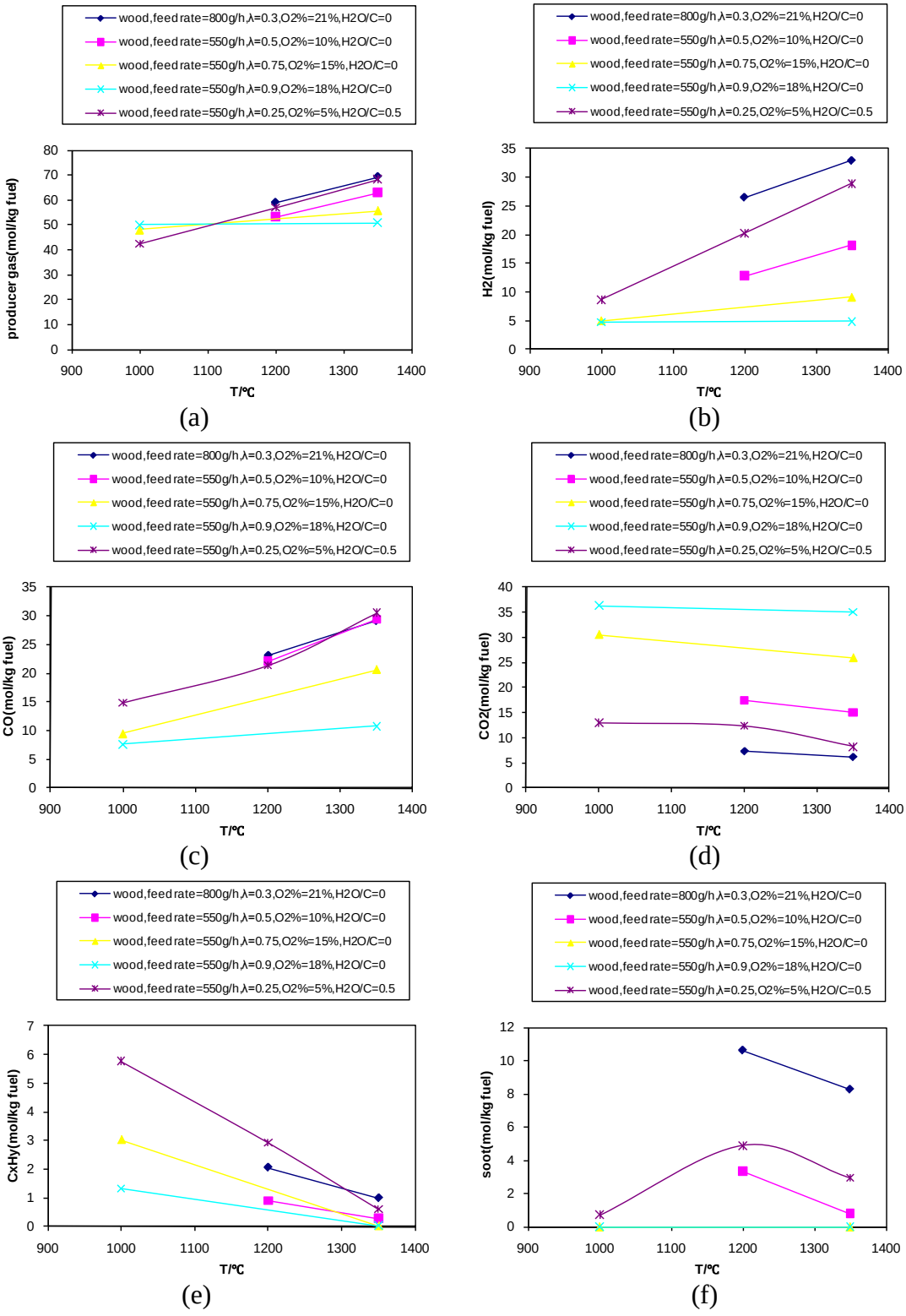

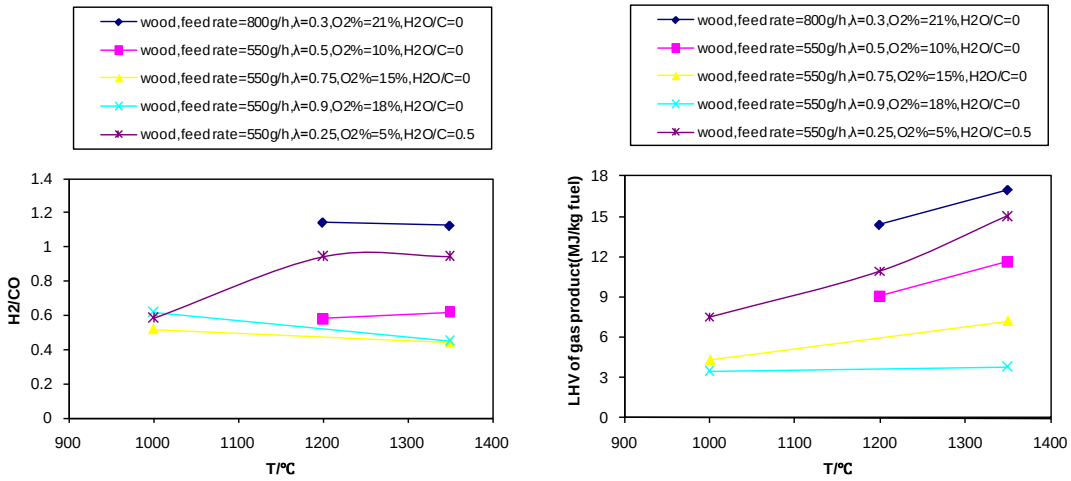

(g) (h)

Figure 21 Effect of temperature on product yield

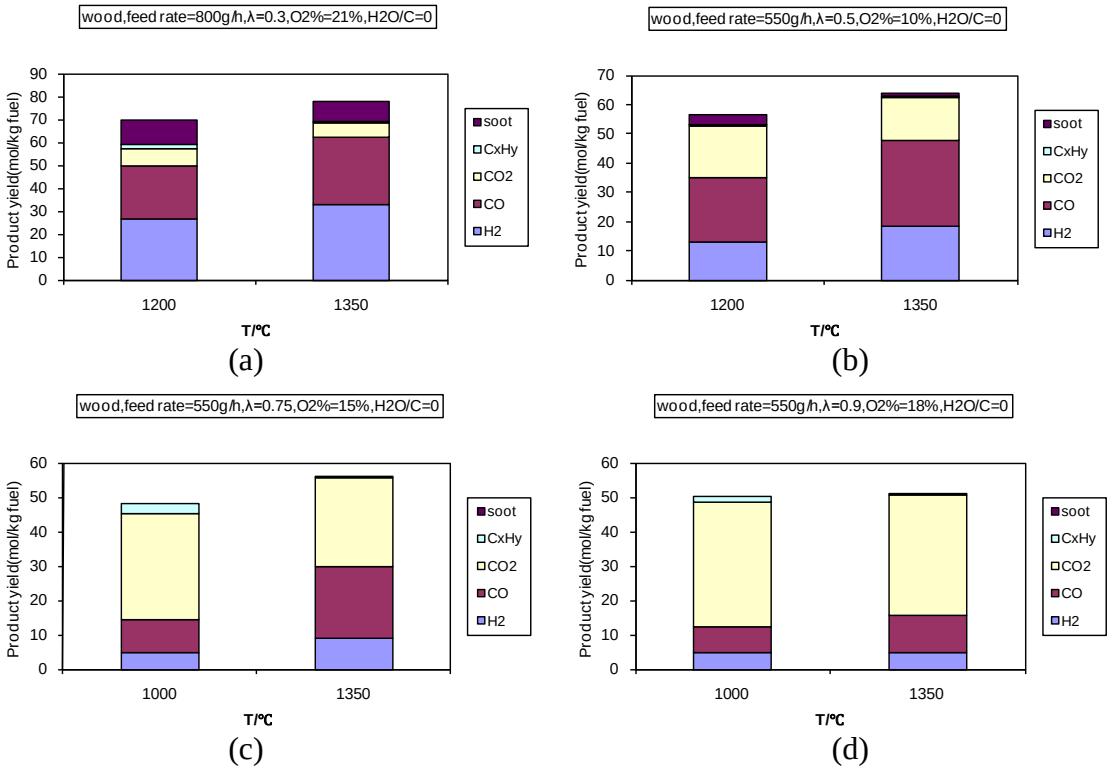

(a) (b) (c) (d)

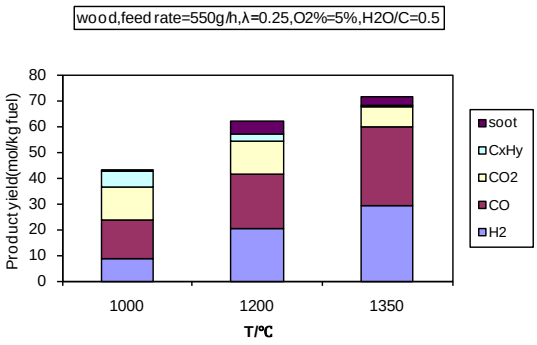

(e)

Figure 22 Effect of temperature on product distribution

Tar is a major compound in the product gas of fixed bed and fluidized bed gasifiers operated at lower temperatures. It was found that at an excess air ratio of 0.25 and a steam/carbon molar ratio of 0.5, the amount of soot is lowest (1.7% g/g fuel) at 1000°C, whereas that of tar (21.8% g/g fuel) is highest (The amount of tar is determined by the carbon mass balance). At 1350°C, the tar content in the syngas is probably close to zero. However, a significant amount of soot (7.1% g/g fuel) was produced at this temperature. This shows that there is a tradeoff between tar and soot formation, which may result partly from soot formation by tar polymerization at high temperatures. Several studies have shown that temperature is an important factor for tar formation [24]-[26].

4.4.4 Effect of steam/carbon molar ratio on product yield and distribution

The effect of steam/carbon molar ratio on products yields are shown in Figure 23 and Figure 24. In general, when steam is introduced, the yield of the producer gas increases slightly due to the promotion of steam gasification of soot and larger hydrocarbons. However, even a high amount of steam injection only small changes in the gas composition is observed. As the steam/carbon ratio increases, the H_2 and CO_2 yields increase, accompanied with a decrease of the CO yield. The steam addition promotes the water gas shift reaction towards formation of H_2 and CO_2 [18][27]. The C_xH_y yield increases when steam is introduced at 1200ºC, which may be caused by the reformation of tar and larger hydrocarbons. The yield of soot decreases with increasing steam/carbon ratio, most likely due to steam gasification of the soot. Steam addition increases the H_2/CO ratio. The heating value of the product gas does not change much with increasing H_2O/C ratio.

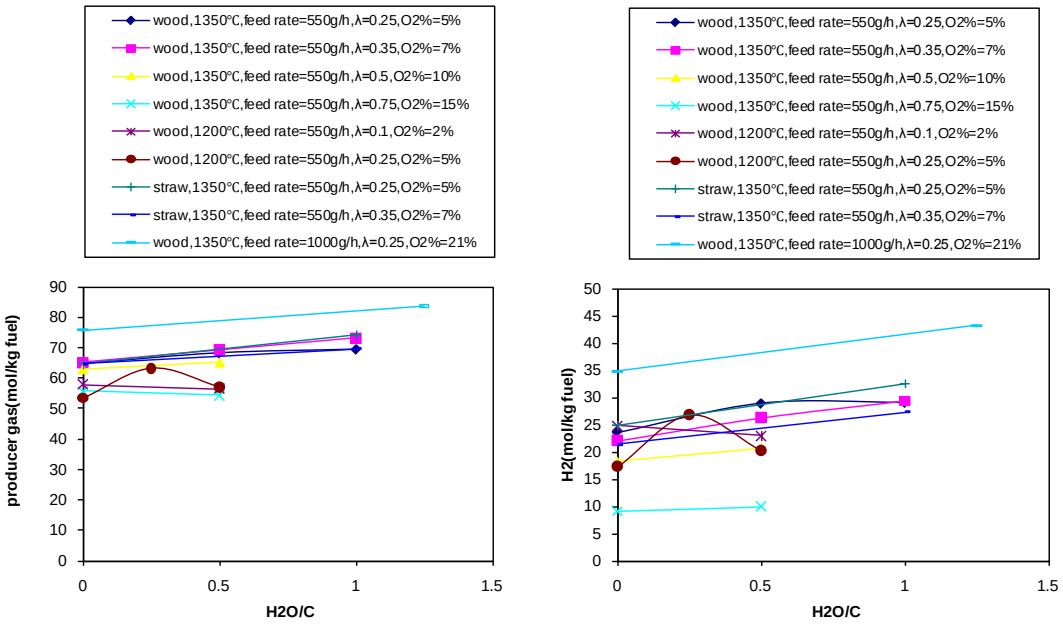
wood,1350℃,feed rate=550g/h,λ=0.25,O2%=5%
wood,1350℃,feed rate=550g/h,λ=0.35,O2%=7%
wood,1350℃,feed rate=550g/h,λ=0.5,O2%=10%
wood,1350℃,feed rate=550g/h,λ=0.75,O2%=15%
wood,1200℃,feed rate=550g/h,λ=0.1,O2%=2%
wood,1200℃,feed rate=550g/h,λ=0.25,O2%=5%
straw,1350℃,feed rate=550g/h,λ=0.25,O2%=5%
straw,1350℃,feed rate=550g/h,λ=0.35,O2%=7%
wood,1350℃,feed rate=1000g/h,λ=0.25,O2%=21%
producer gas(mol/kg fuel)
H2(mol/kg fuel)
H2O/C
(a)
(b)
CO(mol/kg fuel)
CO2(mol/kg fuel)
(c)
(d)

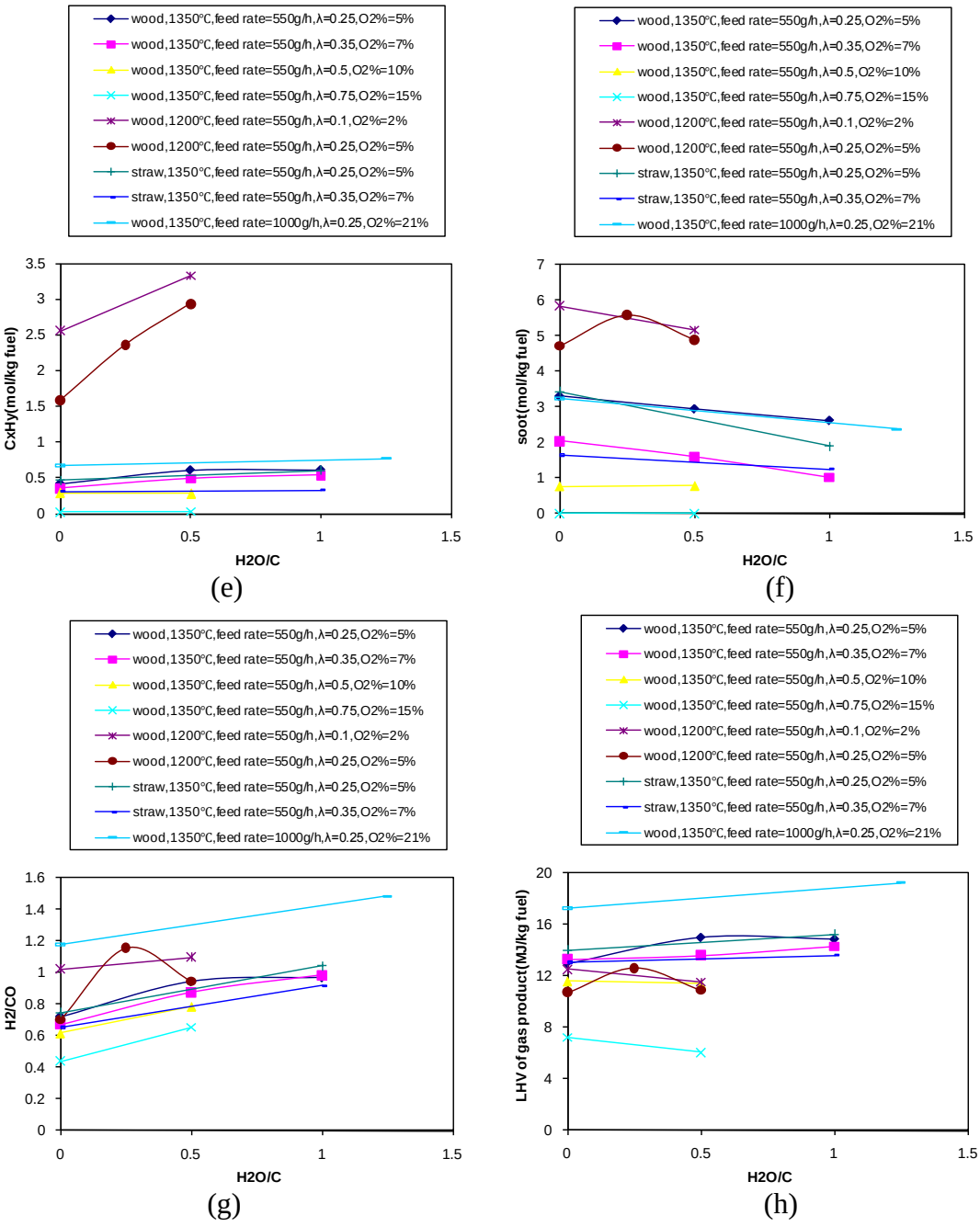

Figure 23 Effect of steam/carbon ratio on product yield

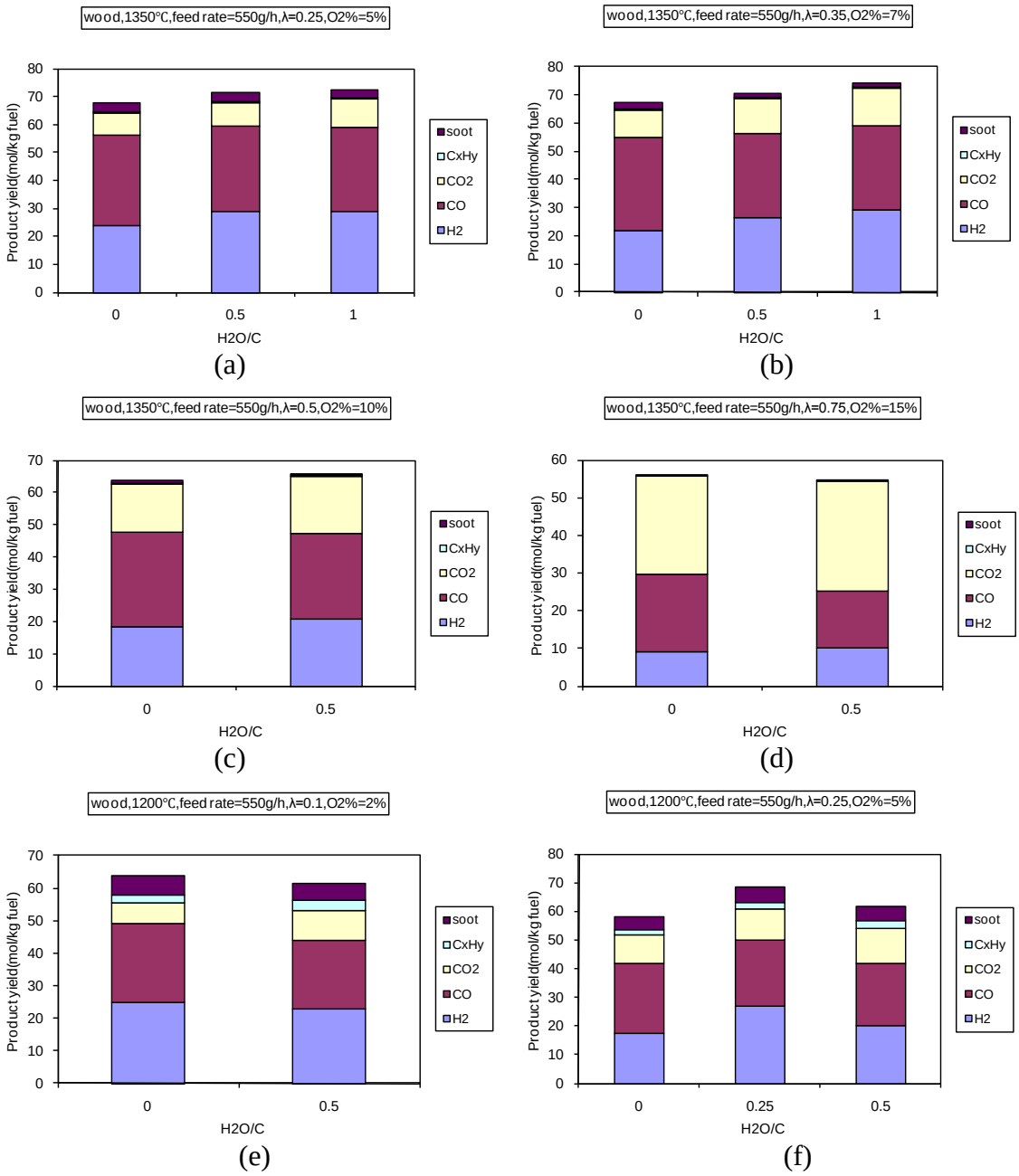
wood,1350℃,feed rate=550g/h,λ=0.25,O2%=5%
Product yield(mol/kg fuel)
H2O/C
soot
CxHy
CO2
CO
H2
(a)
wood,1350℃,feed rate=550g/h,λ=0.35,O2%=7%
(b)
wood,1350℃,feed rate=550g/h,λ=0.5,O2%=10%
(c)
wood,1350℃,feed rate=550g/h,λ=0.75,O2%=15%
(d)
wood,1200℃,feed rate=550g/h,λ=0.1,O2%=2%
(e)
wood,1200℃,feed rate=550g/h,λ=0.25,O2%=5%
(f)

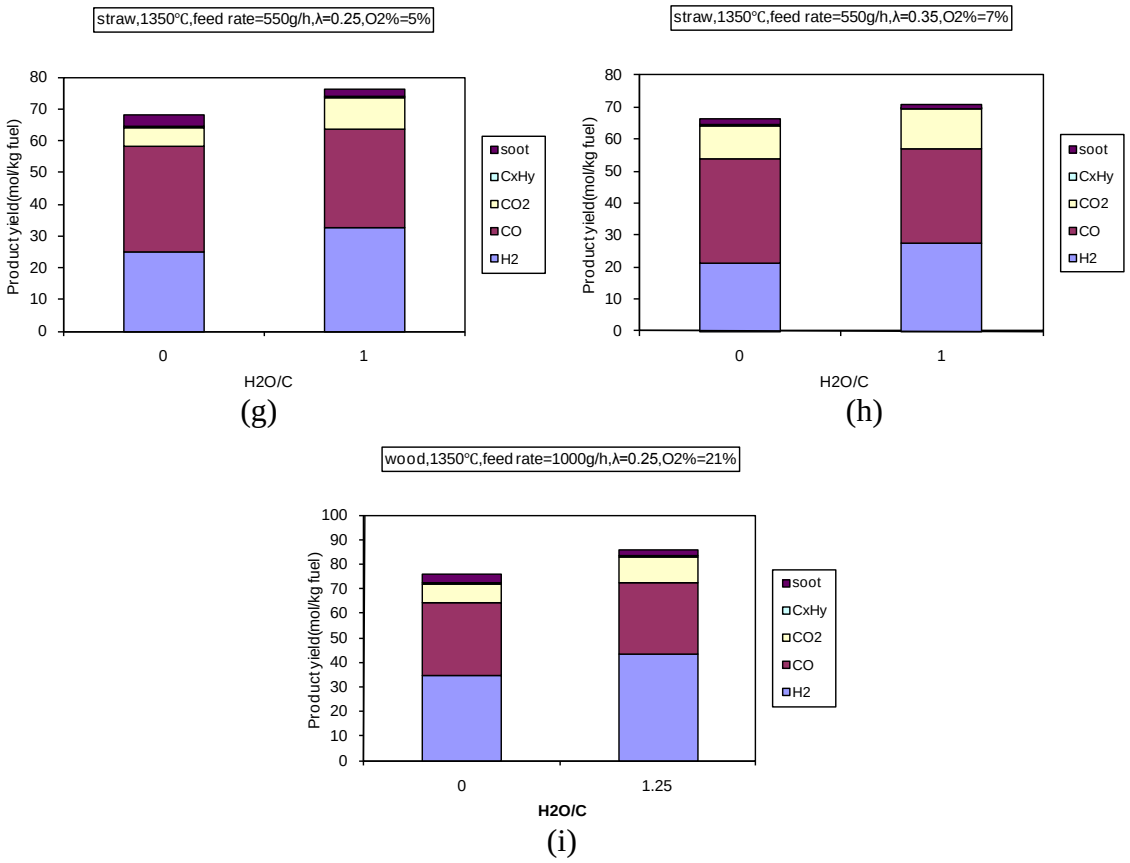

Figure 24 Effect of steam/carbon ratio on product distribution

4.4.5 Effect of fuel type on product yield and distribution

Products yields of wood and straw gasification are compared in Figure 25 and Figure 26. The results indicate that the two types of biomass have similar gasification behavior [16]. An important difference between wood and straw is the high alkali content in straw [9]. The alkali may have a catalytic influence on the gasification of char [10][11]. However, since the wood and straw experiments provided similar results, it can be conclude that the presence of a high amount of alkali metals do not change the gas composition significantly at entrained flow reactor gasification conditions. An influence of alkali on the char conversion rate could not be seen in the experiments since 100% char conversion was obtained in all the biomass experiments.

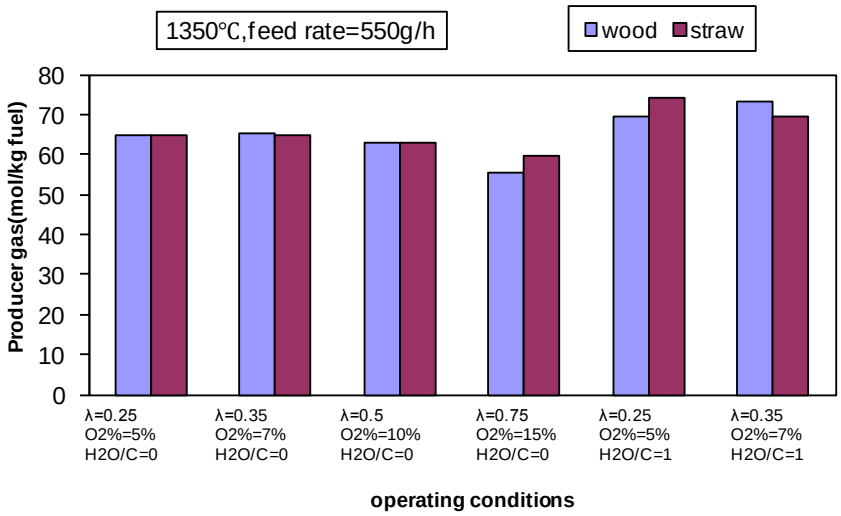
1350℃,feed rate=550g/h
wood
straw
Producer gas(mol/kg fuel)
80
70
60
50
40
30
20
10
0
λ=0.25 O2%=5% H2O/C=0
λ=0.35 O2%=7% H2O/C=0
λ=0.5 O2%=10% H2O/C=0
λ=0.75 O2%=15% H2O/C=0
λ=0.25 O2%=5% H2O/C=1
λ=0.35 O2%=7% H2O/C=1
operating conditions

(a)

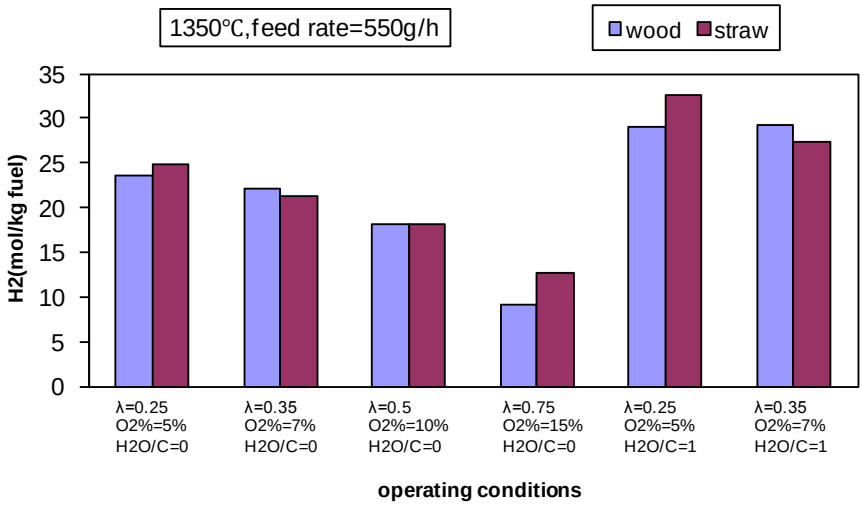
1350℃,feed rate=550g/h
wood
straw
H2(mol/kg fuel)
35
30
25
20
15
10
5
0
λ=0.25 O2%=5% H2O/C=0
λ=0.35 O2%=7% H2O/C=0
λ=0.5 O2%=10% H2O/C=0
λ=0.75 O2%=15% H2O/C=0
λ=0.25 O2%=5% H2O/C=1
λ=0.35 O2%=7% H2O/C=1
operating conditions

(b)

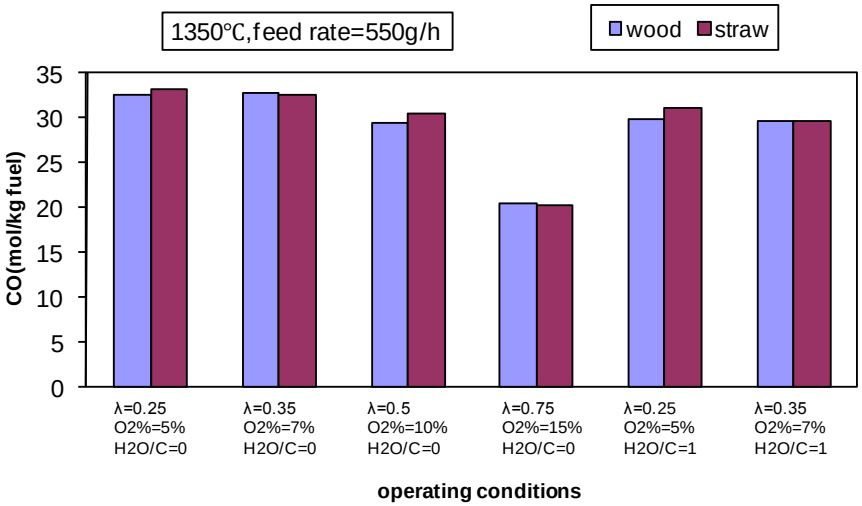
1350℃,feed rate=550g/h
wood
straw
CO(mol/kg fuel)
35
30
25
20
15
10
5
0
λ=0.25 O2%=5% H2O/C=0
λ=0.35 O2%=7% H2O/C=0
λ=0.5 O2%=10% H2O/C=0
λ=0.75 O2%=15% H2O/C=0
λ=0.25 O2%=5% H2O/C=1
λ=0.35 O2%=7% H2O/C=1
operating conditions

(c)

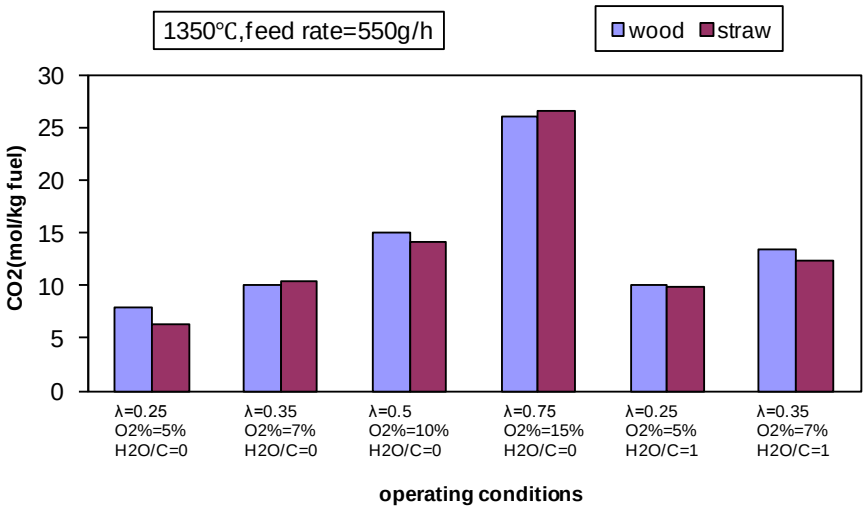
1350℃,feed rate=550g/h
wood
straw
CO2(mol/kg fuel)
30
25
20
15
10
5
0
λ=0.25 O2%=5% H2O/C=0
λ=0.35 O2%=7% H2O/C=0
λ=0.5 O2%=10% H2O/C=0
λ=0.75 O2%=15% H2O/C=0
λ=0.25 O2%=5% H2O/C=1
λ=0.35 O2%=7% H2O/C=1
operating conditions

(d)

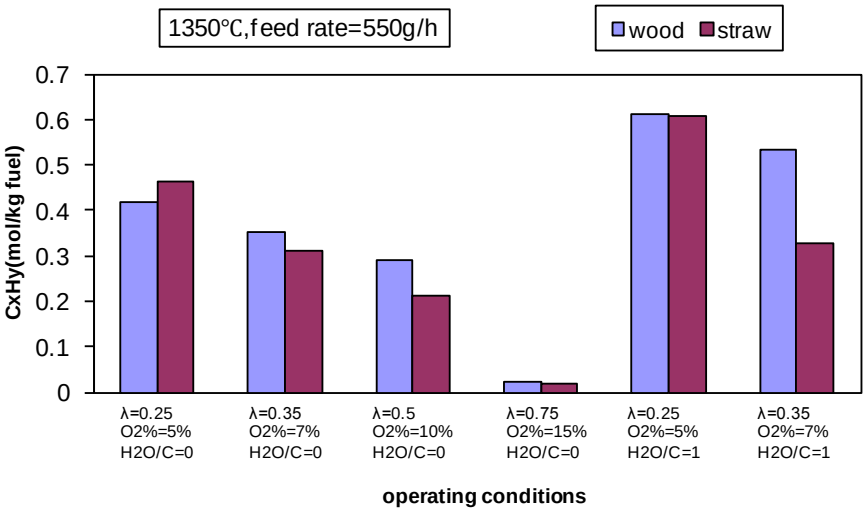
1350℃,feed rate=550g/h
wood
straw
CxHy(mol/kg fuel)
0.7
0.6
0.5
0.4
0.3
0.2
0.1
0
λ=0.25 O2%=5% H2O/C=0
λ=0.35 O2%=7% H2O/C=0
λ=0.5 O2%=10% H2O/C=0
λ=0.75 O2%=15% H2O/C=0
λ=0.25 O2%=5% H2O/C=1
λ=0.35 O2%=7% H2O/C=1
operating conditions

(e)

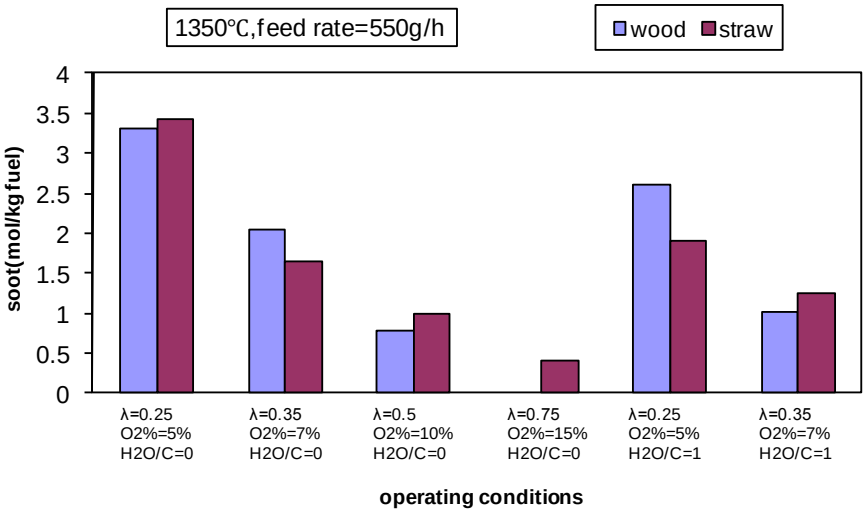
1350℃,feed rate=550g/h
wood
straw
soot(mol/kg fuel)
4
3.5
3
2.5
2
1.5
1
0.5
0
λ=0.25 O2%=5% H2O/C=0
λ=0.35 O2%=7% H2O/C=0
λ=0.5 O2%=10% H2O/C=0
λ=0.75 O2%=15% H2O/C=0
λ=0.25 O2%=5% H2O/C=1
λ=0.35 O2%=7% H2O/C=1
operating conditions

(f)

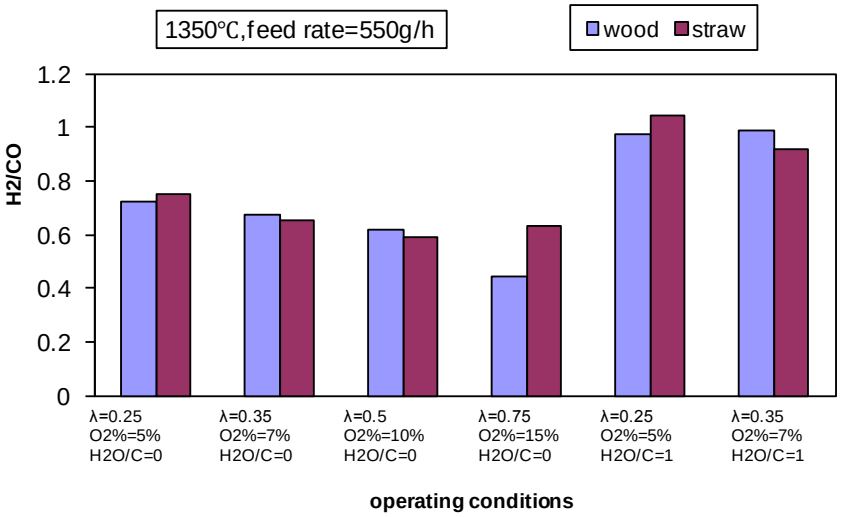

(g)

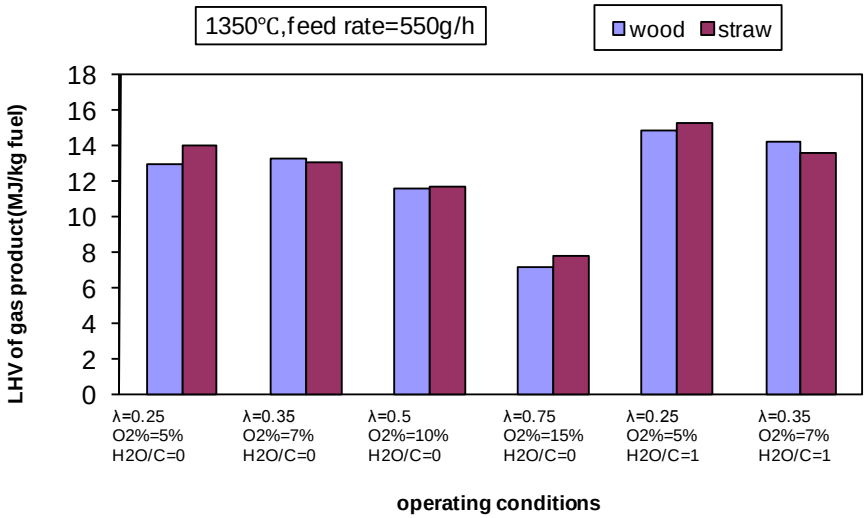

(h)

Figure 25 Effect of biomass type on product yield

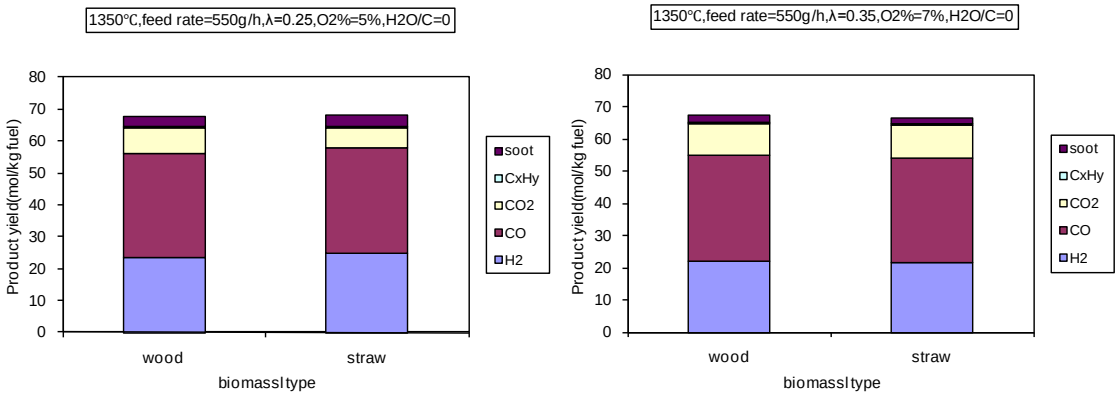

(a) (b)

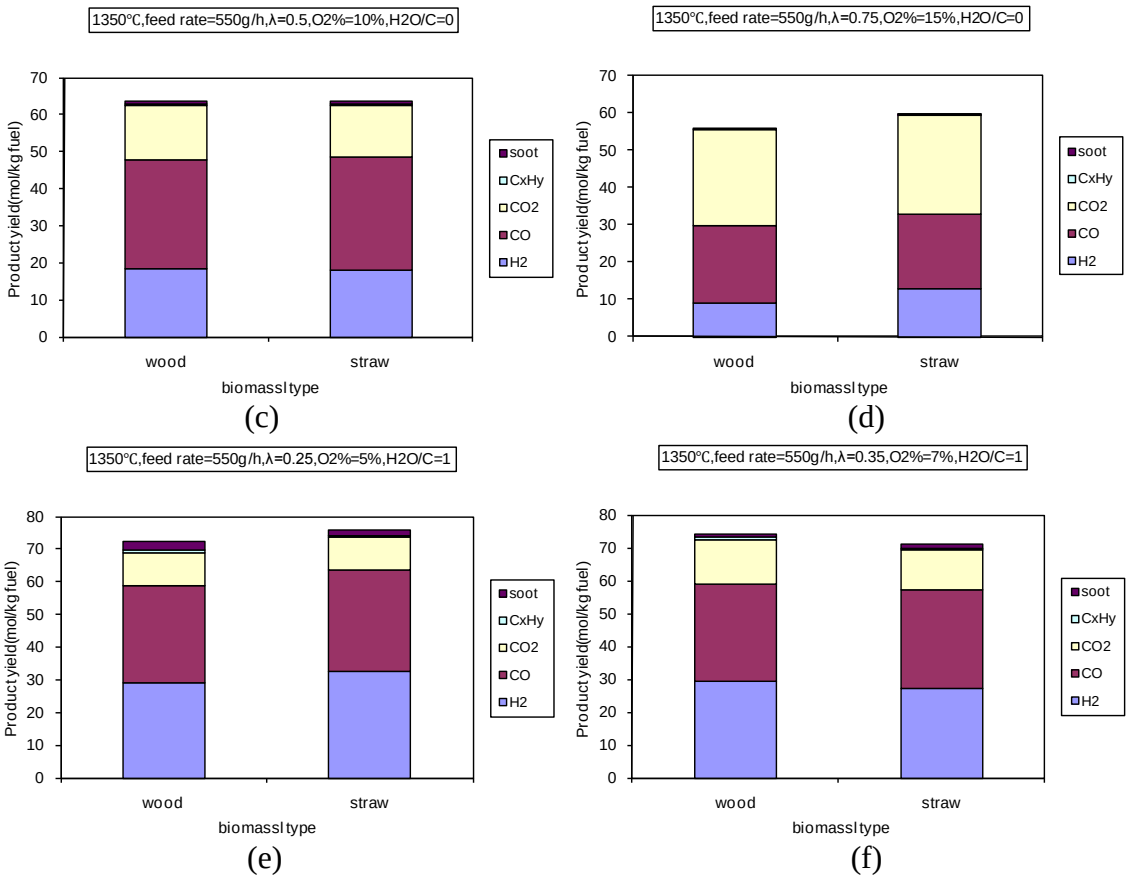

Figure 26 Effect of biomass type on product distribution

A comparison of the products yields of gasifying wood and coal are shown in Figure 27 and Figure 28. In the wood gasification experiment, the wood is completely converted and no char was collected in cyclone. However, in the coal gasification experiment, a significant amount of unconverted char or other solid products were collect in the cyclone. Based on the mass balance calculation 42% of the fuel carbon is not converted. For the same thermal power input, biomass produces more gaseous product and soot, while coal produces more char.

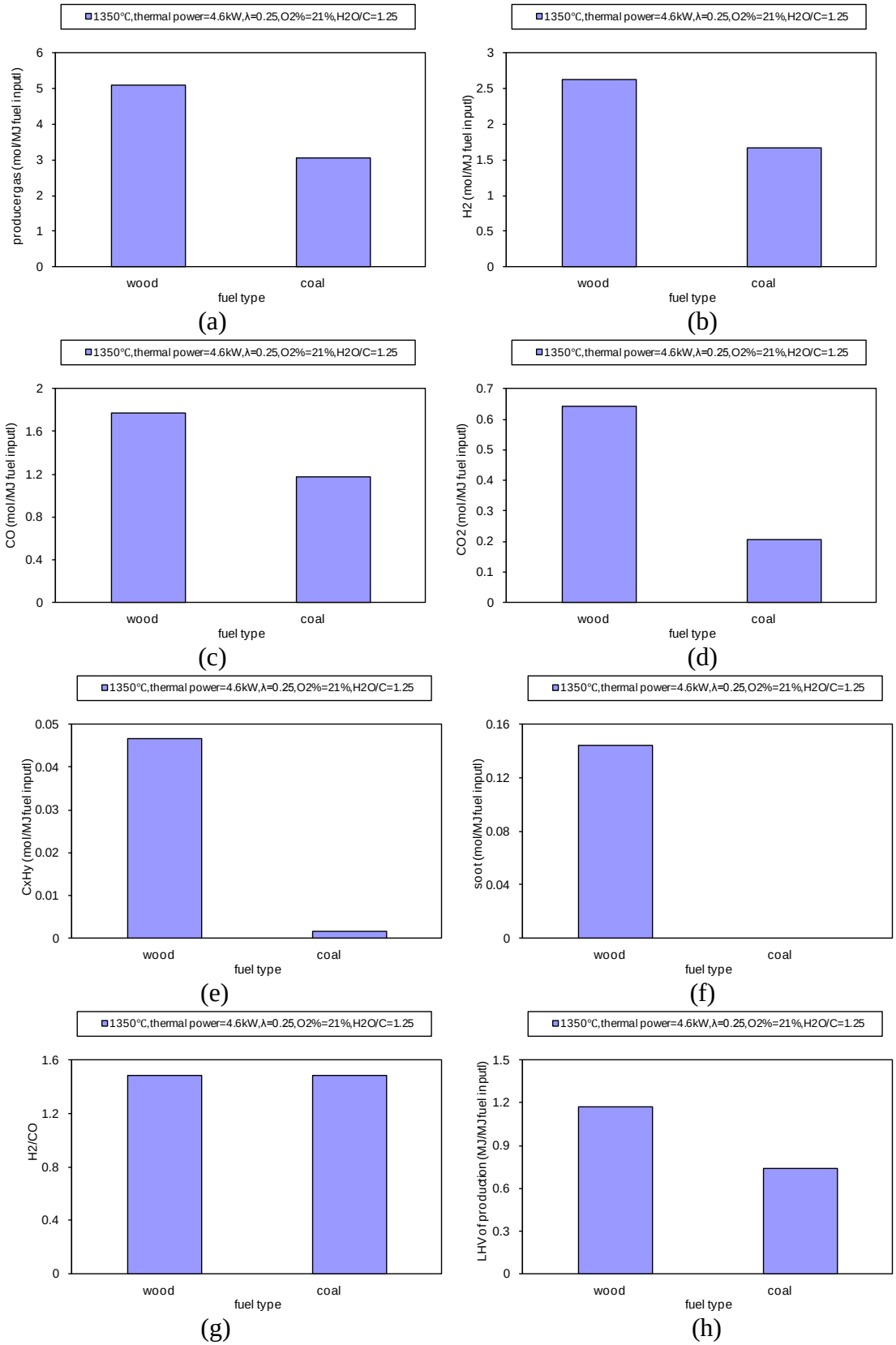

Figure 27 Effect of fuel type on product yield

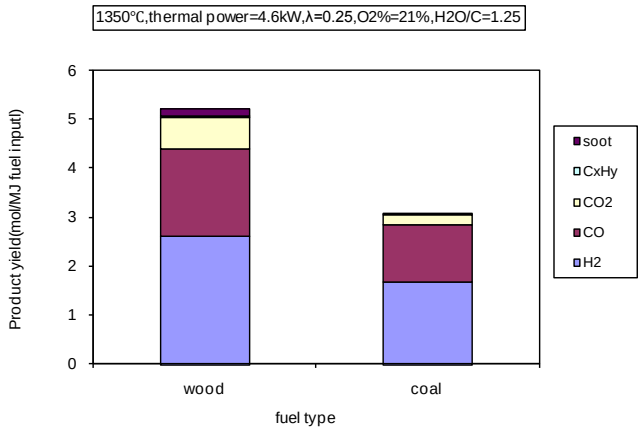

Figure 28 Effect of fuel type on product distribution

4.5 Comparison with thermodynamic equilibrium calculation

The gasification product distribution was predicted by equilibrium calculation using the same input data as in the experiments. All results of experiments and calculation are normalized to 100% and the products compositions are shown in Figure 29. From the figure, it is seen that at the operating conditions at 1350°C and steam addition, the experimental results are reasonably similar to the calculation results. In these cases, the chemical reactions in the experiments are nearly at equilibrium states. When steam is introduced, the reaction of steam with soot and hydrocarbons is faster than the reaction of CO_2 with soot and hydrocarbons [28]. Higher temperature and steam addition help to accelerate attainment of equilibrium.

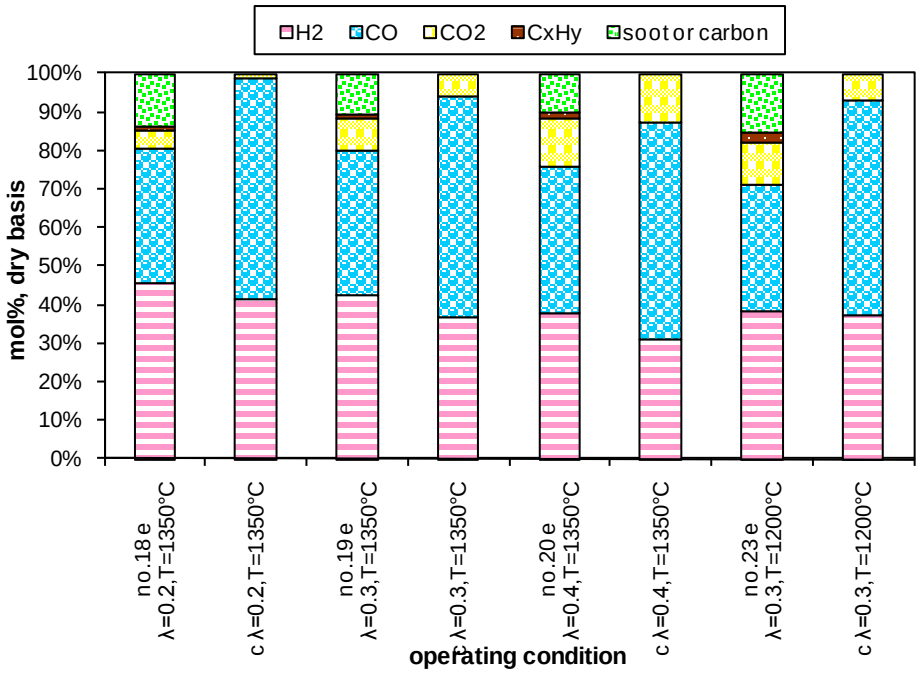

(a) Wood gasification without steam addition, T=1350°C and 1200°C, λ=0.2-0.4

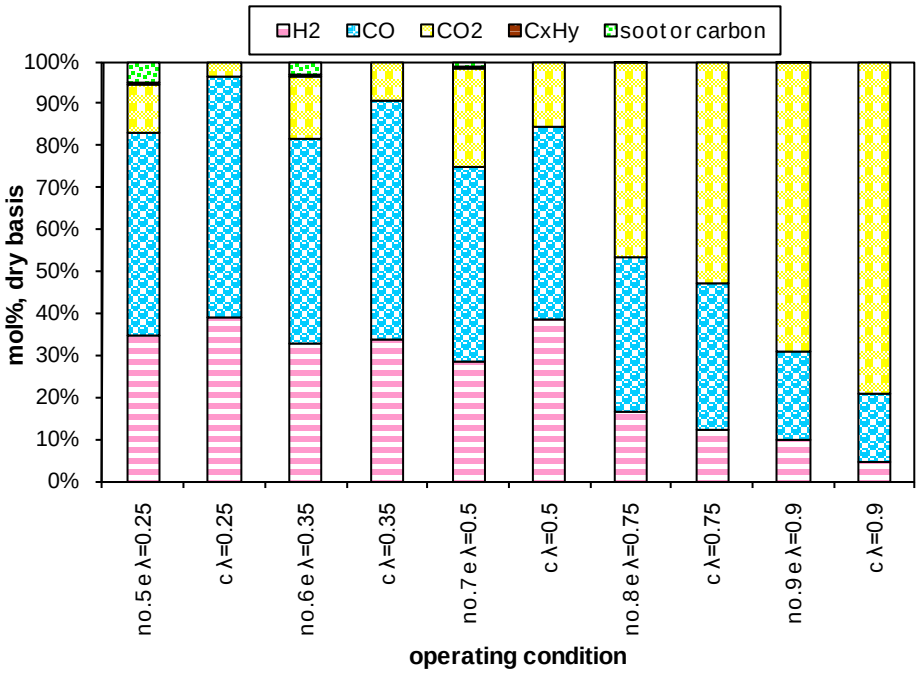

(b) Wood gasification at 1350°C without steam addition, λ=0.25-0.9

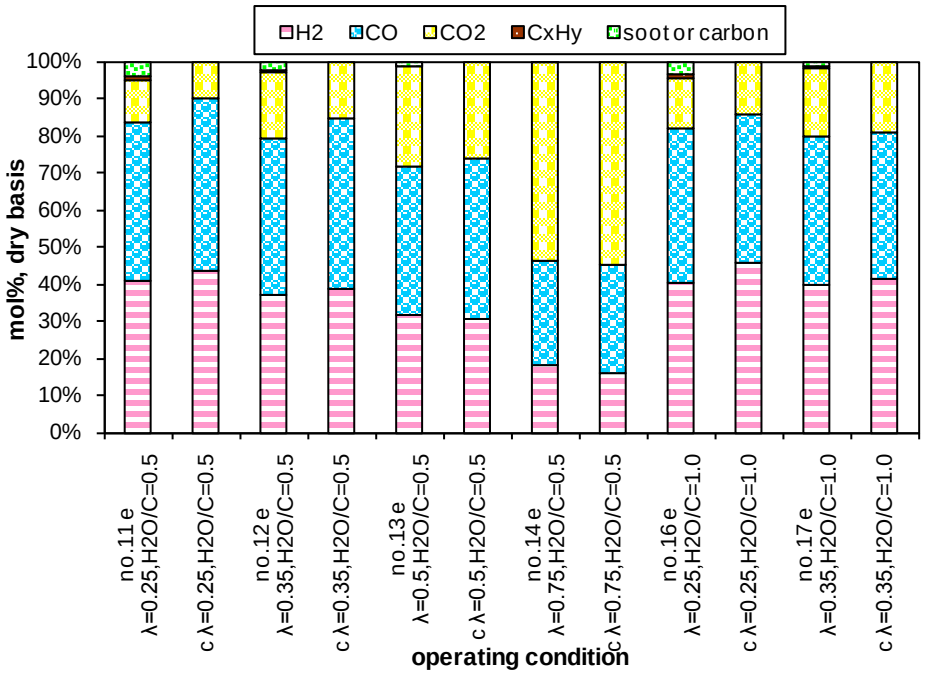

(c) Wood gasification at 1350°C with steam addition, H_2O/C=0.5-1.0, λ=0.25-0.75

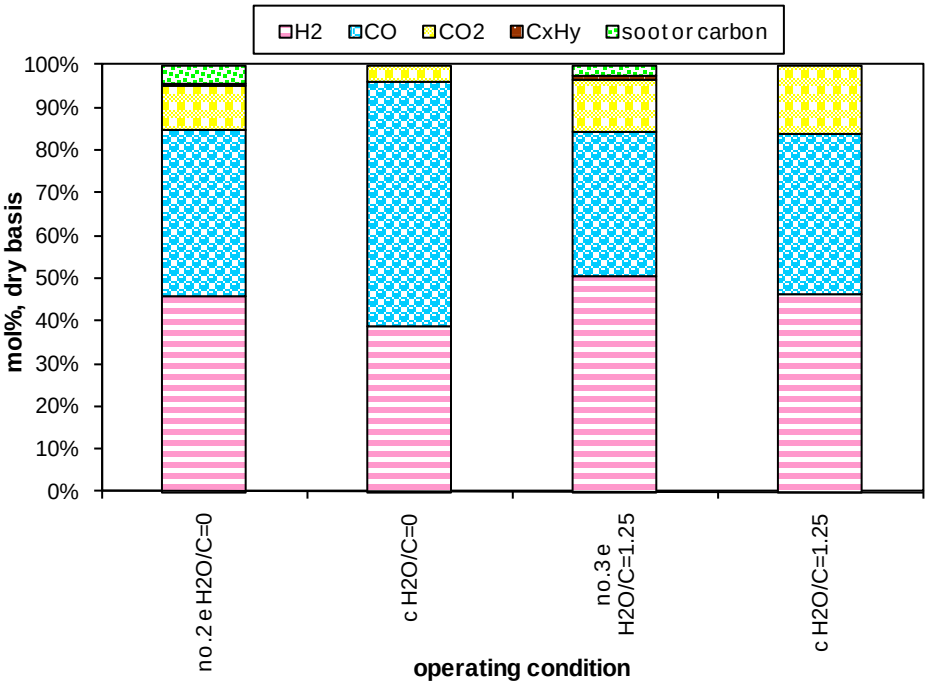

(d) Wood gasification at 1350°C and λ=0.25, H_2O/C=0-1.25

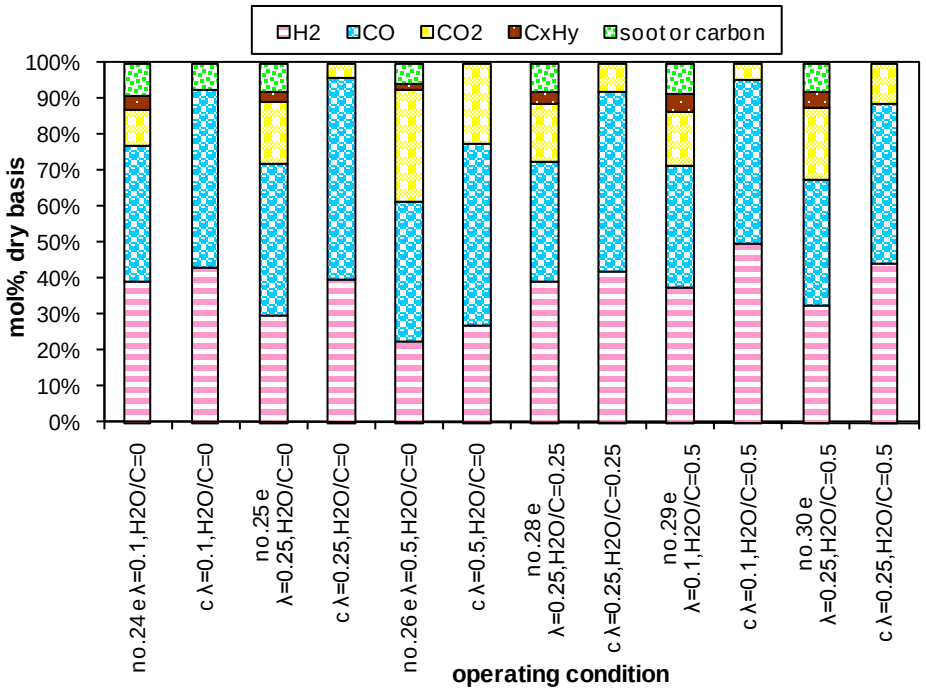

(e) Wood gasification at 1200°C, H_2O/C=0-0.5, λ=0.1-0.5

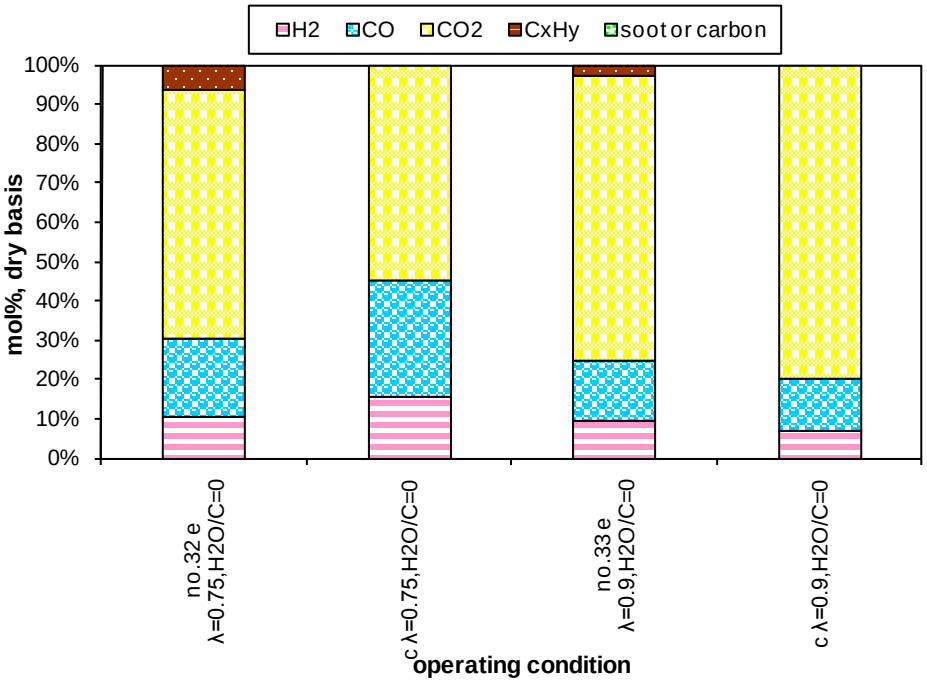

(f) Wood gasification at 1000°C without steam addition, λ =0.75 and 0.9

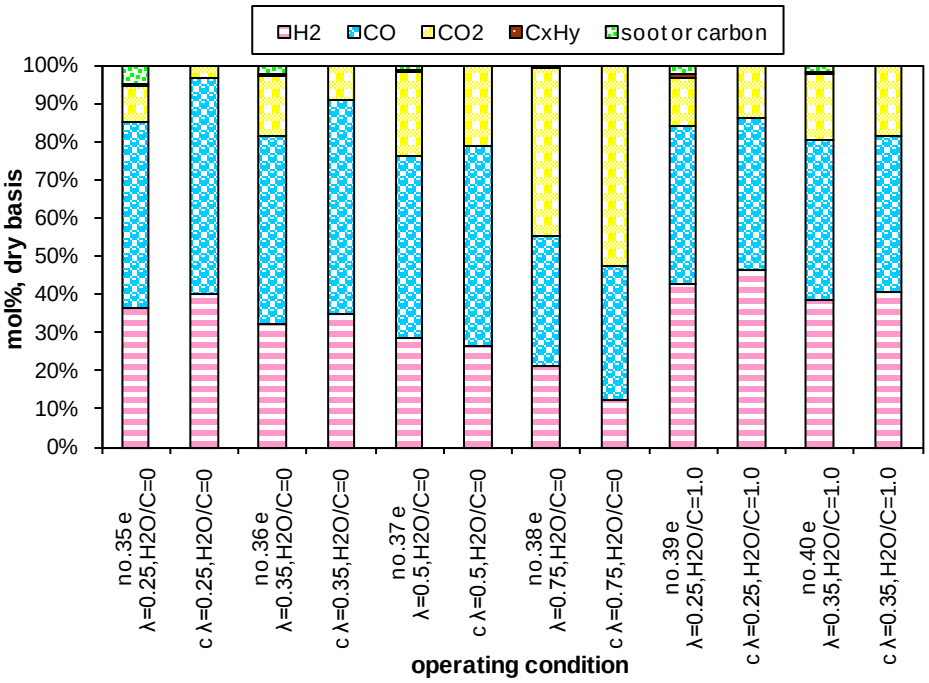

(g) Straw gasification at 1350°C, H_2O/C=0-1, λ =0.25-0.5

*e means the experiment results; c means the calculation results

Figure 29 Comparison of the product compositions from experiments and equilibrium calculations

4.6 Comparison with gas compositions from the Viking gasifier

Some of the results from the entrained flow reactor experiments (exp 2 and 23) are compared with gas compositions obtained on the two step fixed bed Viking gasifier [29] .The tests in the two gasifiers were performed without steam addition, and the product gas compositions are compared in Table 5. The fuel compositions of the applied wood fuels are shown in Table 5. The Viking gasifier wood fuel had higher water content. The yields of H_2 in the two gasifiers are similar. The CO yield of the entrained flow gasifier is higher than of the Viking gasifier, and the CO_2 yield is lower. The formation of CH_4 is strongly affected by the temperature. The CH_4 yield is lowest at 1350°C.

Table 5 The analysis of wood in two gasifiers (on an as delivered basis)

		Entrained flow gasifier	Viking gasifier
Carbon	wt. %	45.05	33.22
Hydrogen	wt. %	5.76	4.07
Oxygen (by diff.)	wt. %	39.41	29.83
Nitrogen	wt. %	0.13	0.27
Sulphur	wt. %	0.01	0.05
Ash	wt. %	0.61	0.62
Moisture	wt. %	9.04	32.20
LHV	MJ/kg	16.44	12.39

Table 6 Comparison with gas compositions

	Operating conditions			Gas compositions			
Gasifier	excess air ratio	temperature	inlet oxygen concentration	H_2	CO	CO_2	CH_4
Entrained flow gasifier	0.3	1200°C	21%	44.5%	38.9%	12.3%	3.5%
Entrained flow gasifier	0.25	1350°C	21%	47.9%	40.6%	10.6%	0.9%
Viking gasifier	0.25	800-1300°C	21%	45.7%	29.4%	23.1%	1.7%

5 Conclusion and summery

In this report entrained flow gasification of biomass is investigated by experiments and equilibrium calculations. Experiments with gasification of two types of biomass, wood and straw, were performed in a laboratory scale atmospheric pressure electrically heated entrained flow reactor. The feeding rate of fuel into the reactor was 550 – 1000 g/h, and the gasification process took place in a two meter long ceramic tube with an inner diameter of 8 cm. It was the objective to quantify the influence of reactor operation conditions on the products composition of gas, tar, char and soot.

The applied operation range included reactor temperatures of 1000 to 1350°C, oxygen inlet concentrations of 2 to 34 vol% O_2, steam carbon molar ratios of 0 – 1,25 H_2O/C (steam inlet to fuel carbon molar ratio), and excess air ratios of λ = 0.2-0.9. The obtained reactor residence time was from 2.1 to 4.7 seconds. In all biomass experiments, the fuel was completely converted and no char was found in the reactor outlet products. At reactor temperatures of 1200°C and 1350°C, all carbon mass balance closures were reasonable, typically within ±9%. At 1000°C the carbon mass balance has a large deviation (22 wt %) probably due to a high content of unmeasured tar and larger hydrocarbons in the product gas. Increasing the reactor temperature from 1000 to 1350°C at otherwise maintained operation conditions led to increased yields of product gas (defined as the sum of H_2, CO, CO_2 and C_xH_y (hydrocarbons up to C_3 species)), H_2 and CO; and a decreased yield of CO_2 and C_xH_y. At 1350°C, a significant yield of soot was produced, while there was nearly no tar formation. Conversely, at 1000°C, the soot yield was lowest, whereas the amount of tar was highest. Thus, there is a tradeoff between soot and tar formation.

The influence of changes in oxygen to fuel ratio was investigated. An increased oxygen to fuel ratio (λ = 0.2-0.9) was obtained by increasing the gas inlet oxygen content from 3 to 17 vol%. The increased oxygen to fuel ratio lead to decreased outlet contents of H_2, CO, C_xH_y and soot, while the CO_2 content increased and the gas heating value decreased. The increased amount of oxygen simply caused an oxidation of the H_2, CO, C_xH_y and soot.

The influence of increased oxygen inlet concentration with otherwise maintained operation conditions at an excess air ratio of λ=0.25, a reactor temperature of 1350°C and no steam injection were investigated. The increased oxygen concentration was obtained by decreasing the N_2 flow to the reactor and this leads to an increased reactor residence time, and probably an increased temperature in the top of the reactor. The soot formation increased from 3 mol/kg fuel at an inlet oxygen concentration of 5 vol% up to 11 mol/kg fuel at an inlet oxygen concentration of 34 vol%. The reason for the large soot formation at high oxygen inlet concentrations is presently not known.

Increased steam injection and thereby increased reactor H_2O/C ratio pushed the water shift reaction towards an increased formation of H_2 and CO_2. However, even a high amount of water injection (H_2O/C ratio changed from 0 to 1) typically caused a H_2 dry gas content increase of only 20%. A moderate reduction of the soot formation was observed with steam injection.

A comparison of product gas composition when using wood and straw fuel showed similar results. This indicates that the high straw fuel alkali content do not significantly influences the gasification process.

Generally some soot was produced in all experiments conducted at 1200 and 1350°C using low λ values. A minimum amount of soot of 2 mol/kg fuel at λ = 0.25 were observed at the operation conditions 1350°C, inlet O_2= 5 vol% and a steam injection level of H_2O/C = 1.0. STA (simultaneous Thermal Analysis) tests showed that the combustion reactivity of soot from straw gasification is higher than that of soot from wood gasification.

Thermodynamic equilibrium calculations were performed by using the Factsage software. The equilibrium calculations were performed using conditions that correspond to entrained flow gasification of wood. Effects of temperature (800-1600°C), steam/carbon molar ratio (0 – 2.0 mol steam added relative to fuel C mol input), excess air ratio (λ = 0.0-1.0), and pressure (1 – 100 Bar) were investigated. As a standard condition were used a temperature of 1350°C, a steam/carbon molar ratio of 0, an excess air ratio λ =

0.25 and pressure of 1 Bar. Using a λ value of 0.2 to 0.25 lead to a maximum CO yield, while using a value of λ bellow 0.2 formation of carbon was predicted. Changes of temperature above 800°C only induced small changes in the gas composition. By increased water injection an increased level of H_2 and CO_2 and a decreased level of CO were observed. Increasing the pressure from 1 to 100 Bar only changed the gas composition slightly; a small amount of methane was predicted to be formed. The gasification product distributions obtained by the experiments and equilibrium calculations were compared. It was observed that at 1350 and 1200°C with no steam addition the experiments gave rise to some soot and hydrocarbon formation that was not predicted by the equilibrium calculations. At 1350 with steam addition smaller amounts of hydrocarbon and soot was formed, and generally the equilibrium calculations provided reasonable predictions of the gas H_2, CO and CO_2 contents.

Appendix A Calibration method for new micro GC

Nine calibrating gas were used to calibrate the new micro GC. The nine calibrating gas are shown in Table 7. Multiple level calibrations are employed. The calibration curves for concerned gas are shown in Figure 30.

Table 7 Calibrating gas

NO.	O_2	N_2	CH_4	CO	CO_2	C_2H_4	C_2H_2	C_3H_8	H_2
1	9.5	67		4.5	19				
2	4.5	94.739		0.38	0.381				
3		90.05							9.95
4		10	35						55
5		49.9001		50				0.0999	
6		99.7247		0.0498	0.0205	0.102	0.103		
7		95	5						
8		98	2						
9		99.001	0.999						

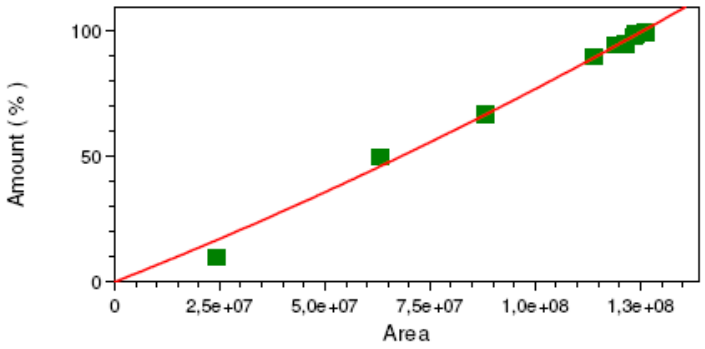

Fit Type: Quadratic

$y = 1{,}06986e\text{-}15x^2 + 6{,}63140e\text{-}7x$

Goodness of fit (r^2): 0.991750

(a) N_2

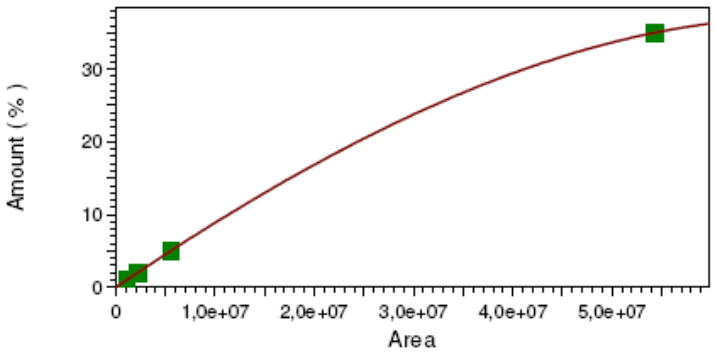

Fit Type: Cubic

$y = -3{,}02292e\text{-}23x^3 - 3{,}52182e\text{-}15x^2 + 9{,}25013e\text{-}7x$

Goodness of fit (r^2): 1.00000

(b) CH_4

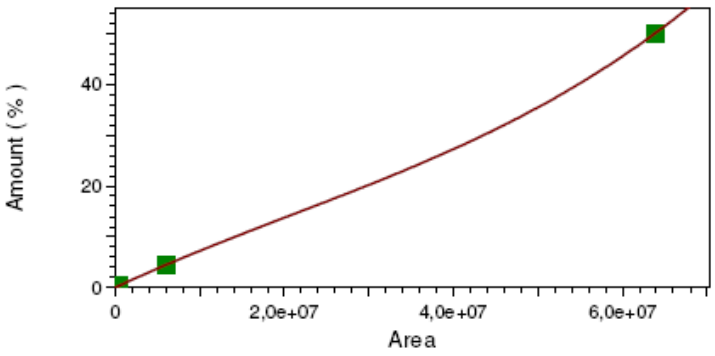

Fit Type: Cubic

$y = 1{,}05392e\text{-}22x^3 - 6{,}64162e\text{-}15x^2 + 7{,}77525e\text{-}7x$

Goodness of fit (r^2): 1.00000

(c) CO

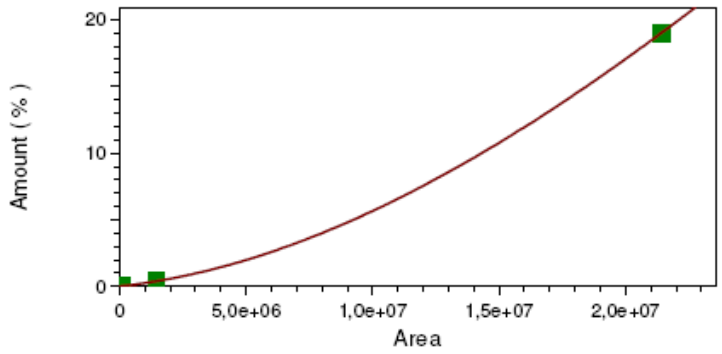

Fit Type: Cubic

$y = -3{,}51117e\text{-}22x^3 + 3{,}92178e\text{-}14x^2 + 2{,}08811e\text{-}7x$

Goodness of fit (r^2): 1.00000

(d) CO_2

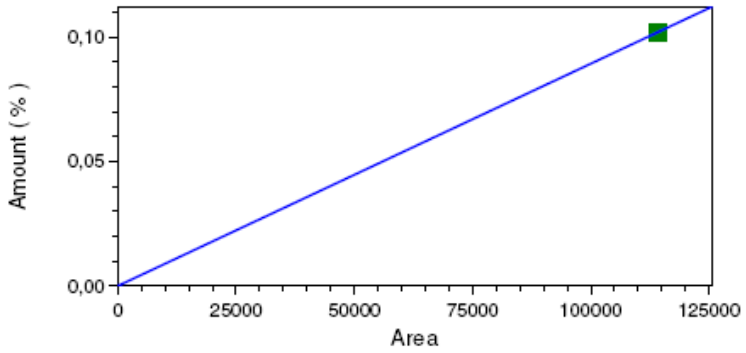

Fit Type: Linear

$y = 8{,}93866e\text{-}7x$

Goodness of fit (r^2): 1.00000

(e) C_2H_4

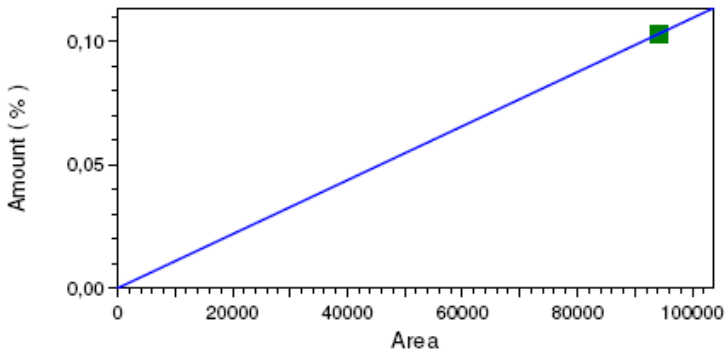

Fit Type: Linear

y = 1,09407e-6x

Goodness of fit (r^2): 1.00000

(f) C_2H_2

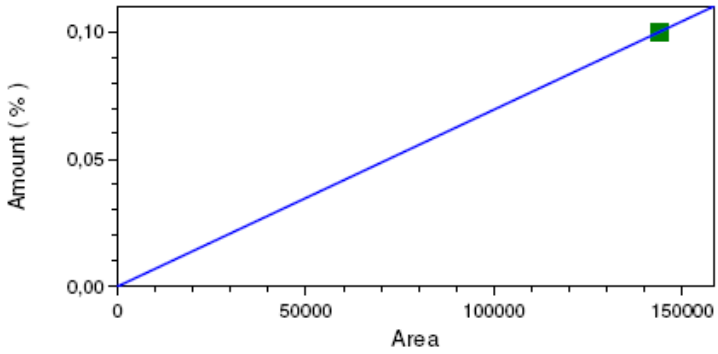

Fit Type: Linear

y = 6,94531e-7x

Goodness of fit (r^2): 1.00000

(g) C_3H_8

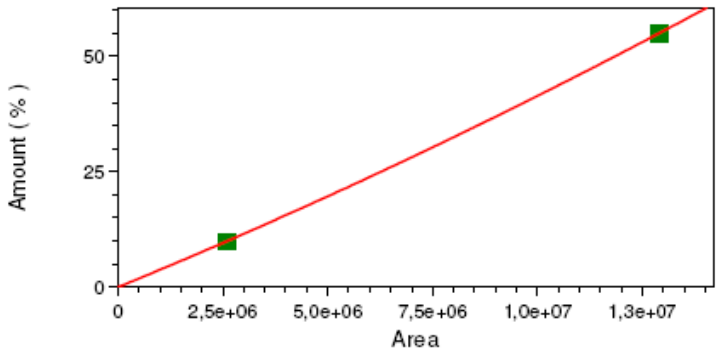

Fit Type: Quadratic

$y = 4{,}17422e\text{-}14x^2 + 3{,}72688e\text{-}6x$

Goodness of fit (r^2): 1.00000

(i) H_2

Figure 30 Calibration curves for concerned gas

Appendix B Calculation method for flow rate of flue gas components

The percent and yield of each gas component in flue gas can be calculated. Figure 31 depicts the gas channel in reactor. The calculation method describes as follows. The values of $C_{measureN2}$, $C_{measureO2}$ and $C_{measure\_components}$ can be measured by GC and flue gas analyzer. To solve below equations, the other unknown quantities can be determined.

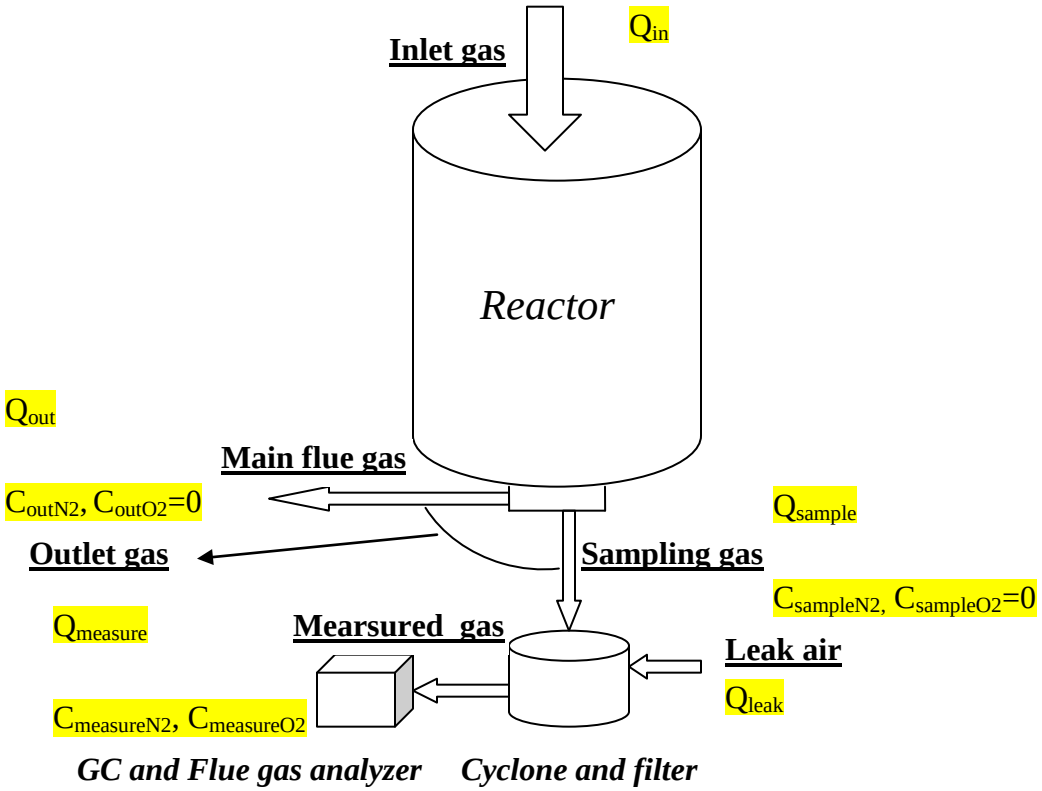

Figure 31 Gas channel in reactor

Equations:

$$Q_{leak} \times 21\% = Q_{measure} \times C_{measureO2} \quad (1)$$

$$Q_{sample} + Q_{leak} = Q_{measure} \quad (2)$$

$$Q_{sample} \times C_{sampleN2} + Q_{leak} \times 79\% = Q_{measure} \times C_{measureN2} \quad (3)$$

$$Q_{in} \times C_{inN2} = Q_{out} \times C_{outN2} \quad (4)$$

$$Q_{sample} \times C_{sample\_components} = Q_{measure} \times C_{measure\_components} \quad (5)$$

$$C_{outN2} = C_{sampleN2} \quad (6)$$

$$C_{outO2} = C_{sampleO2} = 0 \quad (7)$$

$$C_{out\_components} = C_{sample\_components} \quad (8)$$

Appendix C Calculation method for the concentration of solid samples in flue gas

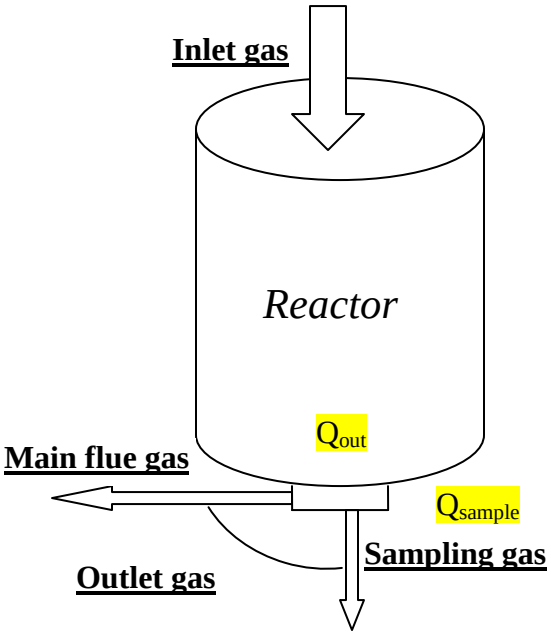

According to the principle of isokinetic sampling, the diameter of the tube of sampling gas is half that of the reactor, so extraction flow of sampling gas should be equal to ¼ of the outlet flow. But in real experiments, it is difficult to ensure isokinetic sampling. The solid sampling time is 20 minutes. The concentration of solid samples in flue gas can be calculated by the equation below.

$$C_{solid} = \frac{m_{solid}}{20} \times \frac{Q_{out}}{Q_{sample}} \tag{9}$$

References

[1] World Energy Outlook 2004

[2] Chum HL, Overend RP. Biomass and renewable fuels. Fuel Processing Technology 71(2001): 187-195

[3] Joshi MM, Lee S. Integrated gasification combined cycle - a review of IGCC technology. Energy Sources 18(1996): 537-568

[4] Stiegel GJ, Maxwell RC. Gasification technologies: the path to clean, affordable energy in the 21st century. Fuel Processing Technology 71(2001): 79-97

[5] Higman C, van der Burgt M. Gasification. America, 2003

[6] Hamelinck CN, Faaij APC, den Uil H, Boerrigter H. Production of FT transportation fuels from biomass; technical options, process analysis and optimisation, and development potential. Energy 29(2004): 1743-1771

[7] Shen J, Schmetz E, Kawalkin GJ. Commercial deployment of Fischer-Tropsch synthesis: the coproduction option. Topics in Catalysis 26(2003): 13-20

[8] Zwart RWR, Boerrigter H. High efficiency co-production of synthetic natural gas (SNG) and Fischer-Tropsch (FT) transportation fuels from biomass. Energy & Fuels 19(2005): 591-597

[9] Capablo J, Jensen PA, Pedersen KH, Hjuler K, Nikolaisen L, Backman R, Frandsen F. Ash properties of alternative biomass. Energy & Fuels 23(2009): 1965-1976

[10] Pang KL, Xiang WG, Liang C, Zhao CS, Xi B, Liu DJ. Gasification reaction of coal char with CO_2 under the catalytic Action of alkali metals. Journal of power engineering 26(2006): 141-144

[11] Wei XF, Huang JJ, Fang YT, Wang Y. Effect of alkali metal on the lignite gasification reactivity. Coal conversion 30(2007): 38-42

[12] Schilling H, Bonn B, Krauss U. Coal gasification: Existing process and new developments. London, 1981

[13] Wang ZH, Zhou JH, Wang QH, Fan JR, Cen KF. Thermodynamic equilibrium analysis of hydrogen production by coal based on Coal/CaO/H2Ogasification system. International Journal of Hydrogen Energy 31 (2006): 945 – 952

[14] Guan J, Wang QH, Li XM, Luo ZY, Cen KF. Thermodynamic analysis of a biomass anaerobic gasification process for hydrogen production with sufficient CaO. Renewable Energy 32 (2007): 2502–2515

[15] Crnomarkovic N, Repic B, Mladenovic R, Neskovic O, Veljkovic M. Experimental investigation of role of steam in entrained flow coal gasification. Fuel 86(2007):194-202

[16] Lapuerta M, Hernandez JJ, Pazo A. Gasification and co-gasification of biomass wastes: effect of the biomass origin and the gasifier operating conditions. Fuel processing technology 89(2008): 828-837

[17] Kim YJ, Lee JM, Kim SD. Coal gasification characteristics in an internally circulating fluidized bed with draught tube. Fuel 76(1997): 1067-1073

[18] Lee JG, Kim JH, Lee HJ, Park TJ, Kim SD. Characteristics of entrained flow coal gasification in a drop tube reactor. Fuel 75(1996): 1035-1042

[19] Na JI, Park SJ, Kim YK, Lee JG, Kim JH. Characteristics of oxygen-blown gasification for combustible waste in a fixed-bed gasifier. Applied energy 75(2003): 275-285

[20] Gil J, Corella J, Aznar PA, Caballero AM. Biomass gasification in atmosphere and bubbling fluidized bed: effect of the type of gasifying agent on the product distribution. Biomass and bioenergy 17(1999): 389-403

[21] Indarto A. Soot growing mechanism from polyynes: a review. Environmental engineering science 26(2009): 1-7

[22] Choi JH, Fujita O, Tsuiki T, Kim J, Chung SH. A study of the effect of oxygen concentration on the soot deposition process in a diffusion flame along a solid wall by in-situ observations in microgravity. JSME International journal 48(2005): 839-848

[23] Xie YR, Shen LH, Xiao J. Experimental research in biomass gasification and reforming to produce hydrogen-rich gas. Journal of xi'an jiaotong university 42(2008): 634-638

[24] Kriengsak SN, Buczynski R, Gmurczyk J, Gupta AK. Hydrogen production by high-temperature steam gasification of biomass and coal. Environmental engineering science 26(2009): 739-744

[25] Lucas C, Szewczyk D, Blasiak W. High-temperature air and steam gasification of densified biofuels. Biomass and bioenergy 27(2004): 563-575

[26] Wei LG, Xu SP, Zhang L, Liu CH, Zhu H, Liu SQ. Steam gasification of biomass for hydrogen-rich gas in a free-fall reactor. International journal of hydrogen energy 32(2007): 24-31

[27] Gil J, Corella J, Aznar PA, Caballero AM. Biomass gasification in atmosphere and bubbling fluidized bed: effect of the type of gasifying agent on the product distribution. Biomass and bioenergy 17(1999): 389-403

[28] Klose W, Wolki M. On the intrinsic reaction rate of biomass char gasification with carbon dioxide and steam. Fuel 84(2005): 885-892

[29] Ahrenfeldt J, Henriksen U, Jensen TK, Gøbel B, Wiese L, Kather A, Egsgaard H. Validation of continuous combined heat and power (CHP) operation of a two-stage biomass gasifier. Energy & Fuels 20(2006): 2672-2680

[30] Hindsgaul G, Schramm J, Gratz L, Henriksen U, Bentzen JD. Physical and chemical characterization of particles in producer gas from wood chips. Bioresource technology 73(2000): 147-155

Appendix F. Influence of operating conditions on gas composition, soot and tar in entrained flow gasification of biomass

Conference paper

Ke Qin, Weigang Lin, Peter Arendt Jensen, Anker Degn Jensen, Helge Egsgaard. Conference paper: Influence of operating conditions on gas composition, soot and tar in entrained flow gasification of biomass. International Conference on Polygeneration strategies, Vienna, September 2009.

2010, DTU no. 50442

Final report - EFP06 – Produktion af methanol/DME ud fra biomasse

Conference paper: Influence of operating conditions on gas composition, soot and tar in entrained flow gasification of biomass. International Conference on Polygeneration strategies, Vienna, September 2009

Ke Qin*, Weigang Lin*, Peter Arendt Jensen*, Anker Degn Jensen*, Helge Egsgaard**

*) Department of Chemical and Biochemical Engineering
Technical University of Denmark
Søltofts Plads, Building 229, DK-2800 Lyngby, Denmark
**Biosystems Department, Risø National Laboratory, Technical University of Denmark, Roskilde, 4000, Denmark

Influence of operating conditions on gas composition, soot and tar in entrained flow gasification of biomass

Ke Qin*, Weigang Lin*, Peter A. Jensen*, Anker D. Jensen*, Helge Egsgaard**

*Department of Chemical and Biochemical Engineering, Technical University of Denmark, Lyngby, 2800, Denmark
**Biosystems Department, Risø National Laboratory, Technical University of Denmark, Roskilde, 4000, Denmark
Email: Wl@kt.dtu.dk

ABSTRACT

In this work, biomass (wood and straw) gasification has been studied in a laboratory scale atmospheric pressure entrained flow reactor, with a focus on the influence of the operating conditions on the gas composition, soot and tar in the syngas. The results show that the amount of producer gas (H_2, CO, CO_2 and hydrocarbon up to C_3 species) increases significantly, from 42.4mol/kg fuel to 68.3mol/kg fuel, with temperature increases in the range of 1000-1350°C, due to the conversion of tar and larger hydrocarbons into lighter gaseous products. With addition of steam, the yield of hydrogen increases at the expense of carbon monoxide. It was found that at an excess air coefficient of 0.25 and a steam/carbon ratio of 0.5, the tar content in the syngas is very low (between 0.27mg/kg fuel and 0.40mg/kg fuel) at 1350°C, while it is relatively high (26.23 mg/kg fuel) at 1000°C. In contrast, the soot content is much higher (35.26g/kg fuel) at 1350°C and has a peak value (58.67g/kg fuel) at 1200°C, whereas it is low (8.49g/kg fuel) at 1000°C. This shows that there is a trade off between tar and soot formation. The soot yield can be reduced by addition of steam, but could not be completely eliminated in the present experiments which were limited to a maximum temperature of 1350°C and a maximum residence time of approximate 2s. Moreover, it appears that wood and straw provide similar compositions of the syngas.

Key words: biomass gasification; entrained flow; soot; tar

INTRODUCTION

Among the renewable energy sources, biomass has a high potential [1], and biomass resources are a major component of strategies to mitigate global climate change. Plant growth "recycles" CO_2 from the atmosphere, and the use of biomass resources for energy and chemicals results in low net emissions of carbon dioxide. There is a world-wide interest in the use of biomass resources as feedstocks for producing power, fuels and chemicals [2]. Gasification is one of the key technologies for utilization of biomass, especially in the field of integrated gasification combined cycle (IGCC) and production of liquid fuels and chemicals [3][4]. Of several gasification methods, the entrained flow gasifier has the advantage to produce a gas with low tar content and possibility to run at high pressure [5].

Although gasification of coal in entrained flow gasifiers have been studied extensively [6]-[11], systematic studies on gasification of biomass in entrained flow gasifiers are scarce. In addition the fundamental processes taking place during biomass gasification at temperatures relevant to entrained flow gasifiers are not fully understood. The production of synthetic liquid fuels for transportation from biomass has a large relevance for the near future [12]. In production of liquid fuels, it is important to control the syngas quality from gasification with respect to both the H_2/CO ratio and harmful impurities [13][14], such as tar.

In this work, gasification of biomass will be investigated under entrained flow reactor conditions with respect to main syngas composition (H_2/CO/CO_2/hydrocarbon), soot and tar as a function of operating conditions, such as temperature (T), excess air coefficient (λ), steam/carbon ratio (H_2O/C) and biomass type.

EXPERIMENTAL

Apparatus

The atmospheric pressure entrained flow reactor used for the gasification experiments is shown schematically in Figure 1. It has an inner diameter of 0.08 meter and a length of 2 meters. The reactor is externally heated by seven independent electric heating elements, which can be heated to a maximum temperature of 1500°C. A reasonably uniform temperature in the reactor can be

realized, and so the influence of temperature and excess air coefficient on the composition of the syngas can be studied independently. Besides the reactor, the complete facility includes equipment for fuel particle feeding, gas supply, solid particle sampling, gas sampling and analysis, liquid sampling, and flue gas treatment. The external height of the facility is 7 meters.

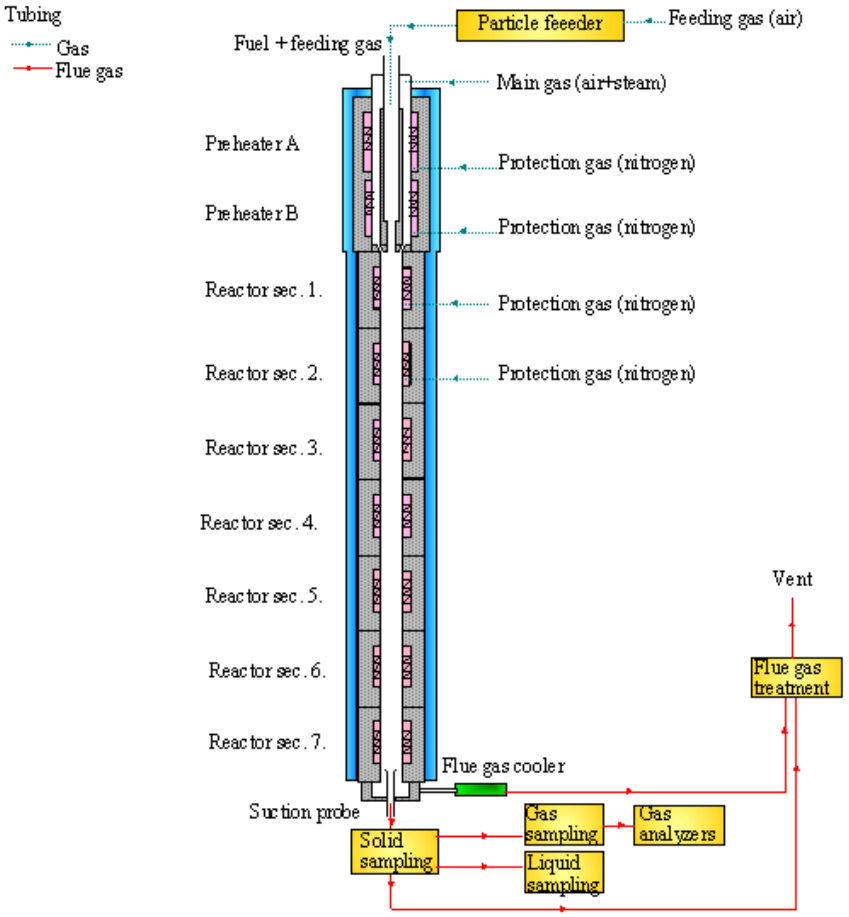

Figure 1 Sketch of experimental setup

Biomass fuels and applied operating condition

Table 1 Proximate and ultimate analysis of biomass (on a delivered basis)

		Wood (Beech saw dust)	Straw (Pulverized wheat straw pellet)
Proximate analysis			
Moisture	wt. %	9.04	8.65
Ash	wt. %	0.61	4.76
Volatile	wt. %	76.70	69.87
Fixed carbon (by diff.)	wt. %	13.65	16.72
Lower Caloric Value	MJ/kg	16.44	15.76
Ultimate analysis			
Carbon	wt. %	45.05	42.88
Hydrogen	wt. %	5.76	5.65
Oxygen (by diff.)	wt. %	39.41	37.51
Nitrogen	wt. %	0.13	0.49
Sulphur	wt. %	0.01	0.06

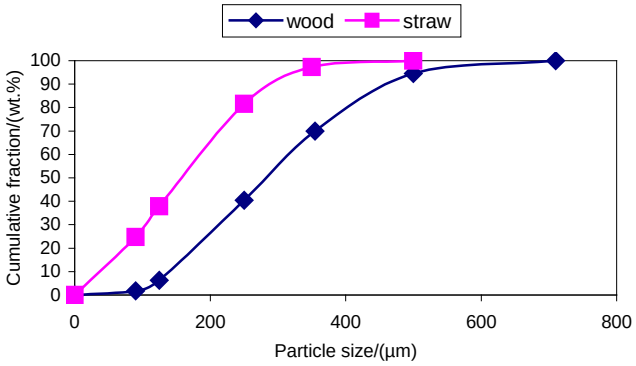

Figure 2 Particle size distributions of wood and straw

Two types of biomass are used in the experiments: wood (beech saw dust) and straw (pulverized wheat straw pellet). The analyses of them are listed in Table 1. It is shown that the compositions of wood and straw are quite similar except for the ash content. Comparing with coal, the content of volatile is higher, the content of fixed carbon and the heating value are lower in biomass. Straw has a high alkali content [15] which may have a catalytic influence on the gasification processes [16][17]. The particle size distribution of the two fuels is shown in Figure 2.

Experiments were conducted in the entrained flow reactor with temperature in the range of 1000-1350°C, excess air coefficient from 0.25 to 0.5, steam/carbon ratio from 0.0 to 1.0, and a fuel input of 0.55kg/h and the residence time in the reactor was 1-2s. The reactor inlet gas consisted of a mix of nitrogen and oxygen.

RESULTS AND DISCUSSION

The solid fuels injected into the gasifier are transformed to gases by several processes that include pyrolysis, oxidation (1 and 2), gasification of char and soot (3 and 4) and gas phase reactions as the water gas shift reaction (5) and the reaction of hydrocarbon with water (6)[5][18].

$$C + O_2 \leftrightarrow CO_2 \qquad \Delta H = -394 kJ/mol \qquad (1)$$

$$C + \tfrac{1}{2} O_2 \leftrightarrow CO \qquad \Delta H = -111 kJ/mol \qquad (2)$$

$$C + CO_2 \leftrightarrow 2CO \qquad \Delta H = +172 kJ/mol \qquad (3)$$

$$C + H_2O \leftrightarrow CO + H_2 \qquad \Delta H = +131 kJ/mol \qquad (4)$$

$$CO + H_2O \leftrightarrow CO_2 + H_2 \qquad \Delta H = -41 kJ/mol \qquad (5)$$

$$C_xH_y + xH_2O \leftrightarrow xCO + \tfrac{2x+y}{2} H_2 \qquad (6)$$

In full scale entrained flow gasifier, the oxidation reaction (1 and 2) provides the energy needed for the endothermic CO_2 and H_2O gasification reactions (3 and 4). In this study the energy for the gasification reactions are supplied by both the electrical heating and a partial oxidation of the fuel.

The measurements conducted in this study on the reactor exit gas included concentration of H_2, CO and CO_2, concentration of some hydrocarbon (C_xH_y includes CH_4, C_2H_4, C_3H_8, C_2H_4O by use of an Agilent 3000 micro GC) and solid particle extraction, and in some of the experiments also tar concentration measurements were conducted. In all experiments, the solid fuel was completely converted and no char was collected. However, in many of the experiments, some soot was observed in the exit gas.

Based on the gas, hydrocarbon and soot measuring data, carbon mass balances were calculated for all conducted experiments, and the results are shown in Figure 3. A reasonable mass balance closure was achieved except for the one experiment performed at 1000°C. Typically the mass balance closure was around ±9%. This largest deviation of the carbon mass balance (22%) at

1000°C may be caused by high tar levels and unmeasured larger hydrocarbon yields at this temperature. The hydrogen and oxygen mass balance could not be closed since water yields were not determined.

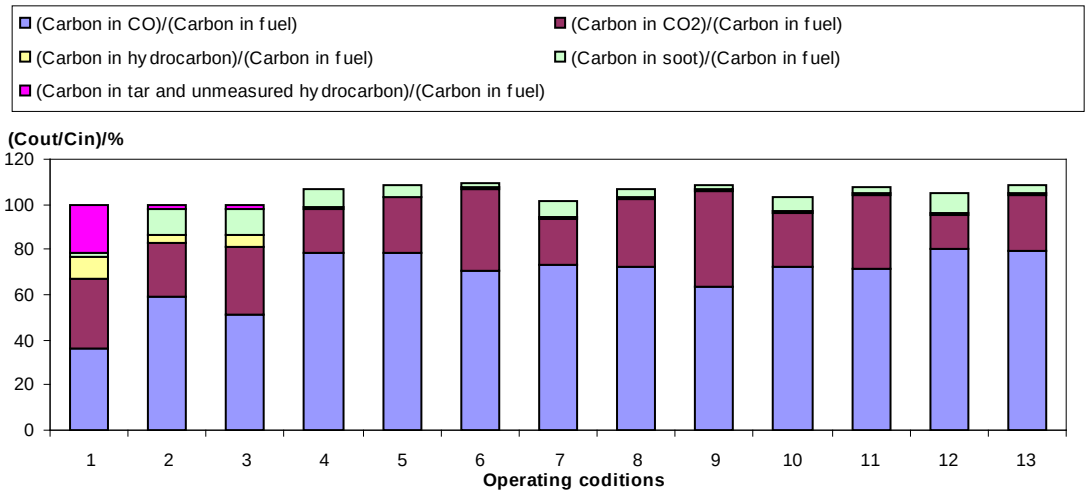

NO.	Operating conditions	NO.	Operating conditions
1	wood,T=1000°C,λ=0.25,H_2O/C=0.5	2	wood,T=1200°C,λ=0.25,H_2O/C=0.0
3	wood,T=1200°C,λ=0.25,H_2O/C=0.5	4	wood,T=1350°C,λ=0.25,H_2O/C=0.0
5	wood,T=1350°C,λ=0.35,H_2O/C=0.0	6	wood,T=1350°C,λ=0.50,H_2O/C=0.0
7	wood,T=1350°C,λ=0.25,H_2O/C=0.5	8	wood,T=1350°C,λ=0.35,H_2O/C=0.5
9	wood,T=1350°C,λ=0.50,H_2O/C=0.5	10	wood,T=1350°C,λ=0.25,H_2O/C=1.0
11	wood,T=1350°C,λ=0.35,H_2O/C=1.0	12	straw,T=1350°C,λ=0.25,H_2O/C=0.0
13	straw,T=1350°C,λ=0.35,H_2O/C=0.0		

Figure 3 Carbon balances all conducted experiments

Influence of temperature

The influence of reactor temperature on the product yield is shown in Figure 4. It can be seen that the amount of producer gas, which is defined as the sum of H_2, CO, CO_2 and C_xH_y up to C_3 species, increases as the temperature increases. The increased gas formation is caused by the conversion of tar and larger hydrocarbons into lighter gaseous products. A large increase in the yields of soot, H_2 and CO is observed when the temperature is increased from 1000°C to 1200°C. At 1000°C, a large amount of undetermined hydrocarbons appear to be present in the gas (see Figure 3). It seems that those hydrocarbons are converted to soot and light gases at 1200 °C. As seen in Figure 4, from 1000°C to 1200°C, the soot yield increases, whereas from 1200°C to 1350°C, there is an opposite trend. Soot is formed at high temperature and the increasing temperature favors soot formation [19]. However, at higher temperature, soot has a higher reactivity for gasification by CO_2 and H_2O. As a result of the competition between formation and destruction of soot, the soot yield decreases above 1200°C.

Tar compounds were sampled by the solid phase absorption method and the measured concentrations of different tar species are shown in Table 2. At 1000°C, only a minor fraction of the total mass of tar and the larger hydrocarbons was determined in this way. The yield of soot is lowest at 1000°C, whereas the yield of tar is highest. At 1350°C, significant soot was produced. However, the tar content in the syngas is very low at this temperature. This shows that there is a trade off between tar and soot formation, which may result from soot formation by tar and hydrocarbon polymerization competing with soot gasification by CO_2 and H_2O at high temperatures [20]-[22].

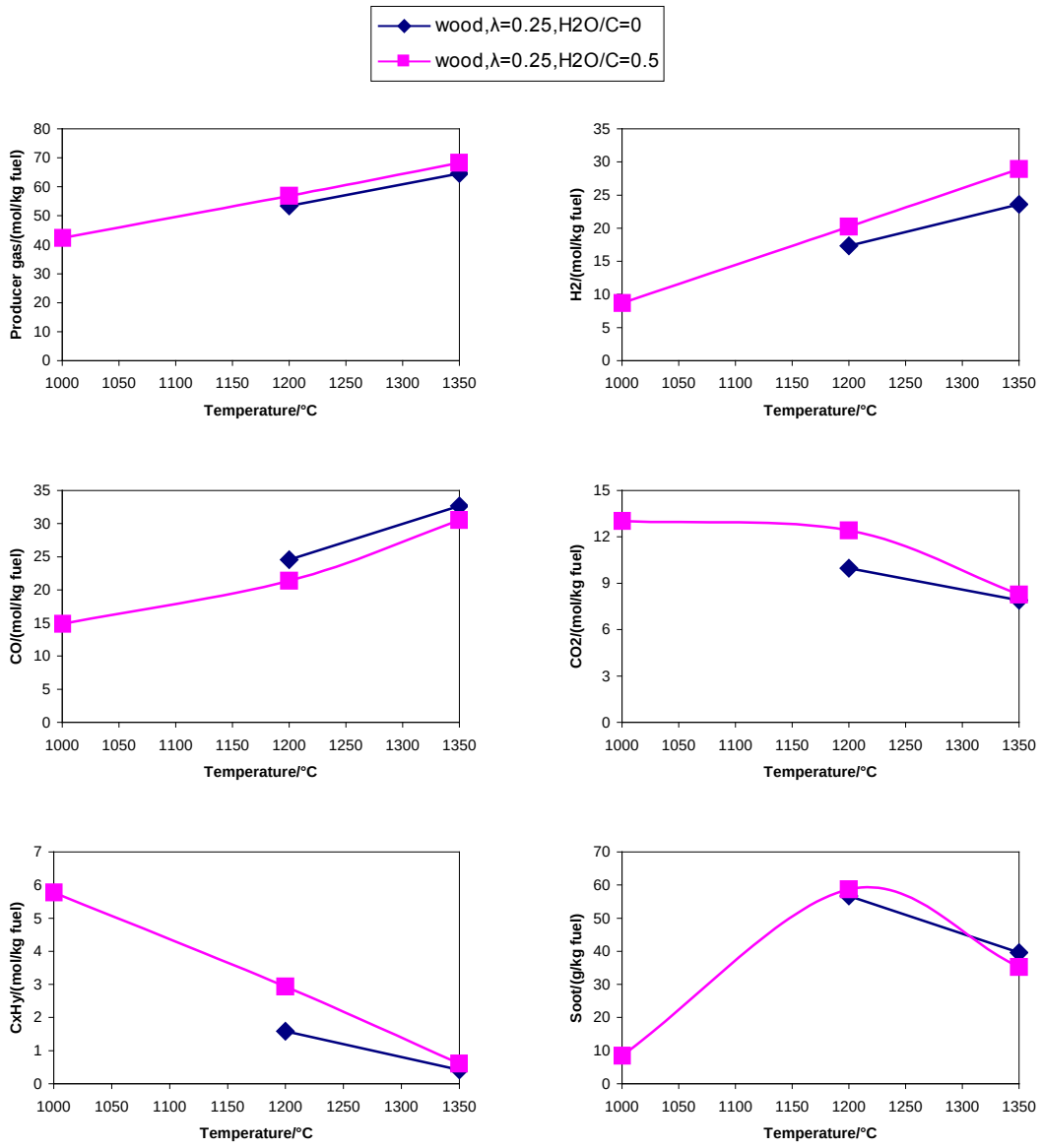

Figure 4 Influence of temperature on product yield for wood gasification at an excess air coefficient of 0.25 and H_2O/C of 0.0 and 0.5 respectively

Table 2 The compounds of tar

Tar compounds (mg/kg fuel)	wood T=1350°C, λ=0.25, H_2O/C=0	wood T=1350°C, λ=0.25, H_2O/C=1	wood T=1000°C, λ=0.25, H2O/C=0
Phenol	0.00	0.01	0.01
Naphthalene	0.00	0.00	0.05
Acenaphthylene	0.00	0.00	3.58
Phenanthrene	0.00	0.00	8.87
Anthracene	0.02	0.01	0.00
Fluoranthene	0.13	0.02	3.65
Pyrene	0.13	0.21	10.05
Unknown	0.13	0.02	0.01
Total tar	**0.40**	**0.27**	**26.23**

Influence of excess air coefficient

The influence of excess air coefficient on product yield is shown in Figure 5. The amount of producer gas nearly keeps constant with an increase of excess air coefficient. The H_2, CO and C_xH_y yields decrease with increasing excess air coefficient, whereas the yield of CO_2 increases due to oxidation of soot, CO and other gaseous species [7][8][23]-[25]. It is observed that the amount of soot decreases with increasing excess air coefficient. As the excess air coefficient increases, a larger part of the soot is combusted.

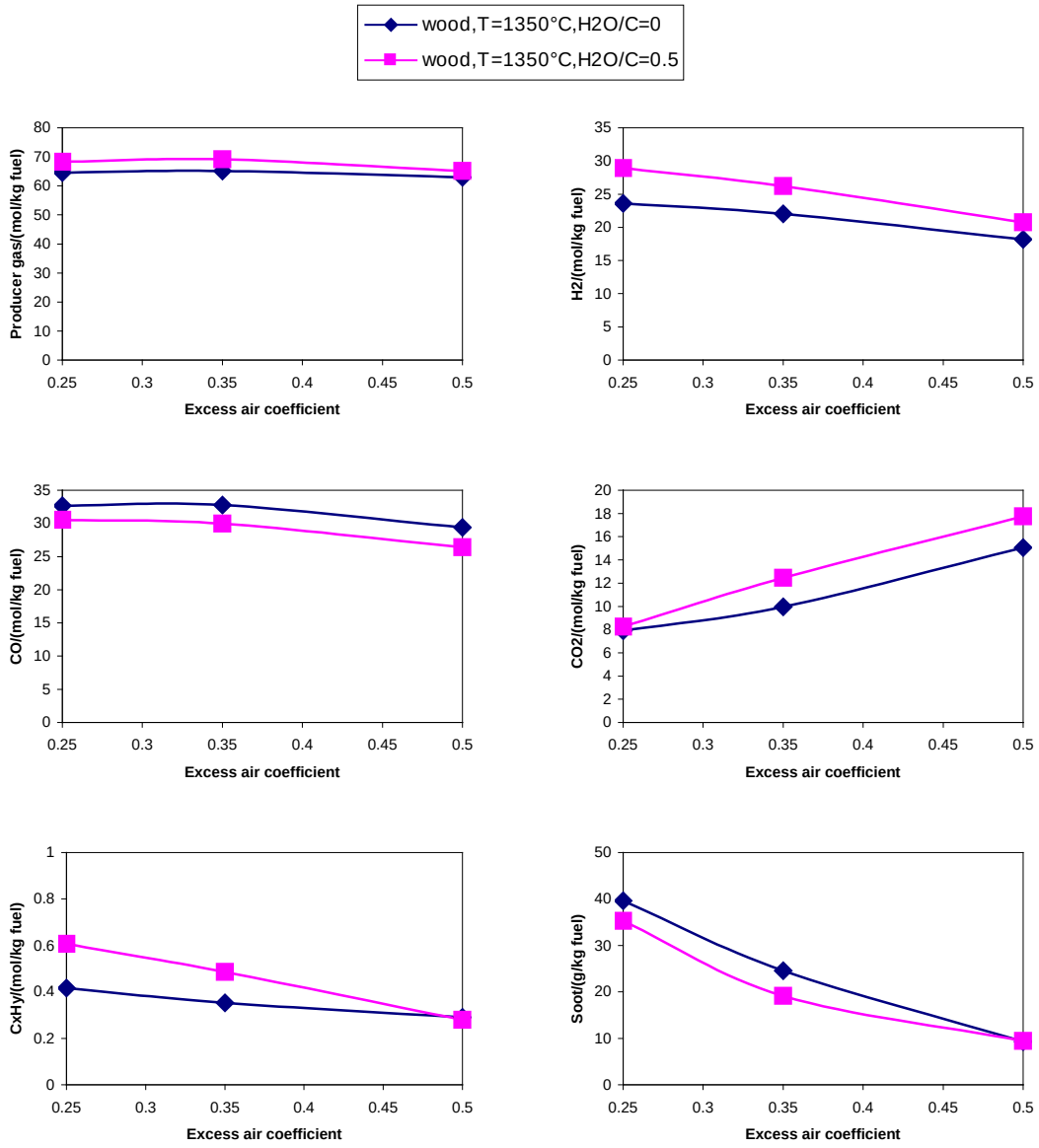

Figure 5 Influence of excess air coefficient on product yield for wood gasification at 1350°C and H_2O/C of 0.0 and 0.5 respectively

Influence of steam/carbon ratio

The influence of steam/carbon ratio on product yield is shown in Figure 6. As steam is introduced, the yield of the producer gas increases slightly due to the promotion of steam gasification of soot and larger hydrocarbons. However, even a high amount of steam injection only gives small changes in the gas composition. As the steam/carbon ratio increases, the H_2 and CO_2 yields increase, accompanied with a decrease of the CO yield, because the steam addition tends to promote the water gas shift reaction (5)[7][26]. The C_xH_y yield increases a little as steam introduced, which is caused by the reformation of tar and larger hydrocarbons. The yield of soot decreases slightly with increasing steam/carbon ratio, most likely due to steam gasification of the soot.

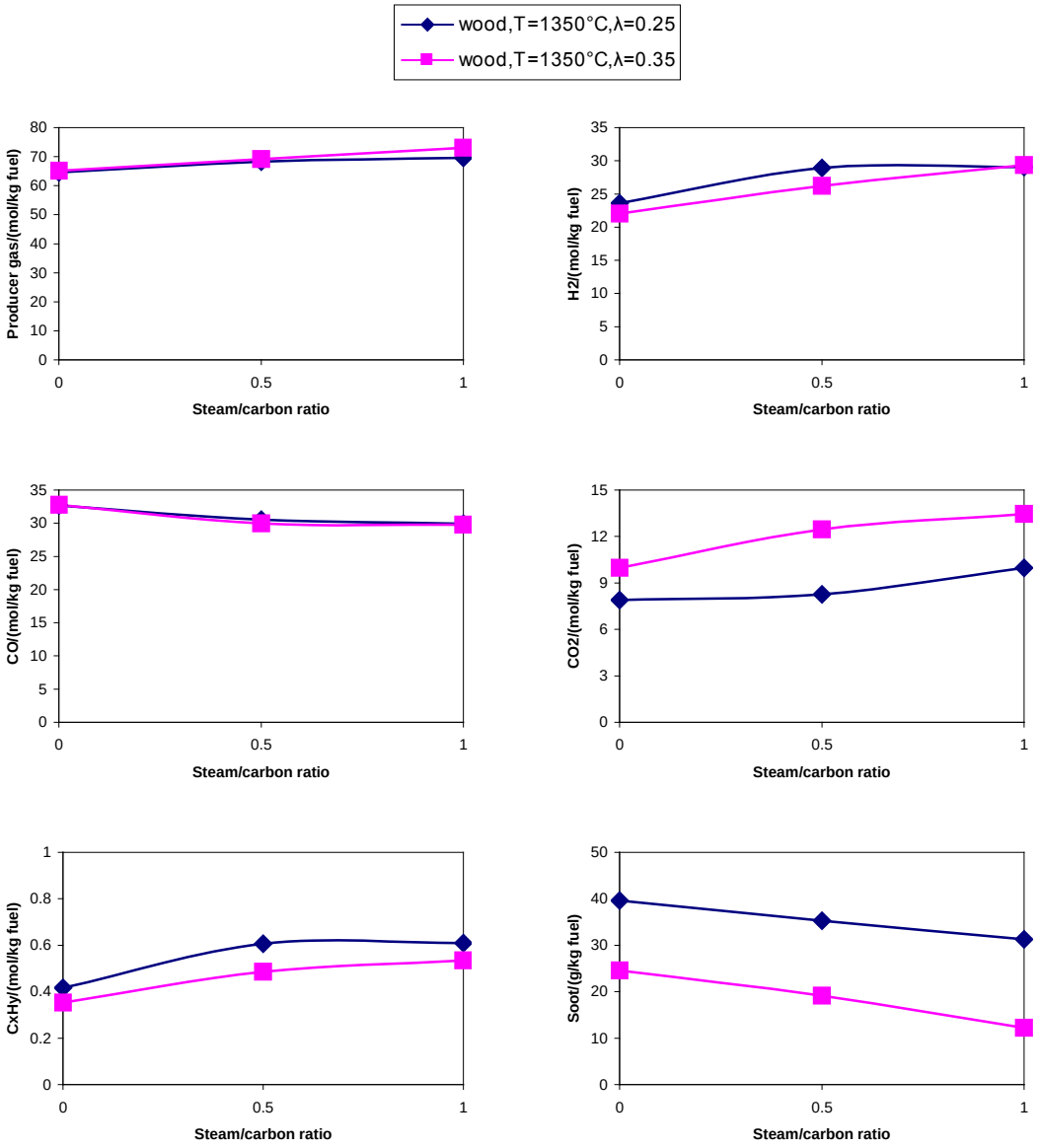

Figure 6 Influence of steam/carbon ratio on product yield for wood gasification at 1350°C and an excess air coefficient of 0.25 and 0.35 respectively

Influence of biomass type

The influence of biomass type on the product yield is shown in Figure 7. The results indicate that the two types of biomass have similar gasification behavior in agreement with the literature [25][27]. An important difference between wood and straw is the high alkali content in straw [15]. The alkali may have a catalytic influence on the gasification experiments [16][17]. However, since the wood and straw experiments provided similar results, it can be conclude that the presence of a high amount of alkali metals do not change the gas composition significantly at entrained flow reactor gasification conditions.

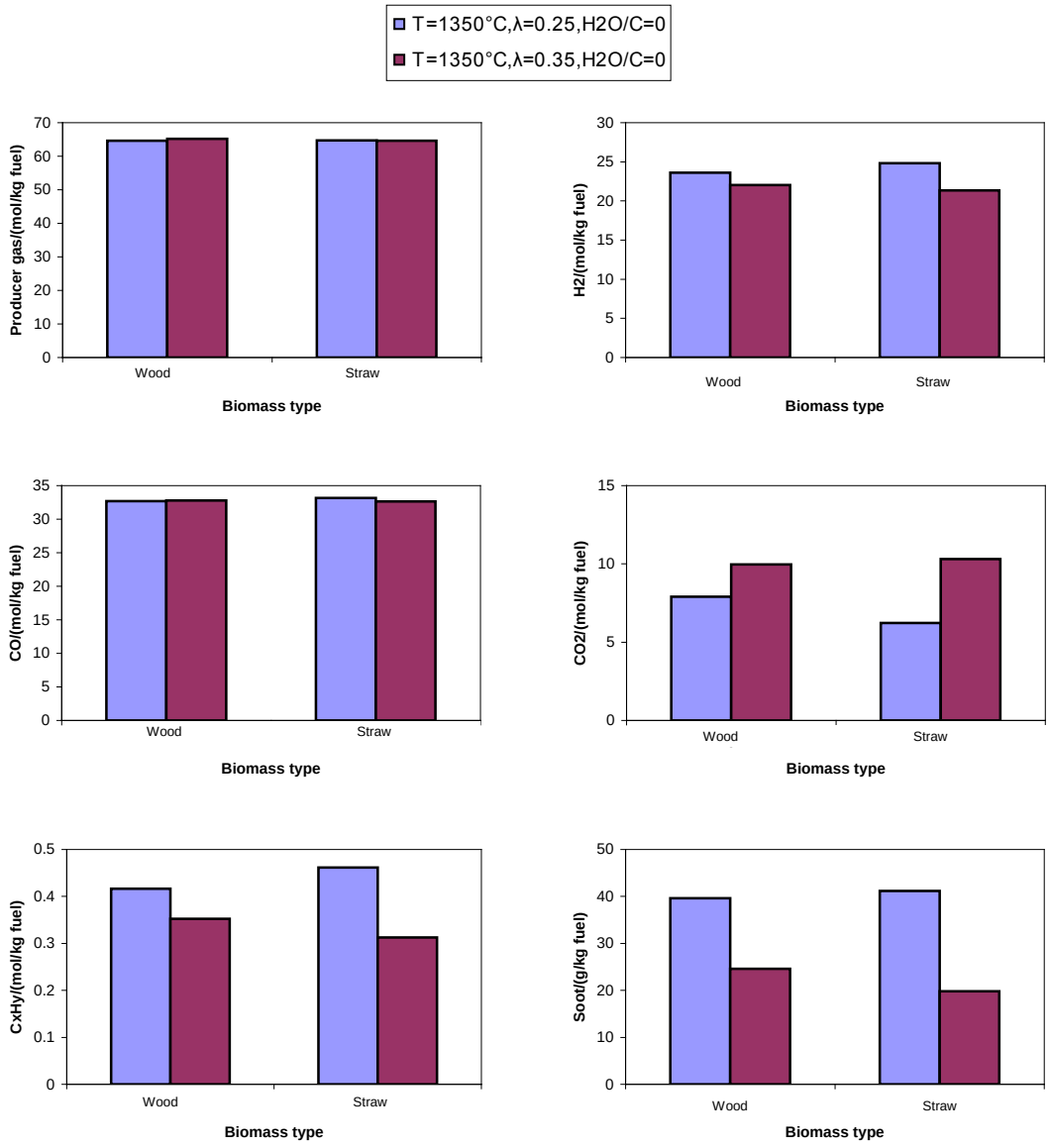

Figure 7 Influence of biomass type on product yield at 1350°C, H_2O/C of 0.0 and an excess air coefficient of 0.25 and 0.35 respectively

CONCLUSIONS

Gasification of two types of biomass, wood and straw, has been investigated in a laboratory scale atmospheric pressure entrained flow reactor. In all experiments, the char was completely converted. The amount of producer gas (defined as H_2, CO, CO_2 and hydrocarbon up to C_3 species) increases significantly, from 42.4mol/kg fuel to 68.3mol/kg fuel, when the temperature is increased from 1000°C to 1350°C. This is caused by the conversion of tar and larger hydrocarbons into lighter gaseous. The yields of hydrogen and carbon monoxide increase as the temperature is increased. It was found that at an excess air coefficient of 0.25 and a steam/carbon ratio of 0.5, the tar content in the syngas is very low (between 0.27mg/kg fuel and 0.40mg/kg fuel) at 1350°C. However, a significant level of soot (35.26g/kg fuel) was produced at this temperature. At 1000°C, the yield of tar is highest (26.23mg/kg fuel), whereas the yield of soot is lowest (8.49g/kg fuel). This trade off between tar and soot formation may result from the competition between soot formation by tar and hydrocarbon polymerization and soot oxidation at high temperatures. The yields of hydrogen and carbon monoxide decrease with increasing excess air coefficient. With addition of steam, the hydrogen yield increases while the carbon monoxide yield decreases due to the water gas shift reaction. The soot yield can be slightly reduced by addition of steam. The applied biomass type has little influence on the composition of the syngas.

REFERENCES

[1] World Energy Outlook 2004

[2] Chum HL, Overend RP. Biomass and renewable fuels. Fuel Processing Technology 71(2001): 187-195

[3] Joshi MM, Lee S. Integrated gasification combined cycle - a review of IGCC technology. Energy Sources 18(1996): 537-568

[4] Stiegel GJ, Maxwell RC. Gasification technologies: the path to clean, affordable energy in the 21st century. Fuel Processing Technology 71(2001): 79-97

[5] Higman C, van der Burgt M. Gasification. America, 2003

[6] Guo XL, Dai ZH, Gong X, Chen XL, Liu HF, Wang FC, Yu ZH. Performance of an entrained-flow gasification technology of pulverized coal in pilot-scale plant. Fuel processing technology 88(2007): 451-459

[7] Lee JG, Kim JH, Lee HJ, Park TJ, Kim SD. Characteristics of entrained flow coal gasification in a drop tube reactor. Fuel 75(1996): 1035-1042

[8] Crnomarkovic N, Repic B, Mladenovic R, Neskovic O, Veljkovic M. Experimental investigation of role of steam in entrained flow coal gasification. Fuel 86(2007): 194-202

[9] Brown BW, Smoot LD, Hedman PO. Effect of coal type on entrained gasification. Fuel 65(1986): 673-678

[10] Azuhata S, Hedman PO, Smoot LD, Sowa WA, Effects of flame type and pressure on entrained coal gasification. Fuel 65(1986): 1511-1515

[11] Harris DJ, Roberts DG, Henderson DG. Gasification behavior of Australian coals at high temperature and pressure. Fuel 85(2006): 134-142

[12] Hamelinck CN, Faaij APC, den Uil H, Boerrigter H. Production of FT transportation fuels from biomass; technical options, process analysis and optimisation, and development potential. Energy 29(2004): 1743-1771

[13] Shen J, Schmetz E, Kawalkin GJ. Commercial deployment of Fischer-Tropsch synthesis: the coproduction option. Topics in Catalysis 26(2003): 13-20

[14] Zwart RWR, Boerrigter H. High efficiency co-production of synthetic natural gas (SNG) and Fischer-Tropsch (FT) transportation fuels from biomass. Energy & Fuels 19(2005): 591-597

[15] Capablo J, Jensen PA, Pedersen KH, Hjuler K, Nikolaisen L, Backman R, Frandsen F. Ash properties of alternative biomass. Energy & Fuels 23(2009): 1965-1976

[16] Pang KL, Xiang WG, Liang C, Zhao CS, Xi B, Liu DJ. Gasification reaction of coal char with CO_2 under the catalytic Action of alkali metals. Journal of power engineering 26(2006): 141-144

[17] Wei XF, Huang JJ, Fang YT, Wang Y. Effect of alkali metal on the lignite gasification reactivity. Coal conversion 30(2007): 38-42

[18] Schilling H, Bonn B, Krauss U. Coal gasification: Existing process and new developments. London, 1981

[19] Indarto A. Soot growing mechanism from polyynes: a review. Environmental engineering science 26(2009): 1-7

[20] Kriengsak SN, Buczynski R, Gmurczyk J, Gupta AK. Hydrogen production by high-temperature steam gasification of biomass and coal. Environmental engineering science 26(2009): 739-744
[21] Lucas C, Szewczyk D, Blasiak W. High-temperature air and steam gasification of densified biofuels. Biomass and bioenergy 27(2004): 563-575
[22] Wei LG, Xu SP, Zhang L, Liu CH, Zhu H, Liu SQ. Steam gasification of biomass for hydrogen-rich gas in a free-fall reactor. International journal of hydrogen energy 32(2007): 24-31
[23] Kim YJ, Lee JM, Kim SD. Coal gasification characteristics in an internally circulating fluidized bed with draught tube. Fuel 76(1997): 1067-1073
[24] Na JI, Park SJ, Kim YK, Lee JG, Kim JH. Characteristics of oxygen-blown gasification for combustible waste in a fixed-bed gasifier. Applied energy 75(2003): 275-285
[25] Lapuerta M, Hernandez JJ, Pazo A. {{49 Kim, Y.J. 1997; 27 Lapuerta, M. 2008; 19 Crnomarkovic, N. 2007; 18 Lee, J.G. 1996}}Gasification and co-gasification of biomass wastes: effect of the biomass origin and the gasifier operating conditions. Fuel processing technology 89(2008): 828-837
[26] Gil J, Corella J, Aznar PA, Caballero AM. Biomass gasification in atmosphere and bubbling fluidized bed: effect of the type of gasifying agent on the product distribution. Biomass and bioenergy 17(1999): 389-403
[27] Lu YJ, Ji CM, Guo LJ. Experimental investigation on hydrogen production by agricultural biomass gasification in supercritical water. Journal of xi'an jiaotong university 39(2005): 238-242

Appendix G. Synthesis of liquid fuels from biomass in a Danish context

Report

Jakob Munkholt Christensen, Anker Degn Jensen, Peter Arendt Jensen. Report: synthesis of liquid fuels from biomass in a Danish context (Syntese af væskeformige brændsler fra biomasse i en dansk kontekst). (in danish)

2009, DTU no. 50442

Final report - EFP06 – Produktion af methanol/DME ud fra biomasse

Rapport: Syntese af væskeformige brændsler fra biomasse i en dansk kontekst

Jakob Munkholt Christensen, Anker Degn Jensen, Peter Arendt Jensen

Department of Chemical and Biochemical Engineering
Technical University of Denmark
Søltofts Plads, Building 229, DK-2800 Lyngby, Denmark

Indledning

Omdannelsen af biomasse til væskeformige transportbrændsler oplever en stigende interesse i takt med det forøgede fokus på den menneskeskabte udledning af CO_2. Det estimeres, at det potentielle energiudbytte fra biomasse på verdensplan udgør 100 EJ/år, hvilket til sammenligning er ca. 30 % af verdens nuværende energiforbrug[1,2]. I dag udnytter man imidlertid blot en mindre fraktion af dette potentiale[1,2]. En mulig rute fra biomasse til væskeformige brændsler er en forgasning af biomassen til såkaldt syntesegas eller syngas. Den dannede syngas kan i en bred vifte af katalytiske reaktioner omdannes til væskeformige transportbrændsler som f.eks. methanol, dimethyl æter (DME), syntetisk diesel (såkaldt Fischer Tropsch eller FT diesel) eller blandede højere alkoholer (forkortet HA og primært bestående af ethanol). Methanol/DME kan endvidere omdannes til syntetisk benzin. Alternativt kan biomassen fermenteres til såkaldt bioethanol. Bioethanol kan fremstilles fra kerner (1. generationsteknologi) eller fra lignocellulose som halm og strå (2. generationsteknologi). Yderligere en metode til fremstilling af transportbrændsel ud fra biomasse er en såkaldt esterificering af planterolier som f.eks. produktionen af rapsoliemethylester (RME) fra rapsolie. En klar fordel ved forgasningsruten er at denne kan anvendes med alle typer af biomasse.

Denne note opsummerer energieffektiviteten for fremstilling og udnyttelse af de ovennævnte væskeformige transportbrændsler afledt af biomasse gennem fermentering eller forgasning/syntese. Produktionen af el fra biomasse i et konventionelt kulfyret kraftværk er inkluderet i studierne som reference. Der er ydermere givet en kort præsentation af teknologiernes modenhed og investeringsbehov, men økonomiske overvejelser mht. brugen af biobrændsler er begrænset til et kvalitativt niveau.

De nærværende undersøgelser er publiceret i Dansk Kemi[3,4]. Denne rapport indeholder de detaljerede resultater samt bilag med beskrivelser af beregningsmetoderne.

Udbytte af afgrøder

Den første væsentlige parameter i en evaluering af effektiviteten i produktion af biobrændsler er markudbyttet. Tabel 1 illustrerer, hvilket udbytte der kan forventes for forskellige typer af afgrøder i Danmark.

Tabel 1 Udbytte af forskellige afgrøder i Danmark

Afgrøde	Tørstofudbytte / ton/(ha&år)	Nedre brændværdi (LHV) / GJ/ton	Energiudbytte / GJ/(ha&år)
Vinterhvede[5-8]	Kerner [a]: 7,19 Strå [b]: 7,48 Samlet: 14,67	Kerner [b]: 18,5 Strå [b]: 18,8	Kerner: 133,0 Strå: 140,6 Samlet: 273,6
Vinterraps[6,7,9-11]	Frø: 3,16[c] Strå: 3,56[d] Samlet: 6,72	Frø: 27,6 Strå: 18,3	Frø: 87,2 Strå: 65,2 Samlet: 152,4
Pil[12,13]	10-15	16,3	163-245
Poppel[8,12]	10-15	17,7	177-266
Elefantgræs[14,15]	8-15	17,9	143-269

[a] Gennemsnit for DK i perioden 2001-2006 [6,7].
[b] Gennemsnit for Roskilde,DK i perioden 1994-1996 [5].
[c] Gennemsnit for DK i perioden 2001-2006 [6,7]. Rapsudbyttet synes dog at være stigende.
[d] Baseret på frøudbyttet og et frø/strå forhold opgivet af Faaij[11].

I denne analyse tages der ikke højde for energiforbruget til dyrkning, høst og transport af biomassen. Det bør dog nævnes, at dyrkningen af såkaldte energiafgrøder som pil, poppel og elefantgræs generelt er mindre energiintensiv end dyrkningen af vinterhvede og raps[15,16]. For skovbrug inden for en radius af 40 km fra forarbejdningsanlægget ligger energiforbruget til produktion og transport på 2-4 % af biomassens energiindhold[17,18]. Nedbrydning af biomassen under eventuel lagring er heller ikke inkluderet i denne analyse.

Effektivitet for brændselssyntese

Biomassen kan som nævnt omdannes til transportbrændsler ad flere ruter. For de fleste af synteserne er der endvidere mulighed for en biproduktion af el. Tabel 2 viser energi-effektiviteten for syntesen af diverse væskeformige brændsler fra biomasse. Tabellen viser den samlede energieffektivitet for forgasning og syntese af brændslet eller effektiviteten for forbehandling og fermentering til bioethanol. Elproduktion kan eksempelvis ske gennem afbrænding af biprodukter fra brændselssyntesen.

Tabel 2 Energieffektivitet for syntetiseringen af væskeformige brændsler og el fra biomasse

	Energieffektivitet / $\%_{LHV}$ [a]	
Brændsel	Brændstof	El
Bioethanol fra hvedekerner[19,20]	40	(-5)
Bioethanol fra lignocellulose (halm, træ etc.) [19,21-25]	26-52 (typisk omkring 35)	0-4
Methanol[20,26-30]	48-55	0-12
Højere alkoholer (HA)[31] [b]	37-38	8
DME[26,30,32]	57-63	(-7)-11
Syntetisk benzin (via methanol/DME)[33] [c]	43-50	0-14[d]
Fischer Tropsch diesel[20,34]	40	4-11
Biodisel (RME) [10] [e]	27	17
Komprimeret brint[29]	33[f]	19
Afbrænding i konventionelt kraftværk[35]	0	40-50[g]

[a] Energi i væskeprodukt eller elproduktion relativt til den tilførte biomasse baseret på den nedre brændværdi (LHV).

[b] Værdier for syntesen fra kul, men disse forventes at afspejle niveauet for biomasse.

[c] Baseret på effektiviteten for methanolsyntesen og 90 % energieffektivitet i omdannelsen fra methanol til benzin rapporteret for Mobils Methanol-to-Gasoline proces[33].

[d] Estimeret ud fra methanoludbyttet og effektiviteten for Mobils Methanol-to-Gasoline proces (se note c).

[e] Effektivitet relativt til frø+strå. Energieffektiviteten for produktion af RME fra rapsfrø er 48 $\%_{LHV}$ [10], mens effektiviteten for produktionen af el fra strå er 40 $\%_{LHV}$ (se evt. note f).

[f] Denne værdi er beregnet ud fra Hamelinck og Faaij[29] og antages at beskrive teknologiens aktuelle niveau. Nuværende anlæg, som producerer brint fra biomasse, rapporteres at operere med en energieffektivitet på 26 %[36]. Det bør dog nævnes at visse studier estimerer højere energieffektiviteter for hydrogenproduktion i størrelsesordnen 50 $\%_{LHV}$[30,37,38]. Ønskes der i stedet væskeformig brint, som har en højere energitæthed, kræves der 12-13 kWh per kg. brint til fortætningen. Dette svarer til 36-39% af den i brinten indeholdte energi[30].

[g] Disse værdier er for kul. Forbrænding af kul og biomasse medfører et mindre effektivitetstab, og hvis dette tab udelukkende tilskrives biomassen, er dennes energieffektitivet 0-10 % mindre[39]. I de videre beregninger er der benyttet en energieffektivitet på 40 $\%_{LHV}$ for biomasse og en værdi på 45 $\%_{LHV}$ for kul.

Det bør nævnes, at energieffektiviteter fundet i de systemstudier, der er opsummeret i tabel 2, generelt udviser en stor spredning – især mht. bioethanol fra lignocellulose (2.generationsteknologi). I efterfølgende beregninger er der benyttet middelværdier for intervallerne opgivet i tabel 2. En undtagelse er ethanol fremstillet fra lignocellulose ved fermentering, hvor en typisk rapporteret værdi på 35 $\%_{LHV}$ er benyttet. Bortset fra biodiesel fra raps er det antaget at hele afgrøden omdannes til biobrændsel. For fremstillingen af bioethanol fra hvede er det f.eks. antaget at der benyttes 1. generationsteknologi til at fremstille ethanol fra kernerne og 2. generationsteknologi til at fremstille ethanol fra stråudbyttet.

For syntesen af højere alkoholer fra syngas har det kun været muligt at finde et realistisk estimat af energieffektiviteten for syntese ud fra kul som dog antages at afspejle niveauet for biomasse. Den primære begrænsning for udnyttelsen af denne syntese er katalysatorens forholdsvis lave selektivitet. I et systemstudie fra US National Renewable Energy Laboratory benyttes forventede forbedringer i katalysatorens produktivitet og selektivitet. I dette studie anslås energieffektiviteten for alkoholproduktion til 58 $\%_{LHV}$, men dette afspejler dog ikke processens aktuelle niveau[40].

Generelt kan det konkluderes, at den største effektivitet opnås gennem forgasning af biomassen og syntese af DME.

Brændstoføkonomi for danske biler

En væsentlig parameter i evalueringen af de væskeformige transportbrændsler er den distance, en bil kan tilbagelægge med den mængde brændsel, der kan udvindes fra årsudbyttet for et givent markareal. I det følgende er der foretaget en evaluering af de forskellige transportbrændsler baseret på brug i forbrændingsmotorer anno 2006. Brugen af hydrogen i en brændselscellebil og el i en elbil er også inkluderet i evalueringen. Dette er gjort selvom disse teknologier ikke for øjeblikket finder bred anvendelse.

Nye benzindrevne biler købt i Danmark i 2006 kører i gennemsnit 14,8 km/L, mens nye dieseldrevne biler i gennemsnit kører 18,6 km/L[41]. Brændstoføkonomien for sådanne biler er benyttet til at estimere den distance, der kan tilbagelægges med biobrændsler fra årsproduktionen for en hektar markareal. De syntetiske alternativer til olieafledt diesel (DME, RME og FT diesel) giver ved brug i en forbrændingsmotor praktisk talt den samme effektivitet, som det fossile brændsel de erstatter[27,32,42,43]. Alkoholer og hydrogen har mærkbart højere oktantal end alm. benzin. Dette betyder, at motorer modificeret til brug af alkoholer kan opereres med et højere kompressionsforhold, hvilket betyder en højere energieffektivitet i forbrændingen. I en sammenligning af de forskellige syntetiske brændsler bør der selvsagt korrigeres for denne effektivitetsforøgelse. Der er dog varierende beskrivelser af den effektivitetsforøgelse, der kan opnås ved brugen af alkoholer som bilbrændsler. Effektiviteten for alkoholer og hydrogen rapporteres generelt at være 10-28 % højere end alm. benzin[20,44,45]. En realistisk værdi under typiske forhold synes at være en forbedring på 10 % i forhold til alm. benzin[46], og denne værdi er benyttet i de indeværende beregninger. Brugen af syntetisk benzin antages at ske med samme effektivitet som alm. olieafledt benzin. Mere ”futuristiske” teknologier som brugen af hydrogen i en brændslescelle eller el i en elbil kan potentielt give mærkbart højere energieffektiviteter end forbrændingsmotorer. I dette studium er det antaget, at en hydrogendrevet brændselscellebil har en effektivitet, der er 100 % større end en alm.

benzinbil[19,20,27]. For elbiler er energieffektiviteten for udnyttelsen af den i tanken/batteriet indeholdte energi antaget at være 400 % større end for benzinbiler benzinbiler[27,47].

Alkoholer, DME og især komprimeret brint har lavere energitætheder end benzin og diesel, hvorfor køretøjer, der benytter disse brændsler, skal have en større brændstoftank for at tilbagelægge den samme distance. Ligeledes er en begrænset batterikapacitet for elbiler årsag til, at disse køretøjer generelt har en mindre aktionsradius end almindelige biler. Disse effekter er ikke inkluderet i beregningerne.

Potentiale for de forskellige biobrændsler

Idet man kender markudbyttet for de forskellige afgrøder, brændselssyntesens effektivitet, og bilernes brændstoføkonomi kan man bestemme den distance der kan tilbagelægges med biobrændsel udvundet af høstudbyttet fra en hektar markareal. Tabel 4 i appendiks A opsummerer transportkapaciteten i et høstudbytte for forskellige kombinationer af syntetiske brændsler og markafgrøder. De fysiske parametre for de undersøgte brændstoffer findes i appendiks B, mens den benyttede beregningsprocedure er beskrevet i appendiks C. Figur 1 herunder illustrerer den transportdistance der kan opnås med syntetiske brændsler fra et års produktion af vinterhvede.

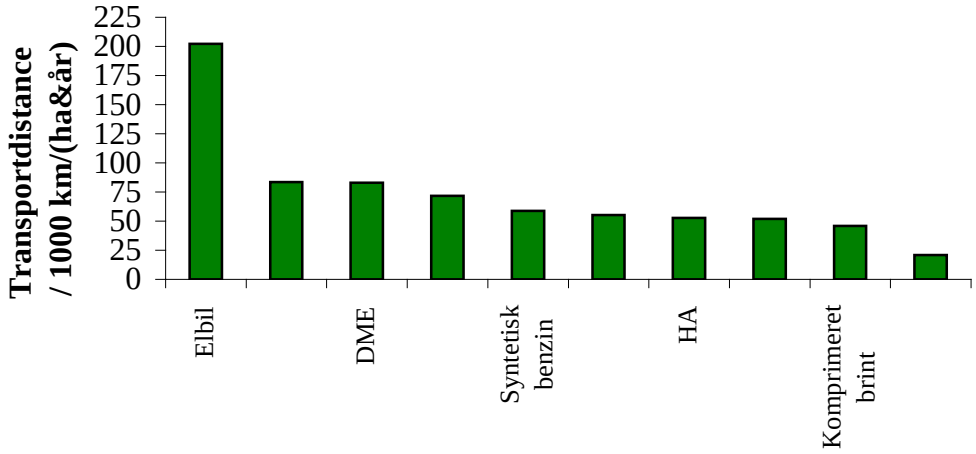

Figur 1 Den distance en gennemsnitsbil kan køre på alternative brændsler udvundet fra årsudbyttet af vinterhvede (strå+kerner). Biodiesel udvundet fra raps er også inkluderet i sammenligningen. "Komprimeret brint BC" indikerer brugen af brint i en bil drevet af en brændselscelle.

Den bedste transportdistance, kan opnås med en elbil efterfulgt af en brintdrevet brændselscellebil. Disse muligheder udgør dog for øjeblikket fremtidsscenarier. Blandt de brændsler, der udnyttes med konventionelle forbrændingsmotorer, er DME den bedste løsning efterfulgt at methanol. Syntetisk benzin og diesel, højere alkoholer samt bioethanol giver næsten lige lange transportdistancer. Produktionen af biodiesel fra raps giver en noget mindre transportdistance end de øvrige undersøgte biobrændsler. Dette skyldes dels, at raps giver et lavere tørstofudbytte end f.eks. hvede, og dels at kun rapsfrøene og ikke stråudbyttet kan udnyttes til produktionen af biodiesel. Figur 2 illustrerer den tilbagelagte distance for forskellige brændsler ud fra et års produktion af piletræ.

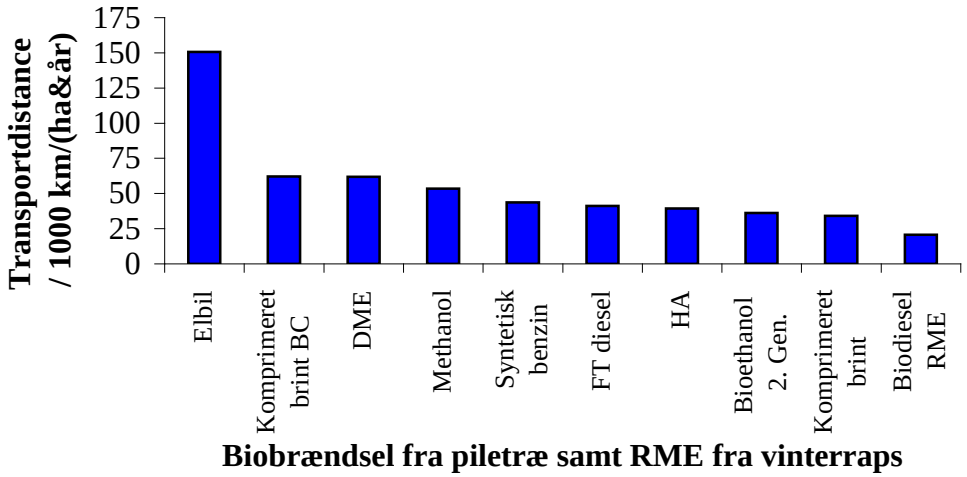

Figur 2 Den distance en gennemsnitsbil kan køre på alternative brændsler udvundet fra årsudbyttet af pil. Biodiesel udvundet fra raps er også inkluderet i sammenligningen.
"Komprimeret brint BC" indikerer brugen af brint i en bil drevet af en brændselscelle.

Figur 2 viser generelt de samme tendenser som figur 1. Med de for øjeblikket bredt anvendte motorteknologier er DME det væskeformige brændsel, der giver den længste transportdistance pr. markareal. Metanol giver dog næsten den samme transportdistance som DME. En sammenligning af figurerne 1 og 2 viser, at bioethanol relativt til de øvrige brændselstyper klarer sig bedre for hvede end for pil. Dette skyldes den højere energieffektivitet for produktionen af ethanol ud fra hvedekerner frem for produktionen fra lignocellulose som strå og træ. Højere alkoholer, FT diesel og syntetisk benzin giver stort set den samme transportdistance pr. markareal.

Som nævnt giver flere af brændselssynteserne mulighed for en biproduktion af elektricitet. Figur 3 viser den mulige elproduktion fra årsudbyttet af piletræ i forbindelse med brændselssynteserne samt for afbrænding af biomassen i et konventionelt kraftværk.

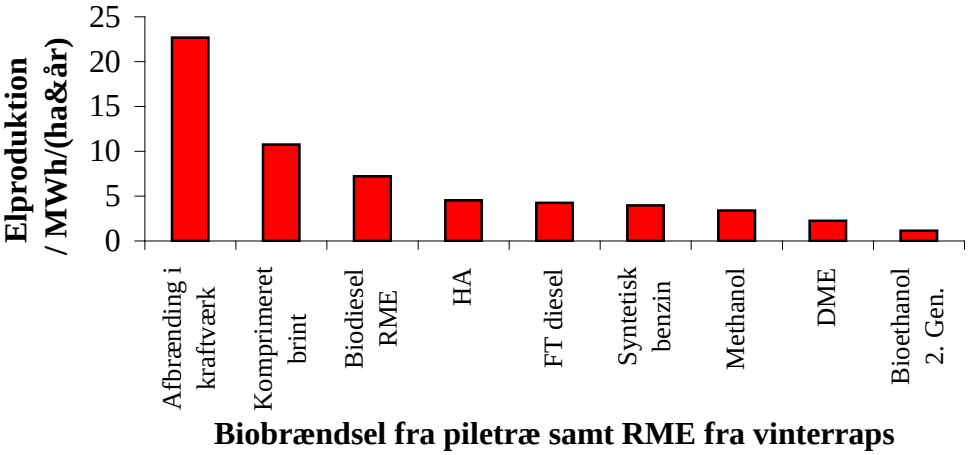

Figur 3 Elproduktionen forbundet med de forskellige processer ud fra årsudbyttet af piletræ. Biodiesel udvundet fra raps er også inkluderet i sammenligningen.

Figur 3 viser, at afbrændingen af hele afgrøden i et konventionelt kraftværk giver den største elproduktion. Den næststørste elproduktion kommer fra samproduceret el i

produktionen af brint. I fremstillingen af biodiesel fra raps indgår udbyttet af strå ikke i brændselssyntesen, men stråene kan potentielt anvendes til elproduktion og derfor har denne syntesevej et vist potentiale for elproduktion. I en række andre brændselssynteser kan el fremstilles fra f.eks. afbrænding af metan, som er et biprodukt i flere af brændselssynteserne.

Modenhed og investeringsbehov for teknologierne

Forgasning af kul og efterfølgende syntese af FT diesel har været udført i stor skala i Sydafrika i en årrække. Energieffektiviteten for denne proces ligger omkring 40 $\%_{LHV}$[48]. Forgasning af biomasse har endnu ikke været udført i kommerciel skala[49]. Der har dog i de senere år været udført en del forgasningsforsøg i mindre skala bl.a. en 4 MW forgasser i Harboøre i Danmark, en 8 MW forgasser i Güssing i Østrig og en 18 MW forgasser i Värnamo i Sverige[49,50]. De fleste af brændselssynteserne opereres også kommercielt, dog typisk med naturgas som føde. Methanol er et af de kemikalier, der på verdensplan produceres i de største mængder[48]. DME fremstilles i langt mindre mængder end methanol, men produktionen på verdensplan er stigende[51]. Et fuld-skala anlæg til produktionen af syntetisk benzin fra naturgas via methanol/DME opereredes i New Zealand igennem en årrække, men produktionen blev indstillet i 1997[52]. Såkaldt 1. generationsanlæg til produktion af bioethanol opereres i dag i kommerciel skala, men 2. genrationsanlæg med ethanolproduktion fra lignocellulose opereres for øjeblikket ikke i kommerciel skala[16]. Heller ikke syntesen af højere alkoholer opereres for øjeblikket i fuld skala, men det førnævnte potentiale for forbedringer i energieffektiviteten og alkoholproduktets gode forbrændingsegenskaber i benzinmotorer er antageligvis årsagerne til, at det første andengenerationsanlæg i kommerciel skala ser ud til at blive baseret på denne teknologi. Firmaet Range Fuels bygger i øjeblikket i USA et anlæg til forgasning af træ-affald til syngas, som efterfølgende katalytisk omdannes til blandede højere alkoholer[53]. Første del af anlægget, som har en projekteret produktionskapacitet på 75 mio. liter ethanol per år, forventes færdiggjort i 2008.

Med hensyn til investeringsbehovet for de forskellige teknologier må det generelt siges, at anlæg til produktion af væskeformige brændsler fra biomasse i kommerciel skala er relativt kapitalintensive. Tabel 4 indeholder estimerede anlægspriser for produktionsanlæg med en indfyret effekt på 400 MW_{HHV} (øvre brændværdi), hvilket svarer til ca. 75 tons træ per time.

Tabel 3 Estimerede investeringsbehov for produktionsanlæg til fremstilling af væskeformige brændsler fra biomasse med en indfyret effekt på 400 MW_{HHV}[20]

Brændsel	Pris / mia. kr	Produktion[†] / tons produkt/dag
Bioethanol (fra lignocellulose)	2,20	398
Methanol	1,78	862
DME	2,32	639
FT Diesel	2,21	278
Biodisel (RME)	3,01	213
Brint	1,87	84

[†] Beregnet ud fra energieffektiviteterne præsenteret i tabel 2, de fysiske parametre presenteret i appendiks B, og det estimat at, at 400 MW_{HHV} svarer til 353 MW_{LHV} i henhold til tal fra Hamelinck og Faaij[29].

Estimat af CO_2-fortrængningen med de forskellige teknologier

På baggrund af energieffektiviteterne for de forskellige brændselssynteser er CO_2-fortrængningen ved slutudnyttelsen estimeret for de forskellige synteseløsninger samt for afbrænding af biomassen i et konventionelt kraftværk. Med slutudnyttelse menes der, at der kun er taget stilling til brugen af brændslet og ikke til miljøforholdene relateret til dyrkning og distribution af biobrændslet. Transportbrændslerne erstatter benzin hhv. diesel, mens elproduktion ud fra biomasse erstatter kul i et konventionelt kraftværk. Brint- og elbiler antages i evalueringen at fortrænge benzinbiler. De fysiske parametre for fossile brændsler som benzin, diesel og kul er givet i appendiks B, og beregningsproceduren er beskrevet i appendiks C. Energieffektiviteten for for-brænding i et kraftværk er givet i tabel 2. Figur 4 herunder viser CO_2-fortrængningen ved slutudnyttelse med de forskellige synteseløsninger.

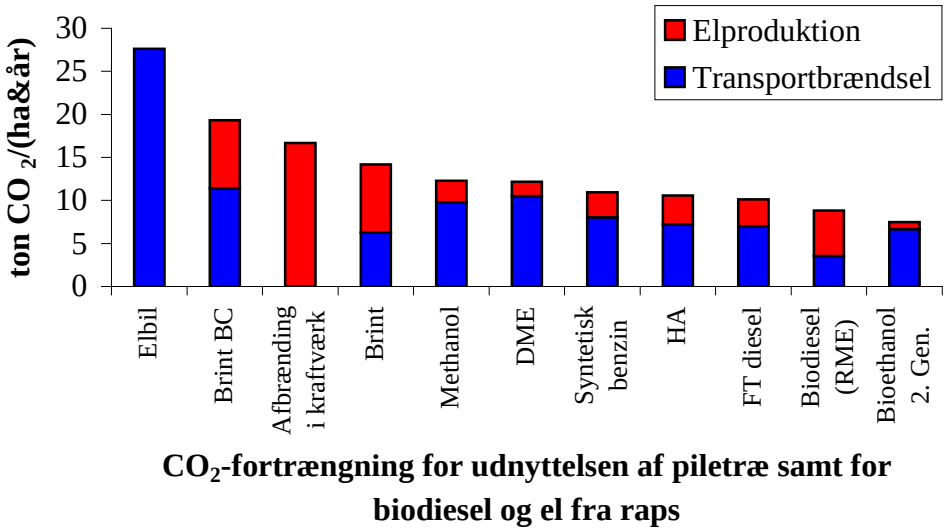

Figur 4 Fortrængningen af CO_2 ved slutudnyttelsen af de forskellige processer.
"Komprimeret brint BC" indikerer brugen af brint i en bil drevet af en brændselscelle.

Den primære konklusion på baggrund af figur 4 er, at den største CO_2-fortrængning, opnås ved at generere el ud fra biomassen. Den dannede elektricitet kan med fordel udnyttes i f.eks. elbiler. Idet elbilen har en mærkbart højere effektivitet, end de benzinbiler den fortrænger, giver dette den bedste CO_2-fortrængning ved slutudnyttelsen. Primært på grund af en anseelig samproduktion af el i syntesen af brint giver denne løsning en den næsthøjeste CO_2-fortrængning. Udnyttelse af brint i en fremtidig brændselscellebil vil potentielt kunne tangere CO_2-fortrængningen ved alm. elproduktion, men det bør nævnes, at det indeværende estimat ikke inkluderer energibehovet for transport af brinten. Transporten af tryksat brint, som har en relativt lav energitæthed, må forventes at være ret energikrævende, hvilket vil nedbringe gevinsten ved udnyttelse af brint betydeligt. Det må derfor forventes, at figur 4 i nogen grad overvurderer CO_2-fortrægningen ved brintproduktion. CO_2-fortrængningen fra brugen af methanol er praktisk talt lige så stor som fortrængningen ved DME-syntesen på grund af en højere elproduktion i forbindelse med methanolsyntesen. Generelt ligger CO_2-fortrængningen med alle transportbrændslerne mærkbart lavere end hvad der opnås ved afbrænding af biomassen i et konventionelt, kulfyret kraftværk. Fremstillingen af biodiesel fra raps

bidrager ikke med nogen nævneværdig CO_2-fortrængning, men en afbrænding af stråproduktet i et konventionelt kraftværk bringer næsten biodiesel på højde med de øvrige synteseløsninger mht. CO_2-fortrængning. Det bør pointeres, at den estimerede CO_2-fortrængning ikke inkluderer produktion af fjernvarme. Hvis denne parameter inkluderes i analysen forøges CO_2-fortrængningen for især afbrændingen i et kraftværk, men også i større eller mindre grad for brændselssynteserne, der alle udvikler varme i forbindelse med syntesereaktionen.

Sammenligning med andre studier på området

De beregnede transportdistancer per markudbytte stemmer udmærket overens med andre lignende studier. Det har ikke været muligt at finde analyser som betragter alle de metoder til brændselssyntese, der er behandlet i det indeværende studium. Det har f.eks. ikke været muligt at finde systemstudier, som behandler produktionen af højere alkoholer eller syntetisk benzin fra mark til motor. I denne sektion er der givet en kort beskrivelse af samhørigheden mellem dette studie og andre lignende analyser.

Et systemstudie fra firmaet Volvo estimerer den transportdistance, en tung lastbil kan tilbagelægge med transportbrændsel udvundet fra et markareals årsudbytte[54]. Det aktuelle studie har beskæftiget sig med personbiler, og de estimerede transportdistancer er derfor længere end hvad der anslås i Volvos analyse. Den indbydes fordeling mellem de transportdistancer, der kan opnås med de forskellige brændsler, stemmer imidlertid udmærket overens med Volvos analyse. Volvos studie estimerer at den bedste transportdistance per markareal opnås med DME, som giver en lidt bedre transportdistance end methanol. Ligesom det indeværende studium anslår Volvos analyse, at FT diesel giver en mærkbart kortere transportdistance end methanol/DME, men en længere distance end bioethanol produceret fra piletræ. Volvos analyse giver også det resultat, at biodiesel fra raps er den af de analyserede muligheder, som giver den korteste transportdistance per markareal.

Et andet studium af Hamelinck og Faaij[20] estimerer transportdistancer for RME og brint, som stemmer overens med det indeværende studium. Hamelinck og Faaij[20] estimerer dog transportdistancer for methanol, FT diesel og bioethanol, som er lidt kortere, end hvad der estimeres i denne analyse. En analyse fra det tyske konsulentfirma L-B Systemtechnik for General Motors finder ligeledes værdier for FT diesel, komprimeret brint og RME, som stemmer overens med værdierne fundet i det indeværende studium[55].

En rapport fra EU kommissionens kontaktgruppe på området indeholder estimerede værdier for den CO_2-fortrængning, som kan opnås ved de forskellige brændselssynteser samt ved el-produktion[37]. De estimater af CO_2-fortrængningen, der er fundet i det indeværende studium, afspejler generelt de værdier, som gives fra EU kommissionens kontaktgruppe. Alt i alt synes resultaterne i denne note at stemme udmærket overens med andre studier på området.

Sammenligning med Energistyrelsens rapport af juni 2007

Energistyrelsen har udarbejdet en ny rapport på området og høringsperioden for denne rapport er i skrivende stund (efteråret 2007) netop afsluttet[56]. Energistyrelsens rapport er baseret på beregninger fra konsulentfirmaet COWI[57]. Dette afsnit indeholder en kort sammenligning mellem den ovenstående analyse og energistyrelsens rapport i den form som er sendt til høring.

I sammenligningen er der benyttet energieffektiveteter fra energistyrelsens rapport, mens markudbyttet er taget fra det indeværende studium. Sammenligningen inkluderer elbiler, samt biler drevet af DME, brint og methanol fremstillet fra biomasse. Disse synteseruter er de eneste, som er fælles for de to studier. I energistyrelsens rapport betragtes brintfremstilling gennem spaltning af vand vha. af dansk blandingsel, mens der i dette studium fokuseres på brintfremstilling via forgasning af biomasse efterfulgt af en såkaldt "shift"-reaktion. Fremstillingen af brint er dog inkluderet i sammenligningen på trods af, at de to analyser fokuserer på forskellige teknologispor til brintfremstilling. Det bør pointeres, at methanol i energistyrelsens rapport udnyttes i en brændselscellebil, mens methanol i den indeværende analyse udnyttes i en konventionel forbrændingsmotor. Figur 5 viser en sammenligning mellem transportdistancerne estimeret i dette studium og distancerne beregnet fra energistyrelsens rapport.

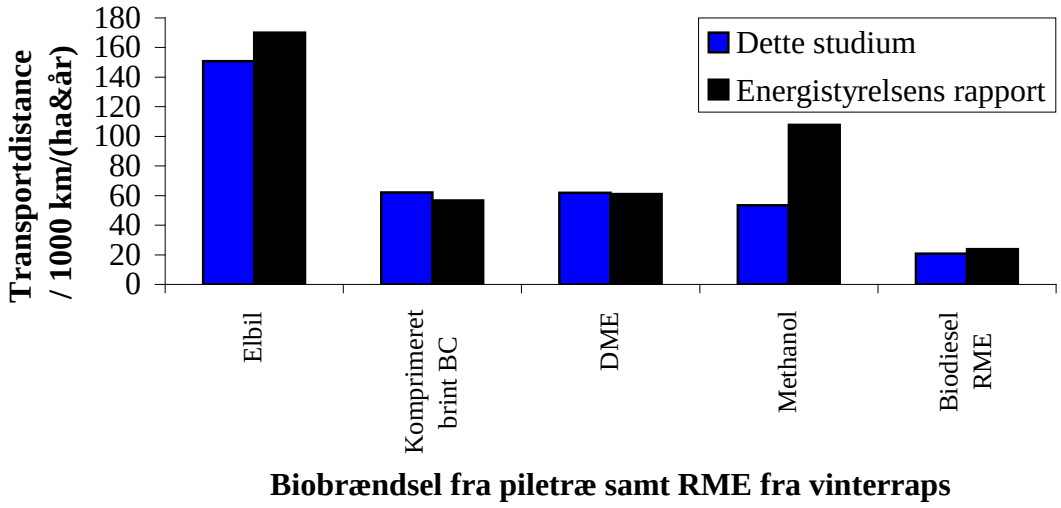

Figur 5 Den distance en gennemsnitsbil kan køre på alternative brændsler udvundet fra årsudbyttet af pil. Biodiesel udvundet fra raps er også inkluderet i sammenligningen. Figuren sammenligner resultaterne fra det indeværende studium med resultaterne fra energistyrelsens rapport[56].
BC indikerer brug i en brændselscelle

Af figur 5 fremgår det, at den estimerede transportdistance for biodiesel, DME, brint og til dels elbiler stemmer relativt godt overens. For elbiler er resultaterne generelt i den samme størrelsesorden, om end energistyrelsens tal giver en længere transportdistance end det indeværende studium. Dette skyldes primært, at elbilen i energistyrelsens rapport antages at være relativt bedre i forhold til benzinbiler. For brugen af brint i en brændselscellebil er der en udmærket overensstemmelse mellem denne note og energistyrelsens rapport. Som nævnt behandler de to studier to forskellige synteseveje til

brint, hvorfor det er svært at drage en konklusion på basis af den relativt gode overensstemmelse, der observeres. Det fremgår også af figur 5, at methanol i energistyrelsens rapport giver en mærkbart højere transportdistance end estimatet for det indeværende studium. Dette skydes, at methanol i energistyrelsens rapport udnyttes i en brændselscellebil med en relativt høj effektivitet, mens det indeværende studium ser på udnyttelsen i en bil med en almindelig forbrændingsmotor, som opererer med en lavere energieffektivitet. Disse værdier er altså ikke direkte sammenlignelige. Det faktum, at methanol i energistyrelsens rapport udnyttes med en mere "futuristisk" og mindre veletableret teknologi (brændselsceller), giver også en vis slagside i forhold til sammenligningerne internt i energistyrelsens rapport. For DME og biodiesel (RME) er der, som det fremgår af figur 5, en glimrende overensstemmelse mellem de to studier.

Konklusion

I de seneste år har der været et stadigt stigende ønske om at nedbringe transportsektorens miljøbelastning og parallelt med dette at opnå en øget uafhængighed af de ofte politiske ustabile olieproducerende lande. Et skridt imod en realisering af disse ønsker er en forøget udnyttelse af biobrændsler i transportsektoren. Denne notes hensigt er ikke at identificere det biobrændsel, som der entydigt bør satses på, men snarere at illustrere de mangfoldige muligheder, der er til stede på området. Udnyttelse af biomassen til elproduktion og brug af den producerede el i el-biler giver generelt den bedste miljøforbedring. Denne løsning vil dog kræve en voldsom forøgelse af elsektoren og synes vanskelig at indfase, hvilket gør, at denne teknologi for øjeblikket snarere ligner "tusindårsriget" end morgendagens transportsektor. Indtil da er der en række mulige biobrændsler, som kan udnyttes med den i dag vidt udbredte motorteknologi. Hidtil har hovedfokus på dette område været på bioethanol (1. generation) og biodiesel. En forgasning af biomassen til såkaldt syntesegas og en efterfølgende syntetisering af et af flere syntetiske brændsler fra syntesegassen åbner imidlertid op for en direkte udnyttelse af lignocellulose som træ og strå - såkaldt 2. generationsteknologi. Med den aktuelle teknologi kan brændsler som DME, methanol, syntetisk benzin og diesel samt blandede højere alkoholer alle give en miljøforbedring, som modsvarer eller overstiger det niveau, der kan realiseres med de hidtil afsøgte løsninger. Den væsentligste konklusion, der kan drages på baggrund af resultaterne i denne note, er derfor som tidligere nævnt, at man bør udvide sit fokus på området til i høj grad også at omfatte forgasningsruten til biobrændsler frem for blot at se på de mere hyppigt omtalte biobrændsler som bioethanol og biodisel. I denne forbindelse er den ting, som er måske vigtigst at huske, Thomas Edisons ord om at: "opportunity is missed by most people, because it is dressed in overalls and looks like work".

Appendiks A: Oversigt over beregnede transportdistancer

Dette appendiks indeholder en oversigt over de beregnede værdier, som er præsenteret grafisk i noten.

Tabel 4 Tilbagelagt distance per markareal for forskellige afgrøder og brændstoftyper

Brændsel	Afgrøde	Brænstoføkonomi / 1000 km/(ha&år)
DME	Vinterhvede (strå+kerner)	82,99
	Pil	61,88
Bioethanol	Vinterhvede (strå+kerner)	52,02
	Pil	36,27
Blandede højere alkoholer	Vinterhvede (strå+kerner)	52,81
	Pil	39,38
Methanol	Vinterhvede (strå+kerner)	71,57
	Pil	53,37
FT diesel	Vinterhvede (strå+kerner)	55,33
	Pil	41,25
Syntetisk benzin (via methanol/DME)	Vinterhvede (strå+kerner)	58,75
	Pil	43,80
Komprimeret brint (forbrændingsmotor)	Vinterhvede (strå+kerner)	45,86
	Pil	34,20
Komprimeret brint (brændselscelle)	Vinterhvede (strå+kerner)	83,39
	Pil	62,17
Biodiesel (RME)	Raps	20,80
Elbil	Vinterhvede (strå+kerner)	202,15
	Pil	150,72

Appendiks B: Parametre benyttet i udregningen

Dette appendiks indeholder de fysiske parametre, der er benyttet i udregningerne til denne note.

Væskeformige transportbrændsler

Tabel 6 herunder indeholder forskellige parametre for de undersøgte væske-formige brændsler.

Tabel 5 Sammenligning af egenskaber for de forskellige væskeformige brændsler behandlet i dette studium[58-67]

	Benzin	Diesel	Methanol	Ethanol	DME	FT diesel	Biodiesel (RME)
Formel	$\approx C_8H_{15}$	$\approx C_{16}H_{34}$	CH_4O	C_2H_6O	C_2H_6O	$\approx C_{16}H_{34}$	$\approx C_{21}H_{28}O_2$
Kulstoffraktion / (w/w)%	86,4	84,9	37,5	52,1	52,1	84,9	77,28
Oktantal	87	8-15	108	115	-	-	-
Cetantal	5-20	40-55	3-5	8	55-60	75	54
Damptryk $P_{37.8°C}^{vap}$ * / bar	0.60	0.03	0.32	0.16	8.44	-	-
Nedre brændværdi (LHV) / $\frac{kJ}{g}$	43.31	42.78	18.23	26.81	28.62	43.9	36,7-40,5
Densitet† / $\frac{g}{cm^3}$	0.74	0.86	0.79	0.79	0.66	0.78	0,88
Energidensitet (LHV) / $\frac{kJ}{cm^3}$	32.05	36.79	14.42	21.16	18.89	34.24	32,3-35,6
Kogepunkt / °C	38-204	163-399	65	78	-25	210-338	-

† DME: T = -25 °C; Benzin, diesel og FT diesel: T = 20 °C; Alkoholer: T = 25 °C; RME: T = 15,5 °C

Det er beskrevet i teksten, at nye benzindrevne biler købt i Danmark i 2006 i gennemsnit kører 14,8 km/L, mens nye dieseldrevne biler i gennemsnit kører 18,6 km/L. Med brændværdierne for benzin og diesel fra tabel 5 bliver den energi, der kræves for at flytte bilen 1 km, omkring 0,46 MJ for benzinbiler og 0,50 MJ. Idet dieselbiler som hovedregel er tungere end benzinbiler, er det ikke urimeligt, at der kræves mere energi for at flytte dieselbilen. For alternative teknologier antages el- og brændselscellebiler at fungere som benzinbiler dog med en højere energieffektivitet som beskrevet i teksten.

Kul

Der er også udført beregninger med den CO_2-fortrængning, der opnås gennem el-produktion, hvor man fortrænger kul afbrændt i et konventionelt kraftværk. Sammensætningen og brændværdien af kul varierer med kvaliteten, ofte betegnet som kullets rang. I dette studium er der benyttet en typisk kulsammensætning refereret fra en rapport fra det amerikanske universitet MIT[68]. De benyttede fysiske parametre for kul er opsummeret i tabel 6.

Tabel 6 Komposition (som leveret) of brændværdi af kul benyttet i dette studium
Den specifikke kultype er Illinois #6.

Øvre brændværdi / $\frac{kJ}{kg}$	25,4
Nedre brændværdi / $\frac{kJ}{kg}$	24,4
Komponent	Indhold / (w/w)%
Karbon	61,20
Brint	4,20
Ilt	6,02
Chlor	0,17
Svovl	3,25
Nitrogen	1,16
Aske	11,00
Fugt	13,00

Energistyrelsens rapport

Til sammenligningsstudierne er der brugt værdier fra energistyrelsens rapport fra 2007[56]. I COWIS rapport[57], der tjener som forlæg for energistyrelsens rapport, antages det, at den effektivt tilførte energi (den fraktion af brændslets energi som rent faktisk overføres til hjulet), der kræves for at flytte en benzinbil, er 0,36 MJ/km. For en dieselbil rapporteres det, at den påkrævede energi pga. en højere vægt er 2 % større, hvilket vil sige 0,3672 MJ/km[57].

I energistyrelsens rapport opgives den totale energieffektivitet for brændsels-synteserne. Dette begreb dækker over den fraktion af energien i biomassen, der reelt kan udnyttes til at drive bilen fremad. Denne effektivitet er rapporteret i tabel 7 herunder.

Tabel 7 Den overordnede energieffektivitet for brændselssynteserne ifølge energistyrelsens rapport[56]

Biorændsel	Effektivitet / $\%_{LHV}$
El	30
Biodiesel (RME)	10*
DME	11
Brint	10
Methanol	19

* Effektivitet for syntesen af RME fra rapsfrø og ikke fra hele afgrøden som for de øvrige værdier.

Appendiks C: Beregningsproceduren

Den transportdistance (D), der kan opnås med et årsudbytte fra en hektar markareal, er beregnet ud fra energiudbyttet fra marken (E), synteseeffektiviteten (η), brændstof-økonomien for en bil drevet af benzin eller diesel (B), energitætheden af benzin hhv. diesel (ρ) og energieffektiviteten af brændslet relativt til olieafledt benzin eller diesel (α).

$$D\left[\frac{km}{ha\cdot år}\right] = E\left[\frac{GJ}{ha\cdot år}\right]\cdot\eta\cdot\left(\frac{B\left[\frac{km}{L}\right]}{\rho\left[\frac{GJ}{L}\right]}\right)\cdot\alpha \qquad \text{C1}$$

Her er $E\cdot\eta$ et mål for den energi, som per markareal kan udnyttes i biler, mens parameteren $\frac{B}{\rho}\cdot\alpha$ er et mål for, hvor langt bilen kører på et givet kvantum energi i brændstoffet. Et eksempel kunne være den transportdistance, der opnås med et års produktion af piletræ gennem forgasning og syntese af methanol. Methanol udnyttes i stedet for olieafledt benzin i en forbrændingsmotor modificeret til brugen af methanol. Middelværdien for energiudbyttet for piletræ kan ses af tabel 1 og er $E = 204\frac{GJ}{ha\cdot år}$. Rapporterede synteseeffektiviteter for methanol ligger mellem 48 og 55 % med en middelværdi på η = 51,5 %. Grundet et højt oktantal antages methanol at give en 10 % højere energieffektitivet end benzin, hvorfor man har α = 110 %. Methanol benyttes i en ny benzinbil, der med benzin som brændstof har en brændstoføkonomi på B = $14,8\frac{km}{L}$. Energitætheden af benzin er ca. ρ = $0.03205\frac{GJ}{L}$. Indsat i ligning C1 ovenfor giver dette:

$$D\left[\frac{km}{ha\cdot år}\right] = 204\frac{GJ}{ha\cdot år}\cdot 0,515\cdot\frac{14,8\frac{km}{L}}{0.03205\frac{GJ}{L}}\cdot 1,10 = 53365,9\frac{km}{ha\cdot år} \qquad \text{C2}$$

Energien af den med brændslet samproducerede el (P) kan beregnes ud fra markens energiudbytte (E) og energieffektiviteten for samproduktionen af el (η_{el}), som kan findes i tabel 2:

$$P\left[\frac{GJ}{ha\cdot år}\right] = E\left[\frac{GJ}{ha\cdot år}\right]\cdot\eta_{el} \qquad \text{C3}$$

For methanol fremstillet fra piletræ har man f.eks. $E = 204\frac{GJ}{ha\cdot år}$ og η_{el} = 6 %:

$$P = 204\frac{GJ}{ha\cdot år}\cdot 0.06 = 12.24\frac{GJ}{ha\cdot år} = 3400\frac{kWh}{ha\cdot år} = 3,4\frac{MWh}{ha\cdot år} \qquad \text{C4}$$

Et givent biobrændsel erstatter et tilsvarende fossilt brændsel (benzin eller diesel). Den del af markens energiindhold, som reelt findes i biobrændslet, er ($E\cdot\eta$). Når denne værdi multipliceres med forholdet mellem effektiviteten for udnyttelse af det syntetiske brændsel og det fortrængte fossile brændsel, α, får man den energi, som "erstattes" af biobrændslet. Den erstattede energi svarer til massen af fortrængt fossilt brændsel

($m_{benzin/diesel}$) ganget med brændværdien af det fossile brændsel ($BV_{benzin/diesel}$). Herudfra kan man så isolere den fortrængte masse af fossilt brændsel:

$$E \cdot \eta \cdot \alpha = m_{benzin/diesel}\left[\frac{kg\,benzin/diesel}{ha \cdot år}\right] \cdot BV_{benzin/diesel}\left[\frac{GJ}{kg}\right] \Leftrightarrow$$

$$m_{benzin/diesel}\left[\frac{kg\,benzin/diesel}{ha \cdot år}\right] = \frac{E\left[\frac{GJ}{ha \cdot år}\right] \cdot \eta \cdot \alpha}{BV_{benzin/diesel}\left[\frac{GJ}{kg}\right]} \qquad \text{C5}$$

Når den fortrængte masse af fossilt brændsel er kendt, kan man ud fra sammensætningen af det fossile brændsel, som er givet i tabel 5 i appendiks B, bestemme den fortrængte masse af CO_2, da et kulstofatom ved forbrænding giver netop et CO_2-molekyle. Efter samme princip beregnes den CO_2 produktion, der fortrænges ved brug af den med transportbrændslerne samproducerede elektricitet. Den fortrængte masse af kul (m_{kul}) kan beregnes ud fra brændværdien af kul (BV_{kul}) givet i tabel 6 i appendiks B og energieffektiviteten af kulforbrænding (η_{kul}) som er opgivet i tabel 2:

$$E\left[\frac{GJ}{ha \cdot år}\right] \cdot \eta_{el} = m_{kul}\left[\frac{kg}{ha \cdot år}\right] \cdot BV_{kul}\left[\frac{GJ}{kg}\right] \cdot \eta_{kul} \Leftrightarrow$$

$$m_{kul}\left[\frac{kg}{ha \cdot år}\right] = \frac{E\left[\frac{GJ}{ha \cdot år}\right] \cdot \eta_{el}}{BV_{kul}\left[\frac{GJ}{kg}\right] \cdot \eta_{kul}} \qquad \text{C6}$$

Når man kender den fortrængte masse af kul, kan man så beregne den fortrængte masse af CO_2 ud fra vægtfraktionen af kulstof i kullet givet i appendiks B.

Sammenligningen med energistyrelsens rapport er udført på følgende måde. Den totale energieffektivitet for brændstoffet (η_{tot}), dvs. den fraktion af markens energi der effektivt går til at flytte bilen, er opgivet i energistyrelsens rapport. Den energi som kræves for at flytte bilen, ε, er givet i COWIS rapport[57], der tjener som forlæg, for energistyrelsens rapport. For markens energiudbytte er værdien fundet i denne note benyttet (se tabel 1). Med disse værdier kan man beregne den transportdistance (D), der kan opnås med et årsudbytte fra en hektar markareal:

$$D\left[\frac{km}{ha \cdot år}\right] = \frac{E\left[\frac{GJ}{ha \cdot år}\right] \cdot \eta_{tot}}{\varepsilon\left[\frac{GJ}{km}\right]} \qquad \text{C7}$$

Et eksempel kunne være beregningen for DME produceret ud fra piletræ. Som det kan ses i appendiks B er beregningsparametrene fra energistyrelsens rapport η_{tot} = 6 % og ε = 0,3672 MJ/km. Med $E = 204\frac{GJ}{ha \cdot år}$ fra denne note har man derfor:

$$D = \frac{204\frac{GJ}{ha \cdot år} \cdot 0{,}11}{0{,}3672\frac{MJ}{km} \cdot 10^{-3}\frac{GJ}{MJ}} = 6111{,}1\frac{km}{ha \cdot år} \qquad \text{C8}$$

Til sammenligning er værdien, som er fundet i denne note $61882\frac{km}{ha \cdot år}$.

Kilder

1 Parikka, M; Global biomass fuel resources; Biomass and Bioenergy; 27; 2004; 613-620

2 Kaltschmitt, M; Dinkelbach, L; in Kaltschmitt, M; Bridgwater, A V editors; Biomass Gasification and Pyrolysis-State of the Art and Future Prospects; 1st ed.; CPL Scientific; Newbury; 1997

3 Christensen, J. M, Jensen, P. A., Jensen, A.D., Effektivitet og CO_2-fortrængning for syntese af væskeformige brændsler fra biomasse I. De mulige synteseveje, Dansk kemi, 10, 2008.

4 Christensen, J. M, Jensen, P. A., Jensen, A.D., Effektivitet og CO_2-fortrængning for syntese af væskeformige brændsler fra biomasse II. Sammenligning af syntesemulighederne, Dansk kemi, 11, 2008.

5 Jørgensen, J R; Deleuran, L C; Wollenweber, B; Prospects of whole grain crops of wheat, rye and triticale under different fertilizer regimes for energy production; Biomass and Bioenergy; 31; 2007; 308-317

6 Danmarks Statistik; Nyt fra Danmarks Statistik; 495; 17/11-2006

7 Danmarks Statistik; Nyt fra Danmarks Statistik; 478; 19/11-2003

8 Dornburg, V; Termeer, G; Faaij, A P C; Economic and greenhouse gas emission analysis of bioenergy production using multi-product crops-case studies for the Netherlands and Poland; Biomass and Bioenergy; 28; 2005; 454-474

9 Diepenbrock, W; Yield analysis of winter oilseed rape (Brassica napus L.): a review; Field Crops Research; 67; 2000; 35-49

10 Bernesson, S; Nielsson, D; Hansson, P-A; A limited LCA comparing large- and small-scale production of rape methyl ester (RME) under Swedish conditions; Biomass and Bioenergy; 26; 2004; 545-559

11 Faaij, A P C; Bio-energy in Europe: changing technology choices; Energy Policy; 34; 2006; 322-342

12 McKendry, P; Energy production from biomass (part 1): overview of biomass; Bioresource Technology; 83; 2002; 37-46

13 Dansk Landbrugsrådgivning; Kalkulationer for Pil; 2007; Tilgængelig fra: http://www.lr.dk/planteavl/informationsserier/info-planter/bioenergi-Kal-pil-helskud.xls

14 Dansk Landbrugsrådgivning; Elefantgræs Dyrkningsvejledning; 2007; Tilgængelig fra: http://www.lr.dk/planteavl/informationsserier/dyrkningsvejledninger/elefantgraesdv.htm

15 Larsen, H; Kossmann, J; Petersen, L S editors; Risø Energy Report 2; Risø National Laboratory; 2003

16 IEA; Biofuels for Transport An International Perspective; 2004

17 Wihersaari, M; Energy Consumption and Greenhouse Gas Emissions from Biomass Production Chains; Energy Conversion Management; 37; 1996; 1217-1221

18 Hamelinck, C N; Suurs, R A A; Faaij, A P C; International bioenergy transport costs and energy balance; Biomass and Bioenergy; 29; 2005; 114-134

19 Towler, G P; Oroskar, A R; Smith, S E; Development of a Sustainable Liquid Fuels Infrastructure Based on Biomass; Environmental Progress; 23; 2004; 334-341

20 Hamelinck, C N; Faaij, A P C; Outlook for advanced biofuels; Energy Policy 34; 2006; 3268-3283

21 Wooley, R; Ruth, M; Sheehan, J; Ibsen, K; Majdeski, H; Galvez, A; Lignocellulosic Biomass to Ethanol Process Design and Economics Utilizing Co-Current Dilute Acid Prehydrolysis and Enzymatic Hydrolysis Current and Futuristic Scenarios; Report NREL/TP-580-26157; National Renewable Energy Laboratory; 1999

22 Alzate, C A; Toro, O J S; Energy consumption analysis of integrated flowsheets for production of fuel ethanol from lignocellulosic biomass; Energy; 31; 2006; 2447-2459

23 MacLean, H L; Lave, L B; Evaluating automobile fuel/propulsion system technologies; Progress in Energy and Combustion Science; 29; 2003; 1-69

24 Delucchi, M; A lifecycle emission analysis: urban air pollutants and greenhouse-gases from petroleum, natural gas, LPG, and other fuels for highway vehicles, forklifts, and household heating in the US; World Reserves Review; 2001; 13; 25-51

25 Hamelinck, C N; van Hooijdonk, G; Faaij, A P C; Ethanol from lignocellulosic biomass: techno-economic performance in short-, middle- and long-term; Biomass and Bioenergy; 28;2005;384-410

26 Wahlund, B; Yan, J; Westermark, M; Increasing biomass utilization in energy systems: A comparative study of CO2 reduction and cost for different bioenergy processing options; Biomass and Bioenergy; 2004; 531-544

27 L-B Systemtechnik GmbH, GM Well-to-Wheel Analysis of Energy Use and Greenhouse Gas Emissions of Advanced Fuel/Vehicle Systems – A European study; 2002

28 Faaij, A; Modern Biomass Conversion Technologies; Mitigation and Adaption Strategies for Global Change; 11; 2006; 343-375

29 Hamelinck, C N; Faaij, A; Future Prospects for production of methanol and hydrogen from biomass; Journal of Power Sources; 111; 2002; 1-22

30 Ahlvik, P; Brandberg, Å; Well-to-Wheel Efficiency For alternative fuels from natural gas or biomass; Report for the Swedish National Road Administration; 2001
31 Shaeiwitz, J A; Whiting, W B; Turton, R; Torries, F; Saymansky, J; Tandon, M; Maier, R W; Haught, B; Dodd, J; The Economical Production of Alcoholic Fuels from Coal-Derived Synthesis Gas, Chapters 7-14; West Virginia University; 1999

32 Elam, N Project Manager; The bio-DME project Phase 1 (Non-confidential version); Report to the Swedish National Energy Administration; Atrax Energi; Stockholm; 2002

33 Kam, A Y; Schreiner, M; Yurchak, S; in Meyers, R A editor; Handbook of Synfuels Technology; McGraw-Hill; USA; 1984

34 Tijmensen, M J A; Faaij, A P C; Hamelinck, C N; van Hardeveld, M R M; Exploration of the possibilities for production of Fischer Tropsch liquids and power via biomass gasification; Biomass and Bioenergy; 23; 2002; 129-152

35 Bugge, J; Kjær, S; Blum, R; High power coal fired power plants developments and perspectives; Energy; 31; 2006; 1437-1445

36 Olag, G A; Goeppert, A; Prakash, G K S; The Methanol Economy; 1st ed.; Wiley-VCH; Germany; 2006

37 Alternative Fuels Contact Group; Market Development of Alternative Fuels; 2003

38 Spath, P L; Mann, M K; Amos, W A; Update of Hydrogen from Biomass – Determination of the Delivered Cost of Hydrogen Milestone Completion Report; Report NREL/MP-510-33112; National Renewable Energy Laboratory; 2003

39 Baxter, L; Biomass-coal co-combustion: opportunity for affordable renewable enery; Fuel; 84; 2005; 1295-1302

40 Phillips, S; Aden, A; Jechura, J; Dayton, D; Eggeman, T; Thermochemical Ethanol via Indirect Gasification and Mixed Alcohol Synthesis of Lignocellulosic biomass; Report NREL/TP-510-41168; National Renewable Energy Laboratory; 2007

41 Danmarks Statistik; Nyt fra Danmarks Statistik; 418; 22/9-2006

42 Semelsberger, T; Borup, R L; Greene, H L; Dimethyl ether (DME) as an alternative fuel; Journal of Power Sources; 156; 2006; 497-511

43 Agarwal, A K; Biofuels (alcohols and biodiesel) applications as fuels for internal combustion engines; Progress in Energy and Combustion Science; 33; 2007; 233-271

44 Lave, L; MacLean, H; Hendrickson, C; Lankey, R; Life-Cycle Analysis of Alternative Automotive Fuel/Propulstion Technologies; Environmental Science and Technology; 34; 2000; 3498-3606

45 Larsen, G; Glejtrup, E redaktører; Morgendagens transportbrændsler Danske perspektiver; Teknologirådet rapport 2006/15; 2006

46 Personal communication with Spencer Sorenson, associate professor at MEK-DTU

47 Delucchi, M A; A Lifecycle Emissions Model(LEM): Lifecycle Emissions from transportation fuels, motor vehicles, transportation modes, electricity use, heating and cooking fuels, and materials; Institute of Transportation Fuels University of California; 2003

48 Wender, I; Reactions of synthesis gas; Fuel Processing Technology; 48; 1996; 189-297

49 Kavalov, B; Peteves, S D; Status and Perspectives of Biomass-to-Liquid Fuels in the European Union; EUR21745EN; Directorate-General Joint Research Centre of the European Commission; 2005

50 Anonymous; Thermal gasification of biomass: success stories; Euroheat and Power; 1; 2005; 18-21

51 Hansen, J B; Syngas Routes to Alternative Fuels Efficiencies and Potential with Update on current projects; SYNBIOS Conference; Stockholm; 2005

52 Fleisch, T H; Sills, R A; Briscoe, M D; 2002 – Emergence of the Gas-to-Liquids Industry: a Review of Global GTL Developments; Journal of Natural Gas Chemistry; 11; 2002; 1-14

53 Anonymous; Range Fuels to build first wood cellulosic ethanol plant in Georgia, USA; Focus on Catalysis; 4; 2007; 5

54 Volvo Truck Corporation; Volvo Trucks and The Environment; 2007

55 Wurster, R; GM Well-to-Wheel Studie – Ergebnisse und Schlüsse sowie Vergleich mit anderen Arbeiten und Ausblick auf Kraftstoffpotentiale und –kosten; L-B Systemtechnik GmBH; 2003

56 Energistyrelsen; Udkast til rapport Alternative drivmidler i transportsektoren (sendt til høring juni 2007); juni 2007

57 COWI; Energistyrelsen Teknologivurdering af alternative drivmidler til transportsektoren rapport; Maj 2007

58 Alternative Fuels Data Center; www.eere.energy.gov/afdc; March 2007

59 Herman, R G; Advances in catalytic synthesis and utilization of higher alcohols; Catalysis Today; 55; 2000; 233-245

60 Sie, S T; Senden, M M G; van Wechem, H M H; Conversion of natural gas to transportation fuels via the shell middle distillate synthesis process (SMDS); Catalysis Today; 8; 1991; 371-394

61 Lide, D R editor; Handbook of Chemistry and Physics; 78th ed.; CRC Press; New York; 1997

62 Minteer, S editor; Alcoholic Fuels; CRC Press; 1st ed.; USA; 2006

63 MacLean, H L; Lave, L B; Evaluating automobile fuel/propulsion system technologies; Progress in Energy and Combustion Sciences; 29; 2003; 1-69

64 Ogawa, T; Inoue, N; Shikada, T; Ohno, Y; Direct Dimethyl Ether Synthesis; Journal of Natural Gas Chemistry; 12; 2003; 219-227

65 Peng, X D; Toseland, B A; Tijm, P J A; Kinetic understanding of the chemical synergy under LPDME conditions - once-through applications; Chemical Engineering Science; 54; 1999; 2787-2792

66 Semelsberger, T A; Borup, R L; Greene, H L; Dimethyl ether (DME) as an alternative fuel; Journal of Power Sources; 156; 2006; 497-511

67 Crookes, R J; Bob-Manuel, K D H; RME or DME: A preferred alternative fuel option for future diesel engine operation; Energy Conversion and Management; 48; 2007; 2971-2977

68 Katzer, J Executive Director; The Future of Coal Options for a Carbon-Constrained World; 2007; Massachusetts Institute of Technology; Available from: http://web.mit.edu/coal/

EFP06

Production of methanol/DME from biomass

Jesper Ahrenfeldt
Ulrik Birk Henriksen
Janus Münster-Swendsen
Anders Fink
Lasse Røngaard Clausen
Jakob Munkholt Christensen
Ke Qin
Weigang Lin
Peter Arendt Jensen
Anker Degn Jensen

National Laboratory for Sustainable Energy (Risø DTU)
Department of Mechanical Engineering (DTU Mekanik - MEK)
Department of Chemical and Biochemical Engineering (DTU Kemiteknik - KT)
TECHNICAL UNIVERSITY OF DENMARK
2011